Accuracy Optimization of anti-TB Drug Assays using Protein Evaluation in Calibration Curves during Pharmacokinetics Quality Assurance

By

SARFARAAZ VALLIE

Thesis presented in Fulfillment of the Requirements for the Degree of Master of Pharmacology at the Stellenbosch University

Supervisor: Prof Marietjie A Stander, Department of Biochemistry, Faculty of Science, Stellenbosch University

Co-Supervisor: Prof Helmuth Reuter, Division of Clinical Pharmacology, Department of Medicine, Faculty of Medicine and Health Sciences, Stellenbosch University

December 2021

Declaration

By submitting this thesis electronically, I declare that the entirety of the work contained therein is my own, original work, that I am the authorship owner thereof (unless to the extent explicitly otherwise stated) and that I have not previously in its entirety or in part submitted it for obtaining any qualification.

Signature: …… Date: .....

Abstract

Quality assurance of drug assaying is an important aspect in clinical testing. Accuracy is important to ensure correct bio-analytical results by constructing calibration curves that took blood matrix interferences into consideration. I have adhered to the United States of America Food and Drug Administration (FDA) call for improved accuracy in bio-equivalence, bio-availability and administering of narrow therapeutic indexed drugs. Significant different plasma levels were observed in clinical trials for the occasional hyperproteinemia (an increase in protein concentration in the bloodstream) and hypoproteinemia (lower-than normal levels of protein in the blood) patients this includes disease-related hyperalbuminemia (an increased concentration of albumin in the blood) and hypoalbuminemia (a deficit of albumin in the blood) patients. This research supported a modeled approach for accuracy improvements by including the patients' plasma protein levels using a combined calibration curve (protein evaluation calibrations curves – PROTECC-PK^{TM}). Levels of albumin were classified as marked hypoalbuminemia (<2.5 g/dL), mild hypoalbuminemia (2.5-3.5 g/dL), normal albumin (3.5-4.5 g/dL), and hyperalbuminemia (>4.5 g/dL). This research was specifically important for drugs with a narrow therapeutic index. The rifampicin method was developed, validated and the concentration calibration curve of rifampicin with and without plasma was assessed. The limit of detection for rifampicin with and without plasma was 0.189 µg/ml ± 0.082 and 0.080 µg/ml ± 0.053 µg/ml respectively (LOD ± mean standard diviation). The limit of quantification of rifampicin with and without plasma was 0.573 µg/ml ± 0.082µg/ml and 0.243 µg/ml ± 0.053µg/ml respectively (LOQ ± mean standard diviation). The r^2 for rifampicin was 0.9971 without plasma and 0.9852 with plasma present. A novel analytical method for determination of the % protein content present in blood plasma was performed using the Karl Fischer Titration process. Results indicated deviation in % protein of blood plasma for patients compared to literature values of about 8 %. Using the data obtained, the PROTECC-PK^{TM} curves indicated that the relative accuracy differed by a minimum of 0.1% for low binding affinity drugs and a maximum of more than 20% for drugs with moderate binding affinities. The relative accuracy of the anti TB drugs was supported by computational modelling and thermodynamic analytical methods for each drug during multiple drug co-administration regimens. This study focused on the drug binding affinity that affects the extrapolation of the patient's sample drug concentration from the slope of LCMS calibration curve. The binding constants calculated from fluorescence spectroscopy data were as follows: rifampicin 5.379 x 10^2 M^{-1} (moderate affinity), isoniazid 9.285 M^{-1} (low affinity), 25-desacetyl rifampicin 3.156 M^{-1} (low affinity), ethambutol 3.443 M^{-1} (low affinity) and pyrazinamide 3.076 X 10^2 M^{-1} (moderate affinity). These drugs Gibbs free energies for these drugs indicated spontaneous binding reactions. Rifampicin, a non-polar weak acid with a higher affinity, showed the most stable complex formation with human serum albumin (HSA) compared to soluble isoniazid. This is because isoniazid in its

ionized form can be easily excreted in the urine resulting in low levels of detection. This will affect the bioavailability and accuracy of the assay levels for patients experiencing hyper and hypoalbuminemia with related competition and induction processes of the enzymes. These complications are apparent where a larger number of patients are involved in clinical trials, bioequivalence and bioavailability studies with varying protein levels that may be more crucial for drugs with a narrow therapeutic index.

Abstrak

Gehalteversekering van medisynemiddel bepalingsprosesse is 'n belangrike aspek in kliniese toetse. Akkuraatheid is belangrik om te verseker korrekte bio-analitiese resultate deur die bou van kalibrasie kurwes wat bloed matriks steuringe in ag neem. Ek het van die Verenigde State van Amerika Food and Drug Administration (FDA) oproep vir 'n beter akkuraatheid in bio-ekwivalensie, bio-beskikbaarheid en administrasie van smal terapeutiese geïndekseer dwelms gevolg. Daar is in kliniese toetse verskille waargeneem in plasmavlakke van hyperproteinemia en hypoproteinemia pasiënte en ook siekte-verwante hyperalbuminemia en hypoalbuminemia pasiënte van die kalibrators. Hierdie navorsing ondersteun akkuraatheid verbeterings deur die insluiting van die pasiënte se plasma proteïen vlakke met behulp van 'n gekombineerde kalibrasie kurwe (proteïen evaluering kalibrasies kurwes - PROTECC-PK^{TM}). Vlakke van albumien is geklassifiseer as gemerk hypoalbuminemia (<2.5 g/dL), ligte hypoalbuminemia (2.5-3.5 g/dL), normale albumien (3.5-4.5 g/dL), en hyperalbuminemia (> 4.5 g/dL). Hierdie navorsing was spesifiek belangrik vir middels met 'n smal terapeutiese indeks. Die metode en kalibrasie kurwe van rifampisien met en sonder plasma is beoordeel. Die limiet van opsporing vir rifampisien met en sonder plasma was 0.189 µg/mL en 0.080 µg/mL onderskeidelik. Die limiet van kwantifisering van rifampisien met en sonder plasma was 0.573 µg/ml en 0.242 µg/ml onderskeidelik. Die r^2 vir rifampisien was 0,9971 sonder plasma en 0,9852 met plasma teenwoordig. 'n Nuwe analitiese metode vir die bepaling van die waterinhoud% teenwoordig in bloedplasma is uitgevoer met behulp van die Karl Fischer Titrasie proses. Resultate dui daarop afwyking in waterinhoud % van bloedplasma van pasiënte in vergelyking met literatuur waardes van ongeveer 92%. Met behulp van die verkry data, die PROTECC-PK^{TM} kurwes het aangedui dat die relatiewe akkuraatheid verskil deur 'n minimum van 0,1% vir lae bindingsaffiniteit dwelms en 'n maksimum van meer as 20% vir dwelms met 'n matige bindende affiniteite. Die relatiewe akkuraatheid van die anti TB-middels is met behulp van die numeriese modellering voorspelling en termodinamiese bindende affiniteit eksperimente van elke dwelm tydens verskeie dwelm mede-administrasie regimens. Dit fokus op die medisynemiddel bindingsaffiniteit dat die ekstrapolasie van die pasiënte monster dwelmkonsentrasie van die helling van die kalibrasie kurwe beïnvloed. Die bindingskonstantes bereken deur fluoressensie spektroskopie data is soos volg: rifampisien 5,379 x 10^2 M^{-1} (matige affiniteit), isoniasied 9,285 M^{-1} (lae affiniteit), 25-desacetyl rifampisien 3,156 M^{-1} (lae affiniteit), ethambutol 3,443 M^{-1} (lae affiniteit) en pyrazinamide 3,076 X 10^2 M^{-1} (matige affiniteit). Hierdie middels se Gibbs vrye energie dui op spontane bindingsreaksies. Rifampisien ’n nie-polêre swak suur met 'n hoër affiniteit en die mees stabiele kompleks vorm met albumien in teenstelling met oplosbare isoniasied. Die rede is die polariteit en die geïoniseerd vorm van isoniasied om maklik in die urine uit geskei te word, lei tot lae vlakke van opsporing. Dit sal die biobeskikbaarheid en akkuraatheid van die toets vlakke vir pasiënte met hiper en hypoalbuminemia

met verwante kompetisie en induksie prosesse van die ensieme beïnvloed. Hierdie komplikasies is duidelik waar 'n groter aantal pasiënte betrokke is by kliniese toetse, bio-ekwivalentestudie en biobeskikbaarheid studies met wisselende proteïen vlakke wat meer belangrik vir middels kan wees met 'n smal terapeutiese indeks.

Acknowledgments

I would like to extend great thanks to my supervisors': Professor Marietjie Stander and Professor Helmuth Reuter for all of the help, time, effort, support, motivation, and intellectual knowledge during this study. I would like to thank Dr Sivapregasen Naidoo for all of the help and support and guidance throughout my research. I would also like to extend thanks to Clinical Pharmacology division and the University of Stellenbosch for all of the support. I would also like to thank Dr. Samual Egieyeh from the University of Western Cape for the help and support of computational, Fluorescence and UV spectroscopy studies. I would also like to send my gratitude to David Kok from the CPUT campus for the aid and assistance of Karl Fischer equipment and equipment software training. I would like to thank the NRF with great gratitude for funding and making my research possible. I would also like to thank my parents, wife and family for supporting me throughout my research.

Table of Contents

List of Figures

List of Tables

Equation Table

Equation	Formula
Concentration	C= n/V
Concentration	$C_1V_1 = C_2V_2$
Limit of detection	$LOD = (3* S_{\frac{Y}{x}}) / m$
Limit of quantitation	$LOQ = \frac{10 \text{ x } {}^{sy}/_{x}}{178188}$
Linear equation	y=mx + c
Entropy equation	$\Delta S° = -\frac{\Delta H°}{T}$
Gibbs free energy	$\Delta G° = \Delta H° - T\Delta S° = -RT\ln K$
Stern-Volmer equation	$\frac{Fo}{F} = 1 + Kq\ \tau[Q] = 1 + Ksv[Q]$....
Stern-Volmer-Line Weaver Burk equation	$Lg\left(\frac{Fo - F}{F}\right) = Lg\ K + n \lg[Q]$
Van't Hoff equation	$\ln K = \frac{-\Delta H°}{RT} + \frac{\Delta S°}{R}$

Chapter 1

Introduction

1. Rationale

The 4-drug regimen of Rifampicin, isoniazid, pyrazinamide and ethambutol has been widely used as a treatment for patients with tuberculosis. It is known that the unbound drug in the blood plasma can freely penetrate to the tissues to produce its physiological effect and that the bound drug binds to the protein in blood plasma and slowly releases to produce an equilibrium in the blood plasma [1]. When using pharmacokinetic/pharmacodynamics models, it is developed using the total drug concentration. For drugs like rifampicin that has a high protein binding affinity the pharmacodynamics effect can lead to overestimated results. The problem that we face is that not every patient is in a good health condition. In critically ill TB patients with health conditions e.g renal failure, HIV or blood disorders such as hypoalbuminea (a deficit of albumin in blood), hyperalbuminia (an increased concentration of albumin levels in blood), hypoproteinemia (low levels of protein in the blood) hyperproteinemia (high protein levels in the blood) dosage of the drugs with a narrow therapeutic index could lead to erroneous drug concentration results and outliers in clinical trials [1]. Therefore in clinical trials, when using bioanlytical methods for monitoring TB patient drug concentration levels, that are administered the same drug dosage, especially for high protein binding drugs like rifampicin, it is important to take the condition of the patient's blood plasma into consideration. This led our research to a hypothesis that varying patient plasma protein levels will affect the accuracy of drug concentration determination by bioanalytical laboratory methods.

1.1 Research Question

When studying patients undergoing TB drug therapy in clinical trials, does the plasma protein concentration:

1. Affect the accuracy and linearity in the calibration curves of different calibrators
2. Cause matrix effects on anti-TB drugs with different physiological properties such as pKa affecting analytical detection?
3. Affect TB-drug binding interaction and can it affect the accuracy of therapeutic drug monitoring in clinical trials?

1.2 Aims

The following aims were outlined indicating the steps taken in our research to investigate and varify our hypothesis which stated that varying patient plasma protein levels will affect the accuracy of drug concentration determination by bioanalytical laboratory methods.

1. To validate the LCMS method of rifampicin **with** and **without** blank blood plasma present in samples, and determine if human blood plasma affects the accuracy and linearity by comparing the two liquid chromatography mass spectroscopy (LCMS) concentration calibration curves produced from the validated methods.

2. To investigate:

- if calibrator plasma used in the laboratory varies from protein water content indicated in the literature.

- if the viscosities of different patients' plasma used exhibit variations that affect the gradient of a calibration curve within clinical drug trial studies.

3. Determine if drug-plasma protein binding interactions occur, using computational modelling, experimental fluorescence excitation, and ultraviolet absorbance spectroscopy

4. Investigate if a modelled approach where albumin levels are taken into account in the calculation of drug concentrations from calibration curves will yield better accuracy.

1.3 Research Overview

Chapter 2 is a detailed literature review explaining the concepts used in this research. The literature outlines, the quality assurance perspective, validation parameters, the laboratory instrumentation used in the study aswell as background of pharmacology, Blood plasma, TB and the anti-TB drugs, clinical trials and compututational modelling of drugs to plasma.

In Chapter 3, a LCMS method was validated to quantify rifampicin using a Shimadzu triple quadrupole mass spectrometer. A mass spectrometer (MS) is a selective detector that detects molecules based on their mass to charge ratio. The system is connected with a liquid chromatograph (LC) that first separates the molecules based on their polarity. Hence LCMS helps us to separate the different molecules in a solution, as well as to identify a molecule like rifampicin by fragmention. This produces a unique fragmentation pattern of the molecule which is measured in mass to charge ratios. Known concentrations of rifampicin were used with and without blood plasma to validate the LCMS method for quantification of rifampicin to obtain the raw data required to construct and plot the LCMS peak area vs concentration calibration curves of rifampicin and to assess if plasma had an impact on the accuracy and linearity of the peak area vs concentration calibration curves with and without plasma.

The study in Chapter 4 was conducted using the Karl Fischer process to assess if the blank plasma standards used in the laboratory to plot LCMS calibration curves for clinical trials varied in water to protein content when compared to the norm reported in the literature of less than 93% water, which could impact accuracy.

In Chapter 5, this study aimed to identify and understand the binding interaction mechanism of the first-line anti-TB drugs INH, RIF, PYR, ETH and 25-desacetyl rifampicin (D-RIF – a major metabolite of RIF) with human serum albumin (HSA) using molecular docking, and with blood plasma using spectroscopic and thermodynamic approaches. We wished to confirm the binding affinity of different drugs with different pKa values to establish a more accurate protein evaluation in calibration curves, since this could affect the recovery and accuracy of calibration curves. Drugs with narrow a therapeutic window, bioequivalence and bioavailability studies are most affected by a less than 100% recovery.

Chapter 6 was a quality assurance-modelled study on the accuracy of calibration curves using the data obtained from Chapter 3, 4 and 5 to construct modelled and calculated calibration curves for patients with normal albumin levels of 4.3 g/dL to low albumin levels of 1.6 g/dL. This was done to assess if the albumin levels caused a decrease in the concentration levels obtained. This research represents a theoretical model for correction of concentration calibration curve extrapolated concentration results by taking patients with blood disorders into account. Where the drug-bound albumin levels affect the

recovery levels in the LCMS calibration curves concentration extrapolation, by using the developed model of taking albumin and protein levels of patients with blood disorders into consideration the error of recovery of concentration results can be optimised and will lead to more accurate extrapolated results from LCMS concentration calibration curves.

Chapter 2

Literature Review

2. Study Background

2.1 Quality Assurance

Quality assurance of drug assaying has become an increasingly challenging factor in bioanalytical lab testing, here we try to increase the confidence level in our results. In this research, the aim was to investigate factors that impact the accuracy of drug assays for validation of therapeutic drug monitoring. The main focus was the difference in protein levels between the calibrator and patients' blood plasma. A quality assurance theoretical model (PROTECC-PK^{TM}) was proposed, where protein evaluation of patients with blood disorders are factored in the LCMS concentration calibration curve for pharmacokinetics optimisation in drug concentration result extrapolation. The PROTECC-PK^{TM} theoretical approach aids in bioanalytical method validation related to patient plasma, and where analysis of plasma levels would lead to more accurate results.

In effective bioanalytical laboratory processes, although the combination of absorption, distribution, metabolism, and excretion (ADME) and the variations that drug molecules offer, without affecting the accuracy and precision supported by validation procedures, drug validated bioanalytical methods still produce less than 100% recovery evident in calibration curves. Here we adhere to the International Organization for Standardization (ISO) and the American Food and Drug Administration (FDA) guidance for industry entitled 'Bioanalytical Method Validation', which includes concerns regarding the matrix effect and recovery during liquid chromatographic-mass spectrometry (LCMS) bioanalytical work [2, 3]. The South African National Accreditation System (SANAS) offers laboratory accreditation that requires similar validation and conformity to these guidelines. Drug bound to plasma proteins suggest that the amount of plasma protein affects the free drug fraction and affects the amount of drug recovered during the analytical process. Tests of patients with a high plasma protein content compared to the calibrator plasma protein content will result in a lower recovery during laboratory experiments. To ensure that the level of accuracy and precision are high in drug quantification, insight into their limits of chemical stability and reactivity during *in vitro* and *in vivo* studies involves conformance in multidisciplinary research centres. During bioanalytical experiments, the range of matrix effects could vary from patient to patient due to the complexity and potential variability of the biological matrix that contains a large variety of endogenous substances, metabolites and, in some cases, the presence of co-administered drug(s). A validated method could be at risk when the actual study samples are tested, since the biological samples from different subjects could have different matrix effects [4, 5]. Whole blood (WB) plays an important role in the

quantification of xenobiotics or drugs within the body, as drug therapeutic and toxicity levels are useful for PK studies. Another factor is that infectious blood diseases such as HIV and malaria could affect the plasma protein quantity and condition. Other atmospheric and airborne substances do enter the blood, as was noted during the informal caterers' study that showed systemic levels of chrome, copper, and arsenate (CCA) in informal settlements and users of firewood as energy [6]. Even though the study used urine samples, the CCA affinity for blood could affect protein and drug stability. This proves that environmental factors like air quality do affect the physiological matrix content, and metals in patient samples could enhance matrix effects during the LCMS analysis. The metal quantification by inductively coupled plasma (ICP) is not always performed in parallel to LCMS drug analysis of patient blood samples.

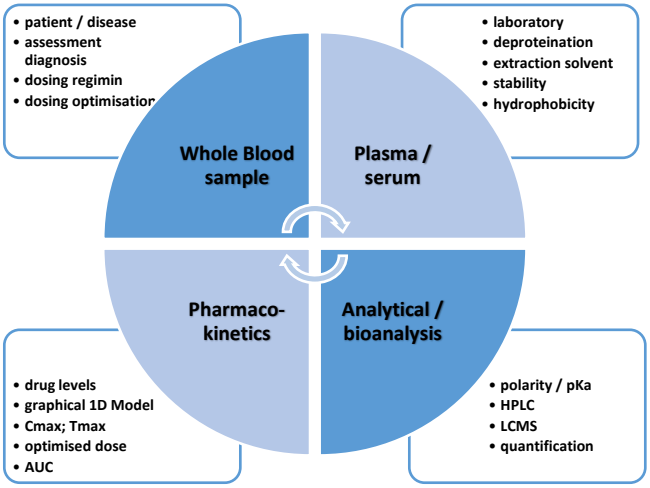

Figure 2.1: The process followed for a dosing optimisation pharmacokinetic study

The quality control parameters and compliance limits are well researched and documented in journals and pharmacopoeias [7, 8, 9]. Pharmacokinetics and ADME of drugs are followed. Whole blood plasma viscosity (WB-PV) can be assessed by the water-protein ratio content. Validation protocols are usually comprehensive quality assurance documents entailing methods and detailed standard operating procedures.

Plasma viscosity is an important analytical biomarker of Hemorheology studies [10]. Hemorheology is the study of flow properties of the blood and its elements of plasma and cells. Hemorheology and drug plasma-tissue equilibrium may be important factors in drug assaying and therapeutic drug monitoring accuracy. Drug plasma-tissue equilibrium is the fraction of unbound drug in the tissue to the fraction of bound drug to plasma protein which is usually a reversible equilibrium reaction, although several factors can cause disequilibrium of the drug concentration in the plasma and tissue [11]. However, it will not be covered within the scope of this research. Plasma viscosity is mostly

dependent on the protein-water ratio. This study focuses on the plasma content presenting challenges in reducing matrix and recovery effects due to drug-plasma binding interaction. This can be achieved by increasing accuracy and optimizing bioanalytical methods by using blood plasma as an added variable to drug sample assays. The body's homeostasis capability in healthy individuals regulates the hydration levels, which are generally varied due to environmental conditions and dietary intake. In drug clinical studies, some patients are critically ill and have contracted opportunistic infectious diseases such as TB, MTB, and XDR-TB, with the possibility of a human immune deficiency virus (HIV) co-infection therefore the accuracy of drug concentration results are important for dose optimizition. Also, bioequivalence (when two different drugs that produce similar blood concentration levels and physiological effect at the active site) and bioavailability (when a drug becomes completely available to the active site) studies require accuracy of the results [12, 13]. These are typically the tests in laboratories where the FDA is supported in proposing cost-effective and practical solutions in improving accuracies. Calibration curves, representative calibrators, and the regression model have been defined in regulatory guidance documents and by the experts [14-25].

2.2 Analytical Method Validation Procedure

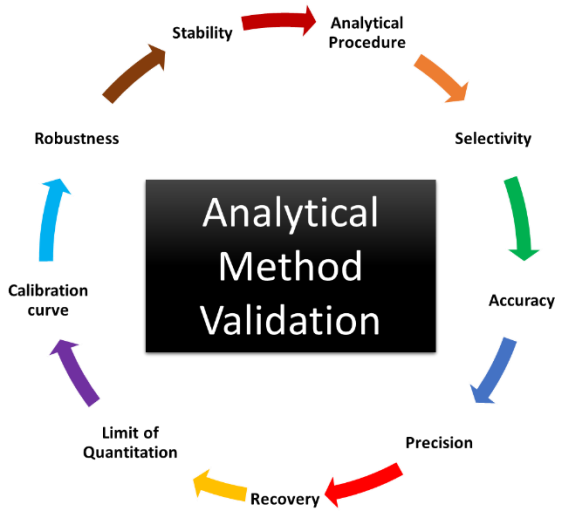

Figure 2.2: Analytical method validation flow chart

Method validation is a vital requirement for any information submitted to regulatory agencies nationally and internationally in support of newly-developed drugs that are released into the market or for clinical trial applications [26]. Method validation provides documented evidence of a method or process (as indicated in Figure 2.2) that provides a great amount of guarantee that the specific method with the instrument used in the analysis will accurately produce results of the tested product [26]. Specific steps are followed and used to validate a method which will be discussed. Method validation should also include information on analytical solutions, stability and system suitability [27].

2.2.1 Specificity

It is required that standard samples of the drug assay are injected to demonstrate the absence of interference of the standard as well as the elution of the analyte sample [28]. No interference of the excipients should occur during the analysis of the analyte being investigated [29].

2.2.2 Linearity

Linearity is an important parameter that helps to confirm the accuracy of experimental findings. Standard solutions are prepared at several concentrations in the typical range of 25 % to 200 % of the aimed concentration [29]. It is required that each standard solution is prepared with three (3) replicates to be analysed at each concentration. The standard preparation and the number of injections remain controlled and the same procedure as the final one used. For each concentration, the mean, standard deviation (SD), and relative standard deviation (RSD) are all calculated. Results are plotted on an x-axis, y-axis graph, which allows the calculation of the regression of the line and coefficient of determination. The correlation coefficient for the range of concentrations used must be more than or equal to 0,999 [29-30].

$$y=mx + c \quad \textbf{Equation 2.1}$$

2.2.3 Range

The range of the data is assessed using the linearity and accuracy data obtained from the method developed [30]. The data used for this assessment would be the precision data prepared for each sample in the three (3) replicates at each analysed concentration in the accuracy study. The range is defined as the concentration at which linearity and accuracy are acquired per replicate analysed. The precision should be less than or equal to 3% of the RSD [30].

2.2.4 Accuracy

The prepared standards range from 50 to 150 % of the specific target concentration. Three replicates are prepared individually for each standard that is analysed [31]. For each standard sample prepared, the actual value, theoretical value (if available), and recovery percentage is reported. The mean, standard deviation, relative standard deviation, and recovery percentage can be calculated. For non-regulated products, the mean recovery should lie between 90 and 110 % of the theoretical value. For active drug ingredients, the mean recovery should be between 80 and 120 % [31].

2.2.5 Precision – Repeatability

A standard with a specifically-selected concentration is prepared and analysed. Ten replicates of the same standard sample concentrations are prepared using the final developed method [32]. The recorded results are then be used to calculate and determine the mean, SD and RSD [32]. According to the FDA, the RSD should be 1 % for drugs substances and products and at 2 % for bulk drugs and final products [30, 32].

2.2.6 Intermediate Precision

Intermediate precision occurs when two analysts using two different HPLCs at concentrations of 50%, 100 % and 150 % on different days test the purity of the data as well as the method used. The mean recovery should range between 80 and 120 % of the analyte assay. The mean area is recorded for each concentration used [30] and the mean, SD and RSD are calculated by the two operators. The results obtained by both operators on different HPLC systems and different days have a statistical RSD of less than or equal to 2% [30].

2.2.7 Limit of Detection

The limit of detection (LOD) is the lowest concentration of the analyte that can be detected by the analytical tool in use [33]. This can be done by sequentially diluting the analyte until it can no longer be detected [34]. Once the lowest concentration is detected, six (6) replicates will be prepared from the sample solution [34]. The chromatogram is then printed, the lowest concentration is detected and the RSD gets recorded [33-34].

$$LOD = (3 * S_{\frac{Y}{x}}) / m \quad \text{.....Equation 2.2}$$

2.2.8 Limit of Quantification

The limit of quantification (LOQ) is an accurate and precise determination of the lowest concentration of the analyte within the sample containing plasma or matrix [35]. The LOQ is determined using the developed method or method in use [35]. This concentration may be the lowest value on the calibration curve. Six replicate samples are prepared for the concentration solution. The chromatographs are recorded. The lowest concentration is then quantified and the RSD determined [36]. The LOQ in chromatography follows acceptance criteria where the concentration provides a signal to noise ratio of 10:1.2. By stating signal to noise ratio, it can be understood as instances where the height of the peak is ten times the height of the baseline noise according to the ratio mentioned above and should have an RSD of approximately 10 % for the six replicates prepared [36].

$$LOQ = \frac{10 \times {}^{sy}/_{x}}{m} \quad \text{.....Equation 2.3}$$

2.2.9 System Suitability

The system suitability of the method can be determined by using two different HPLC systems [37]. The accuracy and precision mentioned above can be determined using both the HPLC systems [37]. Data such as plate count, tailing factor, resolution, and reproducibility can be calculated. All data must be recorded. The retention factor k should be more than or equal to 2 [37]. The resolution should be equal to or more than 2 between the analyte peak and the closest eluted peak. For reproducibility, the peak area, peak height and retention time RSD will be 1 % for the six sample injections. The theoretical plates should be more than equal to 2000 and the tailing factor should theoretically be 2 [37].

2.2.10 Robustness

The United States pharmacopeia defines robustness as a measure of the capacity of the analytical method to work unaffected when small changes are made deliberately to the parameters of the method [38]. This provides the reliability of the developed method when in use. Parameters such as mobile phase pH, temperature, gradient elution, injection volume and organic matter in the mobile phase can be investigated [38]. The parameters can be changed individually or in combination to determine if the method gets affected. If the changes are acceptable and are within the limit of the method, the changes will then be incorporated into the developed analytical method [38].

2.3 Analytical Techniques

2.3.1 High-performance liquid chromatography (HPLC)

High-performance liquid chromatography is by far the most commonly used and versatile elution chromatography technique [39]. HPLC analysis is used by chemists to separate, determine and identify species in a variety of organic, inorganic and biological samples. In liquid chromatography, the mobile phase is the solvent mixture used to carry the analyte through the system [40]. The machine allows complex compounds in a mixture to be separated [39-40] and produces accessible, reproducible and high sensitivity readings. After analysis takes place, the data is recorded onto a chromatogram [39-40]. The chromatogram is a simple and defined output of the HPLC which plots time against detector signal intensity. The chromatogram reflects a profile of the sample analysed where each peak represents a component within the sample [39-40]. HPLC methodologies are used

universally to quantify most drugs of interest in the pharmaceutical industry as well as other industries. In Figure 2.3 a skematic diagram of HPLC is given.

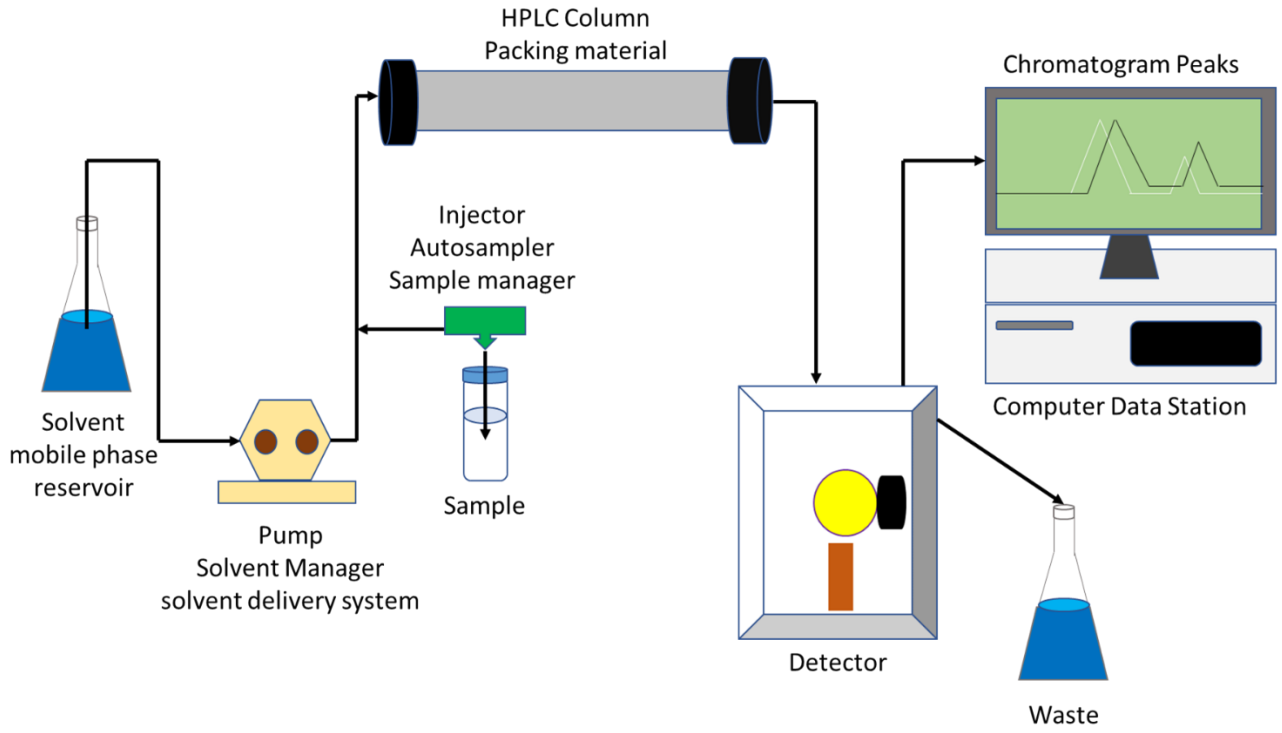

Figure 2.3: HPLC schematic diagram

2.3.2 Reverse-phase chromatography

Reverse-phase chromatography is classified as a type of adsorption chromatography. Adsorption chromatography is dependent on the interaction chemically between the solute molecules and the specific ligands that are chemically bound to a chromatography matrix [41]. Over time, many types of different columns were developed with different ligands bound to the chromatography matrix. The different columns developed were used specifically to separate, purify and exploit the different properties of biomolecules (such as polarity, electronic charge and biological affinity) [41]. Reverse-phase chromatography has been added as an important technique for preparative chromatography of biomolecules [41]. Reverse-phase chromatography involves the retention a solute from the mobile phase or a compound mixture to a stationary phase grafted with an n-alkyl hydrocarbon or aromatic ligand which takes place via a hydrophobic interaction [41].

Reverse-phase chromatography can be used in preparative and analytical applications for separation and purification of biomolecules. Molecules such as protein, nucleic acids, and peptides that have some degree of a hydrophobicity character can be separated with great recovery and resolution when using reverse phase chromatography [41]. Also, the modification of the mobile phase using ion-pairing techniques allows for the reverse phase chromatography of charged solutes, e.g., fully deprotected oligonucleotides and hydrophilic peptides. In preparative reverse phase chromatography, the following application has been developed: protein fragment micro purification is used in the sequencing process, and recombinant protein product purification is used at a process scale [41].

The mechanism of reverse phase chromatography is based on the ability of the solute molecules (within the mobile phase) to effect hydrophobic binding interaction to the stationary phase hydrophobic ligand in the column. Hence, the polarity of the solute is very important for the separation and purification of a sample [42]. Fiigure 2.4 illustrates how non polar molecule in mobile phase interacts with the stationary phase column packing. The mobile phase used in reverse-phase chromatography is primarily aqueous. This indicates a high degree of organized water structure (polar) which surrounds both the solute and the stationary phase ligand [42]. More non-polar solutes will tend to interact more readily with the hydrophobic stationary phase column, which will cause the solute to be retained in the column for a longer period compared to a more polar substance that will be retained for a shorter length of time [42]. It is suggested that the reason for this occurrence could be that, as the solute binds to the hydrophobic ligand stationary phase, the interaction with the mobile in that area of the column is diminished. This causes a favourable increase in entropy, which will allow the solute and stationary phase ligand to associate in terms of an energy point of view [42].

For analysis and separation of biomolecules using reverse phase chromatography, gradient elution is often used instead of the isocratic elution technique [42]. The reason for the use of gradient elution is to provide a sample with a range of aqueous and lipophilic conditions so that biomolecules with different polarities within a sample can be retained and separated into individual compounds on the reverse column stationary phase matrix. Gradient elution also assists biomolecules to desorb easily from the stationary phase matrix when the mobile phase is changed to a more non-polar organic concentration [42]. Most samples analysed contain a mixture of high molecular weight biomolecules with unique adsorption affinities ranges and it is, therefore, more practical to make use of the gradient elution technique [42].

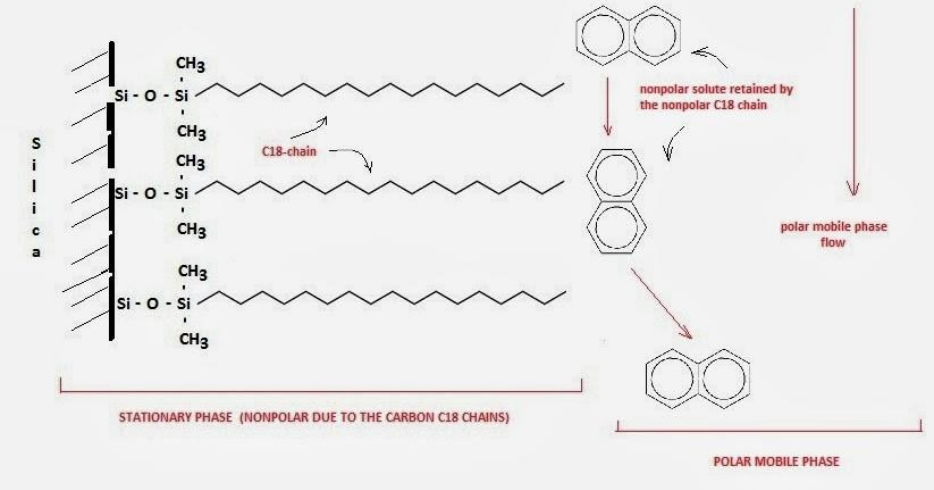

Figure 2.4: Chemical interaction passing through a reversed-phase stationary column (http://chem-net.blogspot.com/2013/11/reversed-phase-chromatography.html)

2.3.3 Mass Spectrometry

Mass spectroscopy is the production and subsequent separation and identification of charged molecules that are produced via a variety of specific ionization methods. Hence, the mass spectrometer (MS) produces ions from chemical compounds that are to be analysed [43]. The MS uses magnetic and electrical fields to measure the mass of the particle ions that have been charged [64].

Mass spectroscopy is a tool that is used to identify the molecular mass to charge ratio (m/z) of a molecule or complex structure by analysing the mass to charge ratios of the molecule [44]. It is a routine method used to identify compounds in an unknown sample by mass to charge ratios [44]. There are many methods of ionization available for specific types of applications and requirements for sample analysis, i.e., fast atom bombardment, desorption chemical ionization, chemical ionization, and electrospray ionization and electron impact ionization. Electrospray ionization is mostly used in pharmaceutical applications and is a soft ionisation technique where the protonated (ESI positive mode) or deprotonated (ESI negative) drug is detected as the molecular ion, which is also known as the parent ion.

Electron impact (EI) ionisation is associated with gas chromatography-mass spectrometry (GCMS) and is a harsher ionisation technique where the molecules get fragmented during ionisation. The result is a unique fingerprint of ions. The ions are arranged on a mass spectrum according to mass to charge ratios [44]. A detailed analysis was possible by resolving the power of the instrument in use for the exact chemical mass, formula, and purity of the compound and could be defined by the depth of the

spectral interpretation. This could be used for structural identification purposes [45]. These characterisation approaches were limited to low molecular weight molecules (<500 Da) with different ranges of thermal lability and polarity [45] if GCMS is used.

The MS is designed as an instrument to separate ions that are in the gas phase according to their mass to charge ratios [45]. The main component of the MS is the analyser. The analyser is responsible for the separation of the gas phase ions. The analyser makes use of the magnetic field or electrical field and can also be used in combination of the two, which aids in moving the ions through the analyser to the detector [45]. The detector then amplifies the signal produced by the analyser so that a reading can take place. The analyser operates under a high vacuum environment [45]. This high vacuum environment aids to move the ions across the analyser to the detector at an adequate yield for amplification. The MS can also be set to detect specific mass to charge ratios through its configuration setting [45]. This is a great advantage when analysts are searching for specific molecules [45].

Several analysers can be used in mass spectroscopy analysis namely ion trap, quadrupole and time of flight analysers [46]. These analysers can also be used in combination (depending on the application required), such as for triple, quadrupole and QTOF (quadrupole time of flight) analyses [46].

During tandem mass spectrometry, a combination of 2 mass analysers is used with a collision cell in between, the ions are fragmented in the collision cell and the detected fragments can be used as fingerprints for additional confidence in the identification of molecules (Figure 2.5; 2.7) [44]. The technique can also be used to increase the selectivity and sensitivity of quantitative LCMS/MS analysis by operating the instrument in multiple reaction monitoring mode whereby the first mass analyser is set at the *m/z* of the molecular ion or precursor ion of an analyte and the second mass analyser on a fragment or product ion after fragmentation in the collision cell.

2.3.4 Quadrupole analyser, and triple quadrupoles

2.3.4.1 The quadrupole analyser operation

The quadrupole consists of four rods. The four rods are metallic and are paired in sets of two. The one pair of rods is positively electrically charged, and the other pair of rods is negatively charged [47]. Voltages are applied in combination to each pair of rods, i.e., direct current (dc) and radio frequency (rf) voltages [47].

Each set of rod pairs acts as a mass filter. The positive pair of rods acts as a high mass filter and the negative rods as a low mass filter. The resolution of the quadrupole analyser is dependent on the dc value and rf value [47]. Hence the dc and rf value must remain constant because the quads are operated at a constant resolution. When the dc and rf voltages are set to a specific amplitude, only ions that resonate with this amplitude with a specific m/z ratio can pass through the quadrupole analyser with the correct trajectory and their speed will be detected [47]. All other ions will be deflected into the two pairs of rods [47].

V(t) = - Vdc - Vrf cost

V(t) = Vdc + Vrf cost.....**Equation 2.4**

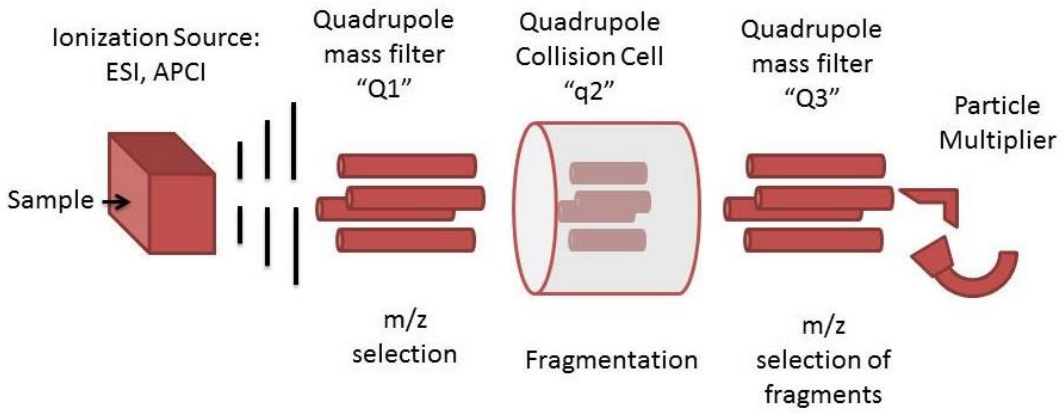

Figure 2.5: Triple quadrupole schematic diagram
(https://upload.wikimedia.org/wikipedia/en/d/d3/Triple_quadrupole_schematic.jpeg)

2.3.5 Liquid chromatographic-mass spectrometry (LCMS)

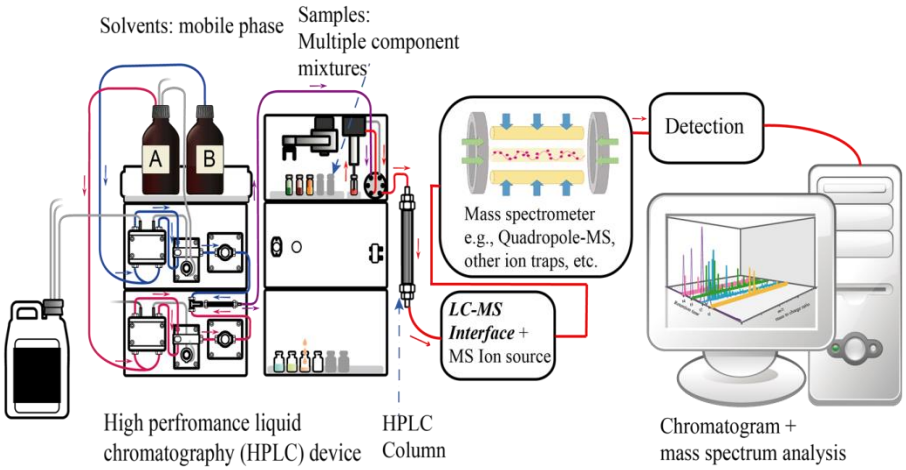

Figure 2.6: LCMS schematic diagram (https://www.slideshare.net/BijiSaro/hyphenated-techniques-154661655)

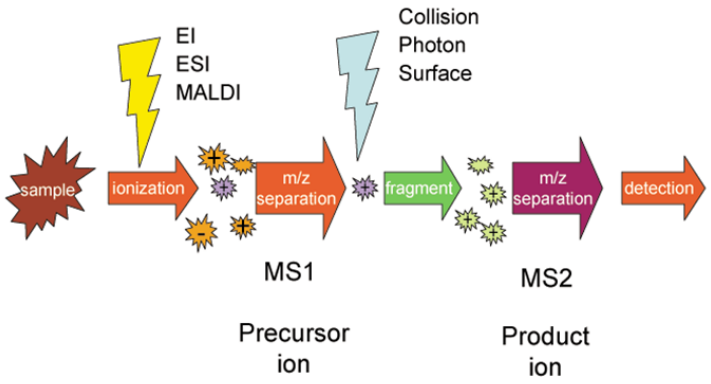

Figure 2.7: Tandem LCMS operation process flow diagram (https://en.wikipedia.org/wiki/Tandem_mass_spectrometry#/media/File:MS_MS.png)

The application of HPLC and mass spectroscopy combined have greatly benefited the pharmaceutical industry in terms of obtaining quantitative and structural information during the beginning stages of drug development compared to the traditional HPLC methods used in the pharmaceutical industry [48].

2.3.6 Liquid chromatographic-mass spectrometry (LCMS) interface

In the pharmaceutical industry, most pharmaceutical analyses favour an ionization technique that can ionize the drug molecule into a single ion that corresponds to the drug's molecular weight with minimal or no fragments of the parent drug compound [49, 50]. The quantification would have a high sensitivity and confirmation of the structure would be easily achieved. The selectivity of the analysis would be achieved by HPLC separation, i.e., separation of the drug component and matrix and MS/MS component, or structural clarification and drug quantification. It was of great importance for pharmaceutical researchers to get the best universal LCMS technique with minimal limitations [49, 50]. A simple procedure was required for the analysis of small and large molecules with a soft ionization technique. Researchers were keen on developing a high-performance method similar to LC/UV with minimal boundaries. The reasons for these requirements were needed more for an industrial perspective than for an analytical perspective, which forms the ultimate basis of acceptance [49, 50].

The applicability and performance of an LCMS interface that showed promise to the industry was due to the original work of Bruins and Fenn [49]. Applications varied from LCMS analysis of small drug molecules using atmospheric pressure chemical ionization (APCI), to the analysis of biomolecules and receptor-ligand interactions using electrospray ionization (ESI) [49]. These new applications increase the performance and broaden the application of LCMS in pharmaceutical analysis [49]. Figure 2.6 represents a schematic diagram of an LCMS instrument

2.3.7 Liquid chromatographic-mass spectrometry (LCMS) Growth

The use of the LCMS technique increased drastically in the pharmaceutical industry once its design was championed by the developers [49]. The growth of LCMS was shown by the number of journal articles published and presented at the conferences held by the American Society for Mass Spectroscopy (ASMS) over the past ten years. For example, in 1998 LCMS papers accounted for 30% of all papers presented and 15% of these consisted of papers on pharmaceutical LCMS applications delivered at the ASMS conference held in Orlando, Florida [49]. The LCMS interface development has led to many new initiatives in different fields of scientific disciplines, which was imperative for understanding, acquiring, and integrating the LCMS interface into the drug development cycle [49].

The impact of the LCMS interface on drug development was non-existent compared to all other techniques at the time. However, the advantages of the LCMS interface, such as fast sample generation, cost-effectiveness and efficiency helped to make the LCMS interface an easily justifiable approach to use [51]. The LCMS instrument became an analysis platform of high efficiency and

productivity in the drug development cycle because of its technological interface advancements and trace mixture high throughput capabilities [51]. Over the past 10 years, a variety of LCMS instruments has been successfully developed and used in the industry – instruments that have specialized features dedicated to specific types of analytes or sample analysis. These developments were made by modification of the MS interface such as using quadrupoles, triple quadrupoles, magnetic sector, time of flight, ion trap and many more analysers [49]. The perception that the MS-techniques were time-consuming, difficult to maintain, hard to operate and limited in application became a negative perception of the past. Further development and growth allowed for matrix-assisted laser desorption/ionization (MALDI) for parallel analysis techniques, as well as capillary electrophoresis and simpler, cheaper and effective instruments. LCMS instruments continue to grow in the drug development industry [49]. New development for increased throughput and efficiency continues, since even better levels and constraints, and new strategies for analysis are required [49].

2.4 Drug reactivity, Permeation and Ionization

2.4.1 Drug reactivity and drug-receptor bond

Drugs react with receptors via three major chemical forces and bonds. A covalent bond is the strongest type of bonding. An electrostatic bond is weaker than the former, while hydrophobic bonds are the weakest of the three types of bonds [51-54].

Covalent bonds are strong and are almost always irreversible bonds in biological interactions. In drug-receptor interaction, electrostatic forces are more common. There are many types of electrostatic forces, such as those between permanently-charged ionic molecules, to weak induced dipole interactions and weaker hydrogen bonds [52-54].

The most notable type of interaction in this context is hydrophobic interactions. These are even weaker than electrostatic and covalent interactions and are important in highly-lipid soluble drugs which can permeate through the lipid cell membrane [52-54].

2.4.2 Permeation of the drug in the body

Permeation is a key process for the drug movement and transfer within the body. There are three types of permeation: aqueous, lipid and special carriers [55]. In this study, aqueous diffusion and lipid diffusion play an important role. Aqueous diffusion occurs when the drug is in its ionized form. This allows the drug to permeate through aqueous parts of the body. Lipid diffusion of the drug takes place when the drug is in its non-ionized neutral form [55]. This is a limiting factor for drug permeation since lipid barriers separate aqueous compartments in the body. The pH has to be taken into consideration for weak acids or bases when permeation takes place between aqueous and lipid layers

[55]. The ratio of the lipid-soluble form to water-soluble form is expressed by the Henderson-Hasselbalch equation [52-55].

2.4.3 Ionization of weak acid and weak bases and the Henderson-Hasselbalch equation

When a molecule is ionized it has an electrostatic charge [56-58]. This electrostatic charge causes attraction of the water molecules or dipoles. The ionize molecules becomes polar which are soluble in hydrophilic solutions and are insoluble to non-polar solutions or lipophilic biomolecules [56-58]. For lipid diffusion to take place, the molecule must have high-lipid solubility. When a drug is ionized it reduces the ability of the drug to permeate through the lipid membrane [56-58]. A molecule with a weak acid or base is considered to be a neutral molecule that can be readily ionized and deionized back to its neutral form, hence weak acid and weak base dissociation is reversible, depending on the pH condition of the molecule [56-58]. This plays an important part in the water-soluble: lipid-soluble permeation coefficient. Therefore, a large fraction of drugs in use today are weak acids and/or bases [56-57].

$$\text{Log}\ \frac{\text{Protonated concentration}}{\text{Unprotonated concentration}} = \text{pKa} - \text{pH}$$

.....**Equation 2.5**

Equation 2.6 is the Henderson-Hasselbalch equation for pH and pKa determination [57]. An acid is a chemical substance that can dissociate into a proton and an ion, and is called a conjugate base. A base is a chemical substance that can accept a proton that forms conjugate acid and a base which is a positively charged cation [57-58].

The pH is a measure of the $[H^+]$ concentration in a solution, while pKa can be defined as the point in a solution when the molecule is in equilibrium in its ionized and unionized forms [58].

It is important to understand and study the pKa of acidic and basic drugs due to the body having different pHs in different compartments. It allows us to manipulate how the body will react to a drug [58]. Only unionized forms of the drug will permeate through cell lipid membranes. The ionized form of the drug is required for administration and distribution of the drug in the plasma due to the ionized form being more water soluble [58].

For acids: a high pKa means that the species is predominantly in its unionized form. It is a bad proton donor and a weak acid. A low pKa means that the species is predominantly in its ionized form, is a good proton donor, and is a strong acid [58-59].

- pH < pKa by 2 units, 99% of the compound is unionized.
- pH > pKa by 2 units, 99% of the compound is ionized.

For bases: A high pKa means that the species is predominantly ionized, is a good proton acceptor, and is a weak base. A low pKa means that the species is predominantly unionized, is a bad proton acceptor, and is a strong base [58-59].

- pH > pKa by 2 units, 99% of the compound is unionized.
- pH < pKa by 2 units, 99% of the compound is ionized.

This information is imperative in assisting chemists and medical researchers to understand and find the best route to administer the drug, as well as to develop methods to detect the drug using HPLC and LCMS. This information allows researchers to manipulate the drug form to permeate through different compartments in the body that have different pH values. The pH, pKa, and concentration of ionized and unionized forms of the drug values can be determined using the Henderson-Hasselbalch equation. This equation can also be manipulated for the use of acid or bases.

2.5 Fluorescence spectroscopy

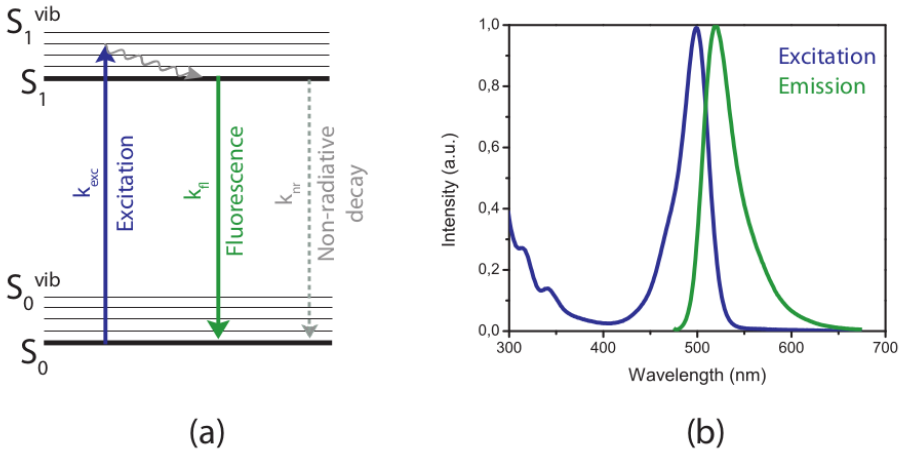

Figure 2.8: Fluorescence excitation process and data output [60]

Fluorescence is a phenomenon that occurs when a specific substance absorbs light and that substance causes an emission of the light absorbed [61]. The light emitted usually has a longer wavelength and lower frequency than the light absorbed [61]. Fluorescence is optimally observed when the electromagnetic radiation light absorbed is in the ultraviolet range of the electromagnetic spectrum. The absorbed light is not visible whereas the emitted light ranges in the visible region. This gives the

emitted fluorescence a distinct color which is only observed when the emitted light is exposed to ultraviolet light. As soon as the radiation source stops the glow produced from the fluorescent material stops [61]. Figure 2.8 illustrates the excitation process and emission spectrum.

2.5.1 Fluorescence Quenching

Quenching of fluorescence emission occurs when the initial emission of a substance is decreased due to the addition of another substance which causes an overall drop in the fluorescence emission [62]. In other words, a small molecule by binding to a protein or near the fluorophore of the protein can cause a great decrease in the quantum yield of the fluorescence. Quenching can occur via dynamic quenching or static quenching [62]. Dynamic quenching occurs whereby a small non-interactive molecule collides with a protein which deactivates the excited state of the fluorophore. Static quenching occurs when the small molecule forms a complex with the fluorophore so that it becomes non-fluorescent [62]. Quenching data were analysed according to the Stern-Volmer method using the following equation. In this study, fluorescence spectroscopy was used to validate that the drug present affects plasma by binding to the plasma [62].

2.6 Ultraviolet spectroscopy

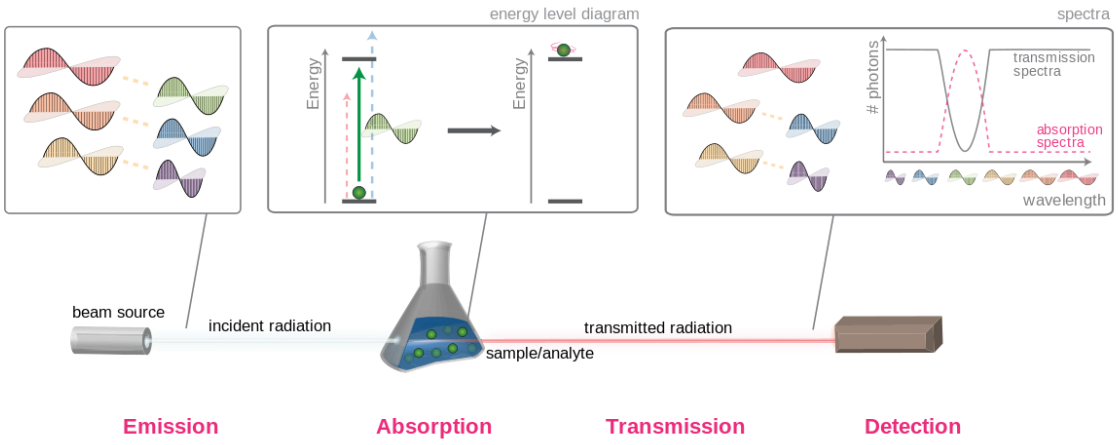

Figure 2.9: Ultraviolet spectroscopy data output and process (https://en.wikipedia.org/wiki/Absorption_spectroscopy)

When a molecule absorbs electromagnetic radiation the light that is absorbed by the molecule is known as the absorbance as indicated in figure 2.9. The absorbance of the molecule is indicated in terms of frequency or wavelength. Absorption spectroscopy is a technique that can be used throughout

the electromagnetic spectrum. When this technique is used in analytical chemistry, it is usually for qualitative analysis to identify if the substance is present as well as quantitative analysis to identify the amount of substance present [63].

Ultraviolet spectroscopy is a very useful and important analysis technique in analytical chemistry. As stated above for absorption spectroscopy UV spectroscopy's main use is for qualitative and quantitative analysis of organic and inorganic substances in a solution. Hence when light interacts with matter, the particles in the sample matter increases in energy, the light that passes through the sample then generates a signal which is amplified to produce a spectrum that is specific to the sample matter [64].

Ultraviolet absorption is stated to cause the ground state electrons to gain the energy required for excitation to occur, this results in excited electrons moving from the ground state to a higher energy state [63]. Hence for excitation of the electron to move to a higher energy state, the ultraviolet radiation absorbed has to resonate with the energy difference between the ground state and the higher energy state [63].

A UV spectrometer follows the principle proposed by the Beer-Lambert Law. Beer Lamberts Law states " whenever a beam of monochromatic light is passed through a solution with an absorbing substance, the decreasing rate of the radiation intensity along with the thickness of the absorbing solution is proportional to the concentration of the solution and the incident radiation."[65]

The law can be applied by the use of the following equation formula:

$$A = \log (I_0/I) = ECl \quad \textbf{Equation 2.6}$$

A is the absorbance, I_0 refers to the intensity of monochromatic light on a sample, I refers to the intensity of light transmitted light from the sample, C indicates the concentration of the sample and E refers to the molar absorptivity [65]

UV spectroscopy has many useful applications whereby functional groups can be detected as well as chromophores in complex mixtures, identification of unknown molecules using known reference material, assistance in geometric isomer configuration determinations as well as purity of substances. In this study, Fluorescence and UV spectroscopy will be used to determine the thermodynamic properties of the TB drugs when bound or interacting with plasma [65].

2.7 Pharmacokinetics

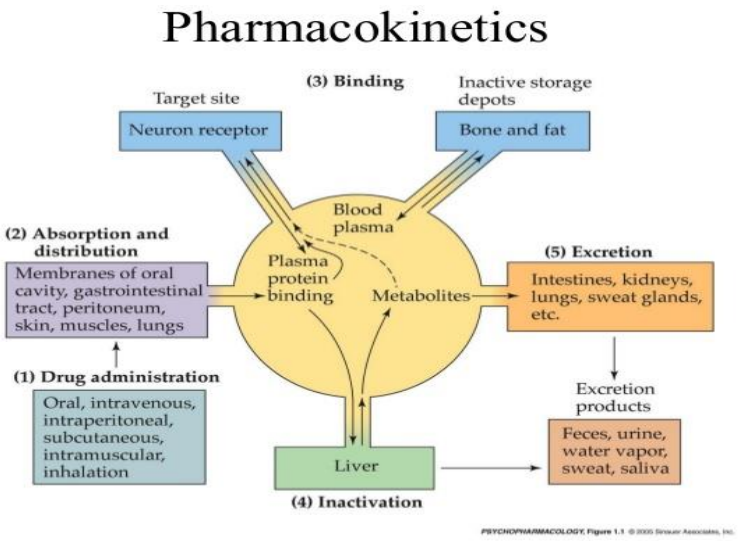

Figure 2.10: Pharmacokinetics process (https://www.slideshare.net/prabhakarchl/pharmacokinetics-31470891)

Researchers in pharmacology look into many studies of drugs such as drugs used to treat diseases, as well as the overuse of drugs, and drug abuse [52]. Since drugs affect different organs and parts of the body, studies are undertaken on almost every area of biomedicine by pharmacological researchers [52].

Pharmacokinetics describes quantitatively the movement of drugs and foreign substances through the body [52]. Figure 2.10 illustrates the pharmacokinetic process. Parameters such as the volume of distribution, bioavailability and distinct clearance are used to indicate the rate and extent of drug absorption in the bloodstream, the movement of the drug administered out of the blood and into the tissue, and the rate of the drug passing out of the body [52]. These parameters can be used to predict the concentration of the drug at any administered dose within the blood. Drugs are processed by the body in four stages, i.e., absorption, distribution, metabolism and excretion (ADME) [52].

2.8 Clinical Trials

Clinical trials are very important in medicine and drug development. A clinical trial is a study undertaken to test if a certain treatment developed or drug developed can solve a problem by testing the developed drug on human volunteers [66-67]. If the clinical trial gets approved, the treatment can be used by the mass population. A treatment could be achieved in many ways e.g., blood products, vaccines, medical devices, biological or gene therapy, etc. The treatment must, however, first be tested on animals to determine toxicity levels and safety of the treatment before tested in humans [66-67].

The Food and Drug Administration is committed to the safety and protection of the participants taking part in the clinical trials. Hence, the FDA strictly regulates and creates guidelines for the clinicians to avoid risks and danger to participants involved [66-68].

Each clinical trial has a protocol. This protocol provides an outline of the participants that are eligible to take part in the trial, the types of tests and procedures used, the drugs and dosages used, the check-ups on participants, as well as the duration and size of the study [66-67].

2.8.1 Four phases in clinical trials:

Phase 1: Consists of a small number of participants, 6-10 healthy volunteers or sick patients. Phase 1 involves information gathering of the effect of the compounds in the human participant. This helps to understand what effect the compound has on the body when swallowed, injected or infused from a safe and acceptable view [66-67].

Phase 2: Takes place when the safety of the drug is confirmed in phase 1. Phase 2 trials are performed on a larger group of participants (about 20-300). Phase 2 is designed to test the efficiency and safety of the treatment. The participants are given various dosages of the treatment and are closely monitored [66-67].

Phase 3: Carried out on participant groups of 300-3000. Phase 3 is carried out to confirm the benefits and treatment safety on a large scale. This information will help to indicate how best to prescribe the treatment to patients [66-67].

Phase 4: Takes place when regulatory approval has been given to the specific treatment. The treatment is then designed safely to have broader efficiency and tested among a larger number of participants. Further research is undertaken to combine developed treatment with existing treatments. These combinatory studies aid in determining the long-term effect of the treatment on the patient.

By implementing these four phases, risk factors and safety issues can be prevented [66-67].

2.9 TUBERCULOSIS (TB)

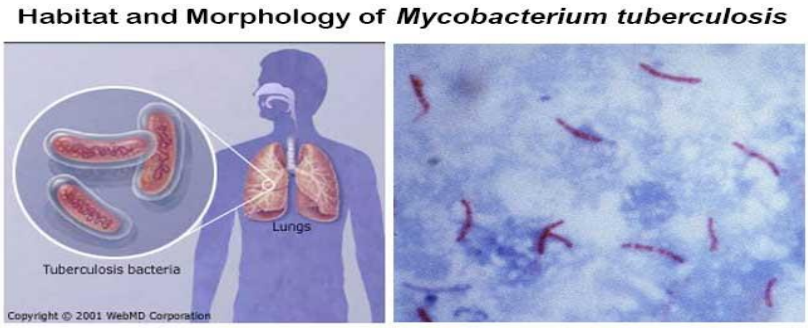

Figure 2.11: Mycobacterium tuberculosis (https://microbenotes.com/habitat-and-morphology-of-mycobacterium-tuberculosis/)

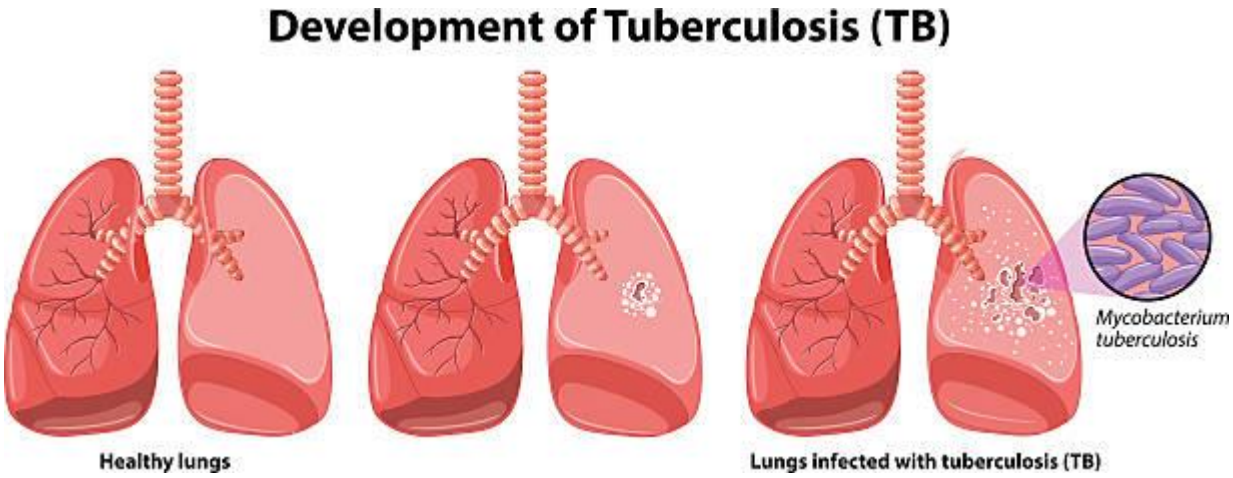

Figure 2.12: Mycobacterium tuberculosis development in the lungs (https://www.vecteezy.com/vector-art/432039-chart-showing-development-of-tuberculosis)

Tuberculosis (TB) is highly contagious and spreads through the air from coughing. TB is caused by a bacterium known as Mycobacterium tuberculosis (*M.tb*), which is rod-shaped in structure as indicated in figure 2.11 [68]. It is the most common cause of death by infectious disease worldwide. The most commonly infected site for TB is known as the pulmonary tract indicate in figure 2.12 [69].

Many types of TB strains exist. However, there are two main forms of TB known as active TB and latent TB [70]. Active TB occurs when the disease causes the production of symptoms in the body that can be transmitted to other living organisms or people, whereas latent TB occurs when the host is infected with the disease but the bacteria cannot produce symptoms in the host due to the immune system of the host causing inhibition of bacterial growth and spreading [69-70]. If the immune system of the host fails, the bacteria will no longer be suppressed. This then results in active TB and the host becomes contagious to others [69-70].

2.9.1 Cell structure and metabolism of TB

Mycobacterium tuberculosis (*M.tb*) has a slow growth rate characteristic due to the tough cell of the bacteria. The cell wall of *M.tb* prevents nutrients from passing in and out [70]. It resembles that of a gram-positive cell wall [69, 72] and consists of a polypeptide layer, peptidoglycan layer, and free lipids. The cell wall contains mycolic acids, which are a complex structure of fatty acids with a glossy appearance [69]. There are three classes of mycolic acids in the TB cell wall i.e., alpha, keto, and methoxymycolates [69, 72]. The TB cell also contains lipid complexes such as the free lipids, acyl glycolipids and sulphanoids. Porins are present in the membrane to facilitate transport. Under the TB cell wall, layers of arabinogalactan and polypeptidoglycan are suspended above the plasma membrane [69, 71, 72].

M.tb transcriptional regulators have learned to adapt to stressful environmental conditions within the host to survive for a longer period [72]. Stressful environmental conditions such as heat, extreme cold conditions, starvation of iron, and oxidation distress are counteracted by the transcriptional regulators of the bacteria by either allowing or inhibiting transcription [73]. The genome of *M.tb* produces approximately 190 transcriptional regulators [71-73].

2.9.2 Treatment of TB

M.tb is a disease that can be cured by using several specific antibiotics prescribed. The treatment consists of a multiple drugs that have to be taken over a period of six (6) months and can even be extended to a year (12 months) [74]. The problem faced is that many Myco tuberculosis strains are resistant to one or more antibiotic TB drugs. This causes major treatment constraints.

The FDA approved ten drugs at this current stage for the treatment of Tuberculosis. Four of the ten drugs are used in first-line anti-tuberculosis treatment. The four drugs are isoniazid (INH), rifampicin (RIF), ethambutol (ETH), and pyrazinamide (PYR). These four drugs form the foundation of the initial stages of TB treatment [74-75].

When TB becomes drug-resistant, major problems arise. MDR-TB (multidrug-resistant TB) is defined as TB that is resistant to at least the two most powerful first-line anti-TB drugs (isoniazid and rifampicin). MDR-TB is very resistant to drugs and the resistance can be intensified when inconsistent or incomplete treatment takes place, e.g., if the TB patient starts feeling well and stops the treatment prescribed, resistant TB bacteria can arise [74]. Drug-resistant TB can be treated. However, the treatment is much longer (about two years) and the patient would need chemotherapy treatment using second-line anti-TB drugs [76]. The second line anti-TB drugs produce more side effects and are much more strenuous when compared to the first-line anti-TB drugs mentioned above [75]. The

second line anti-TB drugs consist of six classes, namely aminoglycosides, fluoroquinolones, polypeptides, thioamides, cycloserine and p-aminosalicylic acid [75].

Over the last few years TB disease has developed into a new form known as exclusively drug-resistant TB (XDR-TB). This strain TB progresses faster than the normal as well as MDR-TB[76]. XDR-TB could lead to fatality within a couple of months or even weeks. XDR-TB is defined by its resistance to INH, Rif, any one member of the fluoroquinolone class, and at least one polypeptide or an aminoglycoside. It was also discovered that XDR-TB is often found in patients that are infected with HIV [75]. This could make it difficult to control this strain of TB [74].

2.10 First line anti-TB drugs

2.10.1 Isoniazid (INH)

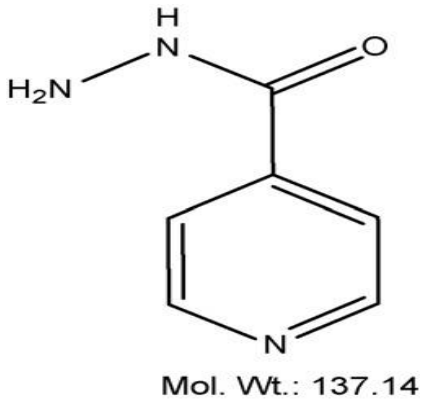

Figure 2.13: Isoniazid molecular structure (https://en.wikipedia.org/wiki/Isoniazid)

As a dangerous microbial disease that requires a long treatment period, TB causes much ill health and death for millions of people every year [70]. The World Health Organization (WHO) has proposed standard counteracting measures to treat the disease. This treatment includes a six-month course of first-line anti-TB drugs: isoniazid (INH), rifampicin (RIF), ethambutol (ETH), and pyrazinamide (PYR), which is also abbreviated as the RIF-4 drugs [75].

Due to the resistance of the TB disease MDR-TB and XDR-TB, many lives are still being claimed by this rapid growth bacterial disease even though strong drugs are available [78]. Isoniazid (INH) (figure 2.13) is one of the TB drugs that have been researched extensively. INH has a molecular weight of 137.14 g/mol and is a pro-drug which activates when oxidation takes place of NADH to form an adduct NAD+. This inhibits the NADP dependent targets such as the enol-acyl carrier protein reductase (INHa) of the Mtb [77]. The disadvantage of INH is its failure to counteract MDR-TB. This has been noticed especially among HIV patients [77]. Recent studies have indicated that lipophilic modification of the INH drug structure could result in an increased permeation of INH through the

bacterium cell wall. Hence due to the hydrazide group, INH can easily be functionalized with carbonyl compounds [77]. Another study specifies that INH reacted with pyrazole molecules indicates good anti-TB activity. Inhibitory action of INH hydrazone analogues may improve by the introduction of pyrazole units [77].

2.10.2 Rifampicin

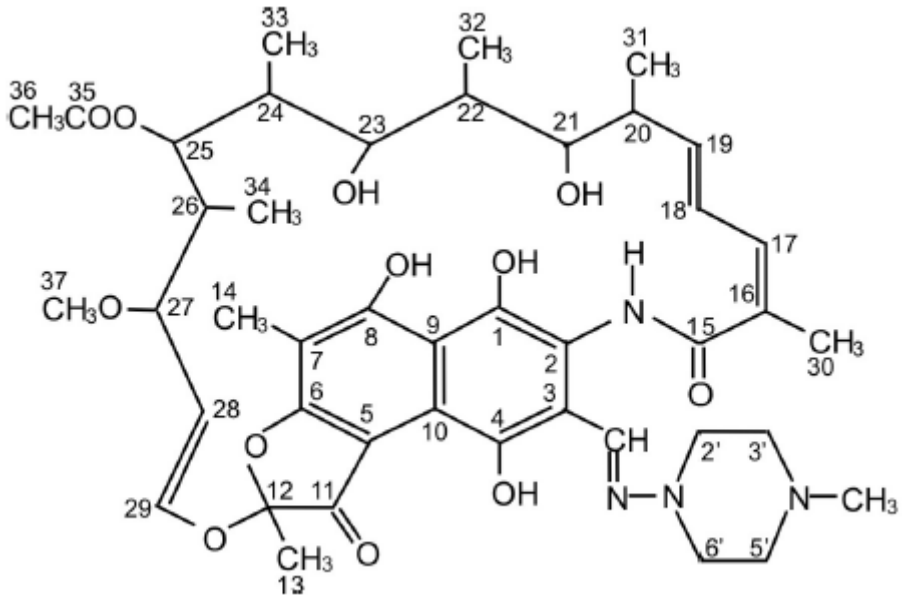

Figure 2.14: Rifampicin Molecular structure (https://en.wikipedia.org/wiki/Rifampicin)

Rifampicin (RIF) is a strong lipophilic liver enzyme inductor and a backbone first-line drug used in the treatment of TB. Figure 2.14 indicates the molecular structure of rifampicin. It has a molecular weight of 822.92g/mol. RIF's mechanism of action takes place via an inhibiting process[79]. It causes inhibition of a gene known as rpoB, which is a B-subunit of DNA-dependent RNA polymerase activity, which occurs during early transcription stages [79]. It is assumed that RIF physically blocks the RNA sequencing process once two to three nucleotides have been added by a binding interaction with a B-subunit occurring close to the RNA/DNA channel [79].

In previous studies, RIF has been used widely by individual's by healthy volunteers and also in TB patients [94]. Most patients respond to the normal dosage treatment of the TB drugs. However, the use of low drug concentrations is usually the result of treatment failure or bacteria resistance, which results in poor clinical outcomes [80].

25-Desacetyl rifampicin (D-RIF) has been identified as the main active metabolite of rifampicin, which is also responsible for the clinical efficiency of the treatment [81]. It has been observed from previous studies that RIF is responsible for stimulating the metabolism of INH and other drugs, as well as inducing its metabolism [82].

Most patients who are affected by renal or hepatic failure should be given reduced drug dosages due to toxicity or given increased dosages of RIF to alleviate under-dosing due to its enzyme-inducing effects. According to a study, due to their large lipophilic binding sites CYP isozymes (especially CYP3A) are induced by RIF.

Another study describes RIF as a strong inductor of the CYP2E1 enzyme [83]. As a result, if INH is co-administered with RIF, it would increase the metabolism of INH to form reactive INH metabolites. This could lead to an increase in hepatic toxicity, which is unfavourable [83].

The identity of the RIF's compound has been determined as using many techniques such as HPLC, LCMS, LCMS/MS, HPTLC, UPLC solid-phase extraction, and LCTOF/MS. The following *m/z* ions have been confirmed for RIF and its metabolite D-RIF respectively, producing a molecular ion of 823 and 781 and base peaks *m/z* 791 and 749 [81].

Multiple drug therapy is often used on an individual patient. In patients diagnosed with multiple illnesses such as HIV and TB, the patient will require a combination of antiretroviral and TB drugs [82-83]. The use of a combination of different drugs could result in drug-drug interactions [82-83]. Drug-drug interactions occur when the presence of one drug affects the bioavailability of another drug in terms of absorption, metabolism, and distribution. This interaction could affect the treatment and toxicity of the drug within the patient, and could lead to adverse effects which can be life-threatening for the patient. These adverse effects can be eliminated or alleviated by rationing the periods of the drugs administered. For the use of the correct dosage adjustment required by the patients, it is important to understand the drug-drug interactions of the drug [84, 85].

The common systemic drug delivery systems used for most administration of drugs occur via a micro-particle delivery system. These micro delivery systems have been researched extensively for achieving targeted site-specificity of the TB infection site to alleviate or reduce its toxic effects. The *M.tb* disease is commonly active in the alveolar macrophage: hence, drug formulations are designed to target these growth sites. For rifampicin to induce its therapeutic effect, it is required that rifampicin penetrates the infected cell wall, where the phagocytized trapped *M.tb* resides within the host cell. For pulmonary TB the most effective drug delivery system used is delivering the drug directly to the active site via an aerosol. The use of this direct delivery system could bypass the first metabolism process, whereby the localized therapeutic effective concentration is maintained and followed by reduced side systemic effects of the drug.

Another study has indicated that rifampicin is sensitive to pH [86]. Therefore, when the RIF drug is in unfavourable conditions, it undergoes degradation. An analysis of the drug and determining drug metabolite formation shows that degradation of the drug causes a hindrance in achieving accurate biotransformation of the drug to metabolites [86]. Ascorbic acid has shown favourable preservation

effect on the rifampicin drug stability in plasma as well as increased the stability of the drug in plasma for 12 hours at room temperature [86]. Hence, the increased stability of the drug will also result in increased bioavailability of the drug [86]. When analysing samples via LCMS analytical techniques, this is an important finding to allow for an increase in accuracy and efficiency of the analyses.

2.10.3 Ethambutol

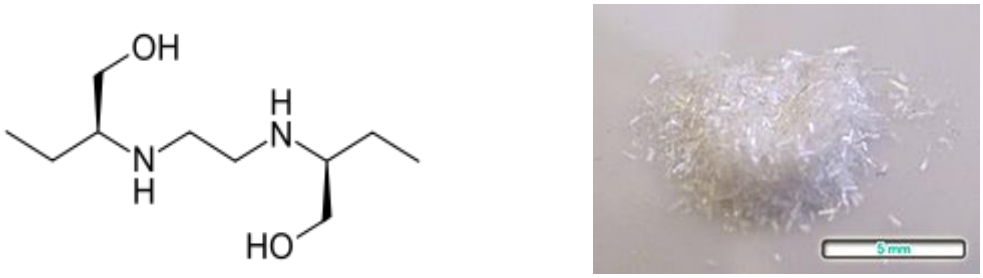

Figure 2.15: Ethambutol molecular and physical structure (https://en.wikipedia.org/wiki/Ethambutol)

Ethambutol (ETH) is a drug used as a combinatorial drug treatment for Tuberculosis. ETH has a molecular weight of 204.31 g/mol [87].The molecular and physical structure is given in figure 2.15. ETH is usually given in combination with INH, RIF, and PYR. It is taken orally. The method of ETH delivery is believed to interfere with the metabolism of the bacteria [87].

ETH obstructs the formation of the wall of the cell of actively growing tuberculosis bacilli. Mycolic acids bind to the 5-hydroxyl groups of the D-arabinose, which is a residue of arabinogalactan [88]. This forms the mycolyl-arabinogalactan-peptidoglycan complex in the cell wall. ETH works by affecting the synthesis of arabinogalactan, by inhibiting the arabinosyl transferase enzyme [88]. This inhibition causes the disruption of the synthesis of arabinogalactan, which increases the permeability of the cell wall [88].

ETH is best administered orally and is absorbed from the gastrointestinal tract. The drug is distributed in the body tissue and fluids very well. When excreted, 50% of ethambutol is unchanged. ETH should be kept out of light and away from moisture at room temperature [88].

ETH is metabolized to an aldehyde intermediate followed by conversion to a dicarboxylic acid. It was observed that no significant drug-drug interactions were observed in animals [89]. Human drug-drug interactions have been observed, namely that ethambutol interacts with antiacids. It is recommended to avoid concurrent administration of aluminium hydroxide containing antacids for at least 4 hours before administering ethambutol [89]. It was reported that a decrease in renal excretion of ETH occurs when administered together with rifampicin [90]. Adverse effects of ETH can lead to reversible blindness or irreversible blindness, which is a major risk for patients.

2.10.4 Pyrazinamide

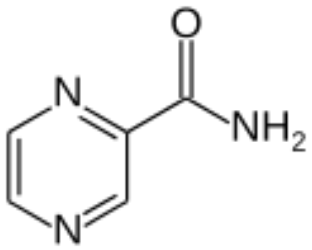

Figure 2.16: Pyrazinamide molecular structure (https://en.wikipedia.org/wiki/Pyrazinamide)

Pyrazinamide (PYR) is a drug used in combination to treat tuberculosis. It is one of the first-line anti-tuberculosis drugs used to treat active TB [91]. PYR has a molecular formula of 123.113 g/mol and it falls under the anti-mycobacterial medication class. The molecular structure is given in figure 2.16. PYR is taken orally and is typically used in combination with INH, RIF, and ethambutol. The mechanism of PYR is not entirely clear as yet Mycobacterium Bovis and Mycobacterium Leprae are resistant to PYR, and hence it cannot be used to treat these TB bacteria [91].

The pharmacokinetics of PYR is based on the drug crossing the meninges that are inflamed [91]. PYR is an important part of the treatment of tuberculosis meningitis [91]. The liver metabolizes the drug and the metabolites produced are excreted by the kidneys.

It has been confirmed by the WHO that PYR is safe when used during pregnancy. PYR works as a pro-drug which inhibits the growth of *M.tb*.

2.10.4.1 How pyrazinamide works

When ingested, the PYR drug passes into the granuloma of *M.tb*. The drug is then converted into pyrazinoic acid by the tuberculosis enzyme pyrazinamidase. The pyrazinoic acid pH conditions range between pH of 5 to 6 and slowly coverts into the conjugated protonated acid which exits from the mycobacterium cell via passive diffusion and an efflux mechanism [92]. This protonated conjugated acid then passes easily back into the bacilli and accumulates. This has a net effect of more pyrazinoic acid inside the bacilli at acidic conditions than at neutral pH conditions [92].

The accumulation of pyrazinoic acid was suggested to interfere with energy production and the membrane potential of the bacteria. Since membrane potential and energy production is a key requirement for the Mtb survival in an acidic infection site, it was though that pyrazinamide caused inhibition to this process. This suggestion of the mechanism was however discounted. This was because of the acid environment not being favourable for pyrazinamide and treatment does not lead to membrane disruption and intrabacterial acidification [92].

The ability of pyrazinamide to kill dormant mycobacteria could be due to the pyrazinoic acid produced and having the ability to bind with the ribosomal protein RpsA that inhibits trans-translation [92].

M.tb mutation occurs via gene mutation where the pcnA gene encodes a pyrazinamidase that causes the transformation of PYR to an active acidic form (pyrazinoic acid). The pcnA gene mutation is responsible for the resistance of PYR in *M.tb* [92]. Furthermore, resistance of PYR has been identified where mutation in the rspA gene in the pyrazinamidase resistive strain occurs. However, a direct link of this type of resistance has not been proven and has recently been disregarded in studies[92].

In 1936 the discovery of PYR took place. PYR was only used in the early 1950s for the treatment of TB [93]. During in vitro processes, the therapeutic effect of PYR was unable to be identified because of the neutral pH environment used. However, in in vivo studies of the drug showed therapeutic effect due to the diverse pH ranges within the body [94]. The discovery of PYR's ability to aid in counteracting the TB bacterium was due to the favourable effect of nicotinamide against TB. From this finding, it was deduced that PYR should have a similar effect [94]. Studies were then undertaken on rodents. This confirmed the PYR activity via elimination of the TB bacterium, and thereafter it became a first-line anti-TB drug in humans [92]. The addition of PYR to the treatment of TB reduced the treatment period from nine to six months. The relapse rates of patients after recovery has also shown a major reduction since the addition of PYR to the TB treatment. The major side effect of the pyrazinamide occurs in the liver via a hepatic reaction which causes hepatotoxicity. The reason for the hepatotoxicity has been indicated to be related to the dosage. These side effects include disturbances in the gastrointestinal tract. The use of PYR is not recommended to patients with severe liver damage or gout – which is a major drawback for the TB treatment process for these patients mentioned [95].

2.11 Blood

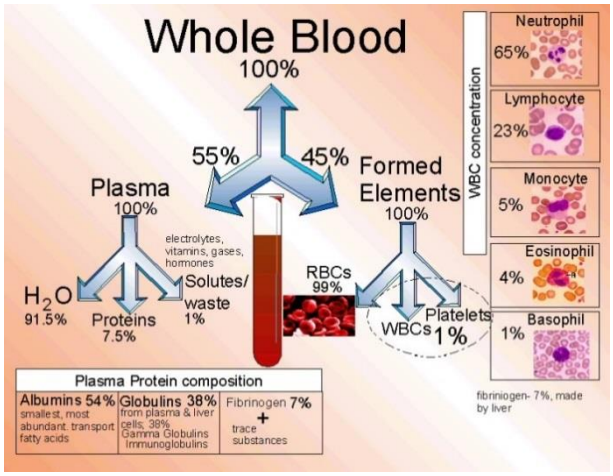

Figure 2.17: The composition of whole blood and its components (https://pantip.com/topic/32055838)

Blood is a very important tissue in the body and the only fluid type of tissue. Blood is a connective tissue comprised of living cells known as blood cells transported by plasma, which is a non-living fluid matrix. Blood is composed of both liquid and cell components [96]. When blood spins in a test tube via a centrifugal process, the whole blood separates into 3 components which consist of many other components as indicated in figure 2.17 above. The component with the lower density moves to the top of the test tube which is known as plasma and the heavier component moves to the bottom of the test tube. This separation occurs due to the centrifugal force. The red component at the bottom of the test tube, when separated, is mostly erythrocytes [96]. These erythrocytes function to transport oxygen through the body. In between the plasma and erythrocytes layer is a buffer coat layer [96]. The buffer coat layer contains white blood cells, which is also referred to as leucocytes. These leucocytes protect the body in many ways. Plasma, erythrocytes, and leucocytes make up 55%, about 45%, and less than 1% respectively of whole blood [96].

2.12 Plasma

Plasma is the clear, light yellow liquid component of blood present when all other components of blood are removed via a centrifugal process [96-97]. The components removed are platelets, red and white blood cells, and many other cellular components present within whole blood [96-97]. Plasma is the largest portion of human blood which occupies about 55% of whole human blood. Plasma is the transport system for cells and other substances important to the body [97]. Plasma is made up of about 93% of water, it also contains salts, enzymes and various proteins [97]. The liver is the organ responsible for most of the plasma protein production. It carries important functions in the body such

as the clotting blood, unbound drug transport within the body and fighting off diseases. One of the major proteins that contribute to 60% of protein present in plasma is known as albumin. The functions of these proteins are to move molecules through the circulatory system, which acts as a blood buffer system and contributes to the osmotic pressure of plasma [97]. The makeup of plasma varies continuously as cells remove or add substances to the blood. However, assuming a healthy diet, plasma composition is kept relatively constant by various homeostatic mechanisms [97]. When the protein levels in blood decrease the protein levels are replenished by the liver. When the blood starts to become too acidic (acidosis), both the respiratory system and the kidneys are called into action to restore plasma's normal, slightly alkaline pH. Body organs make dozens of adjustments, day in and day out, to maintain the many plasma solutes at life-sustaining levels [98]. However, it is important when conducting clinical trials, not to assume that the plasma composition is constant because the health status of most patients varies which could hinder the function of the body to keep the plasma levels constant [98]. According to research, experiments have shown that diet can affect protein levels in the blood. It is stated that a low-calorie diet leads to a slight increase in serum protein and a drop in plasma protein, hence the total circulating proteins diminish [98]. It was proposed that this occurrence was due to low fluid intake. Another study was conducted on patients diagnosed with cirrhosis which resulted in low plasma protein levels [98]. The defective formation of plasma protein is a result of hypoproteinemia which could be due to loss of optimal function in the liver. In this study, source plasma was used which is obtained from human volunteers.

2.13 Computational Pharmacology Modelling

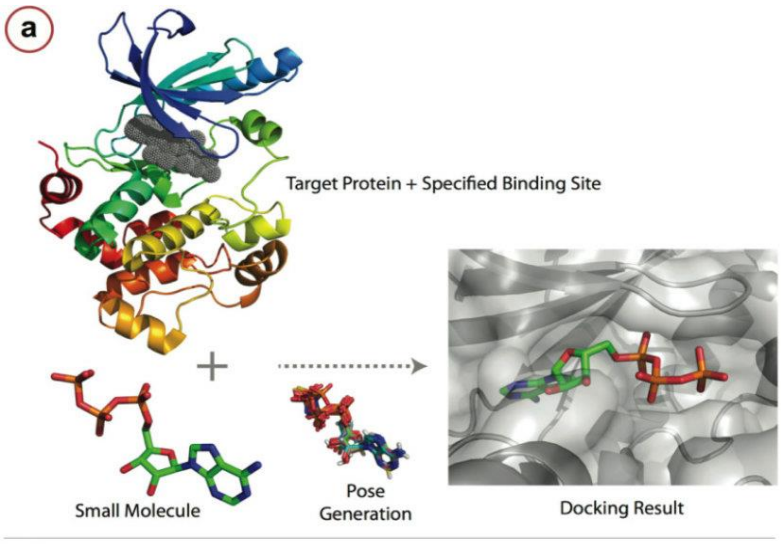

Figure 2.18: Computational modeling structure illustrating the protein, molecule and surface topology of the molecule bound to the protein pocket (https://phys.org/news/2011-05-3d-proteins-big-picture.html)

Computational pharmacology is a technique that has been recently developed. It is a technique that is based on theoretical pharmacological aspects and modelling of many molecules [99]. It is aimed towards rationalizing the relationship between the drug activities when observed experimentally and its structural features derived from computational chemistry and molecular mechanics. The main use of this technique is to provide valuable, efficient, accurate and cost-effective alternative methods for drug study and development [99]. Computational pharmacology is used to determine the possible binding action of molecules within the protein pockets of a specific protein as indicated in figure 2.18. The protein macromolecule is usually obtained from a protein data bank [100]. This protein data bank has already modelled the protein structure to the atomic scale [99]. The molecules that bind to the protein pockets are required to be modelled by the use of a computation pharmacology operating system. The modelled molecules are then docked to the protein pocket according to the most possible binding interaction of the molecule and the protein[100]. The operating system is also responsible for the prediction of the possible interaction between the molecule and the protein pocket site. This interaction can be illustrated in 3d and 2D [100]. The 2D interaction generated indicates specifically how the molecule binds to the pocket of the protein as well as the interaction or binding of the molecule to the amino acid. The 3D surface topography can be illustrated in different modelling imagery such as ribbons, cartoon, or surface topology imagery and many more [99]. When docking the molecule to the protein the process undergoes a search of different positions and conformations within the protein pockets available which generates scores to calculate the binding affinity of the molecule to a specific side chain [99, 101]. The search program is an algorithm that proposes the degree of freedom of the protein-molecule interaction complex. Hence it can be used to rank binding interactions of different molecules and the thermodynamic interactions between the molecule and the protein predicted from these scores [101-102].

2.14 Human Serum Albumin (HSA)

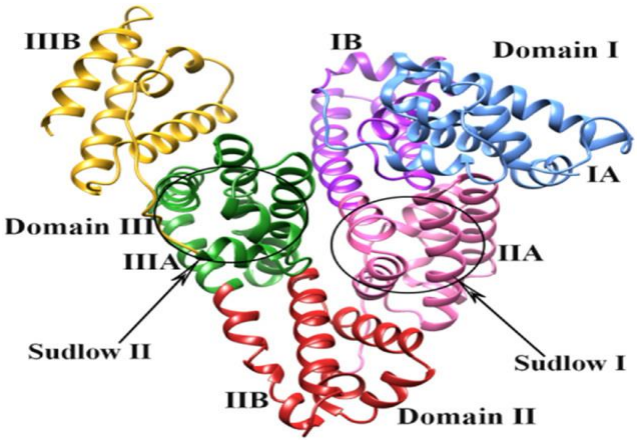

Figure 2.19: Molecular model of HSA protein with possible binding sites [103]

HSA is a major protein component of plasma responsible for the transportation and storage and disposition of compounds or ligands in the blood [104-105]. HSA has a heart conformation 3D geometrical shape consisting of 585 amino acid residues in a single polypeptide chain (shown in figure 2.20) [106-107]. HSA has three domains, connected via 17 disulfide bridges, which can be divided into subunits (I, II and III) and represent similar alpha-helical shapes [108]. Each of the three HSA domains can be further separated into sub-domains A and B [109]. Two principle ligand binding sites within the HSA protein can be found in subdomains IIA and IIIA known as Sudlow's sites I and II respectively. Furthermore, a binding site was identified in subdomain IB [110]. The basic residues (Lys195, Lys199, Arg218 and Arg222) surround the opening of site 1 however the bottom of the site is hydrophobic. An important residue tryptophan 214 often for structural analysis is also present at site 1. Site II is much smaller in size comparatively and accommodates the binding of hydrophobic drugs due to the predominant hydrophobic residues present [110-113]. A study conducted by Ping Li according to the free drug theory states that in an in-vivo system the drug interchanges from protein-bound to unbound states through reversible rapid equilibrium processes [114]. When the drug is distributed to the circulatory bloodstream only the free unbound drug can permeate through the tissue to the active or target site, which produces its effect and after some time reaches its half-life. In studies conducted through in-vitro plasma-protein binding studies, the data is often used to understand and replicate the in-vivo phenomena. This practice provides information in clinical and medicinal sciences which aids in optimizing patient selection in trials. The problem faced with this practice is that the binding kinetics which occurs in living systems is neglected. These kinetic binding effects have great influences on the pharmacokinetic and pharmacodynamics. Thus the insight to the interaction between First-line anti-TB drugs and HSA becomes important [114-115].

2.15 Previous Studies conducted with the use of Blood plasma

According to a study conducted on rifampicin concentrations analysed from arterial plasma vs venous plasma of baboons, the venous blood samples of patients' are used for therapeutic drug monitoring of rifampicin and PK studies. An HPLC-UV method for determination of rifampicin concentration in plasma and the internal standard rifapentine was validated to compare venous and arterial plasma kinetic of baboons after a single dose of rifampicin. Studies suggest that the arterial plasma is more suitable to estimate concentrations of rifampicin at the blood tissue interface. Results of the pharmacokinetic (PK) study indicated that the Arterial Cmax was 2.1 fold higher than venous Cmax. From 0-120 min the area under the PK concentration curve was 80% higher in arterial plasma indicating that Rifampicin venous concentrations, usually measured during conventional PK studies, do not reflect the proper concentration and subsequent tissue exposure in the distribution phase [116].

A clinical study was performed to assess the protein binding of first-line anti-TB drugs to blood plasma [117]. Results indicated that 88% of rifampicin, 14% of isoniazid, 1% of pyrazinamide and 12% of ethambutol drug concentrations were bound to the plasma proteins. Rifampicin plasma concentration positively correlated with its protein binding, whereas isoniazid correlated negatively. Pyrazinamide and ethambutol did not indicate plasma protein binding correlation [117].

A study conducted by Gurevich on the effect of blood protein concentration on drug dosing regimens indicated that terminally ill patients are prone to develop hypoalbuminemia with statistics as high as 40-50% [118]. Hypoalbuminemia occurs when albumin levels in the blood are very low. The blood protein plays a significant role in antibacterial drug dose regimes for these types of patients. Blood proteins also affect the penetration of drug within the tissue. A change in blood protein binding affinity and conjugation can affect antiviral activity. The change in protein binding with drugs affects the bound and unbound concentrations. This fluctuation affects the efficacy of the drug dose regime. Therefore due to hypoalbuminemia changes in free drug concentration can occur which can significantly affect therapeutic effect and cause adverse side effects [118].

An investigation of the binding affinity of RIF to human plasma was conducted via an equilibrium dialysis method [119]. Results indicated that 87-91% of RIF was bound to eleven healthy patient's plasma samples. A binding test was further conducted on ten patients' plasma samples on long term treatment and showed lower binding of rifampicin to the plasma with a percentage of 84-88% [119].

A study conducted states that plasma protein binding determination has an important impact on clinical doses, PK and PD relationships because the free drug is responsible for the pharmacological activity.[120]

2.16 Analytical methods used for detection of TB drugs in blood plasma

Over the years several methods had been developed and validated for the detection of anti-TB drug concentration in blood plasma [121-125]. These developed methods for detection of TB drugs are considered to be a valuable tool for used in therapeutic drug monitoring studies for dose optimization to minimize risk of therapeutic failure and TB drug resistance [121]. Theraputic drug monitoring is also important because of its aid in reducing adverse effects and hepatotoxicity which has been reported in 13-36% of patients [121].

According to a study conducted by Zhifeng Zhou, several HPLC methods have been developed and validated for use in the pharmaceutical industry with effective anlayte elution times [122]. However these methods are limited to analyse only one or two drugs in plasma due to the complexity of plasma. Another limitation to this method was derivertization of the analyte [122].

A study was conducted for therapeutic drug monitoring of TB patient using an Ultra-performance liquid chromatrography tandam mass spectroscopy method for simultaneous detection of nine second-line anti TB drugs in blood concentration [123]. The method was successfully validated and used to monitor 85 patient serum samples. The limitation to the study is that the method was only validated with spiked serum and was not compared to standards without spiked serum. Therefore when monitoring sick patients, if the patient had abnormal serum protein levels concentration results could cause outliers or when extrapolating from the calibration curves.

A rapid LCMS/MS detection method was developed and validated for detection of rifampicin in human plasma and cerebrospinal fluid [124]. The drug and internal standard were isolated from plasma using simple organic solvent to deproteination the samples followed by centrifugation. Detection of the drug was carried out using electrospray positive ionization. The method was successfully validated to study the plasma over a period of 25 hours after a 10 mg/Kg dosage of rifampicin. An observation made in the study was that heat-inactivation significantly affects the size of the rifampicin signal. There it was recommended to avoid heat inactivation where possible. The developed method had a high recovery of 90% and rapid detection of 6 minutes.

A pharmacokinetic study conducted for the detection of pyrazinamide, ethambutol, protionamide andclofazimine in dog plasma was performed using an LCMS/MS coupled with 96-well format plate [125]. The plasma samples were diluted with methanol on the 96-well plate and further diluted to reduce matrix effects. The method was robust and efficient. The validated method was compared with published analytical methods and proved to be advantages for sensitivity, sample time and sample volume.

2.17 Analytical Methods to measure blood plasma protein content

Plasma protein plays an important role in in therapeutic drug monitoring bioanalytical method. When a drug is administered to a patient, only the unbound drug fraction is available to produce its intended effect at the active site. By including the plasma protein as a variable in bioanalytical validation methods, the accuracy of therapeutic monitoring concentration results are increase. However every patient is different. Patient with blood disorders such as hypoalbuminea will have a deficit in albumin in the blood levels [126], therefore when the patient is administered a drug regimen and the drug concentration level in the patients blood is monitored using LCMS concentration calibration curves calibrated using normal albumin levels, the patients blood concentration extrapolation would be inaccurate. Therefore to increase the accuracy in therapeutic drug monitoring trials, it is important to determine the protein content of the patient's blood plasma.

A study to quantify the exact plasma protein content was conducted. The study tested five methods to isolate and measure the plasma protein content [127]. The five methods used were Bradford, Lowry, Biuret, Pesce and Strande and a modified Schaffner-Wesismann method [128-134].

The use of the Biuret assay was considered impractical due to the large sample volume require which could go up to 2mL. However the linearity produced by the signal intensity over a wide range of protein concentration favoured this method [127].

The Bradford assay was based on dye-protein complex. In this method the proteins bind to the dye to form a complex which increased molar absorbance. The method was easy to perform however the method had poor linearity when compared to the biuret assay method [128].

The Lowrey assay is a modification of the biuret assay by using Folin-phenol reagent through subsequent reactions. The problem with this method was that interference occurred due the amino acids tyrosine and tryptophan on the colour development. It was found that interference often occurred when using this method [129].

The Pesce and Strander assay was evaluated as a practical and efficient method to provide accurate measurement of protein content of plasma. The method is based on the simultaneous mixture of protein, Ponceau-S dye with trichloroacetic acid. A precipitate was formed which was then dissolved by sodium hydroxide which produces a violet colour [130].

The Schaffner-Weismann method is based on protein precipitation with Amido black dye in methanol/acetic acid which is dissolved using sodium hydroxide. The method is easy to use and is usually used in dot blot analysis of poteins [131].

The study suggested that each method has its advantages and disadvantages and that the reference range for plasma albumin will vary depending on the method used [127]. In our study the plasma protein content was determined using the Karl Fischer method which was the analysis of the water content present in a sample. This method was used due to instrument availability. The Karl Fischer concept was further discussed in chapter 4.

2.18 Studies on anti TB drug binding interactions with plasma proteins

A study to assess the interaction of anti TB drug with the α_1 – acid glycoprotein (AAG) produced in pulmonary granulomas in drug candidites was conducted [135]. Cicular dichroism and UV/VIS absorbtion spectroscopy methods were use to assess AAG binding properties of anti – TB drug candidates who developed multidrug resistant tb. CD spectroscopic data indicated that AAG molecules were bound within the beta-barrel of the protein in monomeric or dimeric forms. Molecular docking studies suggested the importance of H-Bonds and ligand aromatic residue π-π stacking interactions were important to produce stability to the drug molecule and protein binding site. AAG was considered to be a significant binding competitor to anti TB drugs therefore possibly affecting distribution and bioavailabilty of the drug [135].

The binding effect of INH on the structure and activity of HSA and catalase (CAT) was evaluated through spectroscopic and molecular docking methods under *invitro* physiological conditions [136]. For accurate binding parameters the inner filter effect of all the fluorescence data was eliminated. The stern volmer quenching constant for INH-HSA and INH-CAT was inversely proportional with the temperatures, therefore demonstrating that INH caused static quenching for both HSA and CAT. The conformational investigation of INH with HSA and CAT was performed using UV-VIS spectroscopy synchronous fluorescence and dichroism, results indicated that INH could change the micro-environment by interacting with tryptophan residues and cause structural deformation of the α-helix conformation of the proteins. Molecular docking reveled that INH is probable to interact at sudlow's site 1 of HSA. This study provided helpful information the binding and toxicity of INH with HSA and CAT [136].

The interaction of pyrazinamide with HSA and BSA (Bovine serum albumin) was studied [137]. The methods used for the study was molecular docking, circular dichroism, dynamic light scattering and differential scanning calorimetry. Results indicated that pyrazinamide had a higher binding affinity to BSA with a binding constant of $\approx 10^4$ M^{-1} for both HSA and BSA. The increase in secondary structural content of the protein and the reduction in hydrodynamic radii indicated that pyrazinamide had astabilizing effect on the protein. Pyrazinamide interacted through static quenching and had a stabilizing effect on serum albumin [137].

Researchers studied the binding 4-drug anti-TB regimen to plasma protein [1]. The study was conducted to improve efficacy by determining the free drug concentration. The use of an ultrafiltration technique was employed to determine the protein binding extent and variability of the anti-TB drugs when administed simultaneously to TB patients. Plasma proteins of 22 patients were used and the protein content of 18 of those 22 patients was measured. The median plasma binding extent was determined for all 4 drugs: Rifampicin 88%, INH 14%, PYR 14% and ethambutol 12%. The study indicated that the concentrations of rifampicin and INH are dependant on the plasma concentration. However the plasma proteins were found to be an insignificant predictor for protein binding of first-line anti TB drugs [1].

An *in vitro* pharmacokinetic study was performed using clinical trial data to investigate if a higher administered rifampicin dose regimen would cause saturation of the proteins in blood plasma [138]. Protein free rifampicin standards were spiked with HSA and increasing drug concentrations up to 64mg/L as well as samples obtained from patients which were administed high-dosage of 35 mg/kg of rifampicin. The performance of total (Area under the curve) AUC_{0-24} was evaluated to predict unbound AUC_{0-24}. The study concluded that rifampicin at high doses can saturated plasma proteins, however the high dosage of rifampicin was not high enough to increase free unbound drug fraction in patients with normal albumin levels [138]. Increasing the dosage of rifampicin could also cause adverse effects to TB patient health.

Chapter 3

Rifampicin-plasma assay LCMS method development and validation

3.1 Research Question

Can fields of research used in the laboratory such as bioanalytical drug method development and optimisation, impact and improve the accuracy of LCMS concentration calibration curve results, when assessing and comparing the calibration standards to calibration standards with blood plasma present, as well as improve concentration extrapolation from LCMS calibration curves used for therapeutic drug monitoring for TB patient clinical trials?

3.2 Aims and objectives

- Method validation of the anti-TB drug rifampicin (RIF) using LCMS to create an *in vitro* drug-plasma system to determine calibration curves and drug identification for clinical trial therapeutic drug concentration monitoring.
- To develop an LCMS method for detection and identification of rifampicin within plasma samples.
- To validate the developed LCMS method from rifampicin with and without plasma.
- To assess if the drug-plasma assay has an effect and an impact on the limit of detection and quantification in the validation process, when compared to the validation of the drug without plasma.

3.3 Experimental protocol: rifampicin experimental methods and parameters

3.3.1 Chemicals and Reagents

Rifampicin (≥97%) and phenacetin (≥98%) powder certified reference standards were purchased from Sigma Aldrich (Merck, Darmstadt, Germany). L-ascorbic acid (99%), acetic acid (99.8%) and ammonium acetate (≥98%) were analytical grade and was acquired from Sigma Aldrich. The solvents methanol (99.9%) and acetonitrile (99.9%) were HPLC grade obtained from Sigma Aldrich. Millipore distilled water was obtained from the Stellenbosch Tygerberg Clinical pharmacology department laboratory. Blood samples of healthy patients, for the use of blank plasma were acquired from Tygerberg Hospital Cape Town South Africa. Ethics Approval was obtained from the Health research committee at the University of Stellenbosch for this study Ref: (X17/04/005).

3.3.2 Instrumentation and Chromatographic conditions

The assay analyses were performed using LCMS. A typical analysis used a positive mode, electrospray ionization (ESI) interface hyphenated Shimadzu triple quadrupole mass spectrometer 8040 (MS) connected in tandem to a Shimadzu UFLC-XR HPLC using a 2 channel (binary) pump. Chromatographic separation was achieved using a Shimpack, internal diameter (ID): 2.1 mm, length: 100 mm, particle size: 3.5 µ C18 column with the oven temperature of 40°C by gradient elution using 5mM ammonium acetate in Millipore water at pH 5 (mobile phase A) and 0.01 % acetic acid in methanol: acetonitrile (1: 1) pH 5 (mobile phase B) with a gradient increase from 0% mobile phase B to 100% mobile phase B at a rate of 10% of mobile phase B/min over ten minutes. The mobile phases had a flow rate at 0.1 ml/min-0.5 ml/min over 10 minutes. The sample injection volume was 3 µl. The MS conditions were optimised for best sensitivity as follows, 0.1 µA interface current, nebulizing gas flow of 3 L/min., drying gas (N_2) flow of 15 L/min., desolvation line temperature of 250 °C, heat block temperature of 400 °C and CID gas (argon) at 230 kPa.

3.3.3 Extraction solution

Ascorbic acid was dissolved in methanol to make up a solution with a concentration of 0.1 mg/mL. MeOH was used as an organic extraction solution to precipitate proteins, and as a stock solution for the analyte standards. It can be kept at 6 °C for a maximum of 6 days.

3.3.4 Preparation of stock solutions

Rifampicin and phenacetin reference standards were each dissolved in a separate stock solution consisting of 50:50 ratios of acetonitrile and Millipore water to make up 100 µg/mL concentration in a 100 ml volumetric flask. A second stock solution of rifampicin and phenacetin was prepared in the same manner with a final concentration of 20 µg/mL.

3.3.5 Sample preparation of Rifampicin and internal standard phenacetin without plasma

The stock solutions of rifampicin and phenacetin were used to prepare the plasma free standards for analysis to plot the calibration curve. The following sample concentrations were prepared: 0.1, 0.5, 1, 5, 20 and 25 µg/mL. Table 3.1 illustrates the dilution of the stock solutions to the required rifampicin concentration.The diluted standards were then added to the autosampler vials. The sample injection volume was 3µL.

Table 3.1: Sample preparation and dilution of rifampicin and phenacetin without plasma

RIF	C1	V1 (µL)	C2	V2 (µL)	PHENACETIN (µL)	Extraction solution (µL)	Centrifuge time(min)	Vortex time(min)
0.1 µg/ml	20 µg/ml	5	0.1 µg/ml	1000	100	400	3	1
0.5 µg/ml	20 µg/ml	25	0.5 µg/ml	1000	100	400	3	1
1 µg/ml	20 µg/ml	50	1 µg/ml	1000	100	400	3	1
5 µg/ml	100 µg/ml	50	5 µg/ml	1000	100	400	3	1
10 µg/ml	100 µg/ml	100	10 µg/ml	1000	100	400	3	1
25 µg/ml	100 µg/ml	250	25 µg/ml	1000	100	400	3	1

3.3.6 Sample preparation of rifampicin and internal standard phenacetin with plasma

Blood samples were centrifuged at 2550 rpm for 20 minutes (benchtop centrifuge) to remove particulate matter, sediment and to isolate plasma. Plasma was carefully extracted using a clean pasture pipette and transferred into a suitable container (Eppendorf vial) and frozen immediately for preservation.After thawing, 0.20 mL plasma was placed into an Eppendorf vial. A volume of 0.6 mL (600 µL) of the extraction solution (containing 0.1 mg/mL ascorbic acid) was added to the plasma. The contents (0.8 mL in total) were vortexed for approximately 1 minute. The contents were centrifuged at 2550 rpm for 3 minutes (bench-top centrifuge). The organic supernatant was carefully pippeted and transferred into an eppendorf vial. The solid precipitated proteins were carefully discarded in the biohazardous waste.

The stock solutions of rifampicin and phenacetin were used to prepare the plasma standards for analysis to plot the calibration curve. The following sample concentrations were prepared: 0.25, 0.5, 1, 1.5, and 3 µg/mL. Table 3.2 illustrates the dilution of the rifampicin samples containing blood plasma. The standards were then added to the autosampler vials. The automated injection volume used was 3µL.

Table 3.2: Sample preparation of rifampicin and phenacetin with plasma

RIF	**C1**	**V1 (µL)**	**C2**	**V2 (µL)**	**PHENACETIN (µL)**	**Extraction solution: Plasma (4:1) (µL)**	**Centrifuge time(min)**	**Vortex time(min)**
0.25 µg/ml	20 µg/ml	12.5	0.25 µg/ml	1000	100	400:100	3	1
0.5 µg/ml	20 µg/ml	25	0.5 µg/ml	1000	100	400:100	3	1
1 µg/ml	20 µg/ml	50	1 µg/ml	1000	100	400:100	3	1
1.5 µg/ml	20 µg/ml	75	1.5 µg/ml	1000	100	400:100	3	1
3 µg/ml	20 µg/ml	150	3 µg/ml	1000	100	400:100	3	1
5 µg/ml	20 µg/ml	250	5 µg/ml	1000	100	400:100	3	1

3.3.7 Preparation of mobile phase A

- Preparation of 5 mM ammonium acetate buffer at pH 5.5

Calculation of mass weighed	m = n x Mr
C=n/V	= 0.005 x 77.08
n = CV	= 0.3854 g x 1000
= 5 x 10^{-3} x 1000 ml	= 385.4 mg

- **Mobile phase A**

Ammonium acetate (385.4 mg) was weighed and transferred into a 1-litre volumetric flask and diluted with Millipore water to the meniscus mark on the flask. The pH was measured to be 5.5

3.3.8 Preparation of mobile phase B

- Preparation of 0.01 % of acetic acid in acetonitrile/methanol. 20 µL of acetic acid was pipetted in 200 mL of an acetonitrile/methanol solution. The acetonitrile/methanol solution had a (1:1) mix ratio.

Calculation
0.01 mL in 100 mL make 0.01% 0.01 × 2 = 0.02 mL 0.02 × 1000 = 20 µL

- **Mobile phase B**

20 µL of acetic acid was added 200 mL of acetonitrile/methanol (1:1) ratio to make up a solution of 0.01% of acetic acid in acetonitrile: methanol (1:1) mobile phase solution.

3.4 Results and Discussion

The administration dosage of rifampicin per patient is 10 mg/kg per day [139]. When the drug is administered to a patient, it is transported to the bloodstream via a systemic administration. Systemic administration is an administration route that transports the drug into the circulatory system so that the entire body is affected. Studies indicate that systemic administration is effective for treatment of gram-positive bacteria such as *M.tb* [142]. The drug is then transported to the site of action via the blood plasma. Blood plasma consists of plasma proteins and water and also glucose, electrolytes, hormones etc. Rifampicin is a non-polar drug with a LogP value of 3.719 [73,140]. According to a study by Wanat K, lipophilic drugs can lead to drug plasma binding to occur due to the plasma protein albumin amino acid residues present in the blood plasma [141]. This impacts the pharmacokinetic properties of the drug by decreasing its bioavailability and slowing its passage across biological membranes therefore less than the required therapeutic dose reaches its target [141]. In addition, when multiple drugs are administerd they compete for binding to the plasma proteins. This competition of drug binding to the protein binding site can cause a rise in concentration of free unbound drug. This can have cause serious problems for patients when administered with narrow therapeutic index drugs [141]. This can also lead to errors and outliers in therapeutic drug monitoring data. Therefore, it is important to consider the effect of drug-plasma binding to improve the accuracy of results of LCMS concentration calibration curves.

Method Optimization

The quantification of rifampicin and the internal standard selected was phenacetin with and without human plasma were conducted using an LCMS. During the validation process (validation support data can be found in addendum A), the LCMS instruments conditions were optimized to obtain better resolution of peaks. The pressure was 345 bars, the oven temperature was kept at 40 °C. The flow rate of 0.3 ml/min and the injection volume was 3 µl. Mobile Phase A consisted of ammonium acetate in Millipore water at pH = 5.5 and Mobile Phase B was composed of 0.01 % acetic acid in methanol:acetonitrile ratio of 50:50. Mobile phase B was set to a gradient increase from 0% mobile phase B to 100% mobile phase B at a rate of 10% of mobile phase B/min over ten minutes. The mobile phases had a flow rate at 0.1ml/min-0.5ml/min over 10 minutes.The mobile phases were chosen to keep rifampicin and phenacetin in its non-ionized state due to the pH 5.5 in mobile phase A. This assisted by optimizing recovery and stability of the analyte when passing through the C-18 non-polar stationary phase column. The analytes were kept in the non-ionized state so that the molecule was retained on the non-polar packing carbon-18 column for efficient separation and detection to take place. The extraction organic solvent methanol was used for plasma protein precipitation which was adopted and modified for use in this validation method from a previous study [143].

3.4.1 Limits of detection (LOD) & limit of quantitation (LOQ) Determination for rifampicin without plasma standards based on 0.5 µg/mL concentration and the linear equation gradient

The following data below was obtained using the LCMS method validation data of rifampicin calibration standards without plasma present. The r^2 value 0.9925 was calculated from the LCMS concentration calibration curves linear equation y = 237492x. As indicated in table 3.3 $^{sy}/_{x}$ is the standard deviation that was calculated from the average area of the six LCMS runs performed for the rifampicin concentration 0.5 µg/mL. The standard deviation was then used to calculate the LOD and LOQ as indicated in the formular where m = 237492 which is the gradiant of the linear curve regression line equation y = 237492x.

Table 3.3: LOD, LOQ, Standard deviation, and linear regression equation and correlation coefficient R^2 of rifampicin without plasma

R^2 = 0.9916 y = 237492x	$^{sy}/_{x} = \sqrt{\frac{\varepsilon(y-yi)2}{n-2}}$ = 12542.55286	LOD = $\frac{3.3 \text{ x } ^{sy}/_{x}}{m}$ = $\frac{3.3 \text{ x } ^{sy}/_{x}}{237492}$ = 0.158 µg/mL	LOQ = $\frac{10 \text{ x } ^{sy}/_{x}}{m}$ = $\frac{10 \text{ x } ^{sy}/_{x}}{237492}$ = 0.528 µg/mL

Table 3.4: Sample runs (x 6) of rifampicin and phenacetin (2 µg/mL) with plasma at concentration 0.5µg/ml containing the average area, RSD, retention times and area min and max

Sample Runs	**Rifampicin without plasma**	**Ret. Time**	**Area**	**Std. Conc.**
1	Rifampicin	7.806	246 246	0.5
2	Rifampicin	7.806	223 620	0.5
3	Rifampicin	7.808	209 397	0.5
4	Rifampicin	7.808	225 939	0.5
5	Rifampicin	7.805	216 133	0.5
6	Rifampicin	7.805	220 316	0.5
	Average	**7.806**	**223 608**	
	%RSD	**0.018**	**5.609152**	
	Maximum	**7.808**	**246 246**	
	Minimum	**7.805**	**209 397**	
	Std. Dev.	**0.001**	**12 542.531966**	

Table 3.5: Rifampicin concentration without plasma, Average area, relative standard deviation (RSD) $y = mx + c$, $(y-y_i)^2$

Rifampicin without plasma was injected 6 times and the average area was calculated for each concentration given in table 3.5

CONCENTRATION [x] (µg/ml)	**Average area(y)**	**RSD(%)**	**y=237492x r^2 = 0.9916**
0.1	26 717.33	23.00	
0.5	223 608.5	5.61	
1	292 991.83	2.51	
5	1 667 064.4	7.55	
20	4 583 098.5	1.27	
25	5 970 459.83	2.05	

Internal standard: Phenacetin with a concentration of 2µg/mL

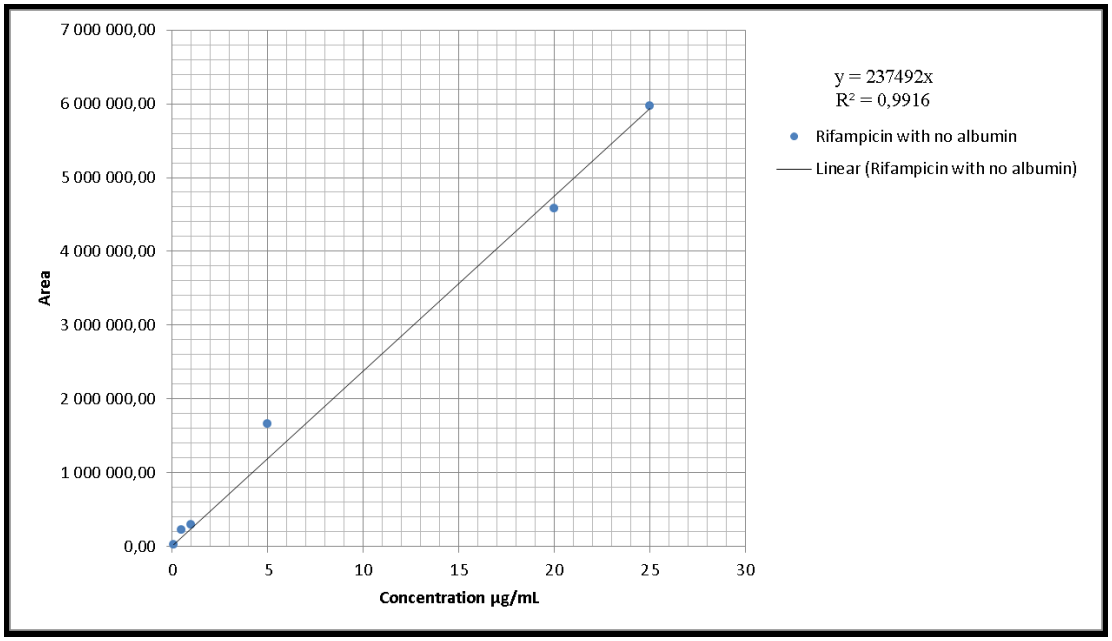

Figure 3.1: Calibration curve for rifampicin plasma free standards at concentration 0.1-25 µg/mL

- **Rifampicin-Plasma free standards:** The calibration curve indicated in figure 3.1 was plotted using the average (6 runs each) concentrations of rifampicin as indicated in table 3.5. The percentages RSDs (Relative standard deviation) of Rifampicin calibration standards without plasma average LCMS peak areas for concentration standards 0.1µg/mL, 0.5µg/mL, 1µg/mL, 5µg/mL, 20µg/mL, 25µg/mL were 23.00 %, 5.61 %, 2.51 %, 7.55 %, 1.27 %, and 2.05 % respectively. The percentage RSD calculated for each concentration of rifampicin without plasma was within the accepted range, except for the rifampicin concentration of 0.1µg/mL. The LOD for plasma standards was found to be 0.158µg/ml and the LOQ was found to be 0.528 µg/mL. The correlation coefficient r^2 generated from the calibration curve with plasma was 0.99712. The mean concentration standard deviation (0.053µg/mL) was calculated using the peak areas of the rifampicin plasma free concentration 0.5µg/mL as indicated in table 3.4, and calculating the x values from the linear regression line. This was performed to represent the error of the data points to the linear plot.

3.4.2 LOD & LOQ Determination for rifampicin-plasma standards based on 0.5 µg/mL concentration and the linear equation gradient

The following data below was obtained using the LCMS method validation data of rifampicin calibration standards with plasma present. The r^2 value 0.9815 was calculated from the LCMS concentration calibration curves linear equation y = 182632x. As indicated in table 3.6 $^{sy}/_{x}$ was the standard deviation that was calculated from the average area of the six LCMS runs performed for the rifampicin concentration 0.5 µg/mL containing blood plasma. The standard deviation was then used to calculate the LOD and LOQ as indicated in the formulars where m = 182632 which is the gradiant of the linear curve regression line equation.

Table 3.6: LOD, LOQ, Standard deviation, linear regression equation and correlation coefficient R^2 of rifampicin with plasma present.

R^2 = 0.9815 y = 182 632	$^{sy}/_{x} = \sqrt{\frac{\varepsilon(y-yi)2}{n-2}}$ = 14 905.89414	LOD = $\frac{3.3x\ ^{sy}/_{x}}{m}$ = 0.2693 µg/ml	LOQ = $\frac{10\ x\ ^{sy}/_{x}}{182632}$ = $\frac{10\ x\ ^{sy}/_{x}}{182632}$ = 0.816 µg/mL

Table 3.7: Sample runs (x 6) of rifampicin and phenacetin (2 µg/mL) with plasma at concentration of 0.5µg/ml containing the average area, &RSD, retention times and area minimum and maximum

Runs	**Sample**	**Ret. Time**	**Area**	**Std. Conc.**
1	Rifampicin + Plasma 0.5µg/ml	7.841	120 523	0.5
2	Rifampicin + Plasma 0.5µg/ml	7.84	126 063	0.5
3	Rifampicin + Plasma 0.5µg/ml	7.84	123 717	0.5
4	Rifampicin + Plasma 0.5µg/ml	7.841	144 757	0.5
5	Rifampicin + Plasma 0.5µg/ml	7.839	126 479	0.5
6	Rifampicin + Plasma 0.5µg/ml	7.834	98 302	0.5
	Average	7.839	123 307	
	%RSD	0.034	12.088506	
	Maximum	7.841	144 757	
	Minimum	7.834	98 302	
	Std. Dev.	0.003	14 905.931953	

Table 3.8: Rifampicin concentration with plasma + phenacetin, Average area, relative standard deviation (RSD) y = mx + c

Rifampicin with plasma was injected 6 times and the average area was calculated for each concentration given in table 3.8

CONCENTRATION [x] (µg/mL)	Average area(y)	RSD(%)	y=182632x R^2 = 0.9815
0.25	25 231	6.25	
0.5	124 195.5	12.09	
1	160 015.33	6.59	
1.5	219 980.16	3.92	
3	619 167.16	2.56	
5	888 844	4.88	

Internal standard: Phenacetin with a concentration of 2µg/mL.

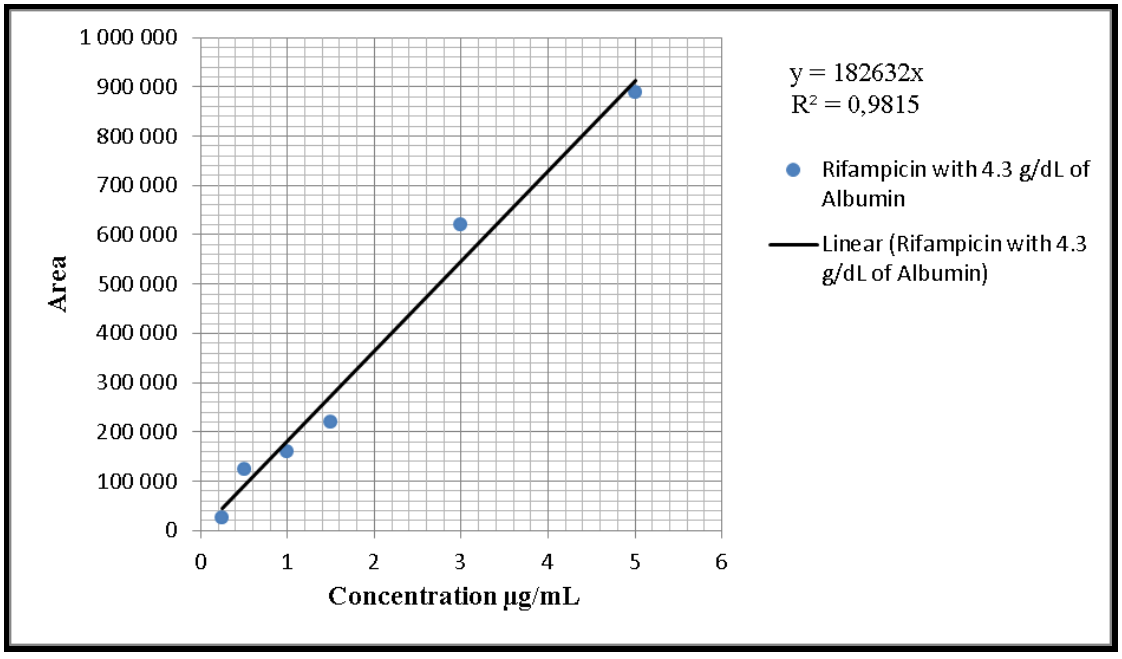

Figure 3.2: Calibration curve for rifampicin standards containing plasma concentration 0.1-5µg/ml

- **Rifampicin plasma standards:** The calibration curve indicated in figure 3.2 was plotted using the average (6 runs each) concentrations of rifampicin with plasma as indicated in table 3.8. The percentage RSD (Relative standard deviation) of the rifampicin standards with plasma average LCMS peak areas for concentration standards 0.25µg/mL, 0.5µg/mL, 1µg/mL, 1.5µg/L, 3µg/mL, 5 µg/mL was 6.25 %, 12.09 %, 6.59 %, 3.92 %, 2.56 %, and 4.88 % respectively. These percentages RSD are in the accepted range, which is % RSD < 20%. The LOD for plasma-free standards was found to be 0.269µg/ml and the LOQ was found to be 0.816µg/ml. The percentage recovery of the rifampicin from the plasma was found to be 55 % when comparing the peak areas at the rifampicin average of concentrations 1µg/mL, 0.5µg/ml with plasma and without plasma. The correlation coefficient r^2 generated from the calibration curve without plasma was 0.9842. The mean concentration standard deviation (0.082µg/mL) was calculated using the peak areas of the rifampicin plasma free concentration 0.5µg/mL as indicated in table 3.7, and calculating the x values from the linear regression line. This was performed to represent the error of the data points to the linear plot.

The linearity of both plasma-free and plasma standards were acceptable however it did not meet the bioanalytical validation requirements of the FDA linearity acceptance criteria for r^2 of > 0.999. The method proposed was found to be very selective and specific for detection and identification of rifampicin and the internal standard phenacetin. The blank sample was prepared containing the methanol extraction solution containing the ascorbic acid, and the blank sample was analysed on the LCMS. The blank sample was used to verify that there was no rifampicin and phenacetin on the column and that the blank sample was free from contaminants. The method developed produced good separation of rifampicin and phenacetin and identified rifampicin and phenacetin peaks. Rifampicin eluted from the column at the retention time of 7.87 minutes (Average retention time ± standard deviation) (see table 9 in addendum A) and phenacetin eluted from the column at the retention time of 6.9 min for samples without plasma. For rifampicin samples containing plasma the average retention time was 7.82 minutes (Average retention time ± standard deviation) (see table 17 in addendum A). When a non-polar stationary phase is used for separation of compounds in a sample, the non-polar compounds are retained for a longer period of time and the polar compounds elute faster from the stationary phase column. Rifampicin was retained for a longer period of time on the non-polar C-18 column which indicates that phenacetin is more polar in nature compared to rifampicin.

Table 3.9 A comparison of rifampicin with albumin levels at 4.3 g/dL and no albumin using the calibration curve equation of the line

	Rif without Albumin	**Rif + 4.3 g/dL albumin**
Concentration in µg/mL	Calculated Area: y = 237492x	Calculated Area: y = 182632x
2	474 984	365 264
4	949 968	730 528
6	1 424 952	1 095 792
8	1 899 936	1 461 056
10	2 374 920	1 826 320
12	2 849 904	2 191 584
14	3 324 888	2 556 848
16	3 799 872	2 922 112
18	4 274 856	3 287 376
20	4 749 840	3 652 640
22	5 224 824	4 017 904
24	5 699 808	4 383 168
26	6 174 792	4 748 432

In figure 3.3 the calibration curve areas were calculated for rifampicin with plasma and without plasma as indicated in table 3.9. The calculated areas were plotted on the same graph to compare the relative accuracy. The graph indicates that as the gradient increases the percentage error increases. The concentration error was illustrated using the calibration curve in figure 3.3 and was calculated by extrapolating the concentration from rifampicin with plasma and rifampicin without plasma at the same area. The extrapolation from the calibration curve for rifampicin without plasma was 25 µg/mL. When compared to the extrapolation from the calibration curve of rifampicin with plasma at the same area, the concentration was 19 µg/mL. The error of the curve without plasma was 24 %. This means that the accuracy of the calibration curve of rifampicin without plasma was 76 %. Therefore, this finding leads to an insight that blood plasma should be a required and should be factored into bioanalytical methods to improve therapeutic monitoring results from LCMS calibration curves. In addition, the concentration extrapolation from LCMS calibration curves without plasma present could lead to large concentration errors especially when administering narrow therapeutic index drugs. This led to the question, does plasma protein to water ratio vary for different patients and if so how could the accuracy of the result be improved for therapeutic drug monitoring? Further research on the plasma content was required.

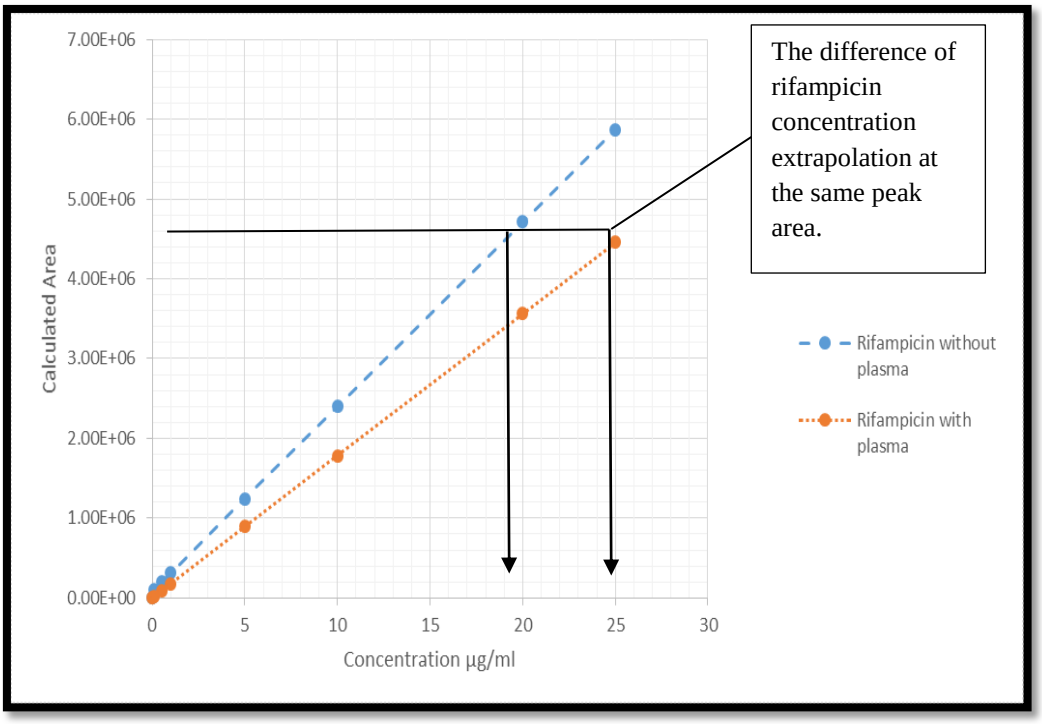

Figure 3.3: Calibration curve of rifampicin with and without plasma from calculated area of each linear equation

3.5 Conclusion

In conclusion a method was successfully developed and validated using the Shimadzu LCMS. The limit of detection and quantification values of the rifampicin plasma free standards was much lower in value than the rifampicin-plasma assay standards. The gradient of the rifampicin plasma assay samples was also lower in value when compared to the plasma-free rifampicin standards. This confirms that the rifampicin drug interacts with the plasma, the recovery of sample concentration decreases and the gradient of the validation calibration curve is affected by the plasma present. Hence for increased accuracy, it is important to consider the use of plasma during validation methods for blood sample analysis to avoid error in concentration results during therapeutic drug monitoring in TB patient clinical trials. Another important parameter to be considered when comparing patients' plasma to the plasma calibration curve is the overall health condition of the patients'.

Chapter 4: Water Content Determination in Human Plasma Using the Karl Fischer process

4.1 Aims and objectives of the variability in plasma stock solutions used to construct calibration curves

- To investigate the influence plasma protein quantity present has on the gradient of the calibration curves by determination of the water: protein content present in calibrator plasma samples.
- To determine the water: protein content of specific patient's plasma.
- To determine if the water content of plasma of patients is approximately ≤ 93 %, as suggested in the literature [144].
- To assess if the % water is impacted when analysing standing plasma samples or mixed (vortexed) plasma samples.
- To use the Karl Fischer process as a novel technique for water content determination of plasma.

4.2 Background

In this experiment, the Karl Fischer process was used to determine the percentage of protein present in plasma samples. As suggested theoretically, and in an article on a new method for determining plasma water content: application in pseudo-hyponatremia, the water content in the plasma is <93 % [144]. The purpose of this study was to determine if the water content in plasma of the same patients was constant, or if the water percentage varies. The determination of the percentage of water content present in plasma samples was acquired by using an automated Karl Fischer titration process. A diagram of the Karl Fischer auto titrator is given in figure 4.1.

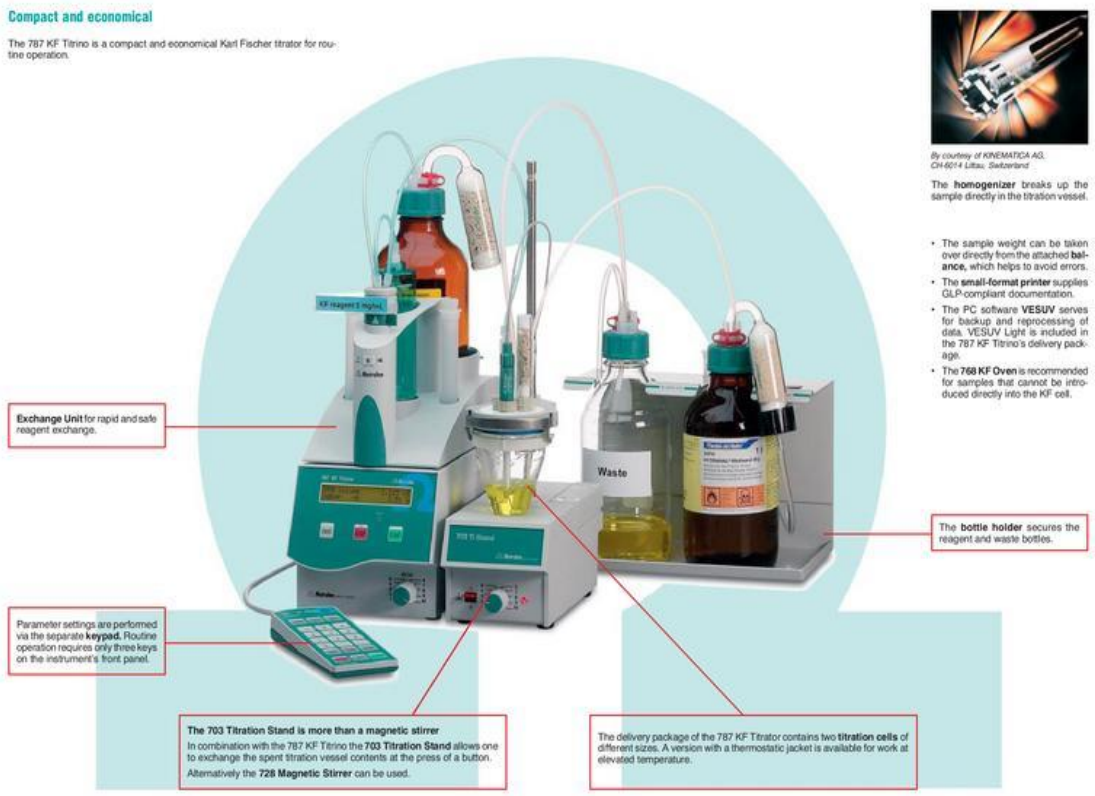

Figure 4.1: Karl Fischer auto-titrator (https://www.metrohm.com/en-us/support-and-service/kf-how-to-operate-sample-processing/#term:auto%20titrator)

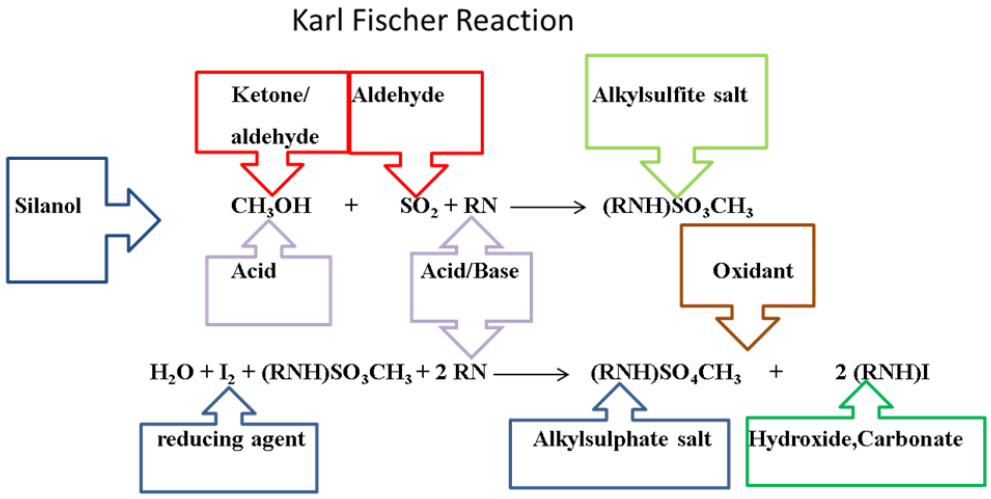

Figure 4.2: The Karl Fischer reaction process (https://www.metrohm.com/en-us/support-and-service/kf-how-to-operate-sample-processing/)

4.2.1 What is the Karl Fischer Reaction?

The Karl Fischer process is an analytical technique used to determine the water content present in a variety of substances [146]. Karl Fischer used the concept of the Bunsen reaction between iodine and sulphur dioxide in an aqueous medium. Karl Fischer identified that the Bunsen reaction between iodine and sulphur dioxide could be modified to determine the water content present in a non-aqueous medium that contained an excess of sulphur dioxide. Methanol was used as a solvent and pyridine was used as a buffering agent [145].

The alcohol reacts with sulphur dioxide and a base to form the intermediate alkylsulfite salt. The alkylsulfite salt is then oxidized by iodine to an alkylsulphate salt. This oxidation reaction consumes the water present [145]. Iodine and water are consumed at a ratio of 1:1. When all the water present in the substance gets consumed, the titrator's indicator electrode detects the excess of iodine present volumetrically. This then gives an amperometric signal based on the detection of a slight excess of iodine when water is no longer present in the KF cell to indicate that the endpoint of the titration has been reached [145]. In Figure 4.2 the Karl Fischer reaction is given.

The amount of Karl Fischer titrant used is directly proportional to the amount of water present in the substance. The water content is calculated based on the iodine concentration present in the Karl Fischer titrating reagent and the amount of Karl Fischer reagent consumed [145].

When the Karl Fischer method was introduced, the Karl Fischer reagent used was a toxic substance pyridine. Due to this toxicity, scientists have looked towards finding pyridine-free substances such as Hydranal that contain imidazole and primary amines. Hydranal-Composite is the most frequently used pyridine free Karl Fischer titrating reagent. Hydranal-Composite contains all the reagents including iodine, sulphur dioxide, and the bases imidazole and 2-methylimidazole, dissolved in diethylene glycol monoethyl ether. Imidazole is stronger base than pyridine and is non-toxic with a higher affinity for alkylsulfite. Imidazole allows the reaction to go to completion rapidly and provides endpoint stability. Later on research indicated that adding 2-methylimidazole (as second base) reduced crystallization and enhanced the stability of the reaction [147].

When determining the percentage of water present in a substance using the Karl Fischer titration process, two types of analytical methods (volumetric and coulometric) can be used [145]. Volumetic analysis occurs via addition of reagent containing iodine to the KF cell. Coulometric analysis occurs by regeneration of iodine electrochemically from the reaction of Karl Fischer reagent and water in the KF cell. However, it is important to select the appropriate method of analysis for the substance in question. The appropriate method is selected by the range of the water content in the substance. For volumetric analysis, the percentage ranges from 0,1 % to100 % and for coulometric analysis, the levels of water detections range below one per cent (<1%) [145]. Since plasma has a high water content of <93 %, the volumetric Karl Fischer titration method would be most appropriate to use in this experiment.

4.2.2 The use of plasma standards to produce calibration curves

When validating an analytical or LCMS method to produce a calibration curve, accuracy is an important factor. The accuracy of the calibration curve will determine the margin of error. If the accuracy is high, the margin of error will be low and results obtained or required from the calibration curve will be reliable and acceptable to use. When taking a closer look at plasma as a component separated from the blood, the plasma component consists of two major components: approximately 90 % water and 10 % protein. However, when using plasma in a standard sample at specific amounts, the gradient of the curve is affected.

The gradient of the curve is derived from the linear equation of a straight line, which is produced from the calibration results. When more plasma is present in the sample, the gradient of the curve will decrease due to more protein content present. When less plasma is present in the sample, the gradient of the curve will increase. Based on this effect of the plasma, when extrapolating results from the calibration curve if the plasma content of the patient varies according to the plasma used to produce the calibration curve, the concentration extrapolated from the calibration curve will give incorrect results. In figure 4.3 a and b and example is given to indicate plasma water ratio of a patient containing a higher protein level compared to the calibrator plasma used in the laboratory study. A comparison using the calibration curve as indicated in the calibration curve in chapter 3 figure 3.3 will result in a concentration extrapolation error. Hence, it is important to use the plasma of the patient to validate the calibration curve.

Another important observation relating to using plasma to prepare calibration curves is that the water to protein percentage ratio is not accurately determined, and is based on the assumption based on literature. Therefore, the purpose of this study was to determine the ratio of water to protein content of different patients and the accuracy of sample plasma used from the same patient using the Karl Fischer auto-titration method.

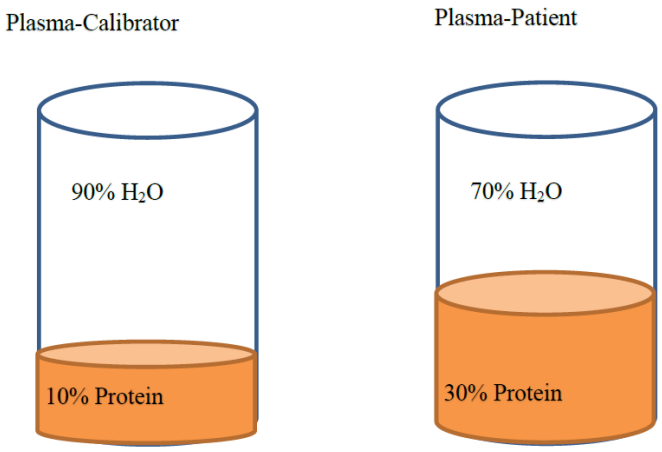

Figure 4.3: a) Plasma-calibrator used to produce a calibration curve with a ratio of 90 % water to 10 % protein. b) Plasma sample of the patient to be analysed with a ratio of 70 % water to 30 % protein.

4.3 Experimental Protocol

4.3.1 Chemicals and Reagents

Blood samples of healthy patients, for the use of blank plasma were acquired from Tygerberg Hospital Cape Town South Africa. Ethics Approval was obtained from the Health research committee at the University of Stellenbosch for this study Ref: (X17/04/005). The standardizing solvent used was Hydranal (Merck, lot. HX85808105). The solvents methanol (99.9%) was HPLC grade obtained from Sigma Aldrich.

4.3.2 Instrumentation and Conditions

A 702 SM Titrino Karl Fischer auto titrator was used to conduct this experiment. A magnetic stirrer was required for mixing the titration solution through the sample analysis. A Mettler Toledo mass balance was used for weighing the plasma samples.The % water, mean and RSD were automatically calculated by the Karl Fischer autotitrator. The following method parameters were set indicated in the figure 4.4 below:

Karl Fischer 702 SM Titrino Parameters

• Titration	
V step	0.10 mL
Titration rate	max. mL/min
Signal drift	50 mV/min
Equilibrium time 26s	
Start V:	off
Pause	0s
Measure input:	1
Temperature	25° C
• Stop Conditions	
Stop V:	abs.
Stop V	20 mL
Stop pH	off
Stop EP	9
Filling rate	max. mL/min
• Statistics	
Status:	on
Mean	n = 4
Rest.tab:	original
Evaluation	
EPC	0.50
EP recognition	all
Fix EP 1 at pH	off
pK/ HNP:	off
• Preselections	
Req.indent:	off
Req.sample size:	value
Activate pulse:	off

Figure 4.4: Karl Fischer method Parameters

4.3.3 Preparation method of plasma samples and sample analysis

Blood samples were centrifuged at 2550 rpm for 20 minutes (benchtop centrifuge) to remove particulate matter, sediment and to isolate plasma. Plasma was carefully extracted using a clean Pasteur pipette and transferred into a suitable container (Eppendorf vial) and frozen immediately for preservation. Sample waste was carefully disposed of in biohardous waste bins.

The samples of frozen preserved plasma from different patients were left to thaw. Once the plasma thawed, 20 µL of plasma was pipetted into a weighing boat and weighed to measure the mass of the plasma. The Methanol solvent used was 99.9% pure HPLC grade and a blank analysis was performed to calibrate the Karl Fischer auto titrator and to indicate that no water was present. Thereafter methanol solvent and a magnetic stirrer were added to the Karl Fischer titrator cell. The magnetic stirrer was used to keep the solution mixed when further addition of solvents were titrated to the titrator cell. The 20 µL of blood plasma was then added to the titrator cell and the Karl Fischer reagent Hydranal was used to titrate and promoted oxidation reaction in the titrator cell to take place. Each addition of hydranal was automatically measured by the auto-titrator until the endpoint of the run was reach. The run reached an end point when all of the water in the titrator cell was consumed.

Two types of analysis on the samples were done:

- Seven (7) x Samples were left to stand and thereafter each sample was analysed four (4) times.
- Seven (7) x Samples were vortexed (3 min) vigorously for homogeneity of the plasma and each sample was analysed four (4) times

4.4 Results and Discussion

The purpose of this experiment was to determine whether the ratio of water content to plasma varied when using an extracted sample from a specific patient. The water content present in the plasma was analysed using a Karl Fischer auto titration method. The volumetric analysis method for Karl Fischer titration was used. Understanding the water content present in a patient's plasma is important because when analysing blood samples of a patient using a specific drug, the drug tends to bind the protein in the plasma.

Table 4.1: Average Plasma water and protein content of sample analysis 1 (unshaken); where each sample was analysed four (4) times

Sample	Mass (g) Average	Water (%) Average	Protein (%) Average	Mass RSD	Water RSD	Protein RSD	Water (%) Max.	Protein (%) Max.
1	0.0337	82.15	17.85	9.43	4.31	19.85	88.04	20.86
2	0.0311	90.39	9.61	12.47	8.52	80.12	95.35	22.94
3	0.0302	89.21	10.79	6.02	4.73	39.08	95.72	14.99
4	0.0311	92.80	7.20	6.32	7.40	65.55	103.97	15.03
5	0.0335	85.21	14.79	1.84	4.77	27.49	90.73	20.75
6	0.0322	88.53	11.47	4.30	4.74	36.58	95.46	15.58
7	0.0313	85.50	14.50	0.14	8.03	47.35	96.81	21.71

When producing a calibration curve of the drug, the results obtained will give a concentration error due to the binding of drug to the plasma. To identify if the proposed hypothesis that error in concentration can occur due to the variation of water content in plasma, two types of analysis were performed. The plasma samples of the patient's water content were analysed when left standing and when shaken to identify if homogenizing the plasma would factor a constant water level in plasma. Seven (7) samples were analysed for both plasma tests and 4 runs were conducted for each sample.

The following results were obtained from the standing plasma sample Analysis 1:

a. Plasma sample 1:(Patient ID)1098435

Runs	Mass in grams	Water%	Protein%
1	0.0306	81.78	18.22
2	0.0326	79.63	20.37
3	0.0390	88.04	11.96
4	0.0325	79.14	20.86
Average	0.0337	82.15	17.85
RSD%	9.43	4.31	19.85

b. Plasma sample 2: (Patient ID)11127901

Runs	Mass in grams	Water%	Protein%
1	0.0316	77.06	22.94
2	0.0281	94.64	5.36
3	0.0274	95.35	4.65
4	0.0372	94.50	5.50
Average	0.0311	90.39	9.61
RSD%	12.47	8.52	80.12

c. Plasma sample 3: (Patient ID)11127901

Runs	Mass in grams	Water%	Protein%
1	0.0322	85.01	14.99
2	0.0294	95.72	4.28
3	0.0272	90.10	9.90
4	0.0320	85.99	14.01
Average	0.0302	89.21	10.79
RSD%	6.02	4.73	39.08

d. Plasma sample 4: (Patient ID)11114623

Runs	Mass in grams	Water%	Protein%
1	0.0344	84.97	15.03
2	0.0301	91.66	8.34
3	0.0294	90.60	9.40
4	0.0303	103.97	0
Average	0.0311	92.80	7.20
RSD%	6.32	7.40	65.55

e. Plasma sample 5: (Patient ID)10984359

Runs	Mass in grams	Water%	Protein%
1	0.0331	85.33	14.67
2	0.0329	85.53	14.47
3	0.0336	90.73	9.27
4	0.0345	79.25	20.75
Average	0.0335	85.21	14.79
RSD%	1.84	4.77	27.49

f. Plasma sample 6: (Patient ID)10984359

Runs	Mass in grams	Water%	Protein%
1	0.0339	84.42	15.58
2	0.0316	86.26	13.74
3	0.0303	88.01	11.99
4	0.0331	95.46	4.54
Average	0.0322	88.53	11.47
RSD%	4.30	4.74	36.58

g. Plasma sample 7: (Patient ID)1114623

Runs	Mass in grams	Water%	Protein%
1	0.0313	83.10	16.90
2	0.0313	78.29	21.71
3	0.0313	96.81	3.19
4	0.0314	83.80	16.20
Average	0.0313	85.50	14.50
RSD%	0.14	8.03	47.35

Figure 4.5: Sample analysis 1 table data: 4 runs were performed for 7 samples to analyse the water content in blood plasma proteins. a) Sample 1 Patient ID (1098435), b) Sample 2 Patient ID (11127901), c) Sample 3 Patient ID (11127901), d) Sample 4 Patient ID (1114623), e) Sample 5 Patient ID (10984359), f) Sample 6 Patient ID (10984359), g) Sample 7 Patient ID (1114623). Each figure contains the mass of the samples, the %water, and the calculated protein content. Each figure indicates the average and relative standard deviation for the mass, %water and protein content.

Table 4.2: Plasma water and protein content sampled (vortexed), where each sample was analysed four (4) times

Sample	Mass (g) Average	Water (%) Average	Protein (%) Average	Mass RSD	Water RSD	Protein RSD	Water (%) Max.	Protein (%) Max.
1	0.0351	83.52	16.48	15.96	9.90	50.14	96.90	23.79
2	0.0309	84.47	15.53	3.00	4.59	25.78	88.26	22.01
3	0.0365	84.35	15.65	8.37	1.61	8.70	86.30	17.55
4	0.0320	86.07	13.93	5.55	2.35	14.52	88.44	17.02
5	0.0370	85.54	14.46	17.69	9.94	58.82	97.49	26.55
6	0.0347	86.22	13.78	4.87	3.12	19.52	89.35	16.99
7	0.0363	85.94	14.06	8.33	9.34	57.65	97.28	22.01

The protein values obtained from the water determination results were calculated using a simple mathematical equation:

Plasma% = water % + protein % = 100 %.....**Equation 4.1**

Therefore

Protein % = 100% - water %

When analysing the water content for both standing and vortexed plasma samples, one of the objectives was to identify if the variation in the plasma volume or mass used to analyse the water content affected the water results. It was observed that the water percentage determined from the sample was independent of the mass of plasma used.

The following results were obtained from the vortexed plasma sample Analysis 2:

a. Plasma sample 1:(Patient ID) 11127901			
Runs	Mass in grams	Water%	Protein%
1	0.0352	77.14	22.86
2	0.0344	76.21	23.79
3	0.0275	96.90	3.10
4	0.0433	83.82	16.18
Average	0.0351	83.52	16.48
RSD%	15.96	9.90	50.14

b. Plasma sample 2: (Patient ID) 11114623			
Runs	Mass in grams	Water%	Protein%
1	0.0305	85.97	14.03
2	0.0301	85.67	14.33
3	0.0306	88.26	11.33
4	0.0325	77.99	22.01
Average	0.0309	84.47	15.53
RSD%	3.00	4.59	25.78

c. Plasma sample 3: (Patient ID) 10984359			
Runs	Mass in grams	Water%	Protein%
1	0.0340	84.35	15.65
2	0.0349	84.29	15.71
3	0.0353	86.30	13.70
4	0.0417	82.45	17.55
Average	0.0365	84.35	15.65
RSD%	8.37	1.61	8.70

d. Plasma sample 4: (Patient ID) 10984359			
Runs	Mass in grams	Water%	Protein%
1	0.0296	88.44	11.56
2	0.0311	85.74	14.26
3	0.0342	82.98	17.02
4	0.0331	87.12	12.88
Average	0.0320	86.07	13.93
RSD%	5.55	2.35	14.52

e. Plasma sample 5: (Patient ID) 11114623			
Runs	Mass in grams	Water%	Protein%
1	0.0356	86.02	13.98
2	0.0336	85.20	14.80
3	0.0480	73.45	26.55
4	0.0309	97.49	2.51
Average	0.0370	85.54	14.46
RSD%	17.69	9.94	58.82

f. Plasma sample 6: (Patient ID) 11114623			
Runs	Mass in grams	Water%	Protein%
1	0.0356	84.15	15.85
2	0.0341	83.01	16.99
3	0.0322	88.36	11.64
4	0.0367	89.35	10.65
Average	0.0347	86.22	13.78
RSD%	4.87	3.12	19.52

g. Plasma sample 7: (Patient ID)1114623			
Runs	Mass in grams	Water%	Protein%
1	0.0407	77.99	22.01
2	0.0374	97.28	2.72
3	0.0329	89.72	10.28
4	0.0342	78.77	21.23
Average	0.0363	85.94	14.06
RSD%	8.33	9.34	57.65

Figure 4.6: Sample analysis 2 table data: 4 runs were performed for 7 samples to analyse the water content in blood plasma proteins. a) Sample 1 Patient ID (11127901), b) Sample 2 Patient ID (1114623), c) Sample 3 Patient ID (10984359), d) Sample 4 Patient ID (10984359), e) Sample 5 Patient ID (1114623), f) Sample 6 Patient ID (1114623), g) Sample 7 Patient ID (1114623). Each figure contains the mass of the samples, the %water, and the calculated protein content. Each figure indicates the average and relative standard deviation for the mass, %water and protein content.

As indicated in figure 4.5 g) of sample Analysis 1 of plasma sample 7:1114623, for runs 1-4, masses of 0.0313, 0.0313, 0.0313 and 0.0314 g of plasma were used with a relative standard deviation of 0.14%. If the water content was dependent on the mass of the plasma used, the water percentage should be constant. However, the water percentage for the masses obtained varied and was 83.10 %, 78.29 %, 96.81 % and 83.80 % respectively. Another observation in figure 4.6 a) of sample Analysis 2 of plasma sample 1:11127901 to support this finding was that the water percentage of a lower mass of 0.0275 in run 3 yielded a higher water content percentage compared to runs 1, 2 and 4 which yielded lower water content percentages.

As a result of this observation, it can be confirmed that the water content percentage determined is independent of the mass of plasma used. The main aim of this study was to determine if the accuracy of plasma used from a specific patient varied in protein content. From the results of Analysis 1 for the standing plasma, it was observed that the water content percentage for each sample in runs 1-4 varied. This is an important finding because plasma is used in analytical standards for blood analysis of the patient to determine the concentration. Hence, when the water content varies in the plasma the protein content varies as well. This could lead to error in calibration curves as well as error in the extrapolation of concentration results per patient. The variation in water to protein content ratio will also cause an increase or decrease in the gradient of the calibration curve validated which will further cause erroneous results. The protein content also plays an important role when preparing standards for validation because the drug could have the ability to bind to the protein. According to the literature, the theoretical plasma content is made up of about 93 % water [144] to 7 % protein. For sample Analysis 1, samples 1-7 per 4 runs for each sample, the average water content percentage ranged from 82.15 to 92.80%. The average calculated protein content (Equation 4.1) for analysis 1 of samples 1-7 was indicated in table 4.1. The average relative standard deviation of samples 1-7 were 19.85%, 80.12%, 39.08%, 65.55%, 27.49%, 36.58%, 47.35%. This indicated that the deviations in protein content between sample runs were large and that the protein content in analysis 1 varied.

From the results of Analysis 2 for the vortexed samples, it was observed that the water content percentage varied as well. For sample Analysis 2, samples 1-7, the water content percentage per four runs for each sample had an average range between 83.52 and 86.22 % which is much smaller compared to the range of the samples from Analysis 1. However, the difference in range cannot confirm that shaking of the samples is the reason for the smaller range between the two analysis methods. The deviation in water content percentage results indicates that when preparing a standard for calibration curves the area under the curve produced at a specific concentration could lead to incorrect results as indicated in Figure 3.3 in chapter 3 (area vs concentration). To alleviate the error of results it would be a requirement to determine the water percentage of each patient's plasma as well as develop a correction factor for the resulted deviation to the literature-based water content in

plasma. From both analysis methods, most of the results obtained were below the literature value of about 93 % water content present in plasma [144]. The average calculated protein content (Equation 4.1) for analysis 2 of samples 1-7 was indicated in table 4.2. The average relative standard deviation of samples 1-7 were 50.14%, 25.78 %, 8.70%, 14.52%, 58.82%, 19.52%, 57.65%. This indicated that the deviations in protein content between sample runs were large and that the protein content in analysis 2 varied aswell and vortexing samples has no effect on when determining plasma protein content.

According to a study of blood plasma content, disorders such as hyperproteinaemia and hyperlipidaemia can be the result of the relative decrease in the water content of plasma and an increase in plasma protein [144]. When conducting clinical studies, these types of disorders could result in incorrect data being obtained. The increase in protein content also affects the sodium concentration in the plasma, since the sodium ion is only present in the water content and the sodium concentration impacts the water content in blood [144]. Hence, the sodium content present in plasma can be used to determine the water content present in blood plasma. Therefore, when the body reabsorbs sodium into the blood the sodium ion gets transported by the water which is absorbed back into the blood circulatory system through the function of the kidneys. If the plasma is extracted from a patient when the sodium level of that patient is low and the water content in the plasma is low, the protein content in the plasma will have a higher concentration ratio [144]. Hence, more of the drug that can bind to the protein in the plasma will bind, leading to erroneous results when conducting LCMS calibration for detection of concentration.

4.5. Conclusion to the Karl Fischer data

Plasma is an important factor to consider in therapeutic drug monitoring of TB patients because it is evident from the results above that the plasma of a single patient and of different patients varies in plasma water content. Therefore, if a plasma calibrator (when compared to a patient with a lower or higher plasma water content) is used, the concentration result of drug present in the patient sample will be inaccurate, due to an increased or decreased amount of drug bound to the protein content. Hence, plasma protein binding interaction should not be considered as a negligible factor during TB clinical trials because it could lead patients to anti-TB drug resistivity, poor absorption, and distribution levels of drugs.

In Conclusion to the Karl Fischer analysis of plasma, the experimental error of the method was very high and was not acceptable for the purpose of analysis of the water/protein content within human

plasma. It is also not possible for a patient to have water content of their plasma of 103% or 77 %. Therefore the results are inconclusive of deviation of the protein/water ratio of human plasma and further research was required to proof these claims. We decided it is better to determine the plasma protein content directly.

4.6 Experimental Protocol: Plasma Protein determination

The data was supplied to us by the SU. CAF Proteomics. laboratory. The protein levels were determined in patient plasma samples to calculate the dilutions needed for Proteomic analysis by LCMS which will be used in a COVID study of Prof Resia Pretorius. Department Physiology. Stellenbosch University. The principal investigator Prof Resia Pretorius gave permission for the data to be used as illustration of what typical patient plasma would look like. Ethical clearance for the study of Prof Pretorius research is in place.

4.6.1 Method

Plasma samples were diluted 20 fold in ammonium bicarbonate (20 mM) and the absorbance measured at 280 nm using a Themo Nanodrop system which calculates the protein concentration based on the absorbance. Single factor ANOVA was performed using the Add on of Microsoft Excel version 2102 with an alpha value of 0.05 to determine of the differences are significant. The statistical analysis was repeated using GraphPad Prism 5, using One-way Anova with Bonferonni's multiple comparison test.

4.7 Results

Table 4.3: Protein concentrations (mg/L) of plasma samples determined by Thermo Nanodrop system

Sample	Conc 1	Conc 2	Conc 3	Minimum	25% Percentile	Median	75% Percentile	Maximum	Mean	Std. Dev.	Std. Error	Lower 95% CI	Upper 95% CI
CL13	55.96	58.54	59.26	56.0	56.0	58.5	59.3	59.3	57.9	1.7	1.0	53.6	62.2
CL14	62.82	72.24	66.30	62.8	62.8	66.3	72.2	72.2	67.1	4.8	2.8	55.3	79.0
CL15	64.98	63.54	61.48	61.5	61.5	63.5	65.0	65.0	63.3	1.8	1.0	59.0	67.7
CL16	43.34	46.82	42.94	42.9	42.9	43.3	46.8	46.8	44.4	2.1	1.2	39.1	49.7
CL17	51.88	55.00	55.94	51.9	51.9	55.0	55.9	55.9	54.3	2.1	1.2	49.0	59.6
CL18	82.34	87.28	88.44	82.3	82.3	87.3	88.4	88.4	86.0	3.2	1.9	78.0	94.1
CL19	27.64	26.30	26.26	26.3	26.3	26.3	27.6	27.6	26.7	0.8	0.5	24.8	28.7
CL20	90.00	89.30	91.68	89.3	89.3	90.0	91.7	91.7	90.3	1.2	0.7	87.3	93.4
CL21	95.64	96.02	99.86	95.6	95.6	96.0	99.9	99.9	97.2	2.3	1.4	91.4	103.0
CL22	98.06	96.60	96.74	96.6	96.6	96.7	98.1	98.1	97.1	0.8	0.5	95.1	99.1
CL23	98.78	97.36	95.70	95.7	95.7	97.4	98.8	98.8	97.3	1.5	0.9	93.5	101.0
CL24	70.88	67.70	71.20	67.7	67.7	70.9	71.2	71.2	69.9	1.9	1.1	65.1	74.7
CL25	67.40	68.52	71.00	67.4	67.4	68.5	71.0	71.0	69.0	1.8	1.1	64.4	73.5
CL26	116.8	128.7	126.8	117.0	117.0	127.0	129.0	129.0	124.0	6.4	3.7	108.0	140.0
CL27	72.92	64.14	76.30	64.1	64.1	72.9	76.3	76.3	71.1	6.3	3.6	55.5	86.7
LCR54	107.5	108.9	107.8	108.0	108.0	108.0	109.0	109.0	108.0	0.7	0.4	106.0	110.0
LCR55	46.22	43.12	54.72	43.1	43.1	46.2	54.7	54.7	48.0	6.0	3.5	33.1	62.9
LCR56	60.08	56.30	67.92	56.3	56.3	60.1	67.9	67.9	61.4	5.9	3.4	46.7	76.2
LCR57	45.96	49.26	47.78	46.0	46.0	47.8	49.3	49.3	47.7	1.7	1.0	43.6	51.8
LCR58	53.46	58.52	58.06	53.5	53.5	58.1	58.5	58.5	56.7	2.8	1.6	49.7	63.6
LCR59	61.64	62.50	61.30	61.3	61.3	61.6	62.5	62.5	61.8	0.6	0.4	60.3	63.3
LCR60	43.64	49.42	42.16	42.2	42.2	43.6	49.4	49.4	45.1	3.8	2.2	35.5	54.6
LCR63	66.78	69.72	71.06	66.8	66.8	69.7	71.1	71.1	69.2	2.2	1.3	63.7	74.6
LCR65	63.78	59.46	55.98	56.0	56.0	59.5	63.8	63.8	59.7	3.9	2.3	50.0	69.4

LCR66	49.46	42.72	42.06	42.1	42.1	42.7	49.5	49.5	44.7	4.1	2.4	34.6	54.9
LCR67	35.60	31.98	23.78	23.8	23.8	32.0	35.6	35.6	30.5	6.1	3.5	15.4	45.5
LCR68	47.22	43.00	47.56	43.0	43.0	47.2	47.6	47.6	45.9	2.5	1.5	39.6	52.2
LCR70	61.08	60.92	61.04	60.9	60.9	61.0	61.1	61.1	61.0	0.1	0.0	60.8	61.2
LCR43	52.84	54.28	53.06	52.8	52.8	53.1	54.3	54.3	53.4	0.8	0.4	51.5	55.3
LCR64	58.16	62.08	57.58	57.6	57.6	58.2	62.1	62.1	59.3	2.5	1.4	53.2	65.4
LCR71	30.12	32.48	37.88	30.1	30.1	32.5	37.9	37.9	33.5	4.0	2.3	23.6	43.4
LCR72	61.48	64.38	66.18	61.5	61.5	64.4	66.2	66.2	64.0	2.4	1.4	58.1	69.9
LCR73	61.66	61.02	60.86	60.9	60.9	61.0	61.7	61.7	61.2	0.4	0.2	60.1	62.2
LCR74	47.36	44.04	41.58	41.6	41.6	44.0	47.4	47.4	44.3	2.9	1.7	37.1	51.5
LCR75	45.52	44.54	44.52	44.5	44.5	44.5	45.5	45.5	44.9	0.6	0.3	43.4	46.3
LCR76	54.82	58.64	59.94	54.8	54.8	58.6	59.9	59.9	57.8	2.7	1.5	51.2	64.4
LCR77	55.54	55.24	58.10	55.2	55.2	55.5	58.1	58.1	56.3	1.6	0.9	52.4	60.2
LCR78	58.06	57.42	57.18	57.2	57.2	57.4	58.1	58.1	57.6	0.5	0.3	56.4	58.7
LCR131	70.40	73.60	74.58	70.4	70.4	73.6	74.6	74.6	72.9	2.2	1.3	67.4	78.3
LCR135	68.54	74.94	63.42	63.4	63.4	68.5	74.9	74.9	69.0	5.8	3.3	54.6	83.3
LV134	45.56	47.62	45.34	45.3	45.3	45.6	47.6	47.6	46.2	1.3	0.7	43.0	49.3
LV136	48.52	44.96	45.68	45.0	45.0	45.7	48.5	48.5	46.4	1.9	1.1	41.7	51.1
LV138	39.68	39.18	38.48	38.5	38.5	39.2	39.7	39.7	39.1	0.6	0.3	37.6	40.6
LV139	47.66	46.54	51.24	46.5	46.5	47.7	51.2	51.2	48.5	2.5	1.4	42.4	54.6
LV140	51.68	52.60	46.92	46.9	46.9	51.7	52.6	52.6	50.4	3.1	1.8	42.8	58.0
LV141	44.82	39.28	38.86	38.9	38.9	39.3	44.8	44.8	41.0	3.3	1.9	32.7	49.2
LV142	31.22	31.16	32.58	31.2	31.2	31.2	32.6	32.6	31.7	0.8	0.5	29.7	33.6
LV143	51.26	54.60	56.48	51.3	51.3	54.6	56.5	56.5	54.1	2.6	1.5	47.5	60.7
LV144	49.62	53.00	50.74	49.6	49.6	50.7	53.0	53.0	51.1	1.7	1.0	46.8	55.4
LV145	59.42	59.80	65.80	59.4	59.4	59.8	65.8	65.8	61.7	3.6	2.1	52.8	70.6

Sample	Conc 1	Conc 2	Conc 3	Minimum	25% Percentile	Median	75% Percentile	Maximum	Mean	Std. Dev.	Std. Error	Lower 95% CI	Upper 95% CI
LV146	28.88	17.90	17.80	17.8	17.8	17.9	28.9	28.9	21.5	6.4	3.7	5.7	37.3
LV161	43.06	49.26	48.54	43.1	43.1	48.5	49.3	49.3	47.0	3.4	2.0	38.5	55.4
LV163	54.34	56.30	54.84	54.3	54.3	54.8	56.3	56.3	55.2	1.0	0.6	52.6	57.7
LV162	36.38	22.53	25.74	22.5	22.5	25.7	36.4	36.4	28.2	7.3	4.2	10.2	46.2
LV164	30.22	31.30	28.56	28.6	28.6	30.2	31.3	31.3	30.0	1.4	0.8	26.6	33.5
LV165	38.02	38.80	38.46	38.0	38.0	38.5	38.8	38.8	38.4	0.4	0.2	37.5	39.4
LV167	46.46	48.42	48.10	46.5	46.5	48.1	48.4	48.4	47.7	1.1	0.6	45.0	50.3
LV168	35.66	33.64	31.46	31.5	31.5	33.6	35.7	35.7	33.6	2.1	1.2	28.4	38.8
LV176	71.42	70.76	70.76	70.8	70.8	70.8	71.4	71.4	71.0	0.4	0.2	70.0	71.9
CV125(L)	67.42	67.04	68.12	67.0	67.0	67.4	68.1	68.1	67.5	0.5	0.3	66.2	68.9
CV126(L)	44.44	40.38	41.46	40.4	40.4	41.5	44.4	44.4	42.1	2.1	1.2	36.9	47.3
CV130	59.06	61.20	65.14	59.1	59.1	61.2	65.1	65.1	61.8	3.1	1.8	54.1	69.5
LV180	55.72	48.14	54.36	48.1	48.1	54.4	55.7	55.7	52.7	4.0	2.3	42.7	62.8
LV183	55.42	50.36	48.94	48.9	48.9	50.4	55.4	55.4	51.6	3.4	2.0	43.1	60.0

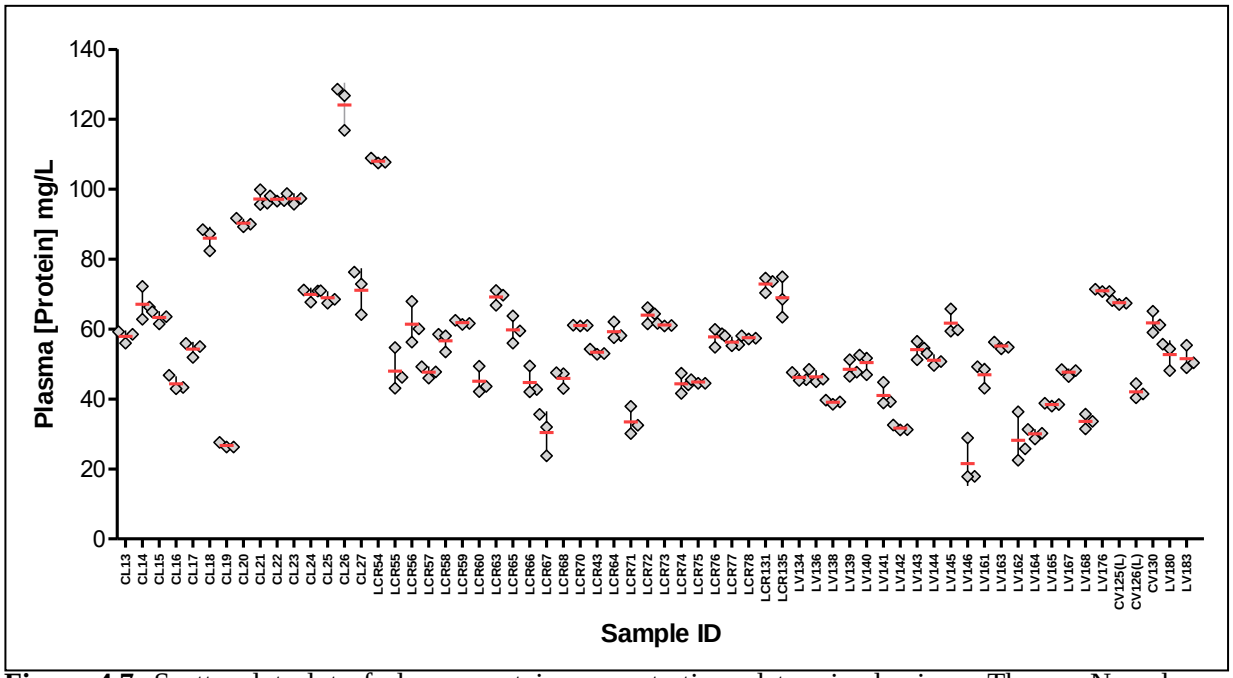

Figure 4.7: Scatter dot plot of plasma protein concentrations determined using a Thermo Nanodrop system in triplicate showing the variance between samples. The error bars show standard deviation and the red bar the mean of the triplicate determination.

Table 4.4: One way Anova global statistical comparison of the [plasma protein] in sample pairs using Bonferonni's multiple comparison test**One-way analysis of variance**

P value	P<0.0001		
P value summary	***		
Are means signif. different? (P < 0.05)	Yes		
Number of groups	64		
F	121		
R^2	0.984		
ANOVA Table	SS	Df	MS
Treatment (between groups)	73800	63	1170
Residual (within groups)	1240	128	9.67
Total	75100	191	

4.8 Discussion and Conclusion

The results from the single factor ANOVA analysis (results not shown) correlated well with the second analysis using One-way Anova with Bonferonni's multiple comparison test. These statistical analyses both indicate that the source of variation is significantly larger between samples than between the replicate determination in each sample. In Figure 4.7 and Table 4.3 the low scatter and low standard deviation is showed and confirms that the replicate variance is within analytical error. One way/Single point Anova analysis of the data confirmed the variance are between sample groups (Table 4.4) The details of this sample to sample variance are given in Table 4.5 which can be viewed in addendum B.

Chapter 5

Computational and In Vitro Evaluation of Plasma Protein Binding of 1st Line Anti-TB Drugs

Plasma proteins are an important component of blood, as they play an important role in the transportation of xenobiotic substances within the body [148]. When drugs are transported in the blood to the target site of interaction, the drug is present in the plasma for a specific time before reaching the targeted site of action [149]. During the transportation period of the drug to the target site, the free drug in the plasma could experience strong or weak binding interactions with the protein present in the plasma, such as HSA and many other proteins [149]. Strong interactions can lead to a decrease in the overall free drug concentration, while weak binding interaction with plasma can lead to degradation of the drug administered or poor drug distribution [149]. These binding interactions could lead to drug resistance by reducing the intensity of the pharmacological effect of the drug and increased toxicity of the drug in the body caused by the action of the drug, or if the drug is degraded to an active metabolite form [150]. Hence it is of importance in pharmacology to understand and identify the binding interactions of drugs and plasma in the blood.

5. Research Question: Can the use of unique validation parameters and analytical methods improve drug-plasma assay accuracy of therapeutic drug monitoring TB clinical trials by determining the extent and mechanism of plasma protein-binding to first-line anti-TB drugs?

5.1 Aims and Objectives

1. To determine if drug-plasma protein binding interactions occur, and the binding affinity of rifampicin (RIF), isoniazid (INH), ethambutol (ETH), pyrazinamide (PYR) and desacetyl-rifampicin (D-RIF), by using computational modeling, experimental fluorescence excitation and ultraviolet absorbance spectroscopy to provide evidence and insight for possible poor anti-TB drug absorption levels and therapeutic effect in TB patients.
2. To investigate drug-HSA binding interaction using computational modeling techniques to predict possible drug binding conformations, intermolecular chemical interactions with HSA amino acids and thermodynamic predicted properties of each drug.
3. Assess if the drug binds to plasma protein using fluorescence spectroscopy.
4. Determine the quenching mechanism of each drug with plasma protein.
5. Determine the binding constants of each drug with plasma to ascertain the change in enthalpy, entropy and Gibbs free energy.

6. To compare the computational intermolecular interactions and thermodynamic properties with the fluorescence experimental intermolecular interactions and thermodynamic properties.
7. Ascertain whether a wavelength shift occurs with plasma for each drug, to identify if a change in the plasma's protein properties occurs.

In this experiment, the degree of TB drugs binding to human serum albumin (HSA) was assessed to determine the binding affinity of the drug to the plasma protein. The following drugs were assessed: isoniazid (INH), rifampicin (RIF), ethambutol (ETH), pyrazinamide (PYR) and the metabolite 25-desacetyl-rifampicin (D-RIF). Computation drug-protein modeling predictions of anti-TB drugs binding to HSA was performed to determine structural conformation of the anti-TB drugs to HSA aswell as the Gibbs free energy to provide insight to the binding affinity of the drugs to the HSA. Fluorescence spectroscopy and UV spectroscopy methods were used to assess the drug binding interactions with blood plasma.

5.2 Experimental Protocol

5.2.1 Chemicals and reagents

RIF (≥97%), INH (≥99%), ETH (≥99%), PYR (≥99%) and D-RIF (≥96%) certified reference material's was obtained from international supplier Sigma Alderich (Merck, Darmstadt, Germany). The blood used in the experienment was obtained from the Tygerberg Hospital in Bellville, Cape Town South Africa from healthy blood donor patients. Ethics approval was obtained from the Health research committee at the University of Stellenbosch for this study Ref: (X17/04/005). All samples were prepared in Phosphate buffer system with a (pH 7.4 with final concentration of 10 mM PO_4^{3-}, 137 mM NaCl, and 2.7 mM KCl). All reagents used were of analytical grade and Millipore distilled water was used throughout the experiment.

5.2.2 Instrumentation and conditions

MOE and Pymol computer software was used to conduct the computational prediction studies. The Fluorescence and UV spectroscopy studies were conducted using an Omega Fluorostar spectroscopic instrument from BMG LABTECH. The Fluorescence emission spectra ranged from 300-700 nm with an excitation wavelength fixed at 278 nm. The emission spectra were recorded of human blood Plasma with and without each drug. The UV absorbance spectra ranged from 220-650 nm. The absorbance spectra were recorded for human blood plasma with and without drug present. The sample runs were conducted using a 96 well plate. The pH measurements were conducted using a calibrated digital pH meter. All spectra were measured at a temperature range of 298.15 K, 310.15 K, 313.15 K and 318.15 K

5.2.3 Computational pharmacological molecular docking of drug bound to HSA computing data

The computer software for prediction of the possible binding affinity and mode of the drug to HSA used was the molecular operating environment (MOE). The molecular docking studies were performed by using MOE software, which is an interactive molecular graphics program to understand the drug-protein interaction. The structure of the complex was drawn in Chemsketch (http://www.acdlabs.com) and converted to a .pdb file from mol format by Openbabel (http://www.vcclab.org/lab/babel/). The crystal structure of the HSA (PDB ID: 1E7I) was downloaded from the protein data bank (http://www.rcsb.org./pdb). All calculations were performed using a Microsoft PC operating system. Visualization of the docked conformations was performed by using the PyMol molecular graphic program (http://www.pymol.sourceforge.net/).

Each drug was constructed and modeled according to its molecular weight and computational codes were build which corresponded to each drug in question as indicated in the table 5.1 below. These drugs constructed in table 5.1 are known as ligands when docking to the HSA protein. Molecular docking feature of MOE is used to predict how the Van de Waals forces, hydrogen bonding and electrostatic bonding interaction of the ligands to the protein pocket binding site as the ligands spacial position and orientation can be changed in the binding pocket of the host [151,152]. Thereafter a full molecular minimization mechanics can be done using the universal force field to indicate the possible binding interaction energy of the specific drug to the HSA binding site. The aim of docking the drug to HSA was to obtain the conformation of the drug to the HSA binding site and to get the lowest possible enthalpy value [153]. The HSA protein used was HSA PDB-1E7I. The constructed molecular protein modeling was then extracted using the 3D software viewer Pymol. In order to successfully use the MOE and docking software to bind drugs to protein, training was required.

In this computational modeling experiment, 3 ΔH^o values were predicted for each drug at 3 best possible predictions of drug binding interactions with HSA. The bindig site of the drug-HSA interaction was predicted by the MOE software. The entropies, as well as the Gibbs free energies, were calculated via the use of the predicted ΔH^o values generated from the MOE molecular docking software. The predicted temperature used was body temperature of 37 ^oC or 310.15 K.

Table 5.1: Computation molecular smiles used for molecular docking of drugs

ID	Smiles (computational codes for compounds)
INH	C1=CN=CC=C1C(=O)NN
RIF	CC1C=CC=C(C(=O)NC2=C(C3=C(C(=C4C(=C3C(=O)C2=CNN5CCN(CC5)C)C(=O)C(O4)(OC=CC(C(C(C(C(C(C1O)C)O)C)OC(=O)C)C)OC)C)C)O)O)C
D-RIF	CC1C=CC=C(C(=O)NC2=C(C3=C(C(=C4C(=C3C(=O)C2=CNN5CCN(CC5)C)C(=O)C(O4)(OC=CC(C(C(C(C(C(C1O)C)O)C)O)C)OC)C)C)O)O)C
PYR	C1=CN=C(C=N1)C(=O)N
ETH	CCC(CO)NCCNC(CC)CO

5.2.4 Preparation of in vitro drug sample and human plasma protein sample for fluorescence and UV spectroscopy analysis

5.2.4.1 Phosphate buffer saline preparation

PBS was prepared using a 1 x stock solution. One (1) litre was prepared. The reagents in the table below were all dissolved in 800 ml H_2O. The pH of the solution was then adjusted to 7.4 using HCl and a pH meter to measure the pH adjustment. Thereafter, 200 ml of H_2O was added to make up the 1 litre solution. The PBS buffer is quite stable and has been shown to maintain its buffer system for one (1) month. Table 5.2 indicates the masses of reagents used to prepare the phosphate buffer solution.

Table 5.2: Phosphate buffer preparation

Reagent	mass	Final concentration
NaCl	8 g	137 mM
KCl	0.2 g	2.7 mM
Na_2HPO_4	1.44 g	10 mM
KH_2PO_4	0.24 g	1.8 mM

5.2.4.2 Blood plasma extraction

Blood samples were centrifuged at 2550 rpm for 20 minutes (benchtop centrifuge) to remove particulate matter, sediment and to isolate plasma. Plasma was carefully extracted using a clean pasture pipette and transferred into a suitable container (Eppendorf vial) and frozen immediately for preservation. Blood samples were carefully handled and all waste was safetly disposed of in the biohazardous waste.

5.2.4.3 Calculations and dilutions of concentration

Stock solution with a concentration of 100 µg/mL were preparation of INH, RIF, ETH, PYR and D-RIF and RIF-4 in phosphate buffer at pH 7.4

- 10 mg ÷ 0.1L = 100 mg/L
- mg/L is equivalent to ppm
- ppm is equivalent to µg/mL

Therefore 10 mg of each drug was diluted in 100 mL of phosphate buffer at pH 7.4 to make up each 100 µg/mL stock solution

Sample Composition:

Total volume = 2 ml

Total volume = 0.5 ml of plasma + 1.5 sample in phosphate buffer

$C_1V_1=C_2V_2$

Where C represents the mass concentration in µg/ml and V represents the volume in mL

Table 5.3: Dilution concentrations for sample composition of INH, RIF, ETH PYR and D-RIF

C1 (µg/mL)	V1 (mL)	C2 (µg/mL)	V2 (mL)
100	0.6	30	2
100	0.5	25	2
100	0.4	20	2
100	0.3	15	2
100	0.2	10	2
100	0.1	5	2
100	0.02	1	2

5.2.4.4 Sample Preparation for fluorescence and UV spectroscopy analysis

The following drugs: RIF, INH, PYR, ETH, D-RIF and RIF-4 were made up in Phosphate buffer to a concentration of 100µg/ml. Further dilutions were made to each stock solution ranging from 1-30 µg/ml in increments of 5 as indicated in table 5.3. Each dilution contained 0.5 mL of plasma. The total sample volume was 2 mL. Each drug was soluble in the phosphate buffer (pH 7.4 with final concentration of 10 mM PO_4^{3-}, 137 mM NaCl, and 2.7 mM KCl) The samples were analysed using a 96 well plate with the set temperatures of 298.15 K, 310.15 K, 313.15 K, and 318.15 K respectively.

5.2.4.5 Formulas for calculation of thermodynamic and fluorescence parameters

$$\Delta S^\circ = -\frac{\Delta H^\circ}{T} \quad \textbf{Equation 5.1}$$

ΔS° represents the change in S^o (Entropy) of the system; ΔH° represents the change in H^o (Enthalpy) of the system and T represents the temperature of the system. Used for the determination of the thermodynamic parameters of the in vitro fluorescence analysis of drug plasma protein samples.

$$\Delta G^\circ = \Delta H^\circ - T\Delta S^\circ = -RT\ln K \quad \textbf{Equation 5.2}$$

The equation 5.2 above is a representation of the relationship of change in Gibbs free energy (ΔG°) based on T, which represents the temperature, ΔH° which represents the change in enthalpy and ΔS° which is the change in entropy of the system. R represents the gas constant. T represents the temperature of the system and K represents the binding constant of the drug to the plasma protein. This equation was used for the Gibbs free energy determination of the in-vitro Fluorescence data obtained.

$$\frac{Fo}{F} = 1 + Ksv[Q] \quad \textbf{Equation 5.3}$$

Representation of the Stern-Volmer equation, where F_o represents the fluorescence intensity of the chromophore without the presence of the quencher, F represents the fluorescence intensity of the chromophore with the presence of the quencher, Ksv is the quenching constant and [Q] is the concentration of the quencher.

$$Lg\left(\frac{Fo-F}{F}\right) = Lg\ K + n\lg[Q] \quad \textbf{Equation 5.4}$$

Stern-Volmer modification to Lineweaver-Burk equation to a double log equation used to determine the equilibrium constant or binding constant K by plotting $Lg\left(\frac{Fo-F}{F}\right)$ vs lg [Q], of the drug bound to the plasma proteins. Here, n represents the number of binding sites available and [Q] represents the concentration of the drug within the plasma sample.

$$\mathbf{lnK} = \frac{-\Delta \mathbf{H}^{\circ}}{\mathbf{RT}} + \frac{\Delta \mathbf{S}^{\circ}}{\mathbf{R}} \quad \textbf{Equation 5.5}$$

Represents the Van't Hoff equation, where K represents the equilibrium constant of the association constant of the drug bound to the plasma protein, R represents the gas constant, T represents the temperature of the system and ΔH° and ΔH° represent the change in enthalpy and entropy of the system respectively. The thermodynamic parameters were calculated using the Van't Hoff equation 5.5, equation 5.1 as well as the change in the Gibbs free energy equation 5.2.

5.3 Results and Discussion

5.3.1 Molecular docking

The following results obtained as described in the experimental protocol which was a statistical computational prediction of how rifampicin, desacetyl rifampicin, isoniazid, pyrazinamide, and ethambutol would bind to the protein human serum albumin (HSA). This computational modeling provides a three-dimensional (3D) view and the ability to construct how the molecule could bind to HSA. It also provided probabilities of the three (3) ΔH° value of each drug when binding to the different pockets of HSA with a specific structural conformation. Only two probability ΔH° for pyrazinamide was used to mathematical error, however this did not impact the study because the two best predicted probabilities were obtained for pyrazinamide. This computational modeling aims to predict the best and most probable interactions of the drug with the HSA and plasma proteins. The large variation between the predicted ΔH° scores in table 5.4 was because the 3 best probable binding interactions of the drugs to HSA binding sites were predicted. The MOE software predicted the best possible binding sites and structural conformation of the drugs bound to HSA. From the data obtained, it was observed that all the drugs could undergo spontaneous reactions with HSA. This was be predicted by the ΔH° values obtained for each drug by calculation of the ΔS° and the Gibbs free energy as indicated in table 5.4.

5.3.2 Results of computational modeling and binding interactions of drugs to HSA protein

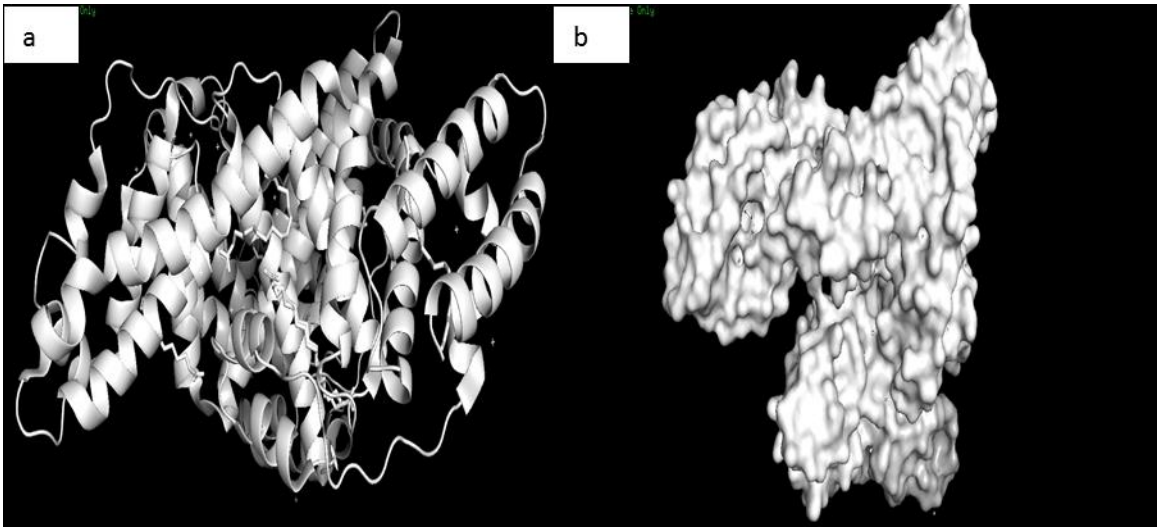

Figure 5.1: a) HSA protein ribbons structure. b) HSA surface topology.

From previous literature studies, it is stated that a negative Gibbs free energy value indicates that the molecule will interact spontaneously with the protein without the need of energy for activation of the binding interactions to take place. When using the Molecular Operating Environment (MOE) software, a prediction is made of how the drug will bind to HSA, as well as of the most probable binding interactions. In this study, the three best possible interactions of each drug – isoniazid (INH), rifampicin (RIF), 25-desacetyl-rifampicin (D-RIF), pyrazinamide (PYR) and ethambutol (ETH) were constructed. The HSA (1E7I) protein structure was obtained from the protein data bank and a cartoon and surface topographical image are illustrated in Figure 5.1 a) and b) respectively. It is of importance to note that the pH environment within the blood is pH 7.4. The following results were obtained:

Table 5.4: Computational modelling Predicted ΔH° results, calculated ΔS° and calculated Gibbs free energy values based on the two or three most probable interactions of the drugs with HSA protein binding site.

Drug	ΔH° (kJ/mol)	ΔS° (kJ/K)	ΔG° (kJ/mol) rounded off to 4 decimals
INH	(1) -25.994383	(1) 0.08381229405	(1) -51.9888
	(2) -22.168131	(2) 0.07147551507	(2) -44.3362
	(3) -16.808249	(3) 0.05419393519	(3) -33.6165
RIF	(1) -52.020626	(1) 0.16772731260	(1) -104.0413
	(2) -37.318169	(2) 0.12032296950	(2) -74.6363
	(3) -23.739071	(3) 0.07654061261	(3) -47.4781
D-RIF	(1) -38.404728	(1) 0.12382630340	(1) -76.8095
	(2) -21.211849	(2) 0.06839222634	(2) -42.4237
	(3) -18.400635	(3) 0.05932817991	(3) -36.8013
PYR	(1) -16.525791	(1) 0.05328322102	(1) -33.0516
	(2) -11.782911	(2) 0.03799100758	(2) -23.5658
	no result obtained	-	-
ETH	(1) -40.259628	(1) 0.12980599060	(1) -80.5190
	(2) -4.5651255	(2) 0.01470660970	(2) -9.1264
	(3) -3.7877724	(3) 0.01221271127	(3) -7.5755

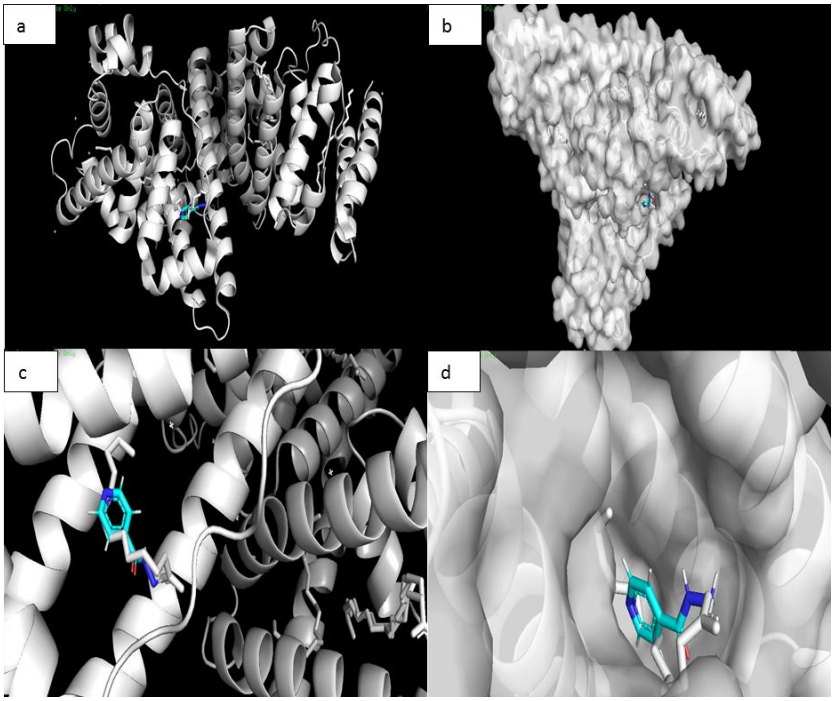

Figure 5.2: a) Isoniazid (INH) conformation 1 binding to HSA ribbon form. b) INH conformation 1 binding to HSA surface topology. c) Image (a) zoomed in. d) Image (b) zoomed in.

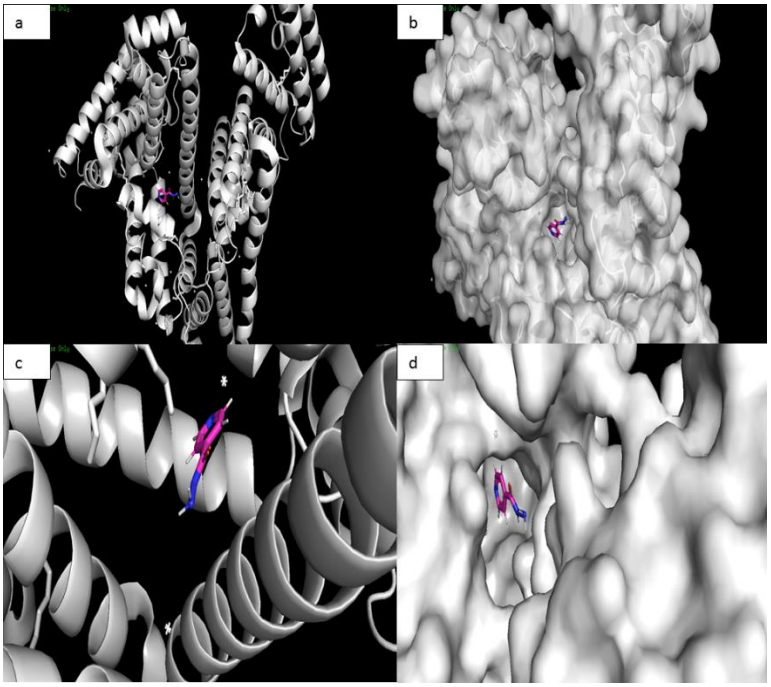

Figure 5.3: a) INH conformation 2 binding to HSA ribbon form. b) INH conformation 2 binding to HSA surface topology. c) Image (a) zoomed in. d) Image (b) zoomed in.

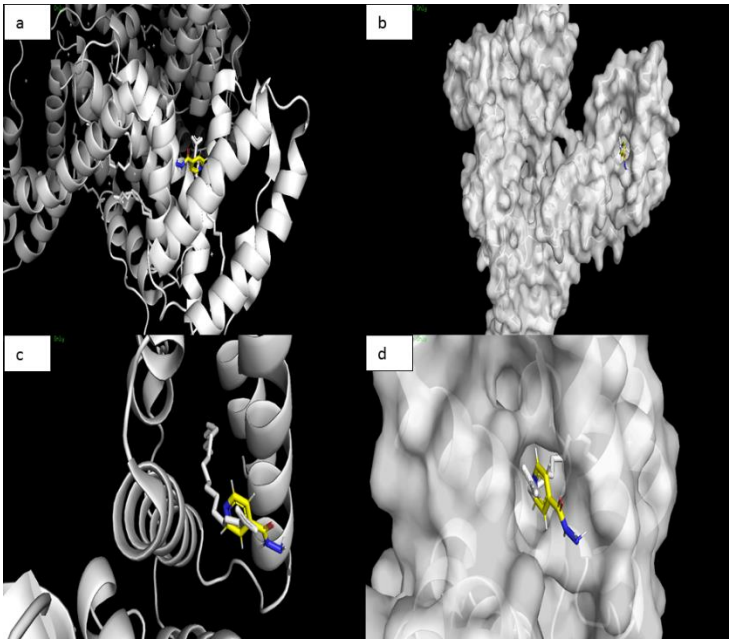

Figure 5.4: a) INH conformation 3 binding to HSA ribbon form. b) INH conformation 3 binding to HSA surface topology. c) Image (a) zoomed in. d) Image (b) zoomed in.

- For INH in Figure 5.2, 5.3 and 5.4 represent the three best probable conformations of drug interactions with the HSA protein.
- Figure 5.16 is a representation of the 2D MOE interaction map of conformations of INH with HSA amino acid terminals.
- In Figure 5.16 a, the hydrogen present on the side chain hydrazine functional group of the INH drug interacts with acidic tyrosine amino acid 161 group present in HSA protein. This indicates that hydrogen bonding is taking place. This interaction occured because the hydroxyl group on the phenol is negatively charged due to deproteination caused by the pH environment of 7.4. The INH hydrazine group in the pH environment is ionized, which allows for the hydrogen interaction to occur between the INH hydrazine group and the tyrosine amino acid hydroxyl group.

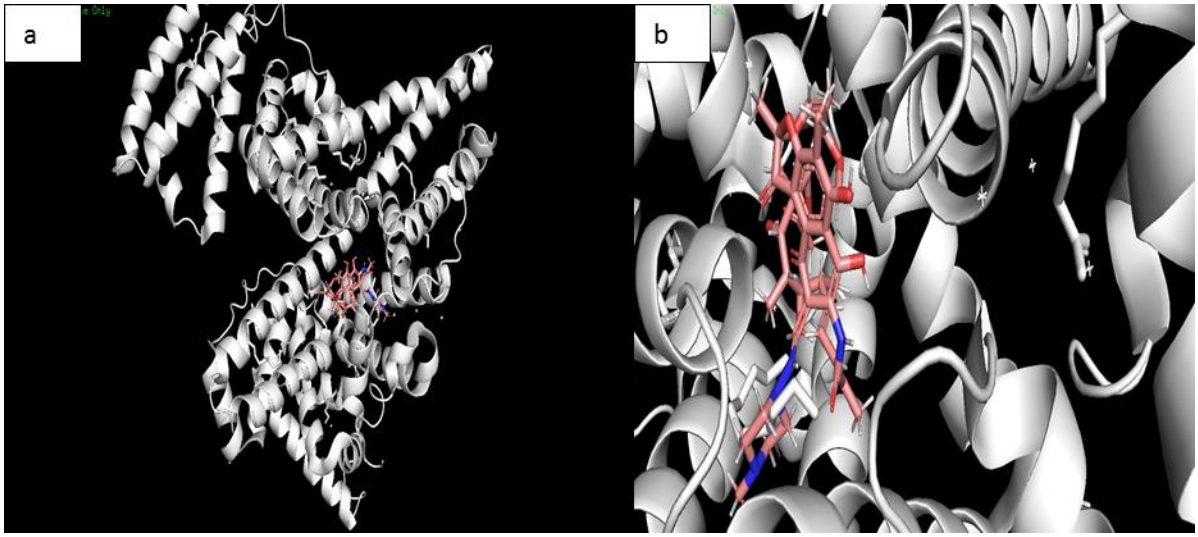

Figure 5.5: a) Rifampicin (RIF) conformation 1 binding to HSA ribbon form. b) RIF conformation 1 binding to HSA surface topology.

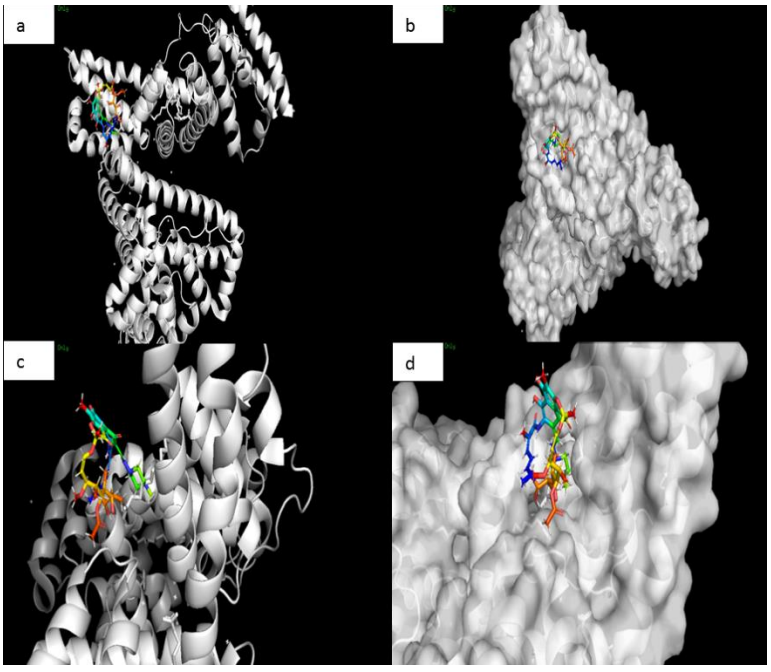

Figure 5.6: a) RIF conformation 2 binding to HSA ribbon form. b) RIF conformation 2 binding to HSA surface topology. c) Image (a) zoomed in. d) Image (b) zoomed in.

- In Figure 5.16 b, the INH molecule is present in the same pocket of the HSA protein as indicated in Figure 5.2 a. However, the INH drug conformation is slightly changed which results in the same hydrogen bonding interaction as with the same amino acid as discussed for

Figure 5.16. The predicted Gibbs free energy value was higher for the Figure 5.16 b MOE binding interaction than the 5.16 a MOE interaction.

- In Figure 5.16 c, the MOE 2d interaction illustrates Van de Waals forces between the hydrogen present on the cyclic group of INH and the aromatic ring present on the polar tyrosine amino acid 150. This interaction could be due to the stability of the aromatic rings of both the amino acid and the INH drug. Therefore, ionization of an aromatic ring would be very unlikely to occur. Furthermore, the Van de Waals interaction could be due to the conformational positing of the drug within the HSA pocket. Another interaction occurs where the nitrogen atom present in the cyclic chain of INH interacts as a side chain donor to the polar cysteine amino acid 253. The cysteine amino acid has a sulfhydryl group present with a pKa of about 8.4. At the pH 7.4 environment, the cysteine amino acid would be in its ionized form – indicating that the sulfhydryl group undergoes deprotonation which will result in a negatively charged. This allows for the polar interaction between INH and cysteine.

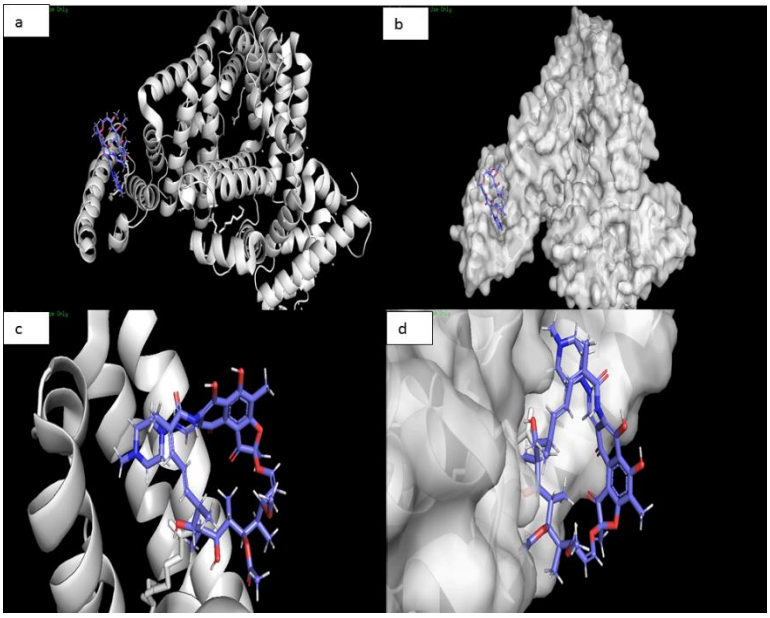

Figure. 5.7: a) RIF conformation 3 binding to HSA ribbon form. b) RIF conformation 3 binding to HSA surface topology. c) Image (a) zoomed in. d) Image (b) zoomed in.

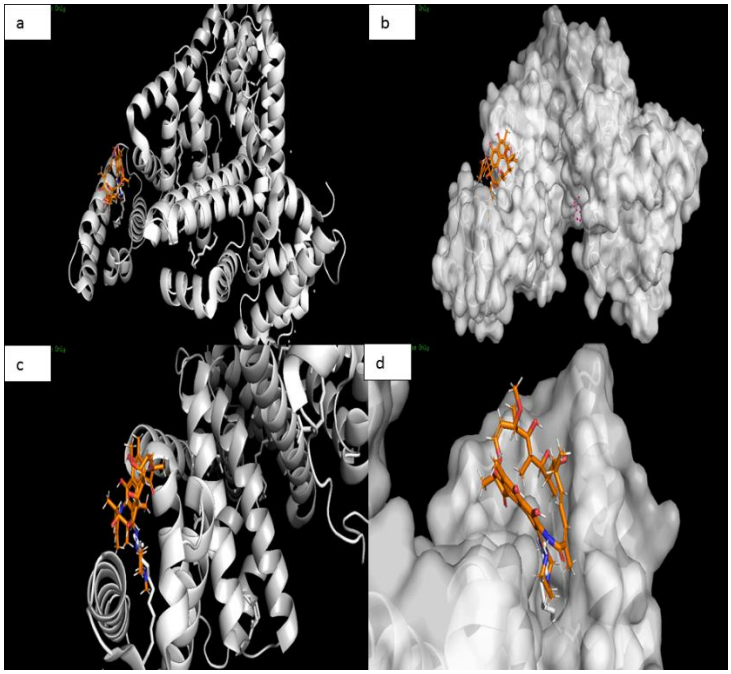

Figure 5.8: a) D-RIF conformation 1 binding to HSA ribbon form. b) D-RIF conformation 1 binding to HSA surface topology. c) Image (a) zoomed in. d) Image (b) zoomed in.

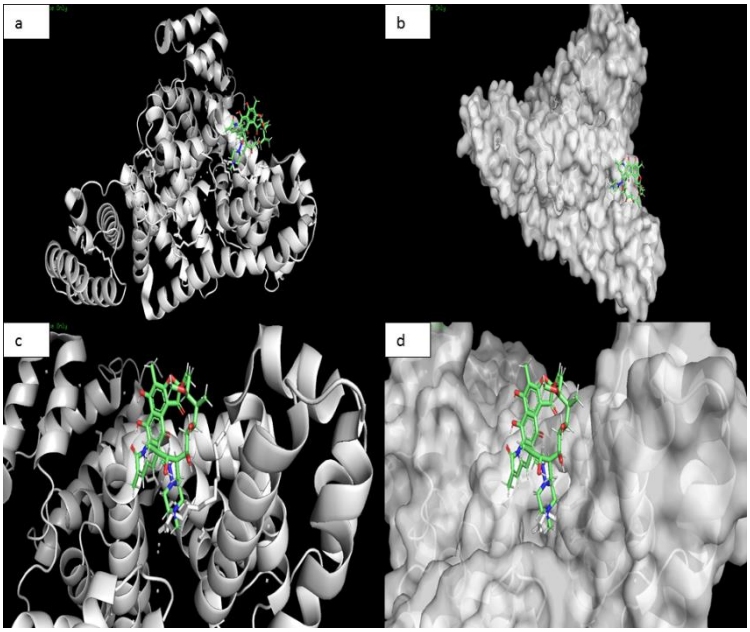

Figure 5.9: a) D-RIF conformation 2 binding to HSA ribbon form. b) D-RIF conformation 2 binding to HSA surface topology. c) Image (a) zoomed in. d) Image (b) zoomed in.

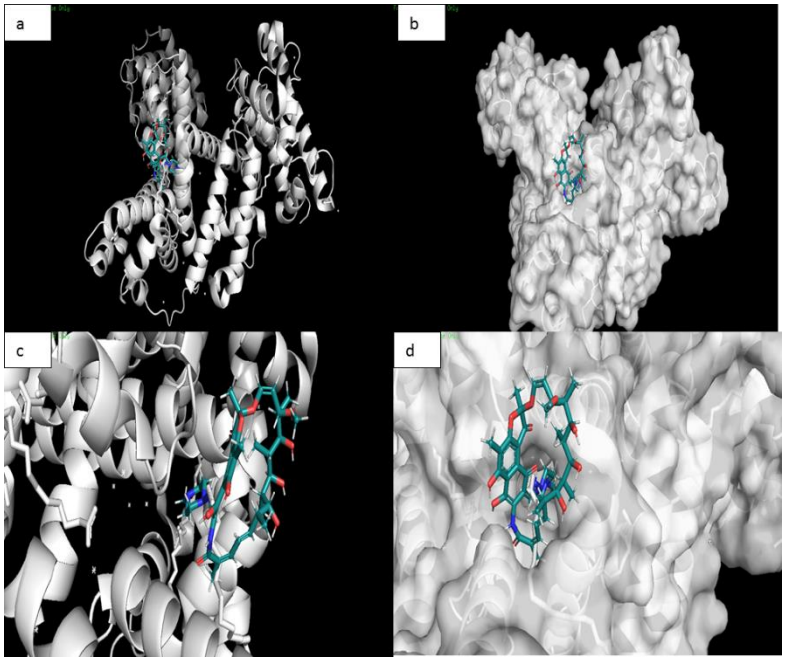

Figure 5.10: a) D-RIF conformation 3 binding to HSA ribbon form. b) D-RIF conformation 3 binding to HSA surface topology. c) Image (a) zoomed in. d) Image (b) zoomed in.

- Figure 5.5, 5.6 and 5.7 represent the three best conformation of drug RIF's interaction with the HSA protein.
- Figure 5.17 illustrates the 2D MOE interaction map of conformation of RIF with HSA amino acid terminals.
- Figure 5.17 a indicates hydrogen bonding of an OH group present on the rifampicin drug with the polar exposed aspartic amino acid 451 residue of HSA. Aspartic acid is a few of the only standard amino acids which contained a carboxylic acid group in the side chain of the amino acid. In the pH 7.4 environment, the functional groups of aspartic acid are usually negatively charged due to the approximate pKa value of 4. The pKa for the hydroxyl group of RIF is 1.7. Therefore, this will allow for hydrogen bonding to occur between the two polar molecules rifampicin and the amino acid aspartic acid. In Figure 5.17 b, the hydrogen present on position 25 of the rifampicin drug interacts with the polar glutamate amino acid 153. Many of the functional groups of the rifampicin drug are exposed as well as many of the HSA amino acids at the specific pocket. The interaction hydrogen present on position 25 of desacetyl rifampicin and glutamate acid has the same type of chemical explanation explained for the interaction between rifampicin and aspartic acid.

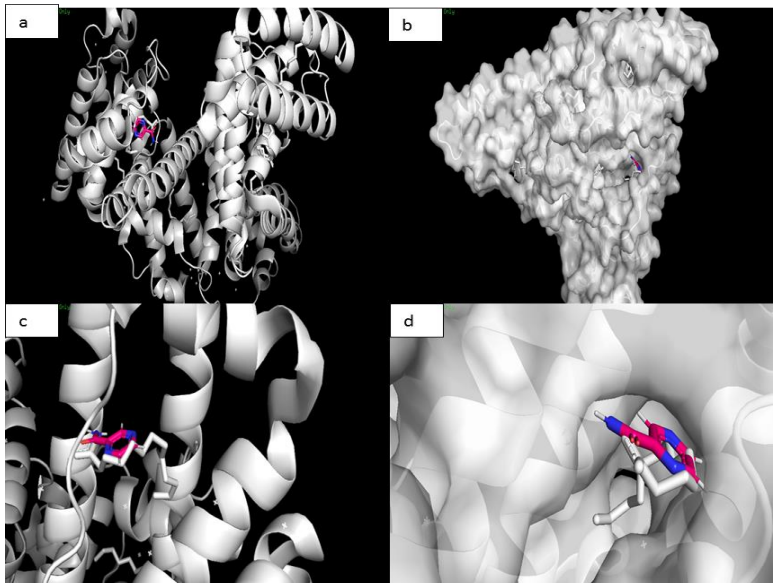

Figure 5.11: a) Pyrazinamide (PYR) conformation 1 binding to HSA ribbon form. b) PYR conformation 1 binding to HSA surface topology. c) Image (a) zoomed in. d) Image (b) zoomed in.

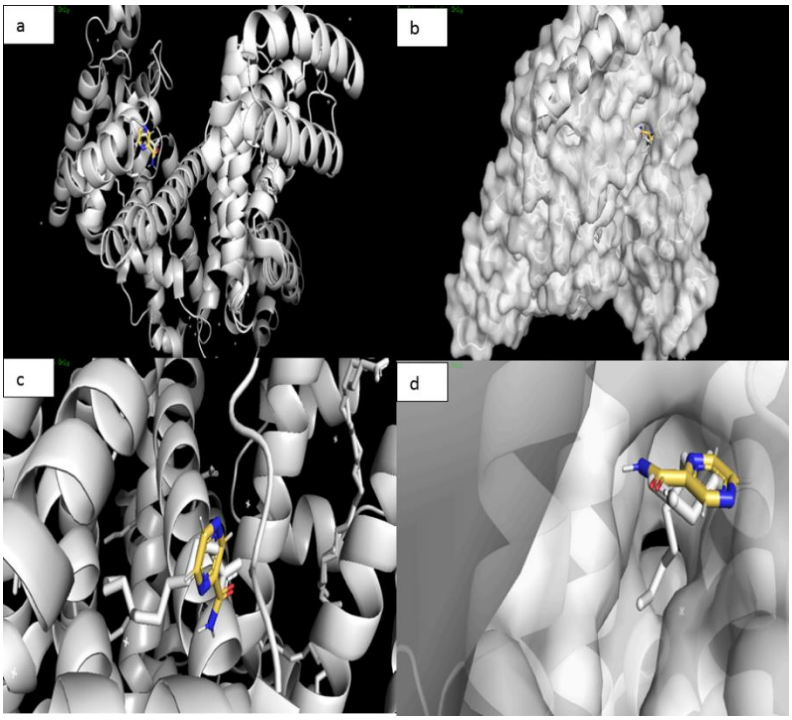

Figure 5.12: a) PYR conformation 2 binding to HSA ribbon form. b) PYR conformation 2 binding to HSA surface topology. c) Image (a)) zoomed in. d) Image (b) zoomed in.

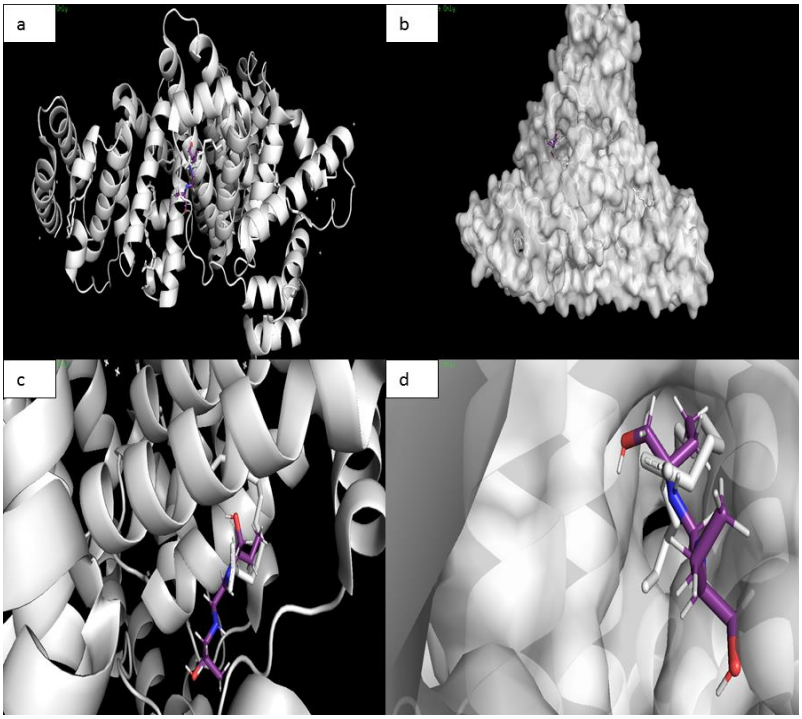

Figure 5.13: a) Ethambutol (ETH) conformation 1 binding to HSA ribbon form. b) ETH conformation 1 binding to HSA surface topology. c) Image (a) zoomed in. d) Image (b) zoomed in.

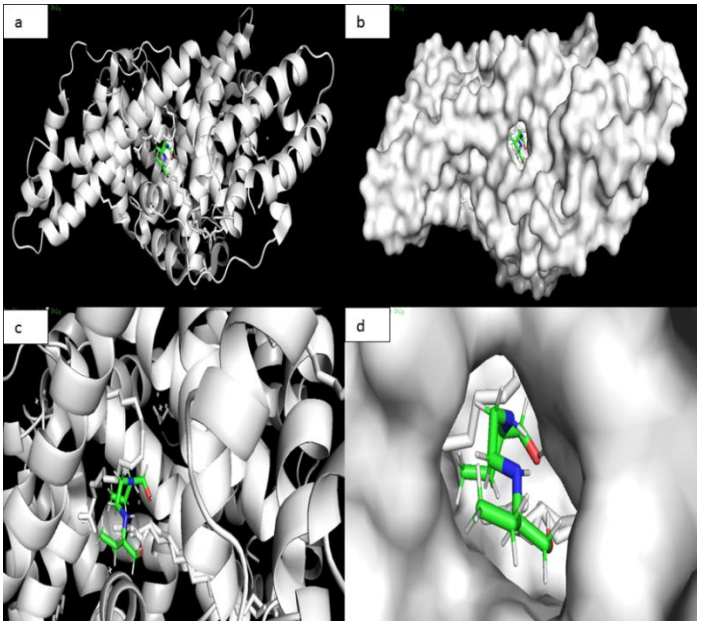

Figure 5.14: a) ETH conformation 2 binding to HSA ribbon form. b) ETH conformation 2 binding to HSA surface topology. c) Image (a) zoomed in. d) Image (b) zoomed in.

- In Figure 5.17 b the rifampicin structure is slightly shifted within the HSA pocket, which results in the same type of MOE interaction as discussed for Figure 5.17 a. However, the MOE interaction from Figure 5.17 b had a higher Gibbs free energy value.
- In Figure 5.17 c no hydrogen bonding occurred, however many of the rifampicin functional groups and HSA amino acid receptors are exposed. The greasy amino acid alanine 552 is close to the hydrogen on the RIF drug which could result in weak Van de Waal forces. However, the Gibbs free energy of the this MOE interaction is the highest generated for the three rifampicin MOE interactions – which could indicate steric hindrance in this specific binding pocket of HSA.
- For 25-desacetyl rifampicin, Figure 5.8, 5.9 and 5.10 represent the three best conformations of drug interaction with the HSA protein.

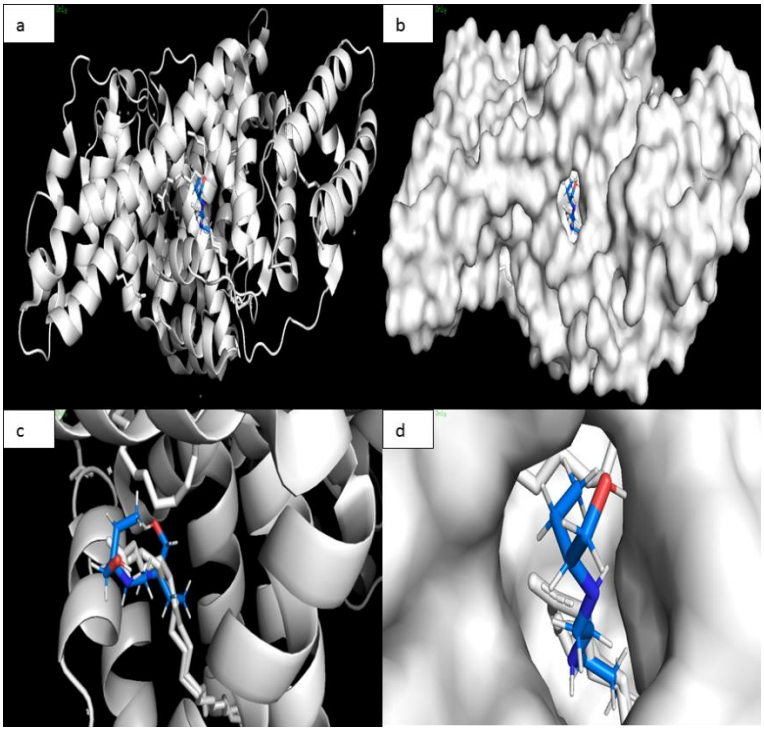

Figure 5.15: a) ETH conformation 3 binding to HSA ribbon form. b) ETH conformation 3 binding to HSA surface topology. c) Image (a) zoomed in. d) Image (b) zoomed in.

- Figure 5.18 illustrates the 2D MOE interaction map of conformations of D-RIF with HSA amino acid terminals. The rifampicin metabolite 25-desacetyl rifampicin in Figure 5.18 a represents hydrogen bonding between the NH group of 25-desacetyl rifampicin, as a backbone donor to the greasy exposed HSA phenylalanine 206 amino acid occurs. Another possible interaction occurs where the hydrogen group with an exposed amino acid arginine

209 could be the result of weak Van de Waal forces or electrostatic interaction. In Figure 5.18 b, the possible interaction between the hydrogen bond of the drug and the greasy valine amino acid 482 could be a result of Van de Waal forces or electrostatic interaction.

- Figure 5.10 c has a similar MOE interaction to the MOE interaction in Figure 5.18 b. However, the Gibbs free energy of the former is higher, which could be a result of molecular shift within the pocket causing steric hindrance of the drug-protein interaction to increase.

- For pyrazinamide, Figure 5.11, 5.12 and 5.13 represent the three best conformations of drug interaction with the HSA protein.
- Figure 5.19 illustrates the 2D MOE interaction map of the conformation of PYR with HSA amino acid terminals. Figure 5.19 a indicates possible interaction by hydrogen bonding between the NH_2 group present in the PYR molecule as a side chain donor to the acid tyrosine 161 amino acid between the NH_2 (as a backbone donor to the greasy Leucine 182 amino acid residue) and the oxygen group present in the pyrazinamide molecule (as a side chain acceptor from the Arginine 117 side-chain donor amino acid).
- In Figure 5.19 b the same MOE interaction was predicted as discussed for Figure 5.19 a. The difference is that the Gibbs free energy predicted calculations were higher for the second MOE interaction for PYR, with a slight shift in position at the HSA protein binding pocket. Figure 5.19 c represents four hydrogen bonding interactions, i.e. the PYR arene group with the polar arginine 117 amino acid via side-chain donor. The oxygen functional group acts a side chain acceptor to the polar arginine 186 donor side-chain amino acid. The NH_2 functional group interacts a backbone chain donor to the greasy Leucine 182 amino acid and the polar arginine 117 amino acid interacts with the oxygen functional group of PYR.

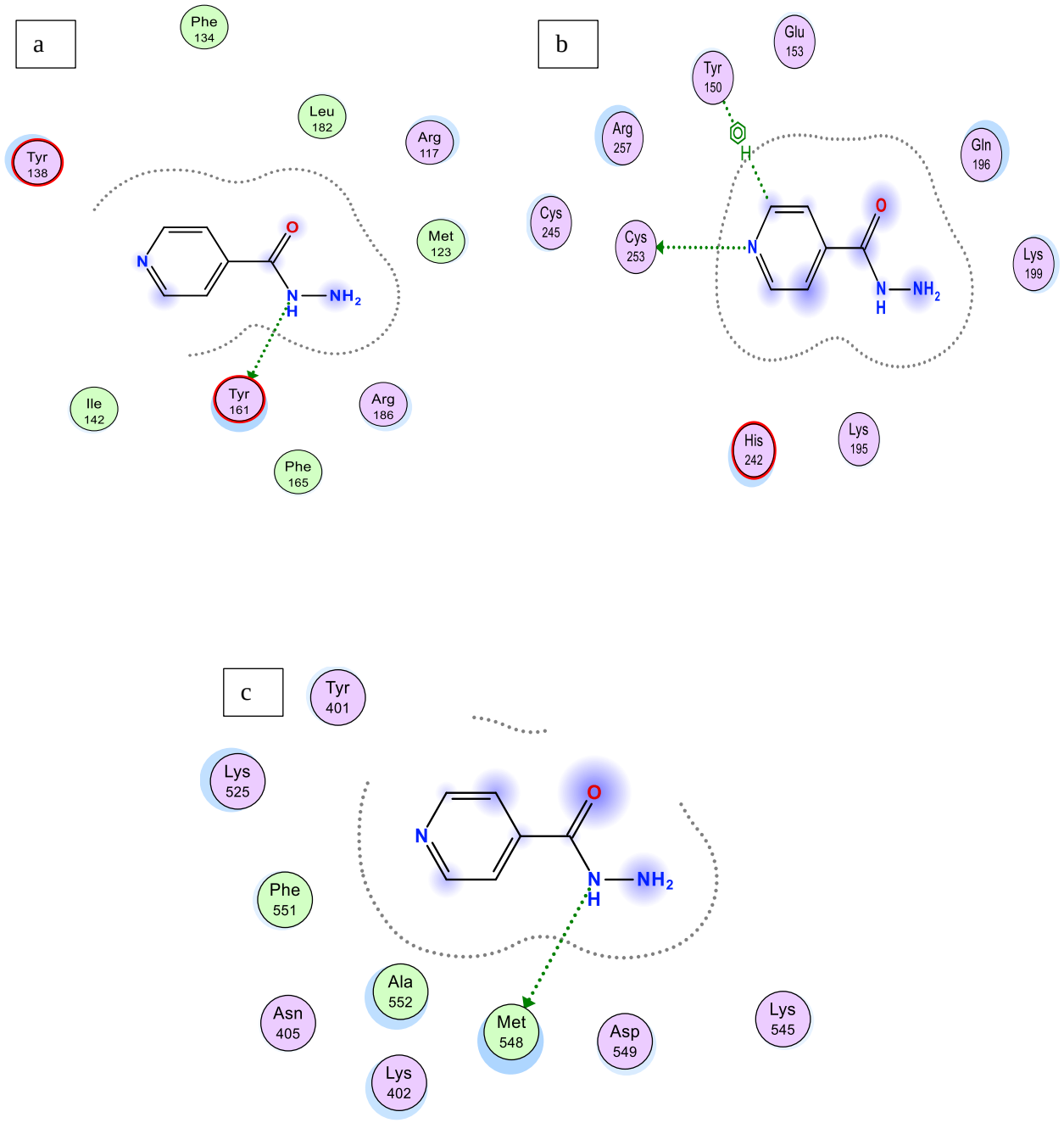

Figure 5.16: MOE interaction map of the conformation of INH with HSA amino acid terminal. a) INH interaction with tyrosine 161. b) INH interaction with tyrosine 150 and cysteine 253. c) INH interaction with methionine 548.

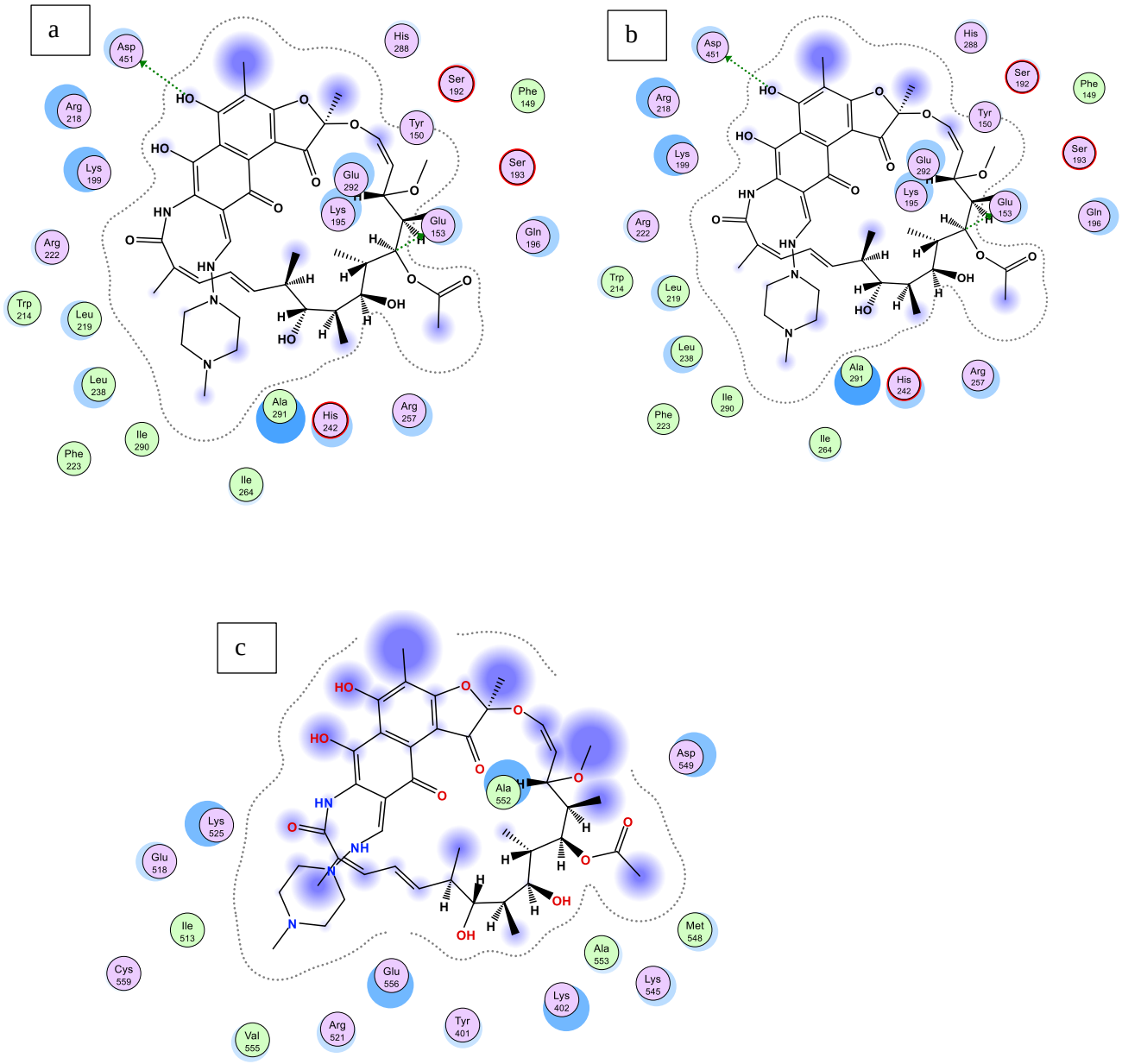

Figure 5.17: MOE interaction map of the conformations of RIF with HSA amino acid terminal. a.) RIF interaction with asparagine 451 and glutamic acid 153. b.) RIF interaction with asparagine 451 and glutamic acid 153 c.) RIF interaction with tyrosine 150 and cysteine 253.

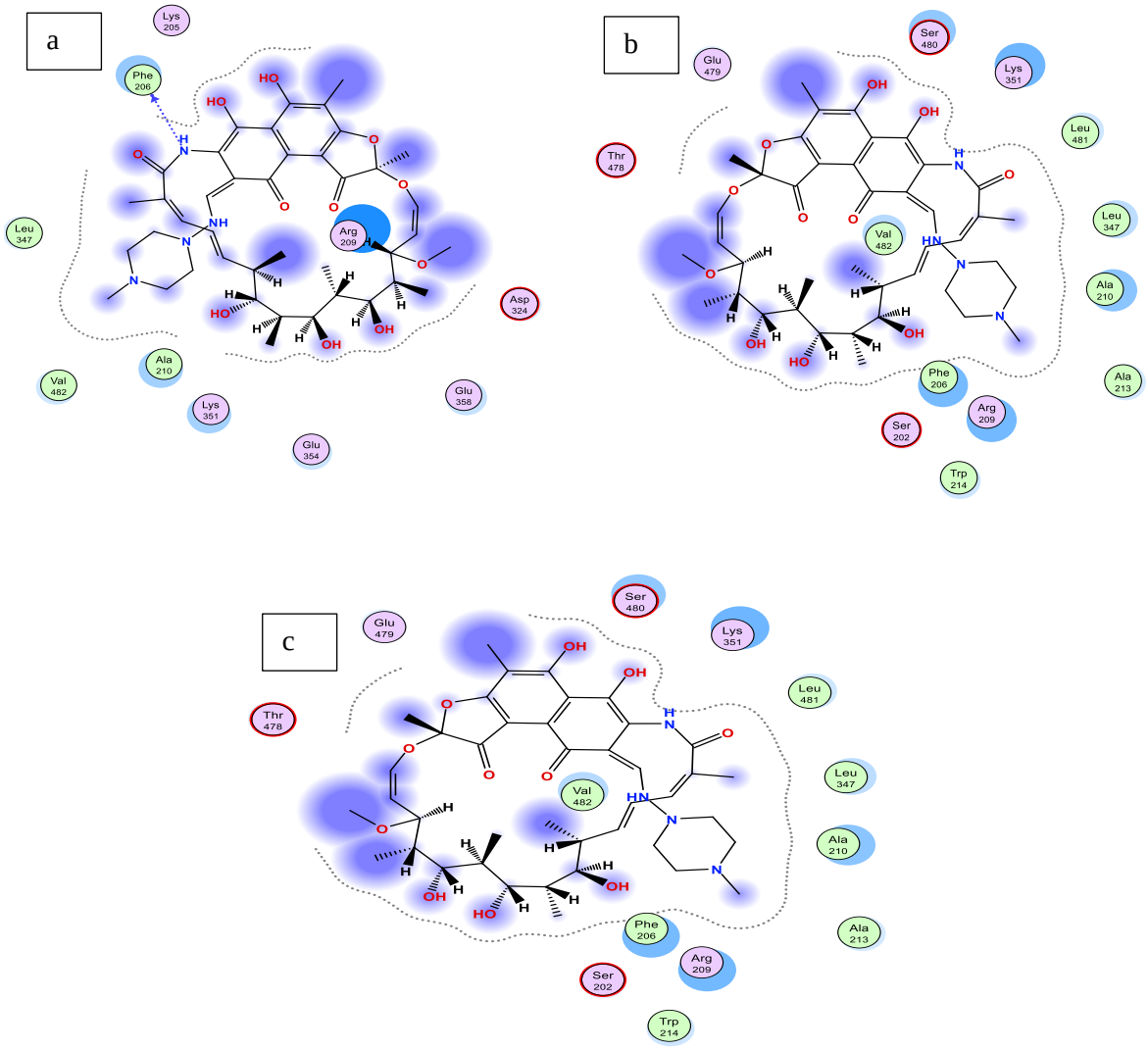

Figure 5.18: MOE interactions map of conformations of D-RIF with HSA amino acid terminal. a) D-RIF interaction with phenylalanine 206 amino acid. b) D-RIF interaction with valine 482. c) D-RIF interactions with valine

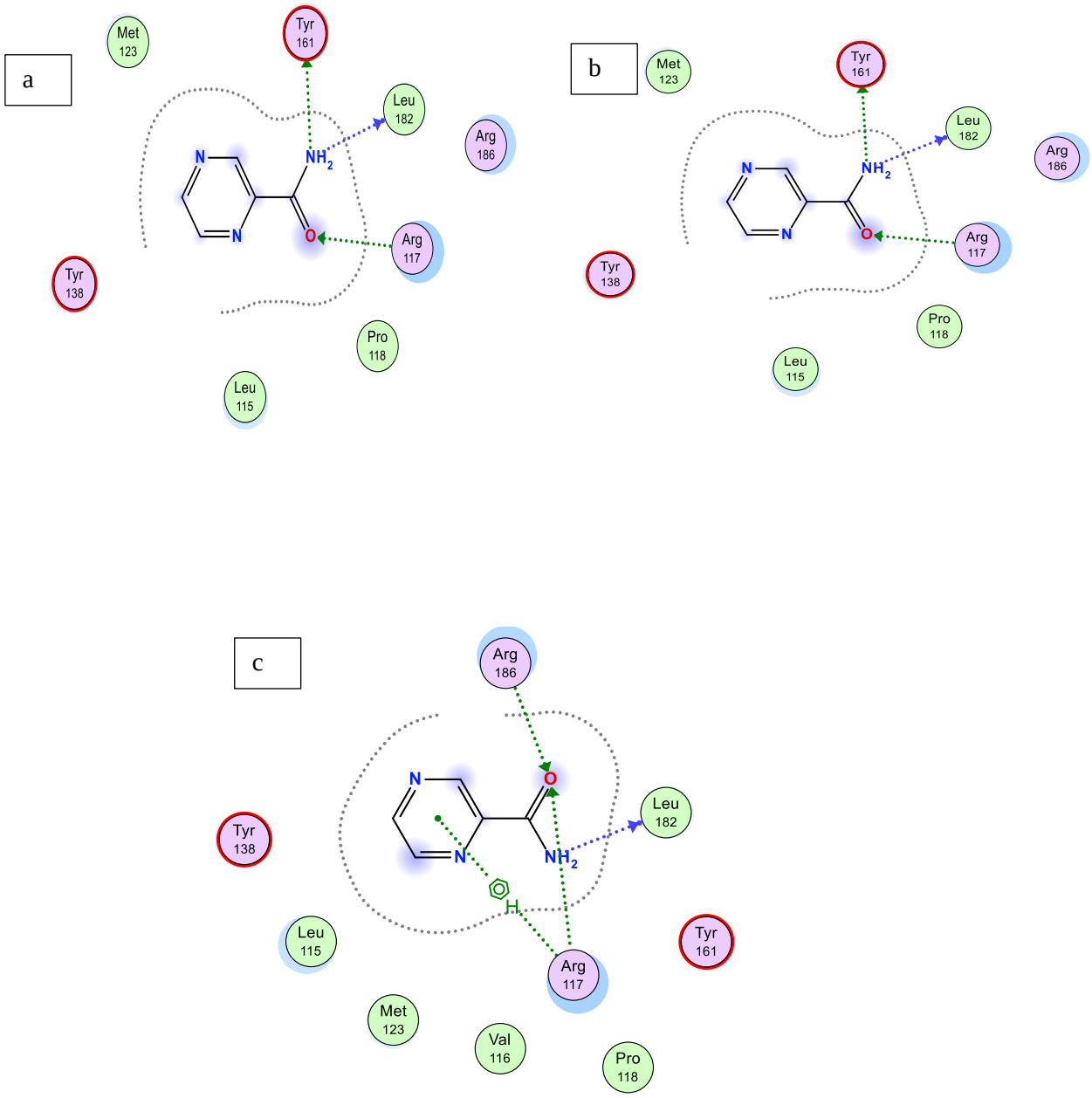

Figure 5.19: MOE interactions map of conformations of PYR with HSA amino acid terminal. a) PYR interaction with tyrosine 161, leucine 182 and arginine 117 amino acid. b) PYR interaction with tyrosine 161, leucine 182 and arginine 117 amino acid. c) PYR interaction with arginine 117, arginine 186, leucine 182 and arginine 117.

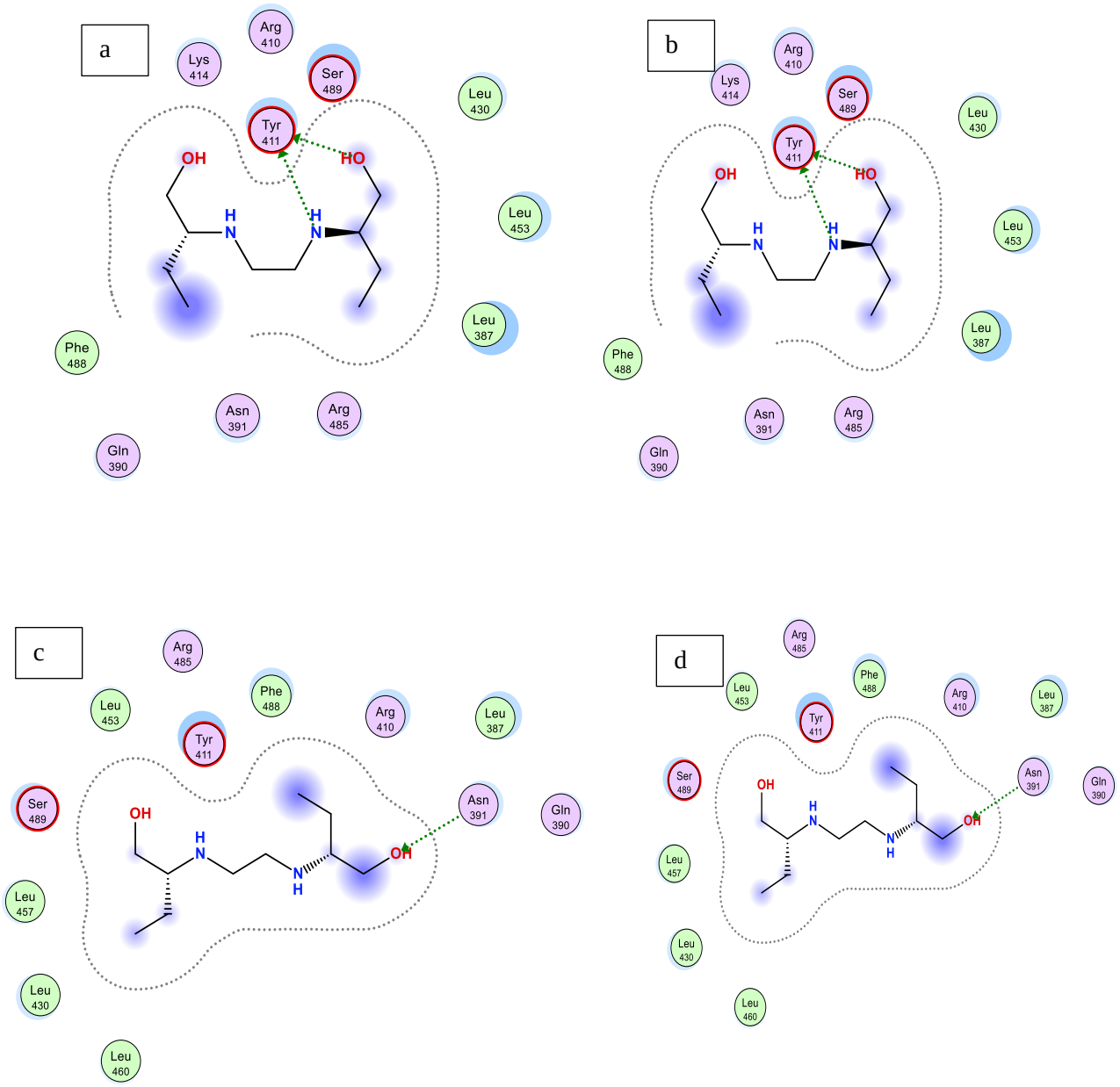

Figure 5.20: MOE interactions map of conformations of ETH with HSA amino acid terminal. a) ETH interaction with tyrosine 411 amino acid. b) ETH interaction with tyrosine 411 amino acid. c) ETH interaction with asparagine 391 amino acid. d) ETH interaction with asparagine 391 amino acid.

- For ethambutol, Figure 5.14, 5.15 and 5.16 represent the three best conformations of drug interaction with the HSA protein. Figure 5.20 illustrates the 2D MOE interaction map of conformations of ethambutol with HSA amino acid terminals. Figure 5.20 a and b show hydrogen bonding via the NH and OH functional groups of ETH with the acidic tyrosine 411

amino acid as side-chain donors. The difference between MOE interactions in Figure 5.20 b is a slight shift in structural position within the HSA pocket. The Gibbs free energy was higher compared to MOE of Figure 5.20 a. Figure 5.20 c and Figure 5.20 d indicate a prediction of hydrogen bonding and structural conformation of ethambutol, where the OH functional group acts as a side chain acceptor, and the polar asparagine 391 amino acid acts as a side chain donor to the oxygen. This indicated that ethambutol is deprotonated within the pH environment, which therefore allows for asparagine to act as a side chain donor for ionized ethambutol, resulting in hydrogen bonding.

- According to literature the enthalpy and entropy thermodynamic parameter can be used to explain interactions between molecules and protein [154]. A positive enthalpy is an indication of hydrophobic interaction [154]. Whereas a negative enthalpy coupled with positive entropy is an indication of electrostatic interaction between ionic species [154]. Whereas negative enthalpy and entropy indicates evidence of weak Van de Waal interactions and hydrogen bonding taking place [154]. However molecules can interact via hydrogen bonding and electrostatic interactions [154].

- For each drug accessed, the MOE software predicted a ΔH° value for each MOE drug-HSA binding interaction. As indicated in Table 5.4, the predicted ΔH° was used to calculate the ΔS° and Gibbs free energy of all the MOE interactions per drug assessed using equations (5.1) and (5.2). From the literature, it is stated that a negative ΔH° value obtained indicates the presence of hydrogen bond formation, positive ΔS° values indicate the presence of electrostatic forces between the drug and the HSA protein, and a negative Gibbs free energy indicates that the drug binding to the protein is spontaneous [155].
- By assessing the best MOE interactions predicted for each drug, the ΔH° prediction for each drug was negative – indicating hydrogen bonding and a positive change in ΔS° values between the drug and the HSA pocket where the drugs were predicted to be situated. This was an indication that the drug interaction of all drugs assessed possibly interacted electrostatically with the HSA protein. RIF indicated the strongest electrostatic interaction from the predicted results and PYR indicates the weakest electrostatic interaction with HSA.
- The Gibbs free binding energy calculated from the predicted ΔH° values indicated the best binding to occur for rifampicin, followed by ethambutol, 25-desacetyl rifampicin, INH, and pyrazinamide with Gibbs free energy values of -104.0413 kJ/mol, -80.5190 kJ/mol, -76.8095 kJ/mol, -51.9888 kJ/mol and -33.0516 kJ/mol respectively. The negative Gibbs free energy value predicted for each drug indicates that the drug could undergo spontaneous binding interaction to the HSA protein.

5.3.3 Results of Preparation of in-vitro drug sample to human plasma protein for fluorescence and UV spectroscopy analysis

5.3.3.1 Fluorescence spectroscopic analysis

In section 5.2.4, the *in vitro* sample preparation of the drugs isoniazid (INH), rifampicin (RIF), 25-desacetyl rifampicin (D-RIF), pyrazinamide (PYR), ethambutol (ETH), and Rifampicin-4 (RIF-4) was done using plasma and a phosphate buffer system at pH of 7.4. The samples were then analysed using fluorescence and UV spectroscopy to confirm the predicted interaction of the drugs with protein. The analysis was performed using a BMG Labtech Omega Fluorostar spectrometer, which has the function to conduct fluorescence as well as UV analysis of samples. The samples were analysed using a 96 well plate with the set temperature at 25 ºC, 37 ºC, 40 ºC, and 45 ºC, or 298.15 K, 310.15 K, 313.15 K, and 318.15 K respectively.

The excitation wavelength was fixed at 278 nm and the analysis wavelength range was from 300 nm to 700 nm. The fluorescence analysis was performed on each drug at different concentrations from 30µg/ml-1µg/ml in increments of 5µg/ml. The temperature used was 310.15 K, which equates to body temperature.

The following results were obtained:

- As indicated in Figure 5.21 (a-f), the fluorescence spectroscopic analysis was conducted for INH, RIF, D-RIF, PYR, ETH and RIF-4 at different concentrations containing plasma and runs conducted with blank plasma for each drug respectively.
- For all the drugs, a trend was noticed that, as the concentration increased, the fluorescence intensity decreased when compared to the blank plasma. This finding indicates that the drug has a quenching effect on the fluorescence emission intensity of the plasma.

This fluorescence data were further analysed to determine what kind of quenching effect each drug had on the plasma proteins as well as the quenching strength. The K_{sv} quenching constant was then calculated using the Stern-Volmer plot.

5.3.3.2 Fluorescence quenching constant Ksv

From the obtained fluorescence data, the quenching constant Ksv was determined for each drug at the different concentrations of 30 µg/ml to 1 µg/ml in increments of 5 µg/ml between the temperature ranges of 298.15 and 318.15 K. The quenching constant was determined using the Stern-Volmer equation (5.4). Hence, a linear plot of F_o/F against [Q] was conducted for each drug were F_o is the fluorescence intensity of the plasma and F is the fluorescence intensity of the sample at specific concentrations against Q which is the concentration per intensity [156]. The following Ksv values were obtained in descending order of the drugs as indicated in table 5.4:

- Rifampicin-4 (RIF-4) 30.742 x 10^3 M^{-1}, 30.506 x 10^3 M^{-1}, 28.283 x 10^3 M^{-1}, at the temperatures 298.15 K 310.15 K and 313.15 K respectively
- Rifampicin (RIF) 15.083 x 10^3 M^{-1}, 16.140 x 10^3 M^{-1}, 16.801 x 10^3 M^{-1}, at the temperatures 310.15 K 313.15 K and 318.15 K respectively
- 25-desacetyl rifampicin (D-RIF) 10.117 x 10^3 M^{-1}, 10.986 x 10^3 M^{-1}, 11.727 x 10^3 M^{-1}, at the temperatures 310.15 K, 313.15 K and 318.15 K respectively
- Isoniazid (INH) 4.6582 x 10^3 M^{-1}, 4.867 x 10^3 M^{-1}, 4.916 x 10^3 M^{-1}, at the temperatures 298.15 K 310.15 K and 318.15 K respectively
- Pyrazinamide (PYR) 2.8702 x 10^3 M^{-1}, 2.961 x 10^3 M^{-1}, 2.9641 x 10^3 M^{-1}, at the temperatures 298.15 K 313.15 K and 318.15 K respectively and
- Ethambutol (ETH) 1.9374 x 10^3 M^{-1}, 1.8896 x 10^3 M^{-1}, 1.9737 x 10^3 M^{-1}, at the temperatures 298.15 K 313.15 K and 318.15 K respectively.

From these results, it is evident that RIF-4 had the strongest quenching effect on plasma followed by RIF, D-RIF , INH, PYR, and ETH. ETH had the weakest quenching effect on plasma. All of the drugs indicate a dynamic quenching mechanism of fluorescence quenching due to the linearity of the Stern-Volmer plots in Figure 5.22 (a-f) [145].

- However, Figure 5.22 (a-f) illustrated the Stern-Volmer plot of each drug at three different temperatures, at the temperature range of 298.15 K to 318.15 K. The Ksv of rifampicin, 25-desacetyl rifampicin, isoniazid and pyrazinamide illustrated that, as the temperature increased, the Ksv quenching constant increased which is also another confirmation of the dynamic quenching mechanism. Ethambutol indicated a decrease in Ksv value between 298.15 K and 313.15 K and thereafter an increase in Ksv value between 313.15 K and 318.15 K. This indicates that ethambutol could have undergone both dynamic and static quenching [157]. RIF-4 indicated a decrease in Ksv quenching constant as the temperature increased. This is an indication that when all four drugs are present, the possibility of static quenching could occur, which could result in a complex formation between RIF-4 and plasma proteins [157-158].

5.3.3.3 Determination of the binding constant K and the experimental thermodynamic properties of the drug interaction with plasma

To calculate the experimental Gibbs free energy of the drugs, it was required to obtain the binding constant value K as indicated in equation (5.4) linear regression of the equation was plotted for each drug at 3 different temperatures ranging between 298.15 K and 318.15 K as indicated in table 5.6 and Figure 5.23 (a-f). The following K values were obtained for each drug:

- Rifampicin 5.379 X 10^2 M^{-1}, 8.422 X 10^2 ,1.585 X 10^3 M^{-1} at temperatures 310.15 K 313.15 K 318.15 K respectively
- Isoniazid 9.285 M^{-1}, 9.674 M^{-1} ,9.874 M^{-1} at temperatures 298.15 K 310.15 K 318.15 K respectively
- 25-Desacetyl rifampicin 3.156 M^{-1}, 3.421 M^{-1}, 3.5002 M^{-1} at temperatures 310.15 K 313.15 K 318.15 K respectively
- Rifampicin-4 (RIF-4) 4.824 X 10^1 M^{-1}, 8.614 X 10^1 M^{-1}, 3.293 X 10^2 M^{-1} at temperatures 310.15 K 313.15 K 318.15 K respectively
- Ethambutol 3.443 M^{-1} ,3.516 M^{-1} ,4.857 M^{-1} at temperatures 298.15 K 313.15 K 318.15 K respectively and
- Pyrazinamide 3.466 X 10^2 M^{-1}, 3.076 X 10^2 M^{-1}, 1.946 X 10^2 M^{-1} at temperatures 298.15 K 310.15 K 318.15 K respectively.

Table 5.5: Stern-Volmer quenching constant Ksv and linear equations of drugs-plasma fluorescence at different temperatures and constant pH 7.4.

DRUG	T (K)	LINEAR EQUATIONS	Ksv X 10^3 (M^{-1})
Isoniazid	298.15	y = 4658.2x + 1.7446 R^2 = 0.9694	4.6582
	310.15	y = 4867x + 1.7031 R^2 = 0.9439	4.867
	318.15	y = 4916.9x + 1.6333 R^2 = 0.9118	4.916
Rifampicin	310.15	y = 15083x + 0.9936 R^2 = 0.9641	15.083
	313.15	y = 16140x + 0.971 R^2 = 0.9517	16.140
	318.15	y = 16801x + 0.972 R^2 = 0.9484	16.801

25-Desacetyl Rifampicin	310.15	y = 10117x + 1.8347 R^2 = 0.8462	10.117
	313.15	y = 10986x + 1.7799 R^2 = 0.842	10.986
	318.15	y = 11727x + 1.7909 R^2 = 0.8378	11.727
Pyrazinamide	298.15	y = 2870.2x + 1.0514 R^2 = 0.9508	2.8702
	313.15	y = 2961x + 1.0692 R^2 = 0.9727	2.961
	318.15	y = 2964.1x + 1.0784 R^2 = 0.9697	2.9641
Ethambutol	298.15	y = 1937.4x + 1.3329 R^2 = 0.8986	1.9374
	313.15	y = 1889.6x + 1.2084 R^2 = 0.9107	1.8896
	318.15	y = 1973.7x + 1.2925 R^2 = 0.9084	1.9737
RIF-4 (combination of INH,RIF,ETH and PYR)	298.15	y = 30742x + 1.115 R^2 = 0.8335	30.742
	310.15	y = 30506x + 1.0728 R^2 = 0.8454	30.506
	313.15	y = 28283x + 1.0155 R^2 = 0.8529	28.283

From the binding constant data K, the binding affinity of each drug was assessed as follows: Rifampicin (moderate affinity), Isoniazid (low affinity), 25-Desacetyl Rifampicin (low affinity), Ethambutol (low affinity) and Pyrazinamide (moderate affinity). RIF had the highest binding constant followed by PYR, INH, ETH and D-RIF. Therefore when co-administration of the anti-TB drug treatment is used on patients, rifampicin could potentially compete with the other drugs for the binding sites on HSA in plasma protein, which means the unbound fraction of the rifampicin drug would be less available to produce therapeutic effect and that hydrophilic drugs like INH for example, would have a higher unbound fraction in blood plasma.

Table 5.6: Stern Volmer Lineweaver-Burk binding parameter K of drugs-plasma fluorescence at different temperatures and constant pH 7.4

DRUG	T(K)	LINEAR EQUATIONS	K (M^{-1})
Isoniazide	298.15	y = 0.2138x + 0.9678 R^2 = 0.7891	9.285
	310.15	y = 0.2202x + 0.9856 R^2 = 0.7512	9.674
	318.15	y = 0.2285x + 0.9945 R^2 = 0.7242	9.874
Rifampicin	310.15	y = 0.6983x + 2.7307 R^2 = 0.8402	5.379 X 10^2
	313.15	y = 0.7502x + 2.9254 R^2 = 0.8186	8.422 X 10^2
	318.15	y = 0.7969x + 3.1999 R^2 = 0.8596	1.585 X 10^3
	310.15	y = 0.1002x + 0.4991 R^2 = 0.7314	3.156
	313.15	y = 0.1109x + 0.5341 R^2 = 0.7125	3.421

25-desacetyl rifampicin			
	318.15	y = 0.1108x + 0.5441 R^2 = 0.6718	3.5002
Pyrazinamide	298.15	y = 0.7495x + 2.5398 R^2 = 0.873	3.466 X 10^2
	310.15	y = 0.731x + 2.488 R^2 = 0.9398	3.076 X 10^2
	318.15	y = 0.6701x + 2.2891 R^2 = 0.9894	1.946 X 10^2
Ethambutol	298.15	y = 0.202x + 0.5369 R^2 = 0.9489	3.443
Ethambutol	313.15	y = 0.2129x + 0.5461 R^2 = 0.9162	3.516
	318.15	y = 0.2703x + 0.6864 R^2 = 0.9283	4.857
RIF-4 (combination of INH,RIF,ETH and PYR)	310.15	y = 0.4143x + 1.6834 R^2 = 0.7266	4.824 X 10^1
	313.15	y = 0.4864x + 1.9352 R^2 = 0.7301	8.614 X 10^1
	318.15	y = 0.6171x + 2.5176 R^2 = 0.7975	3.293 X 10^2

Table 5.7: Calculated thermodynamic parameters of drugs using the binding constant of drugs-plasma fluorescence and the Van't Hoff plot for determination of ΔH◦, ΔS◦ and Gibbs free energy of the drugs at different temperatures and constant pH of 7.4.

DRUG	T(K)	ΔH◦ (KJ/mol)	ΔS◦ (KJ/mol)	Gibbs free energy (KJ/mol)
Isoniazid	298.15	2.443	0.0267	-5.5244
	310.15			-5.8451
	318.15			-6.0689
Rifampicin	310.15	110.2021	0.0407	-16.2518
	313.15			-17.4749
	318.15			-19.5136
25-desacetyl Rifampicin	310.15	9.0969	0.0418	-3.0067
	313.15			-3.1322
	318.15			-3.3414
Pyrazinamide	298.15	-21.3545	-0.0225	-14.6438
	310.15			-14.3738
	318.15			-14.1937
Ethambutol	298.15	50.9249	0.1732	-0.7064
	310.15			-2.7845
	313.15			-3.2780
	318.15			-4.1439
RIF-4	310.15	199.4030	0.6746	-9.8365
	313.15			-11.8604
	318.15			-15.2336

Once the binding constant K was obtained for each drug, the thermodynamic parameters could be calculated using the Van't Hoff equation 5.5, where K is the binding constant and gas and temperature is constant. The ΔH◦ and ΔS◦ values can be calculated from the slope or intercept of the Van't Hoff plot of lnK vs 1/T as indicated in Figure 5.24 (a-f), and the Gibbs free energy equation 5.2.

In Table 5.7 the change in ΔH◦, ΔS◦ and Gibbs free energy was experimentally calculated [156]. The ΔH◦ values were positive for all drugs and the ΔS◦ values were positive for all of the drugs except for the negative ΔH◦ and ΔS◦ of pyrazinamide as indicated in table 5.7.

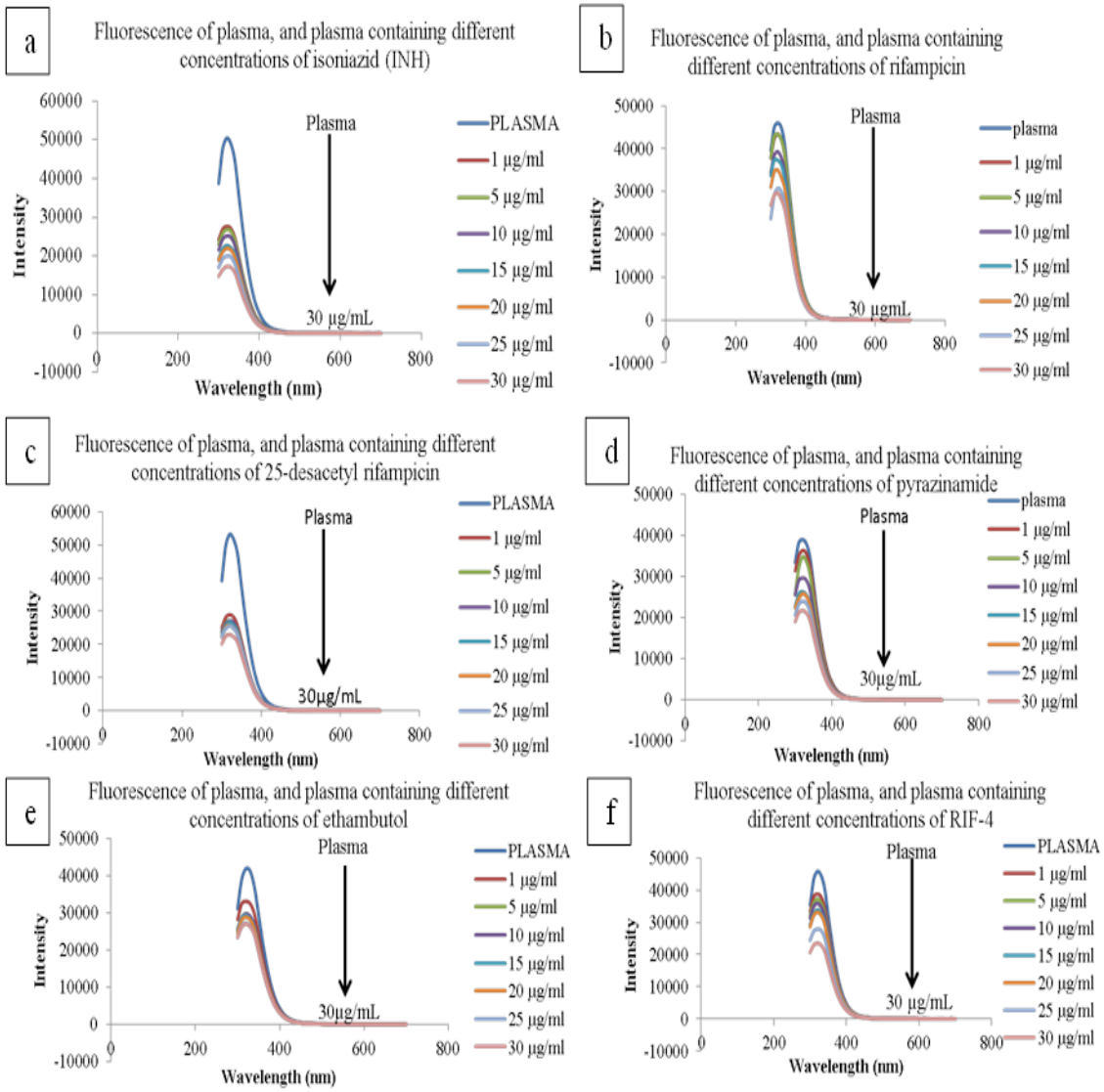

Figure 5.21: Fluorescence comparison of plasma protein and plasma-drug at different sample concentrations ranging from 1 µg/ml–30µg/ml in increments of 5 µg/ml at a temperature of 310.15 K and pH 7.4.a) isoniazid b) rifampicin c) 25-desacetyl rifampicin d) pyrazinamide e) ethambutol f) RIF-4 drug combination

According to the literature, and the fluorescence experimental data, the interaction of pyrazinamide was due to Van de Waals forces and hydrogen bonding in low dielectric media [156]. It is also an indication that pyrazinamide will bind spontaneously at lower temperatures. The drugs that produce positive ΔH° and positive ΔS° are an indication that the drug will bind spontaneously at higher temperatures such as body temperature. The positive values for ΔH° and ΔS° are indicative of a binding process that is controlled by ΔS°. According to the Gibbs free energy equation, a positive ΔH° change is not favourable for the spontaneity of the binding process, unlike a positive ΔS° change that leads to a more negative value for the Gibbs free energy [159].

From Ross and Subramanian's theory, positive values for ΔH° and ΔS° change suggest hydrophobic interaction as the main intermolecular force involved in the binding process [159]. However, this does not indicate that it is the only type of bonding interaction taking place. The experimental fluorescence data calculated do not correlate with the MOE prediction that the drugs analysed will infer drug-protein interactions via hydrogen bonding and electrostatic effects.

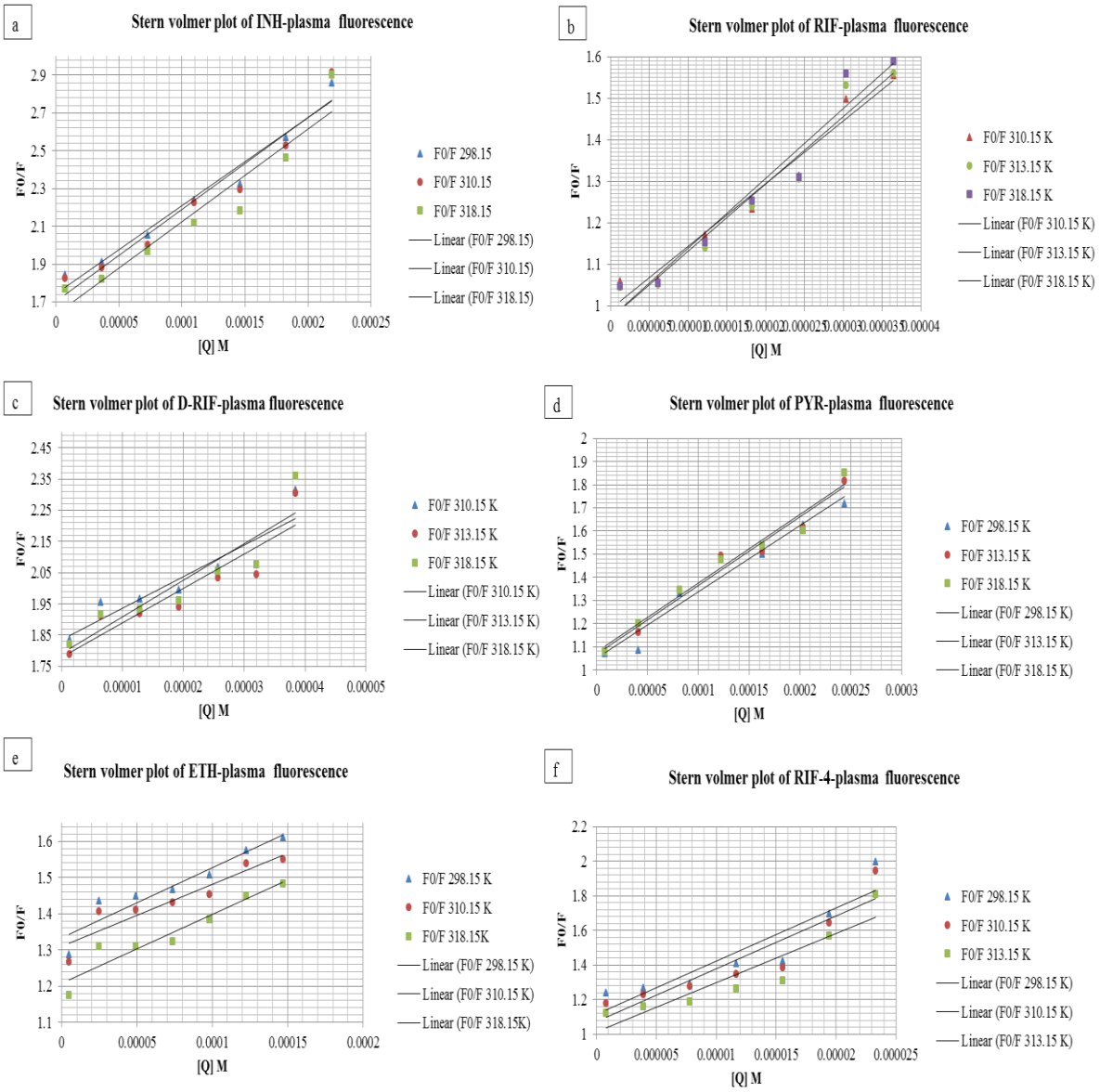

Figure 5.22: Stern-Volmer plot for quenching of drug with plasma proteins at various temperatures and constant pH 7.4 a) INH concentrations: 1µg/ml (7.292 x 10^{-6} M), 5µg/ml (3.646 x 10^{-6} M), 10µg/ml (7.292 x10^{-5} M), 15µg/ml (10.938 x 10^{-5}), 20 µg/ml (14.584 x10^{-5} M), 25 µg/ml (18.23 x 10^{-5} M) and 30 µg/ml (21.876 x 10^{-5} M) b) RIF concentrations: 1µg/ml (1.215 x 10^{-6} M), 5µg/ml (6.076 x 10^{-6} M), 10µg/ml (1.215 x10^{-5} M), 15µg/ml (1.823 x 10^{-5} M), 20 µg/ml (2.43 x10^{-5} M), 25 µg/ml (3.038 x 10^{-5} M) and 30 µg/ml (3.645 x 10^{-5} M), c) PYR: 1µg/ml (8.123 x 10^{-6} M), 5µg/ml (4.061 x 10^{-6} M), 10µg/ml (8.123 x10^{-5} M), 15µg/ml (12.184 x 10^{-5}), 20 µg/ml (16.245 x10^{-5} M), 25 µg/ml (20.307 x 10^{-5} M) and 30 µg/ml (24.368 x 10^{-5} M), d) D-RIF concentrations: 1µg/ml (1.281 x 10^{-6} M), 5µg/ml (6.403 x 10^{-6} M), 10µg/ml (1.281 x10^{-5} M), 15µg/ml (1.921 x 10^{-5} M), 20 µg/ml (2.561 x10^{-5} M), 25 µg/ml (3.201 x 10^{-5} M) and 30 µg/ml (3.842 x 10^{-5} M), e) ETH concentrations: 1µg/ml (4.895 x 10^{-6} M), 5µg/ml (2.447 x 10^{-5} M), 10µg/ml (4.895 x10^{-5} M), 15µg/ml (7.312 x 10^{-5}), 20 µg/ml (9.789 x10^{-5} M), 25 µg/ml (12.236 x 10^{-5} M) and 30 µg/ml (14.683 x 10^{-5} M), f) RIF-4 concentrations: 1µg/ml (7.767 x 10^{-7} M), 5µg/ml (3.883 x 10^{-6} M), 10µg/ml (7.767 x10^{-6} M), 15µg/ml (1.165 x 10^{-5}), 20 µg/ml (1.553 x10^{-5} M), 25 µg/ml (1.942 x 10^{-5} M) and 30 µg/ml (2.33 x 10^{-5} M)

According to literature studies on protein-ligand binding when the change in ΔS◦ is positive, the reaction is endothermic, which means that the drug will require the heat of the body to interact with the protein. This indicates that disruptions of energetically-favourable noncovalent interactions can occur. The Gibbs free energy values obtained for each drug resulted in the following:

- Rifampicin (RIF) -16.2518 kJ/mol -17.4749 kJ/mol -19.5136 kJ/mol at temperatures 310.15 K, 313.15 K, 318.15 K respectively
- Isoniazid (INH) -5.5244 kJ/mol -5.8451 kJ/mol -6.0689 kJ/mol at temperatures 298.15 K,310.15 K, 318.15 K respectively
- 25-desacetyl rifampicin (D-RIF)-3.0067 kJ/mol -3.1322 kJ/mol, -3.3414 kJ/mol, at temperatures 310.15 K, 313.15 K respectively
- Rifampicin-4 (RIF-4) -9.8365 kJ/mol, -11.8604 kJ/mol, -15.2336 kJ/mol, at temperatures 310.15 K, 313.15 K, 318.15 K respectively
- Ethambutol (ETH) -0.7064 kJ/mol, -2.7845 kJ/mol, -3.2780 kJ/mol -4.1439 kJ/mol at temperatures 298.15 K, 310.15 K, 313.15 K, 318.15 K respectively
- Pyrazinamide (PYR) -14.6438 kJ/mol, -14.3738 kJ/mol, -14.1937 kJ/mol, 298.15 K, 310.15 K, 318.15 K respectively.

.

The Gibbs free energy for all the drugs is negative, which indicates that the drug plasma binding will occur spontaneously as predicted. It was observed for all drugs that as the temperature increased, the Gibbs free energy increase except for pyrazinamide which decreased in Gibbs free energy. The possibility of competition between drugs for binding sites within the plasma is high due to the low Gibbs free energy values for all the drugs. The experimental results indicated that rifampicin had the lowest Gibbs free energy and ethambutol had the highest Gibbs free energy. These results deviate from the results predicted. This could be due to the use of plasma which has a higher complexity compared to HSA (which is a component of plasma), incorrect prediction of ΔH◦, or not factoring in the binding constant into the prediction.

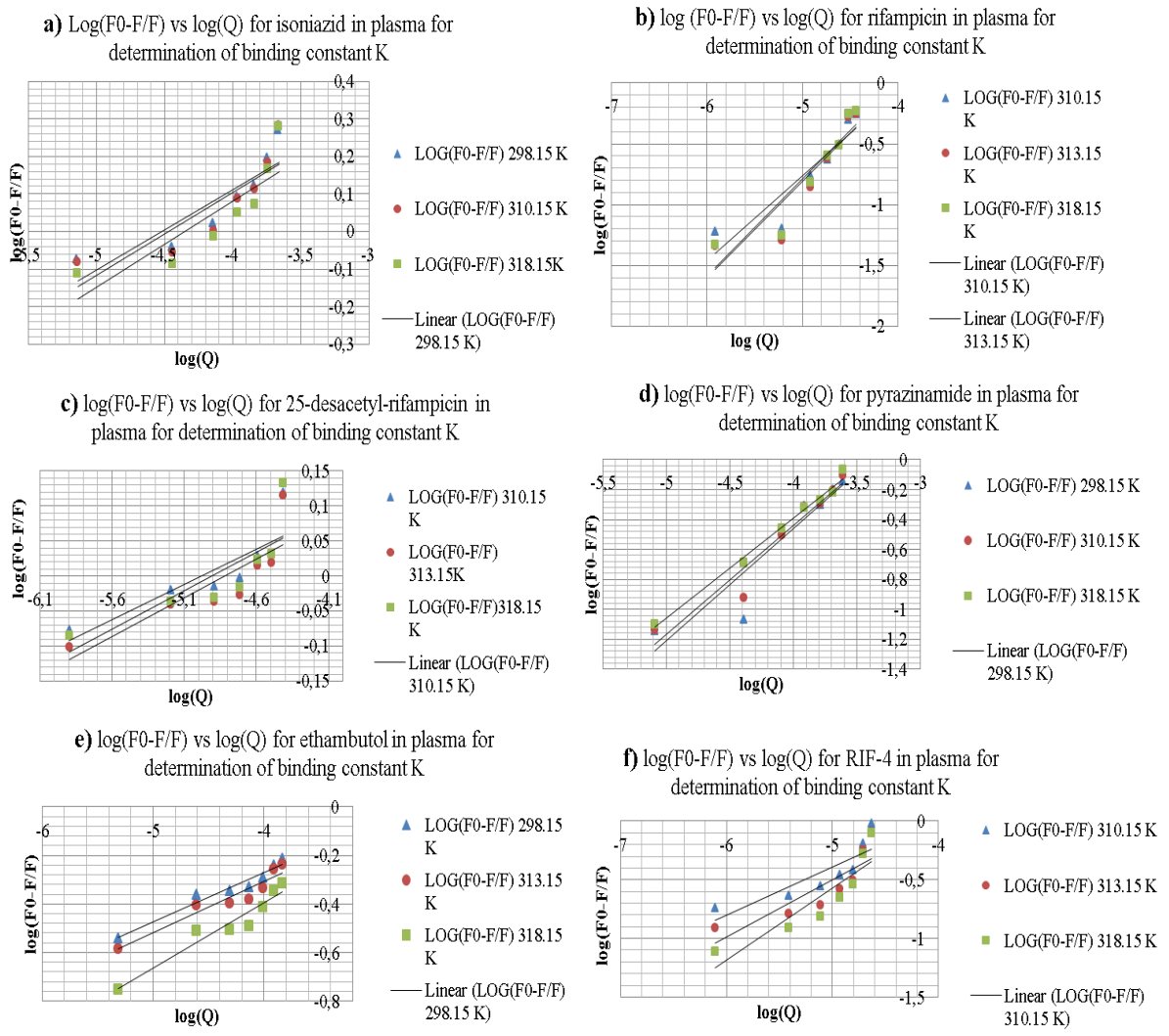

Figure 5.23: Stern-Volmer Lineweaver-Burk plot for determination of binding constants of drug with plasma proteins at various temperatures and constant pH 7.4. a) INH at different concentrations ranging from 1µg/ml (7.292 x 10^{-6} M), 5 µg/ml (3.646 x 10^{-6} M), 10 µg/ml (7.292 x10^{-5} M), 15 µg/ml (10.938 x 10^{-5}), 20 µg/ml (14.584 x10^{-5} M), and 25 µg/ml (18.23 x 10^{-5} M) to30 µg/ml (21.876 x 10^{-5} M) b) RIF at different concentrations ranging from 1µg/ml (1.215 x 10^{-6} M), 5µg/ml (6.076 x 10^{-6} M), 10µg/ml (1.215 x10^{-5} M), 15µg/ml (1.823 x 10^{-5}), 20 µg/ml (2.43 x10^{-5} M), and 25 µg/ml (3.038 x 10^{-5} M) to 30 µg/ml (3.645 x 10^{-5} M) c) D-RIF at different concentrations ranging from 1µg/ml (1.281 x 10^{-6} M), 5µg/ml (6.403 x 10^{-6} M), 10µg/ml (1.281 x10^{-5} M), 15µg/ml (1.921 x 10^{-5}), 20 µg/ml (2.561 x10^{-5} M), and 25 µg/ml (3.201 x 10^{-5} M) to 30 µg/ml (3.842 x 10^{-5} M)d) PYR at different concentrations ranging from 1µg/ml (8.123 x 10^{-6} M), 5µg/ml (4.061 x 10^{-6} M), 10µg/ml (8.123 x10^{-5} M), 15µg/ml (12.184 x 10^{-5}), 20 µg/ml (16.245 x10^{-5} M), and 25 µg/ml (20.307 x 10^{-5} M) to 30 µg/ml (24.368 x 10^{-5} M) e) ETH at different concentrations ranging from 1µg/ml (7.292 x 10^{-6} M), 5µg/ml (3.646 x 10^{-6} M), 10µg/ml (7.292 x10^{-5} M), 15µg/ml (10.938 x 10^{-5}), 20 µg/ml (14.584 x10^{-5} M), 25 µg/ml (18.23 x 10^{-5} M) to 30 µg/ml (21.876 x 10^{-5} M) f) RIF-4 at different concentrations ranging from1 µg/ml (7.767 x 10^{-7} M), 5 µg/ml (3.883 x 10^{-6} M), 10µg/ml (7.767 x10^{-6} M), 15 µg/ml (1.165 x 10^{-5}), 20 µg/ml (1.553 x10^{-5} M), and 25 µg/ml (1.942 x 10^{-5} M) 30 µg/ml (2.33 x 10^{-5} M)

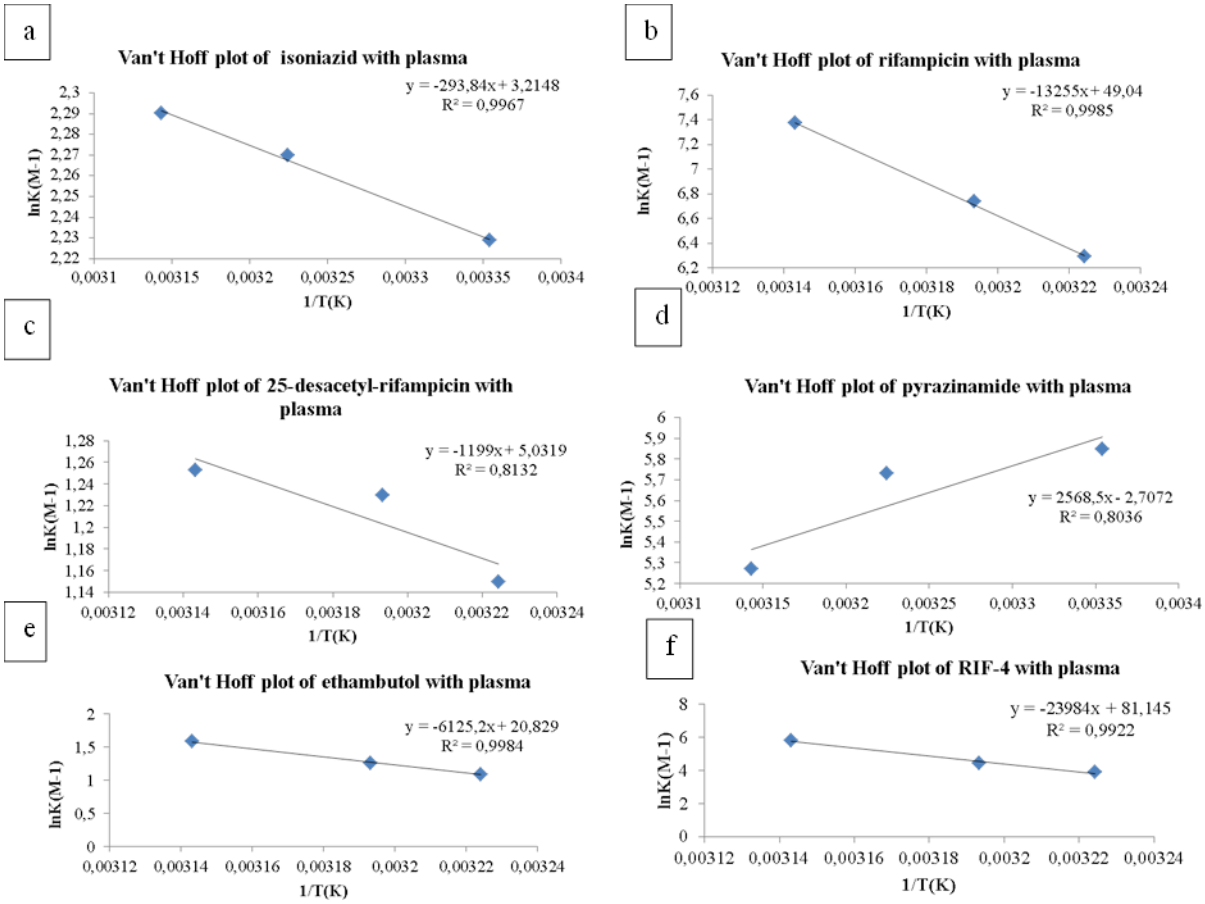

Figure 5.24: Van't Hoff plot lnK vs 1/T at constant pH 7.4 of a) INH and plasma at different temperatures –298.15 K, 313.15 K, and 318.15 K b) RIF and plasma at different temperatures – 310.15 K, 313.15 K, and 318.15 K c) D-RIF and plasma at different temperatures – 310.15 K, 313.15 K and 318.15 K d) PYR and plasma at different temperatures – 298.15 K, 310.15 K, and 318.15 K e) ETH and plasma at different temperatures 298.15 K, 313.15 K, and 318.15 K f) RIF-4 and plasma at different temperatures 310.15 K, 313.15 K, and 318.15 K.

5.3.3.4 Ultraviolet-visible spectroscopy

The UV-vis absorption spectroscopy technique can be used to explore the structural changes of protein and to investigate protein-molecule complex formation. The HSA present in plasma has two main absorption bands. One of them is located in the range of 260 to 300 nm, which is the absorption band of the aromatic amino acids (Trp, Tyr, and Phe).

The absorbance spectra were analysed for all drugs containing plasma with a concentration of 30 µg/ml–1 µg/ml in increments of 5 µg/ml, as well as the drugs without plasma and the plasma blank to identify the effect of the absorbance reading of the plasma.

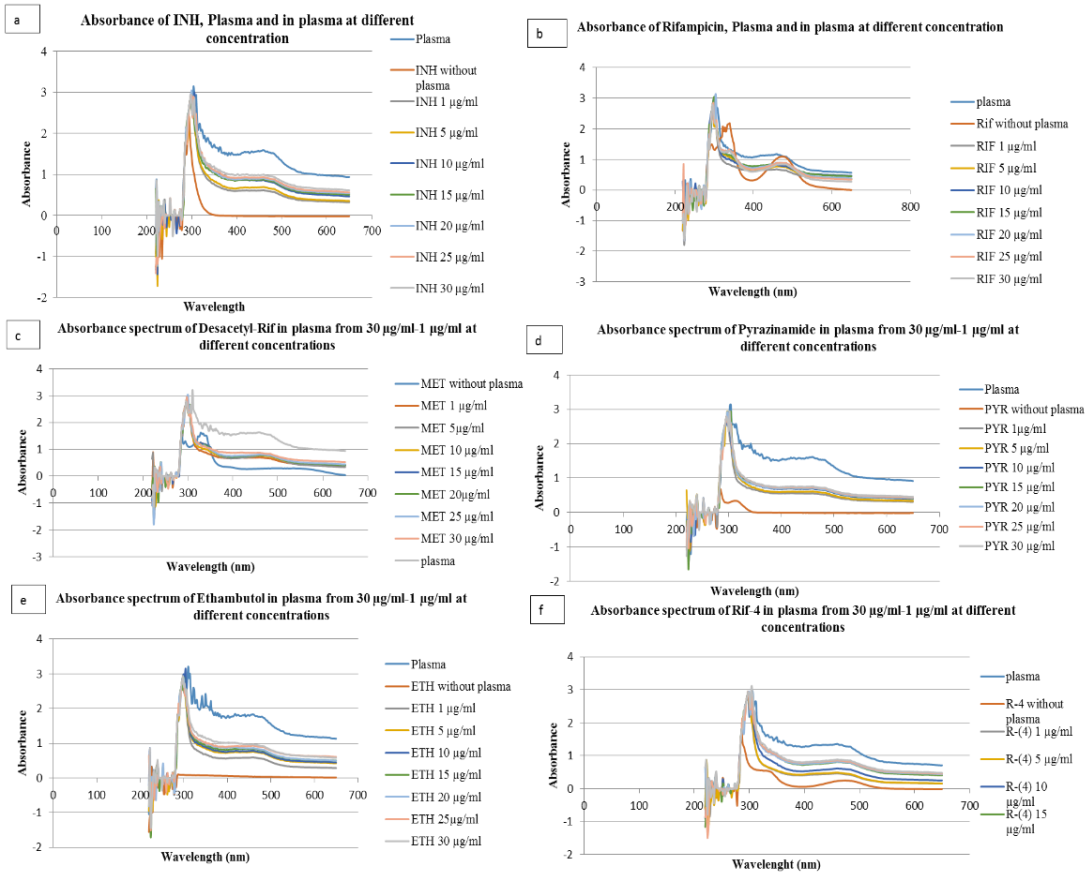

Figure 5.25: Absorbance spectrum of a) blank plasma, INH and INH in plasma from 30 µg/ml to 1 µg/ml. b) Rifampicin in plasma from 30 µg/ml to 1 µg/ml, plasma, and rifampicin. c) D-RIF in plasma from 30 µg/ml to 1 µg/ml , plasma and D-RIF. d.) PYR in plasma from 30 µg/ml to1 µg/ml, plasma and PYR. e) ETH in plasma from 30 µg/ml to1 µg/ml, plasma and ETH. f) RIF-4 in plasma from 30 µg/ml to 1 µg/ml, plasma and RIF-4.

The Omega Fluorostar was used to obtain the UV results with a wavelength analysis range of 220 to 650 nm. As indicated in Figure 5.25 a)-f), a trend was observed for all of the drugs where, as the concentration of the drug increased, the absorbance intensity increased. As shown in Figure 5.26 plasma proteins showed one absorption band at about 280 nm. Upon increasing the concentration of the drugs, the absorbance at 280 nm was gradually increased with a slight red shift to 290 nm, and a new peak appeared between wavelengths of 400–500 nm for the drugs containing plasma. The sample absorbance of the drugs analysed had a slight red shift increase in wavelength at 450nm. The use of the absorbance spectrum was to identify if structural changes in the plasma took place when the drugs were added. This red shift indicates that the macro environment of HSA has been altered by the presence of the drugs. The red shift is also an indication that the hydrophobicity of the plasma protein decreased [156].

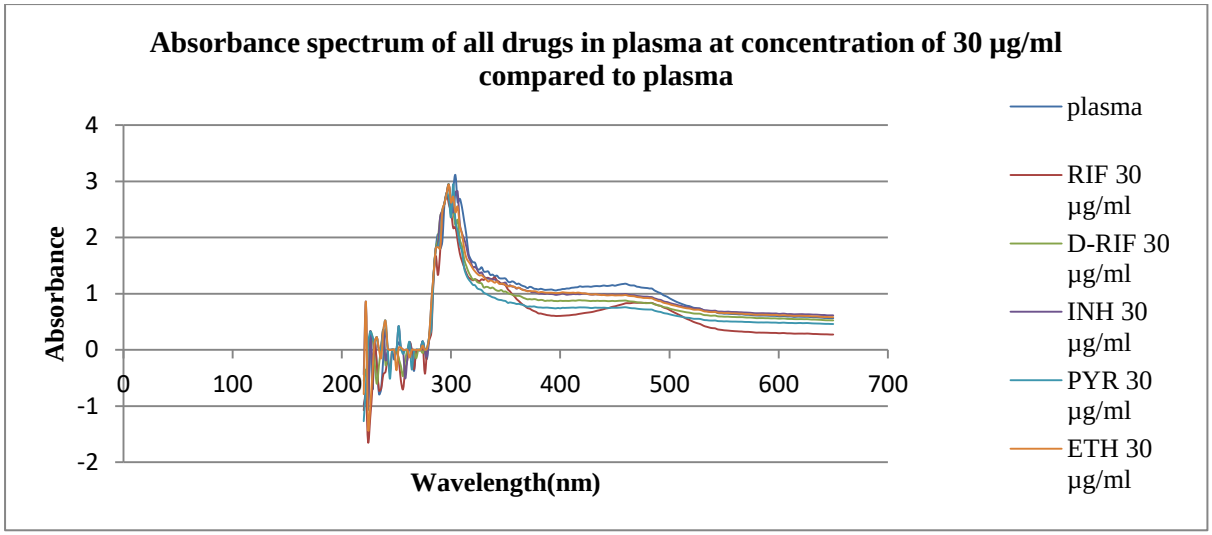

Figure 5.26: Absorbance spectrum of all drugs (rifampicin, 25-desacetyl rifampicin, isoniazid, pyrazinamide, and ethambutol) in plasma at the same concentrations of 30µg/ml.

5.4 Conclusion

In conclusion to the discussion, the computational modeling of each drug provides insight into the possible interactions that occur between the drug and the plasma proteins. From the fluorescence data, it can be observed that as the drug concentration increased, the quenching of plasma increased. This indicates that the more of the drug available in the body, the higher the possibility of drug-plasma binding – which is unfavorable for TB patients. The fluorescence data also confirm that the drug binds to the plasma spontaneously by the negative change in Gibbs free energy values. Therefore, no energy is needed for drug-plasma interaction to be initiated. The use of fluorescence can also be used to increase the accuracy of the drug-plasma assay by assessing the condition of the plasma to the calibrator plasma used during the clinical trial, bioequivalence, bioavailability, and therapeutic drug monitoring.

Chapter 6 Pharmacokinetics – Patient and Calibrator Protein Evaluation in Calibration Curves for Dose Optimization

6.1 Background

As discussed in chapter 1 and the literature review on quality assurance, a proposed thereoretical model was implemented to increase assurance in obtaining an accurate error margin of drug-plasma concentration results. We aimed at exploring factors that influence the accuracy of drug-plasma concentration calibration assays and identifying the most cost-effective and realistic drug bio-analytical methods during validation and therapeutic drug monitoring.

Our main focus was the variations in the calibrator and the patients' protein levels in plasma. A quality assurance perspective was proposed, where protein evaluation of patient plasma or serum protein levels were taken into account for pharmacokinetic (PROTEC-PK^{TM}) optimization recovery in bio-analytical method validation

Plasma protein levels, when discovered, can be used to provide a more accurate assay result. Confirming that the drug bound to plasma proteins does infer that the amount of plasma protein affects the free drug quantity and affects the amount of drug recovered during the analytical process. Individuals with high plasma protein content relative to the calibrator plasma protein content will result in a lower recovery during laboratory procedures. We integrate the significance of whole blood form and multifunctional capability to differences in patient plasma viscosities (PV). The patients mentioned are critically ill and have contracted opportunistic infectious diseases such as TB, MTB, and XDR-TB co-infected with the possibility of the human immune deficiency virus (HIV) infection.

6.2 Aims and objectives

- To study and create an effective method for clinical trial blood patient analysis using a novel design of a plasma calibration curve PROTEC-PK^{TM}

- Evaluation of calibration curves using different plasma protein content.

6.3 Experimental protocol

In this experiment a theoretical method was used to design curves that take patients with plasma protein and albumin levels into account in pharmacokinetic studies. The modelled scenarios of patients with blood disorders such as hypoalbuminea, hyperalbuminia, hypoproteinemia and hyperproteinemia were used to explain the use of the designed curves to improve accuracy of drug concentration recovery in clinical trials. All of the curves were design using a Microsoft offices excel.

- **Scenario 1**

As indicated in figure 6.7 (a) the PROTEC-PK was modelled and constructed for 3 patients (P1-P3) administered with the same (non-polar drug with a pKa range of 1-4 which is regarded as a weak) base. The PROTEC-PK graphs y-axis indicating the plasma drug concentration of the patient in µg/mL and an x-axis indicating the time sampled of the patients blood. The Cmax of each patient was different to indicate drug absorbtion variability. Cmax time was the same for each patient.

Table 6.1: data points used to construct PROTEC-PK in figure 6.1 (a) for patient 1-3

pk Patient 1		**Pk patient 2**		**Pk patient 3**	
Time sampled (hours)	**Plasma drug [] in**	**Time sampled (hours)**	**Plasma drug Concentration (µg/ml)**	**Time sampled (hours)**	**Plasma drug Concentration (µg/ml)**
0	0,00081	0	0,00031	0	-0,00119
0,25	-0,00349	0,25	0,00661	0,25	0,32041
0,5	0,16851	0,5	0,00941	0,5	0,32921
0,75	0,18121	0,75	0,43151	1	0,72121
1	1,21731	1	0,39511	2	0,54071
1,5	1,19691	2	0,45721	4	0,05401
2	0,30561	4	0,30381	8	0,00501
4	0,03411	8	0,13691	24	-0,00219

8	-0,00139	24	-0,00089	0	-0,00119
24	0,00251			0,25	0,32041

- **Scenario 2**

Figure 6.1 (b) was a PROTEC modelled for hyperalbuminea and hyperproteinemia to normalization protein and albumin levels. The designed graph consisted of a y-axis indicating the total protein and total albumin levels and the x-axis indicated the time plasma was sampled. The scenario used pregnant participants with the assumption that they had normal to high protein levels and a low risk cohort

Table 6.2: data points used to construct high albumin and potein to normalization over a specific time for figure 6.1 (b)

Time (hours)	Normal Albumin (g/dL)	High albumin (g/dL)	Normal protein (g/dL)	High protein (g/dL)
0	0,43	0,7	0,8	1,4
5	0,43	0,6	0,8	1
15	0,43	0,48	0,8	0,9
20	0,43	0,47	0,8	0,9
24	0,43	0,46	0,8	0,9

- **Scenario 3**

In figure 6.2 (a) the PROTEC-PK was modelled for a weak acid non-polar drug in below normal albumin levels. The y-axis was the plasma drug concentration and the x-axis indicated the time in hours. In figure 6.2 (b) the Protecc model for hypoalbuminea and hypoproteinemia was constructed where the y-axis indicated the total protein and total albumin levels from low to normalization and the x-axis indicated the time of plasma sample in hours. The scanario used TB/HIV patients treated with rifampicin and had hypoproteinemia blood disorders.

Table 6.3: data points used to construct PROTEC-PK in figure 6.2 (a)

Time (hours)	Plasma drug Concentration (µg/ml)
0	0
2	8
6	2
12	0.1

Table 6.4: Data points for figure 6.2 (b) to construct low albumin and low protein to normalization

Time (hours)	Normal Albumin (g/dL)	Low albumin (g/dL)	Normal protein (g/dL)	Low protein (g/dL)
0	0,43	0,07	0,8	0,5
5	0,43	0,3	0,8	0,59
15	0,43	0,38	0,8	0,69
20	0,43	0,39	0,8	0,73
24	0,43	0,39	0,8	0,75

- **Scenario 4**

In figure 6.3 (a) calibration curve calibration curve was designed and modified to access the relative accuracy of the drugs with moderate to low binding affinity. The concentration errors were compared using the binding constants K of the drugs: rifampicin, isoniazid, ethambutol and pyrazinamide.

Table 6.5: Data points used to construct the plasma concentration calibration comparison curve in figure 6.3 (a).

No Plasma		**1.6g/dL plasma**		**4.3g/dL Plasma**	
Drug Peak area	**Drug Concentration µg/mL**	**Drug Peak area**	**Drug concentration µg/mL**	**Drug Peak area**	**Drug Concentration µg/mL**
0	0	0	0	0	0
440000	3	430000	3,5	400000	4
4000000	25	3200000	25	2500000	25

Table 6.6: Data points used to construct the relative accuracy based on the binding constants of rifampicin, isoniazid, pyrazinamide and ethambutol at specific concentration points.

Concentration (µg/mL)	**Rifampicin**	**Pyrazinamide**	**Isoniazid**	**Ethambutol**
0	100	100	100	100
0,0101	99,0099	99,43376	99,98287	99,99416
0,0203	98,52217	99,15483	99,97443	99,99128
0,051	98,03922	98,87863	99,96608	99,98843
1,03	97,08738	98,33427	99,94961	99,98282
9	83,33333	90,46833	99,71167	99,90167
15,15	81,84818	89,61898	99,68597	99,8929
17,1	81,87135	89,63222	99,68637	99,89304
25	80	88,562	99,654	99,882

The assumptions for the model include:

1. The drug-protein binding affinity is different for each drug where there is a relative decrease in binding affinity to protein and tissue for drugs relative to Rifampicin.

2. The same calibrator stock plasma and content was used for the four drugs calibration curves.

3. The relative accuracy is the difference between the drug concentrations obtained in the calibration curve using patient albumin levels and calibration curves using normal albumin levels (3.5-4.5 g/dL).

4. The concentration of protein in the calibrator is indirectly proportional to the gradient of the calibration curve. Levels of albumin were classified as marked hypoalbuminemia (<2.5 g/dL), mild hypoalbuminemia (2.5-3.5 g/dL), normal albumin (3.5-4.5 g/dL), and hyperalbuminemia (>4.5 g/dL).

5. A single detector response is used to extrapolate the concentrations for both normal and patient albumin levels for the comparison of drug levels.

6. The same amount of protein or albumin stock is used in all the calibrators per calibration curve.

7. The validation recovery is less than 100%.

8. The extraction solvent maintains an optimized concentration levels suitable to chromatographic procedure.

9. The drug polarity is optimized and stabilized during validation in the plasma matrix and extraction solvent.

10. The unionized drug form is suited for reverse phase chromatography hyphenated mass spectrometry (MS) analysis (<2000 g/mol.) and the post column ionization ensues during the MS analysis.

11. Patient absorption and bioavailability is normal (relative) for the condition, disease and body mass index (BMI).

12. The maximum accuracy achievable with protein editing in calibration curves is 100% (estimated).

13. In the protein models, figure 6.3 (b), the accuracy is influenced by the differences of known and unknown patient protein levels and the binding constants of the drugs.

14. Assuming the calibrator protein levels are 4.3g/dL and the patient protein varies from 0 to 4.3g/dL the hypoproteinaemia normal total protein (8.0g/dL) and albumin (4.3g/dL) levels.

15. This would affect the changes in patient protein (Pp) and calibration curve protein (Cp) in would indicate the first model where patient protein levels are known and taken into account during the calibration curve construction.

16. For figure 6.3 (a), the Cp is assumed to be 8.0g/dL for total protein and 4.3g/dL for albumin as the medians in the normal range. The following was calculated for sample A (figure 6.3 (a)):

    Calibration curve (Cp) : 4.3 g/dL (figure 6.3 (a), Calibration curve)

    Measured drug level (Cm) : 25 µg/ml

    Patient protein (Pp) : 1.6 g/dL (figure 6.3 (a), Calibration curve)

    Corrected drug level (P_{dc}) : 21 µg/ml

    Relative error : (| 21 - 25| g/dL / 25 g/dL) * 100 = 16%

    Relative accuracy : 100 – 16 = 84%

17. Although larger drugs (> 75 000g/mol.) are confined to intravascular systems, 3L and prone to slow release from plasma, generally molecular sizes of < 2000 g/mol. will fall within the scope of our research as we are concerned with the parameters affecting the LCMS technique.

18. The drug recovery extraction solvent was different for each drug based upon the stability of the drug in the solvent, as reverse phase chromatography was used the unionised form was optimised relative to its acidity or basicity (pKa).

19. In plasma the drugs considered weak acids usually bind to albumin within the optimised pH range (<pka).

20. The calibrator stock protein condition cannot be assumed to be consistent. The r^2 was acceptable above 0.99. Only one plasma stock was used per batch analysis (calibrations curves).

21. Albumin concentration is the highest in plasma compared to other proteins, drug volume distribution is also affected by the affinity (K_p) tissue has for the drug and drug for the tissue.

22. Fluorescence excitation was used to confirm the different binding energies and affinity. Tryptophan intensity is measured as an indicator of energy necessary for bonding where the intensity is lowered as the binding to the site takes place.

23. Albumin is approximately 50% of the total protein content in plasma, figures 6.1 (b) and 6.2 (b). The calibrator protein (by determining the difference from the water content) content can be determined using a Karl Fischer titration or protein assay analysis.

6.4 Results and Discussion

The plasma protein water content was assessed and modelled against the calibration curves to determine the accuracy. This research was focused on the FDA concern of <100 % recovery in the analytical method validation and its effects on the drug from plasma assay results. This was assumed to be closely related to that of the patient's PV, where the patient therapeutic drug levels fall within a 0.1µg/ml--25 µg/ml range. Chromatography techniques are usually used to determine unknown concentrations within the stated concentration range including LCMS. The plasma content is assumed by literature to be approximately 92 % (m/v) water and 8 % (m/v) protein in healthy patients [144].

In this research the interest was in the occasional protein outliers, where it was discovered that the protein content varied from 8 % to 28%, i.e., 92 % to 2 % (m/v) water variations, where the recovery is below 100 % in the calibrator and sample extraction procedure. This may occur because of patient conditions affecting plasma viscosity or conditions such as hypoproteinaemia, hyperproteinaemia, hypoalbuminaemia, and hyperalbuminaemia. Although there are solvents that can ensure total analysis of protein, the drug structure needs to remain intact, and the extraction solvent must correlate to the stability and pKa of the drug for chromatographic techniques that may not provide optimal deproteination from the compound.

6.4.1 Pharmacokinetic (PK) data show differences in plasma drug levels

An excerpt from a typical clinical trial was used to show variations in patient pharmacokinetics, where the body interacts with the drug (ADME) and we gauge the drug's efficacy by relating the plasma drug levels to patient recovery status (condition). The therapeutic drug monitoring of patients with albumin < 2.5g/dl from TB and MTB hypoalbuminaemia patients was also observed. Where the weak acid and weak base drugs adhere to the pKa status to either ionize or not. The protein and tissue binding affinity changes when the electronic status of the drug changes. These conditions can, however, be controlled in the laboratory to optimize the stability and recovery of the drug during analysis.

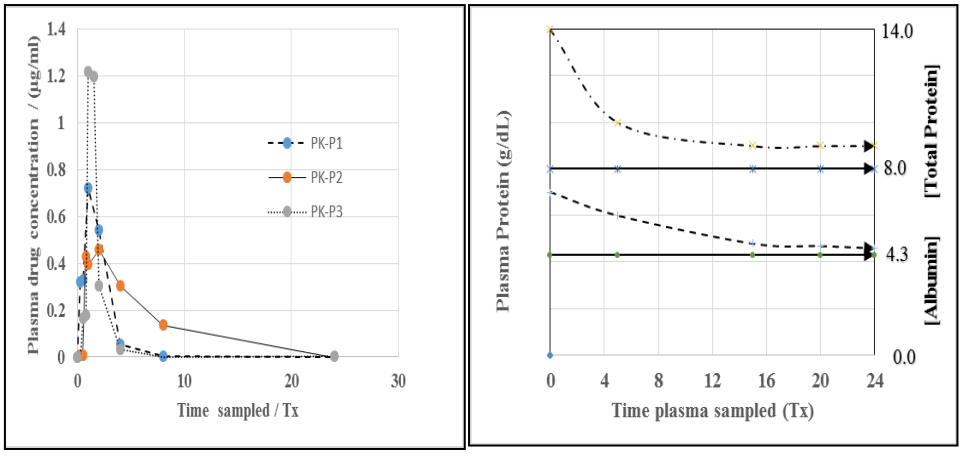

(a) (b)

Figure 6.1: PROTEC-PK (a) Pharmacokinetic study of three patients with a non-polar drug e.g (esomeprazole) (pKa 1.0 & 4.0); weak base). (b) PROTEC model for hyperalbuminea and hyperproteinemia to normalization

In figure 6.1 (a) the total drug (esomeprazole) plasma levels were analysed. A special interest was taken in the differences in the maximum drug levels (C_{max}) reached in a similar time (T_{max}) range (less than two hours). The assumption here is that the three patients (P1-P3) had the same protein concentration in their plasma. Therefore, a single calibration curve with the same plasma protein content calibrators was used. The low level of drug absorption seen could have been related to the drug formulation: for example, an enteric coating is added to the tablet where weak bases with high pKa's are taken orally. The PK curves are typical for oral dose, high absorption weak bases, such as the proton pump inhibitor omeprazole (esomeprazole),which is rapidly absorbed and binds to the receptor of the H^+K^+-ATPase proton pump.

A coating is usually added to the tablet where weak bases with high pKas are taken orally. The PK curves are typical for oral dose high absorption/weak base such as omeprazole (esomeprazole). Proton pump inhibitors block the gastric H, K-ATPase, inhibiting gastric acid secretion. There is rapid absorption and binding of the drug to the receptor of the proton pump that regulates acid (H^+) production during acid reflux. The response duration spans over a longer period than what the vascular esomeprazole levels indicate in figure 6.1 (a). Its primary pK_a of about 4.0 facilitates accumulation in the parietal cell, and a benzimidazole with a second pK_a of about 1.0.

Proton pump inhibitors are prodrugs activated by acids converting to sulphenic acids or sulphonamides. These can bind covalently with one or more cysteines of the ATPase. The drug and metabolites are thought to bind with stable covalently bonded sites on the proton pump and the recovery of these receptors is done over time. The reason for the shifts and the area under the pharmacokinetic in figure 6.1 (a) are the patients physiology relating to variations in plasma protein content of each patient. The *in vivo* drug-plasma interaction when assessing selected drug-protein binding energies and confirming variations in the individuals' plasma, affected current good laboratory practices and recovery rates were always below 100%. The drug-plasma concentration recovery and accuracy improvement was noted after accommodating the varying amounts of plasma protein.

In figure 6.1 (b), the participants were pregnant pregnant patients, a low risk cohort who were assumed to have normal to high plasma protein levels (hyperproteinaemia), and who were being treated for gastric acid reflux. During therapeutic drug monitoring or clinical trials, patient test sample variations in plasma protein levels are usually assumed to be low. The low risk patient cohort were considered to be healthy as they were not admitted with symptoms of dehydration. As such, the amount of albumin used in the calibrators was assumed to be similar to that of the patients (4.3 ± 1.5 g/dL). A possible relative error could have been incurred by not knowing the plasma protein content of an outlying patient sample or by not taking it into account during the preparation of the calibrator. However, the relative error was presumed to be minimal and did not affect the accuracy of the assay relative to the drug recovery process. There would have been significant errors, however, if patients were experiencing hypoalbumenia or if the calibrators contained increased levels of albumin, exceeding the levels in the patients' plasma/serum.

The situation is different for TB/HIV patients being administered rifampicin (RIF-4), Figure 6.2 (a). In figure 6.2 (a), hypoalbuminaemia is usually associated with critically ill HIV and TB patients treated with rifampicin. Rifampicin is soluble in methyl chloride with an octanol/water $\log K_{ow} = 4.24$ (estimated) zwitterion, with pKa 1.7 for the 4-hydroxy and pKa 7.9 due to piperazine nitrogen [79]. This makes it only slightly soluble in water at pH < 6. If plasma were affected by hypoalbuminaemia: a hydrophobicity change could change the solubility levels in the blood. The model in Figure 6.2 (b) uses the protein evaluation calibrations curves (PROTEC-PK) to show the stabilization of the protein and albumin levels during hyperproteinemia and hypoalbuminaemia. Figure 6.2 (b) model also shows the PROTEC analysis for hypoalbuminaemia.

The patients generally admitted had low protein (albumin) content at around 2.3 g/dl and below (where, at the Tygerberg Hospital in the Western Cape, the NHLS normalized range is 3.5--5.2 g/dl). With an increased water concentration in plasma, the ionized rifampicin form may enter the renal elimination pathway [160], with bright red-orange urine usually seen [161]. This is further complicated by socioeconomic factors that affect households in the Western Cape: dietary supplements which are high in protein are generally not affordable [162]. The geographical region is prone to low temperatures, which further exacerbate the situation for many TB and MTB patients – with increased mortality rates in certain sectors affected by their strained socioeconomic situation [162]. Patient data, where admission protein levels need to be documented and followed through to the laboratory, also produce information to predict the drug-plasma interaction where tissue absorbance is likely or not (as an equilibrium of whether plasma proteins is achieved or not). In support of the External Quality Assessment Schemes (EQAS), an accredited proficiency test laboratory to monitor the data was incorporated.

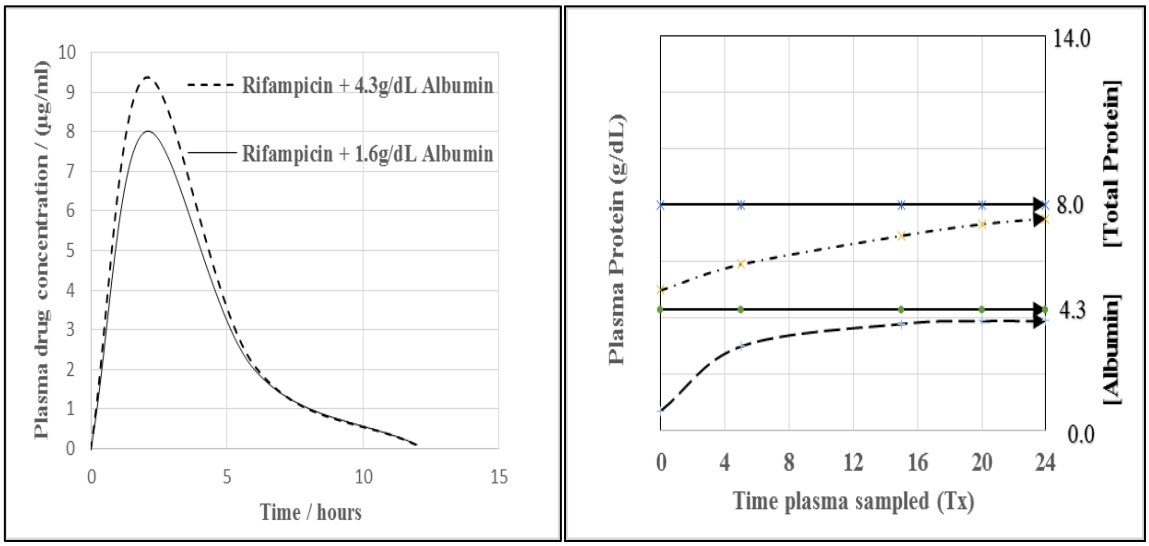

(a) (b)

Figure 6.2: PROTEC-PK (a) Rifampicin (a weakly acidic non-polar drug) concentrations from two calibration curves containing 1.6 g/dL and 4.3 g/dL albumin where patient albumin is below normal albumin levels at 1.6 g/dL (b) Protecc model for hypoalbuminaemia and hypoproteinemia to normalization after an unspecified time, Tx.

In figure 6.2 b, the curve presents the patient protein and albumin levels (broken lines ending with arrows), where the patient albumin is usually in the 1.6 ± 2.0 g/dL region. The straight (solid lines) lines are indicative of normal total protein (8.0 ± 2.0 g/dL) and albumin (4.3 ± 2.0 g/dL) levels used in the calibrator preparation. Plasma viscosity (protein to water ratio) changes from 12:1 to 5:1 in patient plasma and total plasma in calibrators respectively saw a more than 10 % increase in relative error. This would become significantly higher where the plasma volume is increased without adjusting for relative patient and calibrator albumin concentrations. The need for harmonization, standardization, and evidential traceability of the next generation of clinical measurements as an essential mechanism in quality assurance was supported by the design of this study model approach. The International Consortium for Harmonization of Clinical Laboratory Results has the role of reviewing priorities and maintaining a summary of measure and harmonization activities. A test sample was used from an accredited laboratory to verify the proficiency in our results for rifampicin. Patient protein evaluation to determine the content of their plasma protein especially where weak acid drugs are concerned would assist to determine competition and the spontaneity of drugs to bind to albumin which affects the patient-calibrator relative recovery accuracy in bioanalytical methods.

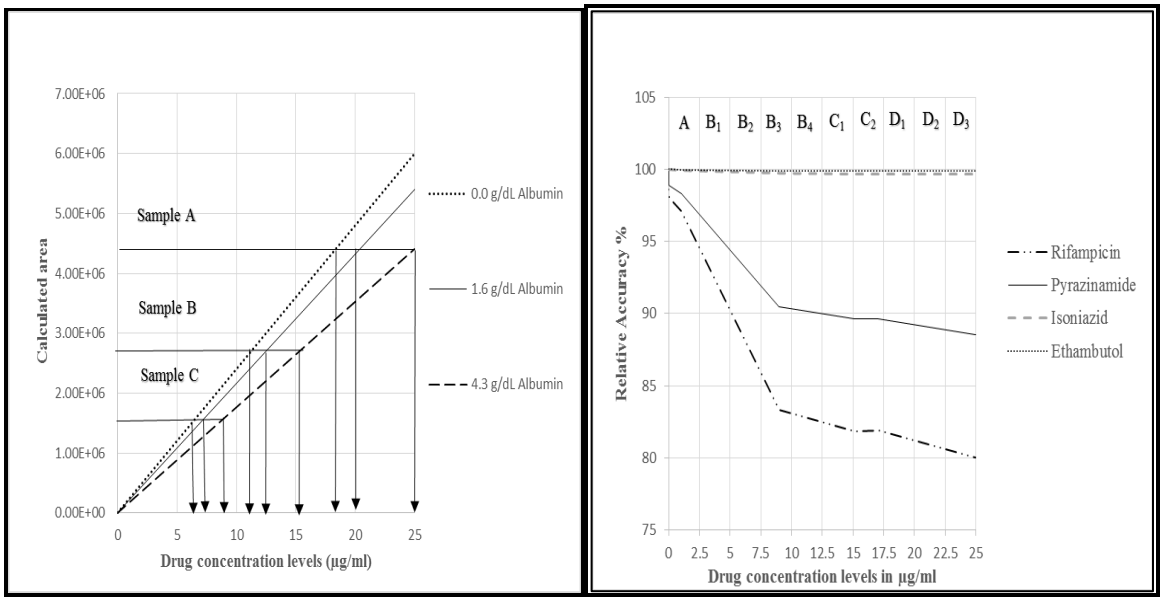

(a) (b)

Figure 6.3: (a) Calibration curves with varied protein content and varying patient protein levels in plasma / serum (b) Modelled accuracy fluctuations for the drug-protein binding affinity (MA - medium affinity and LA - low affinity drugs 1-4). Drug concentration regions A (0-2.49 µg/ml), B_1-B_4 (2.49-12.5 µg/ml), C_1-C_2 (12.5-17.5 µg/ml), D_1-D_3 (17.5-25 µg/ml).

Figure 6.3 (a), illustrates the drug rifampicin concentration ranges affected by protein variation in the calibrators, where < 100 % is noted in the recovery where albumin (plasma) is present. The calibration curve using zero albumin (0.00g/dl) shows the curve for 100 % recovery. This will vary for different drugs and laboratory equipment response. At high calibrator drug concentrations of >4µg/ml, the differences in extrapolated results increase as the amount of calibrator protein remains constant. (The total calibrator protein (plasma) content remains constant, whilst the total diluted volume is maintained.) The drug concentration is thus reduced by the low-end calibrator formation. The deproteination solvent e.g methanol is also kept at a constant volume. The pKa for drugs classified as either weak bases or acids determine the solubility and hydrophobicity of drugs.

The model illustrated in Figure 6.3 (a) shows the three possible drug concentrations for both normal albumin of 4.3 g/dl (calibration curve) and patient protein (albumin) levels at 1.6g/dl (calibration curve) where the level of an unknown patient protein (albumin) will influence the accuracy. The accuracy lies in the differences obtained between the concentrations of the drugs with varied albumin levels in the calibration curves. It can be seen that the accuracy is directly proportional to differences in the patient and calibrator protein levels in the calibration curves.

The calibrator stock plasma protein distribution was noted with the r^2 as 0.9999. However, the ratio of albumin to total protein was significant. Critically ill HIV patients receiving treatment for TB would usually have a low plasma protein (albumin) level below 4.3 g/dl. In plasma, the total protein to water content ratio changes from 12:1 to 5:1 in calibrator stocks. The plasma viscosity in patients is also affected by disease and hydration levels. The efficacy of the ratio of plasma to water adjustments cannot be overlooked, even though most patients will not have significant deviations from the normal blood water to protein ratio, which is approximately 12:1. Changes up to 5:1 were observed. This compounds the error if the patient ratio is affected by disease and metabolic oxidative products. Water level determinations can be a red flag for further investigations to be conducted on patient protein levels, and the calibrator stock albumin levels could be assessed as well.

The curve gradient, m (y=mx+c), was found to be directly affected by the drug-protein binding affinity and albumin levels. The detector response (y) was used in the extrapolation process. In figure 6.3 (b), region A, the accuracy was lowest and closely merged as the low drug bound albumin levels do not affect the recovery by much. A gradual increase in relative error is visible after 2 µg/ml (regions B to D) with significant accuracy decreases noted from D_1 to D_3. Low gradients (m) due to high albumin levels see an exaggerated increase in the extrapolated concentration (x) especially in the higher concentration regions, figure 6.3 (b), D_1-D_3. Here we confirmed drug-protein binding variations and distribution after comparing normal and hypoalbuminaemia albumin conditions.

Shown in figure 6.3 (b) are the relative accuracies (percentages or %) for the drug binding affinity property for protein (albumin). The model is based upon the rifampicin's moderate affinity (MA), with the highest relative binding affinity for albumin. We have already confirmed the binding affinity of figure 6.3 (b) shows the drug-protein binding affinity for four different drugs relative to rifampicin's binding affinity.

In figure 6.3 (b), the naming of the drugs was not of significance, as further validation is needed at the time of use. Since the plasma protein condition (affinity) is prone to changes, here the drug properties are portrayed as relative to rifampicin's experimental binding energy data. The confirmation of drug-albumin complex formation and their spontaneity of binding were covered in the previous chapter, which covered the identification of the binding interaction of anti-TB drugs with albumin: 'A Computational Molecular Docking, Fluorescence and Absorption Spectroscopy Study'.

The binding energies were as follows: rifampicin 5.379 X 10^2 M^{-1} (moderate affinity), isoniazid 9.285 M^{-1} (low affinity), 25-desacetyl rifampicin 3.156 M^{-1} (low affinity), ethambutol 3.443 M^{-1} (low affinity) and pyrazinamide 3.076 X 10^2 M^{-1} (moderate affinity). The Gibbs free energies for the four drugs were below zero indicating spontaneous binding reactions. Rifampicin is a non-polar weak acid with a higher binding affinity, indicating it will form the more stable complex with albumin, as opposed to soluble isoniazid – due to its being polar and in ionized form easily excreted in the urine, resulting in low levels of detection. This will affect the bioavailability and accuracy of the assay levels for patients experiencing hyper and hypoalbuminaemia with related complications and induction processes of the enzymes (CYP3A4/5) as well. The dose optimization will be further complicated where the low binding affinity drugs will have better recoveries and low detector responses due to low bioavailability and because it is also ionized. These complications are apparent in multidrug administering, and where larger numbers of patients (more than 400), are involved in clinical trials. The relative accuracy in bioequivalence and bioavailability studies with varying patient protein levels may be more critical for drugs with a narrow therapeutic index.

6.5 Conclusion

In this study the use of a representative calibrator matrix and albumin levels in relation to the patient's albumin levels was studied. The amount of drug that is bound to albumin and the subsequent recovery levels both affect the gradient (slope) of the calibration curve. The minimizing of relative errors are important for accuracy in clinical trials, bioequivalence and bioavailability studies. The Significant and of concern were narrow therapeutic drug dosage increases that could cause side effects and exceeding the C_{max} in clinical trial dose optimization studies, thus putting the patient at risk. The dose optimization requires accurate bioanalytical drug-plasma assays, as low drug concentrations administered to patients with diseases may cause drug resistance. Patient plasma transporting low

binding affinity drugs such as INH may have metabolites and high excretory levels if co-administered with competitive drugs with higher binding affinities to plasma proteins. Compliance with the FDA and international regulatory guidelines would require reproducibility of a calibration curve that closely resembles calibrator and patient drug-protein interactions. Plasma viscosity (protein to water ratio) changes from 12:1 to 5:1 in patient plasma and total plasma in calibrators showed the relative error increased more than 10%. Further increases in the difference between patient and calibrator albumin (protein) levels could see a further 20 % increase in relative error. Hypoalbuminemia (or hypoproteinaemia in cases of related low total protein levels) patients show the lowest accuracy in assay test results and the highest risk of mortality. The use of the patient-calibrator PROTEC-PK™ was proposed.

Chapter 7

Conclusion

7.1 The analytical liquid chromatography–mass spectrometry (LCMS) method for rifampicin was developed and validated using phenacetin as an internal standard combined with human plasma. The extraction solution for deproteination of the plasma standards used was ascorbic acid and methanol. The main focus of the study was to compare the LCMS calibration curves from the validation data of rifampicin known standard without plasma and rifampicin known standards spiked with plasma. The comparison of the calibration curve data with and without plasma was as follows: Limit of detection (LOD) for plasma-free standards was found to be 0.19 µg/ml and the limit of quantification (LOQ) LOQ was found to be 0.57 µg/ml. The LOD for rifampicin plasma standards was found to be 0.0801µg/ml and the LOQ was found to be 0.24 µg/ml. The % relative standard deviation (RSD) for rifampicin-free plasma concentration of 0.5 µg/ml is 12.1%. The % RSDs rifampicin-plasma standard concentration of 0.5 µg/ml, are 5.6% respectively. The percentages of RSD are in the accepted range, which is % RSD < 20%. The correlation coefficient r^2 generated from the calibration curve without plasma was 0.985. The correlation coefficient r^2 generated from the calibration curve with plasma was 0.997. From the linearity comparison of the calibration curves the gradient of the plasma calibration was lower than the rifampicin-plasma free curve which indicated that plasma caused decreasing effect on the gradiant of the calibration curve. This indicated that the drug recovery for plasma standards directly affected the area response of the LCMS detection due to drug-plasma interference. Therefore we conclude that when validating bioanalytical methods for clinical trials it is important to incorporate plasma as a variable in the method validation.

7.2 Plasma is a unique substance, and when extracted the plasma content is dependent on whether the patient is healthy or not.

7.3 Using plasma from different patients can cause deviation when compared to a plasma calibrator derived from one patient due to the different protein (α and β globulins and albumin) concentrations of plasma of different patients containing a water percentage that is lower or higher than 90%.

7.4 The plasma used to prepare samples should be isolated from one specific patient.

7.5 The water content percentage in the plasma of the patient being assessed can be tested using the Karl Fischer process however error of results are possible. Direct determination of plasma concentration levels using systems like the Thermo Nanodrop system is more accurate.

7.6 A recommendation is that plasma from different patients can cause fluctuations in calibration curves which can cause a change in the gradient of the calibration curve leading to erroneous results.

7.7 The results obtained from the computational pharmacology data predicted that rifampicin (RIF), isoniazid (INH), pyrazinamide (PYR) ethambutol (ETH), (D-RIF) spontaneously bind to HSA by hydrogen bonding via electrostatic interactions.

7.8 The predicted enthalpy values for the three best possible conformations of each drug to the plasma protein human serum albumin (HSA) were used to calculate the change in entropy and Gibbs free energy of the drugs assessed. The calculated Gibbs free energy from the predicted enthalpy values indicates that, of the five drugs assessed, rifampicin has the highest binding affinity of -104.04 kJ/mol and pyrazinamide has the lowest binding affinity of -33.05 kJ/mol to the HSA protein.

7.9 The fluorescence spectroscopy was used to confirm the computational prediction of binding. However, in the experiment plasma which consists of the HSA protein was used instead of HSA due to unavailability of the reference material, therefore we could not validate the computational data with the fluorescence data. The quenching constant Ksv and Gibbs free energies were calculated for rifampicin, isoniazid, pyrazinamide, ethambutol, 25-desacetyl rifampicin, and RIF-4. RIF-4 combination sample was the strongest quencher of plasma with the values of (RIF-4 30.742 x 10^3 M^{-1}, 30.506 x 10^3 M^{-1}, 28.283 x 10^3 M^{-1}, at the temperatures 298.15 K 310.15 K and 313.15 K respectively). Of the the 4 anti TB samples (RIF, INH, PYR and ETH) and 25-desacetyl rifampicin drugs, rifampicin was the strongest quencher of plasma with a Ksv of (rifampicin 15.083 x 10^3 M^{-1}, 16.140 x 10^3 M^{-1}, 16.801 x 10^3 M^{-1}, at the temperatures 310.15 K 313.15 K and 318.15 K respectively). Ethambutol was the weakest quencher of plasma with a value of (ethambutol 1.9374 x 10^3 M^{-1}, 1.8896 x 10^3 M^{-1}, 1.9737 x 10^3 M^{-1}, at the temperatures 298.15 K 313.15 K and 318.15 K respectively).

The quenching mechanism of each drug was found to be dynamic quenching except for ethambutol, which indicated a combination of dynamic and static quenching and RIF-4 which indicated a decrease in the quenching constant as the temperature was increased. This is an indication of static quenching taking place. The binding constants were used to calculate the experimental thermodynamic parameters. The enthalpy values obtained were positive and the entropy values calculated were positive, which according to the literature, indicates that the hydrophobic forces were the main interactions that took place between the drugs accessed and the plasma proteins – except for pyrazinamide, which had a negative change in entropy and enthalpy values. The literature states that this could be due to Van de Waals forces and hydrogen bonding at low dielectric media.

The Gibbs free energies obtained from the experimental data were negative, which indicates that all of the drugs accessed binds spontaneously to the plasma proteins present. Rifampicin had the lowest Gibbs free energy with values (-16.25 kJ/mol, -17.47 kJ/mol and -19.51 kJ/mol at temperatures of 310.15 K, 313.15 K, and 318.15 K respectively) and the highest binding affinity. Ethambutol had the highest Gibbs free energy with values of -0.706 kJ/mol, -2.785 kJ/mol, -3.278 kJ/mol and -4.144 kJ/mol at temperatures 298.15 K, 310.15 K, 313.15 K, 318.15 K respectively) and the lowest binding affinity. Hence, the prediction that rifampicin would bind most to the HSA protein was correct. However, the binding interaction of the prediction and the experimental data obtained did not coincide. This could be due to the fact that the protein used in the experiment was full plasma protein due to financial constraints, and not only HSA as in the computational modeling prediction. However HSA is the main protein in plasma that caused drug-plasma binding interactions.

7.10 The *UV*-vis spectroscopy results of the drugs assessed indicated red shifts to longer wavelengths, which confirm the decrease in hydrophobicity of the plasma protein. Hence, from this finding, it can be confirmed that hydrogen bonding is taking place between the drug and the protein.

7.11 Protein to water ratio (PV) changes from 12:1 to 5:1 in patient plasma, and total plasma in calibrators caused the relative error to be increased by more than 10 %. Additional increases in the difference between patient and calibrator albumin (protein) levels could produce a further 20% increase in relative error. Patients with hypoalbuminemia (or hypoproteinaemia in cases of related low total protein levels) show the lowest accuracy in assay test results and have the highest risk of mortality. This study therefore proposes the use of the patient-calibrator PROTEC-PK^{TM} in validation assay development and therapeutic drug monitoring to ensure that patient albumin levels are within acceptable validation accuracy ranges.

7.12 To conclude, all of the parameters assessed are important in terms of improving the accuracy of the therapeutic drug monitoring process of TB patient blood samples in clinical studies. This includes increased accuracy of calibrator drug-plasma assay calibration curves, detailed protein plasma calibrator level analysis, and thorough insight into drug-binding interactions of TB drugs with plasma proteins.

7.13 Future work

The LCMS rifampicin quantification method validated should be further optimized for faster elution time. The method should also go through precision and intermediate-precision tests to confirm that the method is reproducible, and free from sample preparation error.

To research fast and accurate methods to obtain plasma protein content of clinical patients in therapeutic monitoring drugs trials which will improve bioanalytical methods and concentration

Further analysis of fluorescence and UV spectroscopy should be performed using HSA to compare and validate the computational modeling data obtained by performing the analysis with HSA instead of full blood plasma.

Molecular dynamic with HSA interacting with rifampicin, isoniazid, ethambutol and pyrazinamide will be performed using a video modeling tool of a particle in a box therefore it would illustrate through video visuals how anti-TB drugs bind to HSA.

The PROTEC-PK^{TM} curves should be assessed and modified on a mathematical and statistical method approach which could be test for use in clinical trials in the future.

References

1. Alghamdi WA, Al-Shaer MH, Peloquin CA. Protein Binding of First-Line Antituberculosis Drugs. Antimicrobial Agents Chemotherapy. Journal of clinical microbiology 2018;62(7):e00641-18. Published 2018 Jun 26. doi:10.1128/AAC.00641-18

2. Food and Drug Administration. Bioavailability and Bioequivalence Requirements, 21 Code of federal regulations Part 320 (2006).

3. US Department of Health and Human Services, Food and Drug Administration, Center for Drug Evaluation and Research, Centre for Veterinary Medicine. Guidance for Industry: Bioanalytical Method Validation. Biopharmaceutics May 2001.

4. Weng N, Halls TDJ. Systematic troubleshooting for LC/MS/MS. Pharm Tech. Biopharm international 2001; 28–38.

5. James CA, Breda M, Frigerio E. Bioanalytical method validation: A risk-based approach? Journal Pharmaceutical and biomedical analysis 2004; 5(4): 887–893.

6. Naidoo S, Africa A, Dalvie MA. Exposure to CCA-treated wood amongst food caterers and residents in informal areas of Cape Town. South African journal of science 2013;109(7/8). http://dx.doi.org/10.1590/ sajs.2013/20120043

7. Deedwania PC, Carbajal EV. Getting with the ACC/AHA guidelines for the treatment of chronic angina as a disease state. Reviews in Cardiovascular Medicine 2009;10 Suppl 1:S11–20.

8. Lloyd-Jones D, Adams R, Carnethon M, De Simone G, Ferguson TB, Flegal K, Ford E, Furie K, Go A, Greenlund K, Haase N, Hailpern S, Ho M, Howard V, Kissela B, Kittner S, Lackland D, Lisabeth L, Marelli A, McDermott M, Meigs J, Mozaffarian D, Nichol G, O'Donnell C, Roger V, Rosamond W, Sacco R, Sorlie P, Stafford R, Steinberger J, Thom T, Wasserthiel-Smoller S, Wong N, Wylie-Rosett J, Hong Y. Heart disease and stroke statistics–2009 update: a report from the American Heart Association Statistics Committee and Stroke Statistics Subcommittee, Circulation , 2009, vol. 119 (pg. 480-486)

9. Virmani R, Burke AP, Farb A, Kolodgie FD. Pathology of the vulnerable plaque, Journal of the American College of Cardiology, 2006, vol. 47 (pg. C13-C18)

10. Naghavi M, Libby P, Falk E, Casscells SW, Litovsky S, Rumberger J, Badimon JJ, Stefanadis C, Moreno P, Pasterkamp G, Fayad Z, Stone PH, Waxman S, Raggi P, Madjid M, Zarrabi A, Burke A, Yuan C, Fitzgerald PJ, Siscovick DS, de Korte CL, Aikawa M, Juhani Airaksinen KE, Assmann G, Becker CR, Chesebro JH, Farb A, Galis ZS, Jackson C, Jang IK, Koenig W, Lodder RA, March K, Demirovic J, Navab M, Priori SG, Rekhter MD, Bahr R, Grundy SM, Mehran R, Colombo A, Boerwinkle E, Ballantyne C, Insull WJr, Schwartz RS, Vogel R, Serruys PW, Hansson GK, Faxon DP, Kaul S, Drexler H, Greenland P, Muller JE, Virmani R, Ridker PM, Zipes DP, Shah PK, Willerson JT. From vulnerable plaque to vulnerable patient: a call for new definitions and risk assessment strategies: part I, Circulation , 2003, vol. 108 (pg. 1664-1672)

11. W. Maetzler, A.K. Stapf, C. Schulte, A.K. Hauser, S. Lerche, I. Wurster, E. Schleicher, A. Melms, D. Berg, Serum and cerebrospinal fluid uric acid levels in lewy body disorders: associations with disease occurrence and amyloid-beta pathway, Journal of Alzheimers Disease, 27 (2011) 119–126.

12. M.Q. Pan, H.M. Gao, L. Long, Y.Q. Xu, M. Liu, J. Zou, A.M. Wu, X.B. Wei, X.H. Chen, B.S. Tang, Q. Wang, Serum uric acid in patients with Parkinson's disease and vascular parkinsonism: a cross-sectional study, Neuroimmunomodulation 20 (2013) 19–28.

13. I. Schlesinger, N. Schlesinger, Uric acid in Parkinson's disease, Mov. Disord. Off. Journal of Movement Disorder Society, 23 (2008) 1653–1657.

14. Findlay JWA, Dillard RF. Appropriate calibration curve fitting in ligand binding assays. American Association of Pharmaceutical Scientists Journal 2007; 9(2): E260 https://doi.org/10.1208/aapsj0902029.CrossRefPubMedPubMedCentralGoogle Scholar

15. Booth B, Arnold ME, DeSilva B, Amaravadi L, Dudal S, Fluhler E, et al. Workshop report: crystal city V-quantitative bioanalytical method validation and implementation: the 2013 revised FDA guidance. American Association of Pharmaceutical Scientists Journal 2015; 17(2): 277–88. https://doi.org/10.1208/s12248-014-9696-2.

16. EMA, European Medicines Agency. Guideline on bioanalytical method validation. [Online] July 21, 2011. EMEA/CHMP/EWP/192217/2009.Google Scholar

17. U.S. Food and Drug Administration. Guidance for industry bioanalytical method validation. [Online] May 2001. http://www.fda.gov/cder/guidance/index.htm.

18. U.S. Food and Drug Administration, US Department of Health and Human Services. Draft guidance for industry: bioanalytical method validation (Revised). [Online] September 2013. http://www.fda.gov/downloads/Drugs/GuidanceComplianceRegulatoryInformation/Guidances/UCM368107.pdf.

19. Guideline on bioanalytical method validation in pharmaceutical development. Japan: Pharmaceutical Manufacturers Association; 2013.Google Scholar

20. Guide for validation of analytical and bioanalytical methods, Resolution - RE n. 899, of May 29, 2003, Agência Nacional de Vigilância Sanitária. www.anvisa.gov.br.

21. Bioanalytical Guidance Resolution – RDC # 27 of 17 MAY 2012, Agência Nacional de Vigilância Sanitária. www.anvisa.gov.br.

22. Viswanathan CT, Bansal S, Booth B, DeStafano J, Rose MJ, Sailstad J, et al. Quantitative bioanalytical methods validation and implementation: best practices for chromatographic and ligand binding assays. Journal of Pharmaceutical Research 2007;24(10):1962–73.Google Scholar

23. Nowatzke W, Woolf E. Best practices during bioanalytical method validation for the characterization of assay reagents and the evaluation of analyte stability in assay standards, quality controls, and study samples. American Association of Pharmaceutical Scientists Journal 2007; 9(2):F117–E122.CrossRefGoogle Scholar

24. Yantih N., Hafilah S., Harahap Y., Wahono, (2018) Partial Validation of High Performance Liquid Chromatography for Analysis of Isoniazid in Rat Plasma Jurnal Ilmu Kefarmasian Indonesia, April 2018, 67-71 Vol. 16 No. 1 ISSN 1693-1831,

25. Kolmer E.W.J.E.B, Marga J.A., Erik T., C.A. van den Hombergh Nielka E. van Erp Lindsey H.M. te Brake, Aarnoutse RE,(2017) Determination of protein-unbound, active rifampicin in serum by ultrafiltration and Ultra Performance Liquid Chromatography with UV detection. A method suitable for standard and high doses of rifampicin Journal of Chromatography B Volume 1063, 15 September 2017, Pages 42-49 https://doi.org/10.1016/j.jchromb.2017.08.004

26. Sheets, Rebecca. 2018. 'Chapter 16 - Lot Release, Analytics, and Analytical Validation.' in Rebecca Sheets (ed.), Fundamentals of Biologicals Regulation (Academic Press).

27. McMillan, J. 2016. '13 - Principles of Analytical Validation.' in P. Ciborowski and J. Silberring (eds.), Proteomic Profiling and Analytical Chemistry (Second Edition) (Elsevier: Boston).

28. Vessman, Jörgen. 1996. 'Selectivity or specificity? Validation of analytical methods from the perspective of an analytical chemist in the pharmaceutical industry', Journal of Pharmaceutical and Biomedical Analysis, 14: 867-69.

29. Bouabidi, A., E. Rozet, M. Fillet, E. Ziemons, E. Chapuzet, B. Mertens, R. Klinkenberg, A. Ceccato, M. Talbi, B. Streel, A. Bouklouze, B. Boulanger, and Ph Hubert. 2010. 'Critical analysis of several analytical method validation strategies in the framework of the fit for purpose concept', Journal of Chromatography A, 1217: 3180-92.

30. Ye, Christine, June Liu, Feiyan Ren, and Ngozi Okafo. 2000. 'Design of experiment and data analysis by JMP® (SAS institute) in analytical method validation', Journal of Pharmaceutical and Biomedical Analysis, 23: 581-89.

31. Enderle, Yeliz, Kathrin Foerster, and Jürgen Burhenne. 2016. 'Clinical feasibility of dried blood spots: Analytics, validation, and applications', Journal of Pharmaceutical and Biomedical Analysis, 130: 231-43.

32. Knapen, Lotte M., Yvo de Beer, Roger J. M. Brüggemann, Leo M. Stolk, Frank de Vries, Vivianne C. G. Tjan-Heijnen, Nielka P. van Erp, and Sander Croes. 2018. 'Development and validation of an analytical method using UPLC–MS/MS to quantify everolimus in dried blood spots in the oncology setting', Journal of Pharmaceutical and Biomedical Analysis, 149: 106-13.

33. Brkljača, Robert, and Sylvia Urban. 2015. 'Limit of detection studies for application to natural product identification using high performance liquid chromatography coupled to nuclear magnetic resonance spectroscopy', Journal of Chromatography A, 1375: 69-75.

34. Pérez-Lozano, P., E. García-Montoya, A. Orriols, M. Miñarro, J. R. Ticó, and J. M. Suñé-Negre. 2004. 'Development and validation of a new HPLC analytical method for the determination of alprazolam in tablets', Journal of Pharmaceutical and Biomedical Analysis, 34: 979-87.

35. Carlson, Jill, Artur Wysoczanski, and Edward Voigtman. 2014. 'Limits of quantitation — Yet another suggestion', Spectrochimica Acta Part B: Atomic Spectroscopy, 96: 69-73.

36. Kirkwood, Jay S., Corey D. Broeckling, Seth Donahue, and Jessica E. Prenni. 2016. 'A novel microflow LCMS method for the quantitation of endocannabinoids in serum', Journal of Chromatography B, 1033-1034: 271-77.

37. Soboleva, Eugenia, and Árpád Ambrus. 2004. 'Application of a system suitability test for quality assurance and performance optimisation of a gas chromatographic system for pesticide residue analysis', Journal of Chromatography A, 1027: 55-65.

38. Ferreira, Sergio L. C., Adriana O. Caires, Thaise da S. Borges, Ariana M. D. S. Lima, Laiana O. B. Silva, and Walter N. L. dos Santos. 2017. 'Robustness evaluation in analytical methods optimized using experimental designs', Microchemical Journal, 131: 163-69.

39. Moldoveanu and Victor David (eds.), Essentials in Modern HPLC Separations (Elsevier). 2017. 'Chapter 4 - Basic Information Regarding the HPLC Techniques.' in Serban C.

40. Ahuja, Satinder. 2005. '1 - Overview: Handbook of Pharmaceutical Analysis by HPLC.' in Satinder Ahuja and Michael W. Dong (eds.), Separation Science and Technology (Academic Press).

41. Gika, H., G. Kaklamanos, P. Manesiotis, and G. Theodoridis. 2016. 'Chromatography: High-Performance Liquid Chromatography.' in Benjamin Caballero, Paul M. Finglas and Fidel Toldrá (eds.), Encyclopedia of Food and Health (Academic Press: Oxford).

42. Soliven, A., S. Kayillo, and R. A. Shalliker. 2013. 'LIQUID CHROMATOGRAPHY | Reversed Phase☆.' in, Reference Module in Chemistry, Molecular Sciences and Chemical Engineering (Elsevier).

43. Perutka, Zdeněk, and Marek Šebela. 2018. 'Chapter Two - Basis of Mass Spectrometry: Technical Variants.' in Fernando Cobo (ed.), The Use of Mass Spectrometry Technology (MALDI-TOF) in Clinical Microbiology (Academic Press).

44. Picó, Yolanda. 2015. 'Chapter 2 - Advanced Mass Spectrometry.' in Yolanda Picó (ed.), Comprehensive Analytical Chemistry (Elsevier).

45. David Sparkman, O. 2016. 'A Perspective on Books on Mass Spectrometry in Chemistry.' in Michael L. Gross and Richard M. Caprioli (eds.), The Encyclopedia of Mass Spectrometry (Elsevier: Boston).

46. Crotti, Sara, Ilena Isak, and Pietro Traldi. 2017. 'Chapter 18 - Advanced spectroscopic detectors for identification and quantification: Mass spectrometry.' in Salvatore Fanali, Paul R. Haddad, Colin F. Poole and Marja-Liisa Riekkola (eds.), Liquid Chromatography (Second Edition) (Elsevier).

47. March, Raymond E., and John F. J. Todd. 2016. 'The Development of the Quadrupole Mass Filter and Quadrupole Ion Trap.' in Michael L. Gross and Richard M. Caprioli (eds.), The Encyclopedia of Mass Spectrometry (Elsevier: Boston).

48. Sumner, Neil. 2011. 'Developing counter current chromatography to meet the needs of pharmaceutical discovery', Journal of Chromatography A, 1218: 6107-13.

49. Lee, M. S., and E. H. Kerns. 1999. 'LC/MS applications in drug development', Mass Spectrometry Reviews, 18: 187-279.

50. Zhou, Leon Z. 2005. '19 - Applications of LC/MS in Pharmaceutical Analysis.' in Satinder Ahuja and Michael W. Dong (eds.), Separation Science and Technology (Academic Press).

51. Holčapek, Michal, Robert Jirásko, and Miroslav Lísa. 2012. 'Recent developments in liquid chromatography–mass spectrometry and related techniques', Journal of Chromatography A, 1259: 3-15.

52. Katzung, B.G., Basic & clinical pharmacology. 2018.

53. Davis, J.L., Chapter 2 - Pharmacologic Principles, in Equine Internal Medicine (Fourth Edition), S.M. Reed, W.M. Bayly, and D.C. Sellon, Editors. 2018, W.B. Saunders. p. 79-137.

54. Raza, K., et al., 9 - Pharmacokinetics and biodistribution of the nanoparticles, in Advances in Nanomedicine for the Delivery of Therapeutic Nucleic Acids, S. Nimesh, R. Chandra, and N. Gupta, Editors. 2017, Woodhead Publishing. p. 165-186.

55. Kenakin, T.P., Chapter 7 - Pharmacokinetics I: Permeation and Metabolism, in Pharmacology in Drug Discovery and Development (Second Edition), T.P. Kenakin, Editor. 2017, Academic Press. p. 157-191.

56. Sarmini, K. and E. Kenndler, Ionization constants of weak acids and bases in organic solvents. Journal of Biochemical and Biophysical Methods, 1999. **38**(2): p. 123-137.

57. Hills, A.G., pH and the Henderson-Hasselbalch equation. The American Journal of Medicine, 1973. **55**(2): p. 131-133.

58. Gaffney, J.S. and N.A. Marley, Chapter 5 - Acids and Bases, in General Chemistry for Engineers, J.S. Gaffney and N.A. Marley, Editors. 2018, Elsevier. p. 147-180.

59. Barret, R., 2 - Importance and Evaluation of the pKa, in Therapeutical Chemistry, R. Barret, Editor. 2018, Elsevier. p. 21-51.

60. Schreiber, B., Selective and enhanced fluorescence by biocompatible nanocoatings to monitor G-protein-coupled receptor dynamics. 2018.

61. Powell, A.L., The fundamentals of fluorescence. Journal of Chemical Education, 1947. **24**(9): p. 423.

62. Fraiji, L.K., D.M. Hayes, and T.C. Werner, Static and dynamic fluorescence quenching experiments for the physical chemistry laboratory. Journal of Chemical Education, 1992. **69**(5): p. 424.

63. Tissue, B.M., Ultraviolet and Visible Absorption Spectroscopy, in Characterization of Materials. 2002.

64. Young, J.K., et al., The use of UV-visible spectroscopy for the determination of hydrophobic interactions between neuropeptides and membrane model systems. Biopolymers, 1992. **32**(8): p. 1061-4.

65. Swinehart, D.F., The Beer-Lambert Law. Journal of Chemical Education, 1962. **39**(7): p. 333.

66. Kukreja, J.B., I.M. Thompson, and B.F. Chapin, Organizing a clinical trial for the new investigator. Urologic Oncology: Seminars and Original Investigations, 2018.

67. Mead, S. and F. Tagliavini, Chapter 24 - Clinical trials, in Handbook of Clinical Neurology, M. Pocchiari and J. Manson, Editors. 2018, Elsevier. p. 431-444.

68. Dal-Ré, R., Clinical Trials Transparency: Where Are We Today? Trends in Cancer, 2018. **4**(1): p. 1-3.

69. Velayati, A.A. and P. Farnia, Chapter 2 - Microscopic Anatomy of Mycobacterium tuberculosis, in Atlas of Mycobacterium Tuberculosis, A.A. Velayati and P. Farnia, Editors. 2017, Academic Press: Boston. p. 17-69.

70. Kumar, N., B. Das, and S. Patra, Chapter 10 - Drug Resistance in Tuberculosis: Nanomedicines at Rescue, in Antimicrobial Nanoarchitectonics, A.M. Grumezescu, Editor. 2017, Elsevier. p. 261-278.

71. Talbot, E.A. and B.J. Raffa, Chapter 92 - Mycobacterium tuberculosis, in Molecular Medical Microbiology (Second Edition), Y.-W. Tang, et al., Editors. 2015, Academic Press: Boston. p. 1637-1653.

72. Bhat, Z.S., et al., Cell wall: A versatile fountain of drug targets in Mycobacterium tuberculosis. Biomedicine & Pharmacotherapy, 2017. **95**: p. 1520-1534.

73. Gravier-Hernández, R. and L. Gil-del Valle, Chapter 2 - Oxidative Stress and Tuberculosis–Human Immunodeficiency Virus Coinfection, in HIV/AIDS, V.R. Preedy and R.R. Watson, Editors. 2018, Academic Press. p. 17-27.

74. Pascual-Pareja, J.F., et al., Treatment of pulmonary and extrapulmonary tuberculosis. Enfermedades infecciosas y microbiologia clinica (English ed.), 2018. **36**(8): p. 507-516.

75. Caminero, J.A., et al., Diagnosis and Treatment of Drug-Resistant Tuberculosis. Archivos de Bronconeumología (English Edition), 2017. **53**(9): p. 501-509.

76. T. Ogawa, W.R. Matson, M.F. Beal, R.H. Myers, E.D. Bird, P. Milbury, S. Saso, Kynurenine pathway abnormalities in Parkinsons-disease, Neurology 42 (1992) 1702–1706.

77. Nayak, N., J. Ramprasad, and U. Dalimba, New INH–pyrazole analogs: Design, synthesis and evaluation of antitubercular and antibacterial activity. Bioorganic & Medicinal Chemistry Letters, 2015. **25**(23): p. 5540-5545.

78. H. Luan, L.-F. Liu, N. Meng, Z. Tang, K.-K. Chua, L.-L. Chen, J.-X. Song, V.C.T. Mok, L.-X. Xie, M. Li, Z. Cai, L.C. MS-Based Urinary, Metabolite signatures in idiopathic Parkinson's disease, Journal of Proteome Research 14 (2015) 467–478.

79. Rifampin. Tuberculosis, 2008. **88**(2): p. 151-154.

80. Khadka, P., et al., Considerations in preparing for clinical studies of inhaled rifampicin to enhance tuberculosis treatment. International Journal of Pharmaceutics, 2018. **548**(1): p. 244-254.

81. Ghiciuc, C., et al., Rapid simultaneous LC/MS2 determination of rifampicin and 25-desacetyl rifampicin in human plasma for therapeutic drug monitoring. Studia Universitatis Babes-Bolyai. Chemia, vol. 60, no. 2, June 2015, pp. 309+

82. Chen, J. and K. Raymond, Roles of rifampicin in drug-drug interactions: underlying molecular mechanisms involving the nuclear pregnane X receptor. Annals of Clinical Microbiology Antimicrobials, 2006. **5**: p. 3.

83. Baldan, H.M., et al., The effect of rifampicin and pyrazinamide on isoniazid pharmacokinetics in rats. Biopharmaceuticals and Drug Disposition, 2007. **28**(8): p. 409-13.

84. A.W. Amara, D.G. Standaert, Metabolomics and the search for biomarkers in Parkinson's disease, Movement Disorders. 28 (2013) 1620–1621.

85. S. Lei, R. Powers, NMR metabolomics analysis of Parkinson's disease, Current drug metabolism 1 (2013) 191–209.

86. Rajaram, S., V.D. Vemuri, and R. Natham, Ascorbic acid improves stability and pharmacokinetics of rifampicin in the presence of isoniazid. Journal of Pharmaceutical Biomedical Analysis, 2014. **100**: p. 103-108.

87. Ethambutol. Tuberculosis, 2008. **88**(2): p. 102-105.

88. Jadaun, G.P.S., et al., Role of embCAB gene mutations in ethambutol resistance in Mycobacterium tuberculosis isolates from India. International Journal of Antimicrobial Agents, 2009. **33**(5): p. 483-486.

89. Islam, M.M., et al., Drug resistance mechanisms and novel drug targets for tuberculosis therapy. Journal of Genetics and Genomics, 2017. **44**(1): p. 21-37.

90. Ethambutol, in Meyler's Side Effects of Drugs (Sixteenth Edition), J.K. Aronson, Editor. 2016, Elsevier: Oxford. p. 172-178.

91. Njire, M., et al., Pyrazinamide resistance in Mycobacterium tuberculosis: Review and update. Advances in Medical Sciences, 2016. **61**(1): p. 63-71.

92. Momekov, G., et al., Pyrazinamide - Pharmaceutical, biochemical and pharmacological properties and reappraisal of its role in the chemotherapy of tuberculosis.Pharmacia Vol. 61. 2014. 38-67.

93. Zhang, Y., et al., Mechanisms of Pyrazinamide Action and Resistance. Microbiology Spectrum, 2014. **2**(4).

94. Zhang, Y. and D. Mitchison, The curious characteristics of pyrazinamide: a review. Int J Tuberc Lung Dis, 2003. **7**(1): p. 6-21.

95. Pyrazinamide, in Meyler's Side Effects of Drugs (Sixteenth Edition), J.K. Aronson, Editor. 2016, Elsevier: Oxford. p. 1053-1056.

96. Sobolewski, K., et al., Blood, Blood Components, Plasma, and Plasma Products, in Side Effects of Drugs Annual. 2018, Elsevier.

97. Cardinale, M., K. Owusu, and T. Malm, Chapter 29 - Blood, Blood Components, Plasma, and Plasma Products, in Side Effects of Drugs Annual, S.D. Ray, Editor. 2017, Elsevier. p. 331-343.

98. Holman, R.L., E.B. Mahoney, and G.H. Whipple, BLOOD PLASMA PROTEIN REGENERATION CONTROLLED BY DIET : I. LIVER AND CASEIN AS POTENT DIET FACTORS. The Journal of Experimental Medicine, 1934. **59**(3): p. 251-267.

99. Sliwoski, G., et al., Computational Methods in Drug Discovery. Pharmacological Reviews, 2014. **66**(1): p. 334-395.

100. Tami J. Marrone, et al., STRUCTURE-BASED DRUG DESIGN: Computational Advances. Annual Review of Pharmacology and Toxicology, 1997. **37**(1): p. 71-90.

101. Nisius, B., F. Sha, and H. Gohlke, Structure-based computational analysis of protein binding sites for function and druggability prediction. Journal of Biotechnology, 2012. **159**(3): p. 123-34.

102. Grunberg, R., M. Nilges, and J. Leckner, Flexibility and conformational entropy in protein-protein binding. Structure, 2006. **14**(4): p. 683-93.

103. Mondal, M., et al., Molecular interaction between human serum albumin (HSA) and phloroglucinol derivative that shows selective anti-proliferative potential. Journal of Luminescence, 2017. 192: p. 990-998.

104. Schoenmakers, I. and K.S. Jones, Chapter 37 - Pharmacology and Pharmacokinetics, in Vitamin D (Fourth Edition), D. Feldman, Editor. 2018, Academic Press. p. 635-661. eBook ISBN:9780128099667

105. Katzung, B.G., Basic & clinical pharmacology. 2018.

106. Rabbani, G.; Ahn, S.N. Structure, enzymatic activities, glycation and therapeutic potential of human serumalbumin: A natural cargo. International Journal of Biological Macromolecules 2019, 123, 979–990. doi: 10.1016/j.ijbiomac.2018.11.053

107. Sugio, S.; Kashima, A.; Mochizuki, S.; Noda, M.; Kobayashi, K. Crystal structure of human serum albumin at2.5 Å resolution. Protein Engineering Design and Selection 1999, 12, 439–446. DOI: 10.1093/protein/12.6.439

108. He, X.M.; Carter, D.C. Atomic structure and chemistry of human serum albumin. Nature 1992, 358, 209–215. DOI: 10.1038/358209a0

109. Curry, S.; Mandelkow, H.; Brick, P.; Franks, N. Crystal structure of human serum albumin complexed with fatty acid reveals an asymmetric distribution of binding sites. Nature Structural and molecular Biology 1998, 5, 827–835. DOI: 10.1038/1869

110. Ahmad, E.; Rabbani, G.; Zaidi, N.; Singh, S.; Rehan, M.; Khan, M.M.; Rahman, S.K.; Quadri, Z.; Shadab, M.;Ashraf, M.T.; et al. Stereo-selectivity of human serum albumin to enantiomeric and isoelectronic pollutantsdissected by spectroscopy, calorimetry and bioinformatics. PloS ONE 2011, 6, e26186. https://doi.org/10.1371/journal.pone.0026186

111. Rabbani, G.; Baig, M.H.; Lee, E.J.; Cho, W.K.; Ma, J.Y.; Choi, I. Biophysical Study on the Interaction betweenEperisone Hydrochloride and Human Serum Albumin Using Spectroscopic, Calorimetric, and MolecularDocking Analyses. Molecular Pharmaceutics 2017, 14, 1656–1665. https://doi.org/10.1021/acs.molpharmaceut.6b01124

112. Rabbani, G.; Khan, M.J.; Ahmad, A.; Maskat, M.Y.; Khan, R.H. Effect of copper oxide nanoparticles on the conformation and activity of beta-galactosidase. Colloids and Surfaces B Biointerfaces 2014, 123, 96–105. doi: 10.1016/j.colsurfb.2014.08.035

113. Rehman, M.T.; Dey, P.; Hassan, M.I.; Ahmad, F.; Batra, J.K. Functional role of glutamine 28 and arginine 39 in double stranded RNA cleavage by human pancreatic ribonuclease. PLOS ONE 2011, 6, e17159. https://doi.org/10.1371/journal.pone.0017159

114. Li, P., et al., Characterization of plasma protein binding dissociation with online SPE-HPLC. Scientific Reports, 2015. **5**: p. 14866.

115. Rehman, M.T.; Faheem, M.; Khan, A.U. Insignificant beta-lactamase activity of human serum albumin:No panic to nonmicrobial-based drug resistance. Letters in Applied Microbiology 2013, 57, 325–329. doi: 10.1111/lam.12116

116. Goutal, S., et al., Validation of a simple HPLC-UV method for rifampicin determination in plasma: Application to the study of rifampicin arteriovenous concentration gradient. Journal of Pharmaceutical Biomedical Analysis, 2016. 123: p. 173-8.

117. Alghamdi, W.A., M.H. Al-Shaer, and C.A. Peloquin, Protein Binding of First-Line Antituberculosis Drugs. Antimicrobials Agents and Chemotherapy, 2018. 62(7).

118. Gurevich, K.G., Effect of blood protein concentrations on drug-dosing regimes: practical guidance. Theoretical biology & medical modelling, 2013. 10: p. 20-20.

119. Boman, G. and V.A. Ringberger, Binding of rifampicin by human plasma proteins. European Journal of Clinical Pharmacology, 1974. 7(5): p. 369-73.

120. Kalamaridis, D. and N. Patel, Assessment of Drug Plasma Protein Binding in Drug Discovery, in Optimization in Drug Discovery: In Vitro Methods, G.W. Caldwell and Z. Yan, Editors. 2014, Humana Press: Totowa, NJ. p. 21-37.

121. Temova Rakuša, Ž., et al., Fast and Simple LC-MS/MS Method for Rifampicin Quantification in Human Plasma. International Journal of Analytical Chemistry, 2019. 2019: p. 4848236.

122. Zhou, Z., et al., Simultaneous Determination of Isoniazid, Pyrazinamide, Rifampicin and Acetylisoniazid in Human Plasma by High-Performance Liquid Chromatography. Analytical Sciences, 2010. 26(11): p. 1133-1138.

123. Han, M., et al., Method for simultaneous analysis of nine second-line anti-tuberculosis drugs using UPLC-MS/MS. Journal of Antimicrobial Chemotherapy, 2013. 68(9): p. 2066-2073.

124. Srivastava, A., et al., Quantification of rifampicin in human plasma and cerebrospinal fluid by a highly sensitive and rapid liquid chromatographic–tandem mass spectrometric method. Journal of Pharmaceutical and Biomedical Analysis, 2012. 70: p. 523-528.

125. Wu, S., et al., Simultaneous determination of the potent anti-tuberculosis regimen-Pyrazinamide, ethambutol, protionamide, clofazimine in beagle dog plasma using LC-MS/MS method coupled with 96-well format plate. Journal of pharmaceutical and biomedical analysis, 2019. 168: p. 44-54.

126. Vincent, J.-L., et al., Hypoalbuminemia in acute illness: is there a rationale for intervention? A meta-analysis of cohort studies and controlled trials. Annals of surgery, 2003. 237(3): p. 319-334.

127. Osakwe, O., Chapter 9 - Clinical Development: Ethics and Realities, in Social Aspects of Drug Discovery, Development and Commercialization, O. Osakwe and S.A.A. Rizvi, Editors. 2016, Academic Press: Boston. p. 191-220.

128. BradfordMM.Arapid and sensitive method for the quantitation of microgram quantities of protein utilizing the principle of protein–dye-binding. Analytical Biochemistry 1976;72:248–54.

129. Lowry OH, Rosebrough NJ, Farr AL, et al. Protein measurement with the Folin phenol reagent. Journal of Biological Chemistry 1951;193:265–75.

130. Pesce MA, Strande CS. A new micromethod for determination of protein in cerebrospinal fluid and urine. Clinical Chemistry 1973;19:1265–7.

131. Dube J, Girouard J, Leclere P, et al. Problems with the estimation of urine protein by automated assays. Clinical Biochemistry 2005;38:479–85.

132. Zhong H, Xu J, Chen H. A rapid and sensitive method for the determination of trace proteins based on the interaction between proteins and Ponceau 4R. Talanta 2005;67:749–54.

133. Schaffner W, Weissmann C. A rapid, sensitive, and specific method for the determination of protein in dilute solution. Analytical Biochemistry 1973;56:502–14.

134. Zaia DAM, Marques FR, Zaia CTB. Spectrophotometric determination of total proteins in blood plasma: a comparative study among dye-binding methods. Brazillian Archieves of Biology and Technology 2005;48:385–8.

135. Zsila, F., S. Bősze, and T. Beke-Somfai, Interaction of antitubercular drug candidates with α1-acid glycoprotein produced in pulmonary granulomas. International Journal of Biological Macromolecules, 2020. 147: p. 1318-1327.

136. Wang, Y.-r., et al., Spectroscopic and Molecular Docking Study on Specific Binding and Inhibition of Isoniazid to Human Serum Albumin and Catalase. Guang pu xue yu guang pu fen xi = Guang pu, 2016. 36: p. 3789-3795.

137. Chaturvedi, S., et al., Comparative binding study of anti-tuberculosis drug pyrazinamide with serum albumins. The Royal Society of Chemistry Advances, 2016. 6.

138. Litjens, C.H.C., et al., Protein binding of rifampicin is not saturated when using high-dose rifampicin. Journal of Antimicrobial Chemotherapy, 2018. 74(4): p. 986-990.

139. Boeree MJ, et al.,. A dose-ranging trial to optimize the dose of rifampin in the treatment of tuberculosis. American Journal of Respiratory and Critical Care Medicine 2015 May 1;191(9):1058-65. doi: 10.1164/rccm.201407-1264OC. PMID: 25654354.

140. C. Stephens, ... R.J. Andrade, in Comprehensive Toxicology (Third Edition), 2018

141. Wanat, K. Biological barriers, and the influence of protein binding on the passage of drugs across them. Molecular Biological Reports 47, 3221–3231 (2020). https://doi.org/10.1007/s11033-020-05361-2

142. Beloor Suresh A, Rosani A, Wadhwa R. Rifampin. 2021 Jun 7. In: StatPearls [Internet]. Treasure Island (FL): StatPearls Publishing; 2021 Jan–. PMID: 32491420.

143. Bruce, S.J., et al., Investigation of Human Blood Plasma Sample Preparation for Performing Metabolomics Using Ultrahigh Performance Liquid Chromatography/Mass Spectrometry. Analytical Chemistry, 2009. 81(9): p. 3285-3296.

144. Nguyen, M. K., V. Ornekian, A. W. Butch, and I. Kurtz. 2007. 'A new method for determining plasma water content: application in pseudohyponatremia', American Journal of Physiology-Renal Physiology, 292: F1652-6.

145. Osakai, Toshiyuki. 2017. 'The Principle of Water-Content Determination by Karl Fischer Titration', Review of Polarography, 63: 101-07.

146. Supartono, W., S. Rückold, and H. D. Isengard. 1998. 'Karl Fischer Titration as an Alternative Method for Determining the Water Content of Cloves', LWT - Food Science and Technology, 31: 402-05.

147. Tavčar, E., E. Turk, and S. Kreft, Simple modification of karl-Fischer titration method for determination of water content in colored samples. Journal of analytical methods in chemistry, 2012. 2012: p. 379724-379724.

148. Cardinale, Maria, Kent Owusu, and Tamara Malm. 2017. 'Chapter 29 - Blood, Blood Components, Plasma, and Plasma Products.' in Sidhartha D. Ray (ed.), Side Effects of Drugs Annual (Elsevier).

149. L Howard, Monique, John Hill, Gerald R Galluppi, and Matthew McLean. 2010. Plasma Protein Binding in Drug Discovery and Development. Combinatorial Chemistry and High Throughput Screening. 2010 Feb;13(2):170-87. doi: 10.2174/138620710790596745. PMID: 20053162.

150. Fanali, G., A. di Masi, V. Trezza, M. Marino, M. Fasano, and P. Ascenzi. 2012. 'Human serum albumin: from bench to bedside', Molecular Aspects in Medicine, 33: 209-90.

151. Clark, A. M., Labute, P., & Santavy, M. (2006). 2D Structure Depiction. Journal of Chemical Information and Modeling, 46(3),1107-1123. doi:10.1021/ci050550m

152. Wallace AC, Laskowski RA, Thornton JM. LIGPLOT: a program to generate schematic diagrams of protein-ligand interactions. Protein engineering, design and selection. 1995 Feb 1;8(2):127-134. doi:10.1093/protein/8.2.127

153. Kitchen DB, Decornez H, Furr JR, Bajorath J. Docking and scoring in virtual screening for drug discovery: methods and applications. Nature reviews Drug discovery. 2004 Nov; 3(11) 935-949. doi:10.1038/nrd1549

154. Yang GD, Li C, Zeng AG, Zhao Y, Yang R, Bian XL. Fluorescence spectroscopy of osthole binding to human serum albumin. Journal of pharmaceutical analysis. 2013 Jun 1; 3(3): 200-204. doi:https://doi.org/10.1016/j.jpha.2012.10.002

155. Tabassum, S., et al., Synthesis, characterization and interaction studies of copper based drug with Human Serum Albumin (HSA): Spectroscopic and molecular docking investigations. Journal of photochemistry and photobiology. B, Biology, 2012. 114: p. 132-9.

156. Yang, Guang-De, Cong Li, Ai-Guo Zeng, Yuan Zhao, Rong Yang, and Xiao-Li Bian. 2013. 'Fluorescence spectroscopy of osthole binding to human serum albumin', Journal of Pharmaceutical Analysis, 3: 200-04.

157. Albani, J. R. 2004. 'Chapter 4 - Fluorescence Quenching.' in J. R. Albani (ed.), Structure and Dynamics of Macromolecules: Absorption and Fluorescence Studies (Elsevier Science: Amsterdam).

158. Behera, P. K., T. Mukherjee, and A. K. Mishra. 1995. 'Simultaneous presence of static and dynamic component in the fluorescence quenching for substituted naphthalene—CCl4 system', Journal of Luminescence, 65: 131-36.

159. Chaves, O. A., M. T. Tavares, M. R. Cunha, R. Parise-Filho, C. M. R. Sant'Anna, and J. C. Netto-Ferreira. 2018. 'Multi-Spectroscopic and Theoretical Analysis on the Interaction between Human Serum Albumin and a Capsaicin Derivative-RPF101', Biomolecules, 8

160. Panchagnula, R., et al., Determination of rifampicin and its main metabolite in plasma and urine in presence of pyrazinamide and isoniazid by HPLC method. Journal of Pharmaceutical and Biomedical Analysis, 1999. 18(6): p. 1013-20.

161. Snider, D.E., Jr and L.S. Farer, Rifampin and Red Urine. Journal of American Medical Association, 1977. 238(15): p. 1628-1628.

162. Misselhorn A, Hendriks SL (2017) A systematic review of sub-national food insecurity research in South Africa: Missed opportunities for policy insights. PLOS ONE 12(8): e0182399. https://doi.org/10.1371/journal.pone.0182399

Addenda

Addendum A: Chapter 3: Rifampicin validation tables raw data

Part A: Rifampicin Validation Support Data

3. TABLES

3.1 Rifampicin + internal standard with ascorbic acid dilution table

- **Stock Solution: 100µg/ml**
- **2nd Stock solution: 20 µg/ml**

Table 1: Mass of standard and Internal standard weighed

Mass of Rifampicin (mg)	Mass of Phenacetin (mg)
5.19	5.38

Table 2: Dilution table for Rifampicin, Phenacetin and Ascorbic acid, Centrifuge time and Vortex time

RIF at 340nm	C1	V1 (µL)	C2	V2 (µL)	PHENACITIN (µL)	Ascorbic Acid	Centrifuge time (min)	Vortex time (min)
0.1 µg/ml	100 µg/ml	250	0.1 µg/ml	1000	100	400	15	1
0.5 µg/ml	100 µg/ml	100	0.5 µg/ml	1000	100	400	15	1
1µg/ml	100 µg/ml	50	1 µg/ml	1000	100	400	15	1
5 µg/ml	20 µg/ml	50	5 µg/ml	1000	100	400	15	1

10µg/ml	20 µg/ml	25	10 µg/ml	1000	100	400	15	1
25 µg/ml	20µg/ml	5	25 µg/ml	1000	100	400	15	1

Preparation of 20 µg/ml Phenacetin

$C_1V_1 = C_2V_2$

$100V_1 = 20 \times 10$

$V_1 = \frac{20 \times 10}{100}$

= 2 ml

100 µL of phenacetin was taken from 20 µg/ml to make up 2 µg/ml

$C_1V_1 = C_2V_2$

$20 \times 100 = C_2 \times 1000$

$C_2 = \frac{20 \times 100}{1000}$

= 2 µg/ml

3.2 Tables for Rifampicin Data file name, Ret.time, Area and Concentration Level, S/N

Table 3: Rifampicin Data file name, Ret.time, Area and 0.1 µg/ml Concentration Level, S/N

Data#	Data Filename	Level#	Ret. Time	Area	Std. Conc.	S/N
1	std's+Blank_20160614_001.lcd	1	7.816	28 374	0.1	27.8
2	std's+Blank_20160614_002.lcd	1	7.812	26 513	0.1	26.6
3	std's+Blank_20160614_004.lcd	1	7.808	25 627	0.1	27.8
4	std's+Blank_20160614_005.lcd	1	7.806	22 140	0.1	21.5
5	std's+Blank_20160614_006.lcd	1	7.807	20 019	0.1	19.7
6	std's+Blank_20160614_003.lcd	1	7.807	37 631	0.1	46.5
	Average		7.809	26 717		28.3
	%RSD		0.052	23.006099		33.7
	Maximum		7.816	37 631		46.5
	Minimum		7.806	20 019		19.7

	Std. Dev.		0.004	6 146.614114		9.53

Table 4: Rifampicin Data file name, Ret.time, Area and 0.5 µg/ml Concentration Level, S/N

Data#	Data Filename	Level#	Ret. Time	Area	Std. Conc.	S/N
1	std's+Blank_20160614_007.lcd	2	7.806	246 246	0.5	389
2	std's+Blank_20160614_008.lcd	2	7.806	223 620	0.5	259
3	std's+Blank_20160614_009.lcd	2	7.808	209 397	0.5	280
4	std's+Blank_20160614_010.lcd	2	7.808	225 939	0.5	296
5	std's+Blank_20160614_011.lcd	2	7.805	216 133	0.5	336
6	std's+Blank_20160614_012.lcd	2	7.805	220 316	0.5	361
	Average		**7.806**	**223 608**		**320**
	%RSD		**0.018**	**5.609152**		**15.6**
	Maximum		**7.808**	**246 246**		**389**
	Minimum		**7.805**	**209 397**		**259**
	Std. Dev.		**0.001**	**12 542.531966**		**50**

Table 5: Rifampicin Data file name, Ret.time, Area and 1 µg/ml Concentration Level, S/N

Data#	Data Filename	Level#	Ret. Time	Area	Std. Conc.	S/N
1	std's+Blank_20160614_013.lcd	3	7.802	284 494	1	479
2	std's+Blank_20160614_014.lcd	3	7.812	296 920	1	483
3	std's+Blank_20160614_015.lcd	3	7.805	283 763	1	458
4	std's+Blank_20160614_016.lcd	3	7.811	298 546	1	531
5	std's+Blank_20160614_017.lcd	3	7.812	301 136	1	479
6	std's+Blank_20160614_018.lcd	3	7.806	293 092	1	396
	Average		**7.808**	**292 992**		**471**
	%RSD		**0.053**	**2.508147**		**9.3**
	Maximum		**7.812**	**301 136**		**531**
	Minimum		**7.802**	**283 763**		**396**
	Std. Dev.		**0.004**	**7 348.665646**		**43.8**

Table 6: Rifampicin Data file name, Ret.time, Area and 5 µg/ml Concentration Level, S/N

Data#	Data Filename	Level#	Ret. Time	Area	Std. Conc.	S/N
1	std's+Blank_20160614_019.lcd	4	7.81	1 770 174	5	2 585.46
2	std's+Blank_20160614_020.lcd	4	7.807	1 401 186	5	2 285.25
3	std's+Blank_20160614_021.lcd	4	7.817	1 644 398	5	2 544.28
4	std's+Blank_20160614_022.lcd	4	7.812	1 598 758	5	2 264.78
5	std's+Blank_20160614_023.lcd	4	7.812	1 649 362	5	2 303.77
6	std's+Blank_20160614_024.lcd	4	7.812	1 672 630	5	2 373.03
	Average		**7.812**	**1 622 751**		**2 392.76**
	%RSD		**0.044**	**7.550602**		**5.8**
	Maximum		**7.817**	**1 770 174**	**0**	**2 585.46**
	Minimum		**7.807**	**1 401 186**	**0**	**2 264.78**
	Std. Dev.		**0.003**	**122 527.491313**	**0**	**139**

Table 7: Rifampicin Data file name, Ret.time, Area and 20 µg/ml Concentration Level, S/N

Data#	Data Filename	Level#	Ret. Time	Area	Std. Conc.	S/N
1	std's+Blank_20160614_025.lcd	5	7.814	4 504 281	20	5 048.55
2	std's+Blank_20160614_026.lcd	5	7.82	4 630 015	20	4 965.01
3	std's+Blank_20160614_027.lcd	5	7.823	4 598 456	20	4 001.52
4	std's+Blank_20160614_028.lcd	5	7.827	4 516 306	20	4 192.19
5	std's+Blank_20160614_029.lcd	5	7.826	4 612 855	20	4 653.16
6	std's+Blank_20160614_030.lcd	5	7.826	4 636 678	20	4 148.67
	Average		**7.823**	**4 583 099**		**4 501.52**
	%RSD		**0.066**	**1.267276**		**9.97**
	Maximum		**7.827**	**4 636 678**		**5 048.55**
	Minimum		**7.814**	**4 504 281**		**4 001.52**
	Std. Dev.		**0.005**	**58 080.522187**		**449**

Table 8: Rifampicin Data file name, Ret.time, Area and 25 µg/ml Concentration Level, S/N

Data#	Data Filename	Level#	Ret. Time	Area	Std. Conc.	S/N
1	std's+Blank_20160614_031.lcd	6	7.818	5 990 112	25	5 093.05
2	std's+Blank_20160614_032.lcd	6	7.818	6 089 410	25	5 193.42
3	std's+Blank_20160614_033.lcd	6	7.824	6 011 362	25	4 892.88
4	std's+Blank_20160614_034.lcd	6	7.816	6 085 114	25	4 656.58
5	std's+Blank_20160614_035.lcd	6	7.824	5 857 478	25	4 644.90
6	std's+Blank_20160614_036.lcd	6	7.824	5 789 273	25	4 499.15
	Average		7.821	5 970 458		4 830.00
	%RSD		**0.049**	**2.050624**		**5.7**
	Maximum		**7.824**	**6 089 410**		**5 193.42**
	Minimum		**7.816**	**5 789 273**		**4 499.15**
	Std. Dev.		**0.004**	**122 431.674515**		**275**

Table 9: showing data, data file name, level, retention time, area, concentration of all plasma-Free standards

Data#	Data Filename	Level#	Ret. Time	Area	Std. Conc.
1	std's+Blank_20160614_001.lcd	1	7.816	28 374	0.1
2	std's+Blank_20160614_002.lcd	1	7.812	26 513	0.1
3	std's+Blank_20160614_003.lcd	1	7.807	37 631	0.1
4	std's+Blank_20160614_004.lcd	1	7.808	25 627	0.1
5	std's+Blank_20160614_005.lcd	1	7.806	22 140	0.1
6	std's+Blank_20160614_006.lcd	1	7.807	20 019	0.1
7	std's+Blank_20160614_007.lcd	2	7.806	246 246	0.5
8	std's+Blank_20160614_008.lcd	2	7.806	223 620	0.5
9	std's+Blank_20160614_009.lcd	2	7.808	209 397	0.5
10	std's+Blank_20160614_010.lcd	2	7.808	225 939	0.5
11	std's+Blank_20160614_011.lcd	2	7.805	216 133	0.5
12	std's+Blank_20160614_012.lcd	2	7.805	220 316	0.5
13	std's+Blank_20160614_013.lcd	3	7.802	284 494	1
14	std's+Blank_20160614_014.lcd	3	7.812	296 920	1

15	std's+Blank_20160614_015.lcd	3	7.805	283 763	1
16	std's+Blank_20160614_016.lcd	3	7.811	298 546	1
17	std's+Blank_20160614_017.lcd	3	7.812	301 136	1
18	std's+Blank_20160614_018.lcd	3	7.806	293 092	1
19	std's+Blank_20160614_019.lcd	4	7.81	1 770 174	5
20	std's+Blank_20160614_020.lcd	4	7.807	1 401 186	5
21	std's+Blank_20160614_021.lcd	4	7.817	1 644 398	5
22	std's+Blank_20160614_022.lcd	4	7.812	1 598 758	5
23	std's+Blank_20160614_023.lcd	4	7.812	1 649 362	5
24	std's+Blank_20160614_024.lcd	4	7.812	1 672 630	5
25	std's+Blank_20160614_025.lcd	5	7.814	4 504 281	20
26	std's+Blank_20160614_026.lcd	5	7.82	4 630 015	20
27	std's+Blank_20160614_027.lcd	5	7.823	4 598 456	20
28	std's+Blank_20160614_028.lcd	5	7.827	4 516 306	20
29	std's+Blank_20160614_029.lcd	5	7.826	4 612 855	20
30	std's+Blank_20160614_030.lcd	5	7.826	4 636 678	20
31	std's+Blank_20160614_031.lcd	6	7.818	5 990 112	25
32	std's+Blank_20160614_032.lcd	6	7.818	6 089 410	25
33	std's+Blank_20160614_033.lcd	6	7.824	6 011 362	25
34	std's+Blank_20160614_034.lcd	6	7.816	6 085 114	25
35	std's+Blank_20160614_035.lcd	6	7.824	5 857 478	25
36	std's+Blank_20160614_036.lcd	6	7.824	5 789 273	25
	Average		**7.813**	**2 119 938**	
	%RSD		**0.094**	**111.31533**	
	Maximum		**7.827**	**6 089 410**	
	Minimum		**7.802**	**20 019**	
	Std. Dev.		**0.007**	**2 359 815.488220**	

3.3 Plasma-Rifampicin Standard dilution tables

Table 10: Dilution table for Rifampicin, Phenacetin, plasma and Ascorbic acid, Centrifuge time and Vortex time

RIF at 340nm	C1	V1 (µL)	C2	V2 (µL)	PHENACITIN (µL)	Ascorbic Acid: Plasma (µL)	Centrifuge time(min)	Vortex time(min)
0.25 µg/ml	20 µg/ml	12.5	0.25 µg/ml	1000	250	400:100	15	1
0.5 µg/ml	20 µg/ml	25	0.5 µg/ml	1000	250	400:100	15	1
1µg/ml	20 µg/ml	50	1 µg/ml	1000	250	400:100	15	1
1.5 µg/ml	20 µg/ml	75	1.5 µg/ml	1000	250	400:100	15	1
3µg/ml	20 µg/ml	150	3 µg/ml	1000	250	400:100	15	1
5 µg/ml	20µg/ml	250	5 µg/ml	1000	250	400:100	15	1

Preparation of 20 µg/ml phenacetin

$\mathbf{C_1V_1=C_2V_2}$

$100V_1 = 20 \times 10$

$V_1 = \frac{20 \times 10}{100}$

= 2 ml

250 µL of Phenacetin was taken from 20 µg/ml to make up 5 µg/ml

$\mathbf{C_1V_1=C_2V_2}$

$20 \times 250 = C_2 \times 1000$

$C_2 = \frac{20 \times 250}{1000}$

= 5 µg/ml

3.4 Tables for Rifampicin with plasma and internal standard Data file name, Ret.time, Area and Concentration Level

Table 11: Rifampicin Data file name, Ret.time, Area and 0.25 µg/ml Concentration Level

Data#	Data Filename	Level#	Ret. Time	Area	Conc. (µg/ml)	Std. Conc.
1	Rif&Phen precision_20160608_003.lcd	1	8.539	17 396	0	0.25
2	Rif&Phen precision_20160608_004.lcd	1	8.542	18 087	0	0.25
3	Rif&Phen precision_20160608_005.lcd	1	8.524	15 982	0	0.25
	Average		8.535	17 155	0	
	%RSD		0.11	6.25326	0	
	Maximum		8.542	18 087	0	
	Minimum		8.524	15 982	0	
	Std. Dev.		0.009	1 072.750593	0	

$$SNR = \frac{\mu}{\delta}$$

$$= \frac{17155}{1072.750593}$$

$$= 15.99$$

Table 12: Rifampicin Data file name, Ret.time, Area and 0.5 µg/ml Concentration Level

Data#	Data Filename	Level#	Ret. Time	Area	Conc. (µg/ml)	Std. Conc.
1	Plasma 0.25-5µg/ml x6_20160613_008.lcd	2	7.841	120 523	0.5	0.5
2	Plasma 0.25-5µg/ml x6_20160613_009.lcd	2	7.84	126 063	0.52	0.5
3	Plasma 0.25-5µg/ml x6_20160613_010.lcd	2	7.84	123 717	0.51	0.5
4	Plasma 0.25-5µg/ml x6_20160613_011.lcd	2	7.841	144 757	0.6	0.5

5	Plasma 0.25-5µg/ml x6_20160613_012.lcd	2	7.839	126 479	0.53	0.5
6	Plasma 0.25-5µg/ml x6_20160613_007.lcd	2	7.834	98 302	0.41	0.5
	Average		7.839	123 307	0.51	
	%RSD		0.034	12.088506	12.1	
	Maximum		7.841	144 757	0.6	
	Minimum		7.834	98 302	0.41	
	Std. Dev.		0.003	14 905.931953	0.06	

$$\textbf{SNR} = \frac{\mu}{\delta}$$

$$= \frac{123307}{14905.931953} = 8.27$$

Table 13: Rifampicin Data file name, Ret.time, Area and 1 µg/ml Concentration Level

Data#	**Data Filename**	**Level#**	**Ret. Time**	**Area**	**Conc. (µg/ml)**	**Std. Conc.**
1	Plasma 0.25-5µg/ml x6_20160613_013.lcd	3	7.839	178 708	1	1
2	Plasma 0.25-5µg/ml x6_20160613_014.lcd	3	7.833	163 221	0.91	1
3	Plasma 0.25-5µg/ml x6_20160613_015.lcd	3	7.827	150 567	0.84	1
4	Plasma 0.25-5µg/ml x6_20160613_016.lcd	3	7.836	161 438	0.9	1
5	Plasma 0.25-5µg/ml x6_20160613_017.lcd	3	7.834	155 284	0.87	1
6	Plasma 0.25-5µg/ml x6_20160613_018.lcd	3	7.828	150 874	0.84	1
	Average		7.833	160 015	0.9	
	%RSD		0.058	6.595679	6.59	
	Maximum		7.839	178 708	1	
	Minimum		7.827	150 567	0.84	
	Std. Dev.		0.005	10 554.098412	0.06	

SNR = $\frac{\mu}{\delta}$

= $\frac{160015}{10554.098412}$

= 15.16

Table 14: Rifampicin Data file name, Ret.time, Area and 1.5 µg/ml Concentration Level

Data#	**Data Filename**	**Level#**	**Ret. Time**	**Area**	**Conc. (µg/ml)**	**Std. Conc.**
1	Plasma 0.25-5µg/ml x6_20160613_019.lcd	4	6.831	803 606	1	1.5
2	Plasma 0.25-5µg/ml x6_20160613_020.lcd	4	6.834	807 140	1	1.5
3	Plasma 0.25-5µg/ml x6_20160613_021.lcd	4	6.838	733 282	1	1.5
4	Plasma 0.25-5µg/ml x6_20160613_022.lcd	4	6.839	756 061	1	1.5
5	Plasma 0.25-5µg/ml x6_20160613_023.lcd	4	6.839	750 884	1	1.5
6	Plasma 0.25-5µg/ml x6_20160613_024.lcd	4	6.835	757 899	1	1.5
	Average		6.836	768 145	1	
	%RSD		0.045	3.923893	0	
	Maximum		6.839	807 140	1	
	Minimum		6.831	733 282	1	
	Std. Dev.		0.003	30 141.205248	0	

SNR = $\frac{\mu}{\delta}$

= $\frac{768145}{30141.205248}$

= 2.55 X 10^{-5}

Table 15: Rifampicin Data file name, Retention Time, Area and 3 µg/ml Concentration Level

Data#	Data Filename	Level#	Ret. Time	Area	Conc. (µg/ml)	Std. Conc.
1	Plasma 0.25-5µg/ml x6_20160613_026.lcd	5	6.833	643 519	1	3
2	Plasma 0.25-5µg/ml x6_20160613_027.lcd	5	6.83	667 450	1	3
3	Plasma 0.25-5µg/ml x6_20160613_028.lcd	5	6.828	659 553	1	3
4	Plasma 0.25-5µg/ml x6_20160613_029.lcd	5	6.818	693 295	1	3
5	Plasma 0.25-5µg/ml x6_20160613_030.lcd	5	6.831	673 244	1	3
6	Plasma 0.25-5µg/ml x6_20160613_025.lcd	5	6.827	680 053	1	3
	Average		6.828	669 519	1	
	%RSD		0.076	2.560786	0	
	Maximum		6.833	693 295	1	
	Minimum		6.818	643 519	1	
	Std. Dev.		0.005	17 144.944640	0	

$$\textbf{SNR} = \frac{\mu}{\boldsymbol{\delta}}$$

$$= \frac{669519}{17144.944640}$$

$$= 39.05$$

Table 16: Rifampicin Data file name, Retention Time, Area and 5 µg/ml Concentration Level

Data#	Data Filename	Level#	Ret. Time	Area	Conc. (µg/ml)	Std. Conc.
1	Plasma 0.25-5µg/ml x6_20160613_031.lcd	6	7.817	824 345	5	5
2	Plasma 0.25-5µg/ml x6_20160613_032.lcd	6	7.816	860 499	5.22	5

3	Plasma 0.25-5µg/ml x6_20160613_033.lcd	6	7.816	888 503	5.39	5
4	Plasma 0.25-5µg/ml x6_20160613_034.lcd	6	7.816	904 489	5.49	5
5	Plasma 0.25-5µg/ml x6_20160613_035.lcd	6	7.829	903 090	5.48	5
6	Plasma 0.25-5µg/ml x6_20160613_036.lcd	6	7.832	952 138	5.78	5
	Average		7.821	888 844	5.39	
	%RSD		0.096	4.882691	4.88	
	Maximum		7.832	952 138	5.78	
	Minimum		7.816	824 345	5	
	Std. Dev.		0.008	43 399.498103	0.26	

SNR = $\frac{\mu}{\boldsymbol{\delta}}$

$= \frac{888844}{43399.498103}$

= 20.48

Table 17: showing data, data file name, level, retention time, area, concentration of all Rifampicin-Plasma standards

Data#	**Data Filename**	**Level#**	**Ret. Time**	**Area**	**Conc. (µg/ml)**	**Std. Conc.**
1	Plasma 0.25-5µg/ml x6_20160613_001.lcd	1	7.76	24 098	0.17	0.25
2	Plasma 0.25-5µg/ml x6_20160613_002.lcd	1	7.78	22 682	0.16	0.25
3	Plasma 0.25-5µg/ml x6_20160613_003.lcd	1	7.798	10 937	0.1	0.25
4	Plasma 0.25-5µg/ml x6_20160613_005.lcd	1	7.799	28 913	0.19	0.25
5	Plasma 0.25-5µg/ml x6_20160613_006.lcd	1	7.834	42 475	0.27	0.25
6	Plasma 0.25-5µg/ml x6_20160613_007.lcd	2	7.834	98 302	0.57	0.5

7	Plasma 0.25-5µg/ml x6_20160613_008.lcd	2	7.841	120 523	0.69	0.5
8	Plasma 0.25-5µg/ml x6_20160613_009.lcd	2	7.84	126 063	0.72	0.5
9	Plasma 0.25-5µg/ml x6_20160613_010.lcd	2	7.84	123 717	0.71	0.5
10	Plasma 0.25-5µg/ml x6_20160613_011.lcd	2	7.841	144 757	0.82	0.5
11	Plasma 0.25-5µg/ml x6_20160613_012.lcd	2	7.839	126 479	0.72	0.5
12	Plasma 0.25-5µg/ml x6_20160613_013.lcd	3	7.839	178 708	1	1
13	Plasma 0.25-5µg/ml x6_20160613_014.lcd	3	7.833	163 221	0.92	1
14	Plasma 0.25-5µg/ml x6_20160613_015.lcd	3	7.827	150 567	0.85	1
15	Plasma 0.25-5µg/ml x6_20160613_016.lcd	3	7.836	161 438	0.91	1
16	Plasma 0.25-5µg/ml x6_20160613_017.lcd	3	7.834	155 284	0.88	1
17	Plasma 0.25-5µg/ml x6_20160613_018.lcd	3	7.828	150 874	0.85	1
18	Plasma 0.25-5µg/ml x6_20160613_019.lcd	4	7.829	228 777	1.28	1.5
19	Plasma 0.25-5µg/ml x6_20160613_020.lcd	4	7.829	216 957	1.21	1.5
20	Plasma 0.25-5µg/ml x6_20160613_021.lcd	4	7.832	219 969	1.23	1.5
21	Plasma 0.25-5µg/ml x6_20160613_022.lcd	4	7.831	217 800	1.22	1.5
22	Plasma 0.25-5µg/ml x6_20160613_023.lcd	4	7.829	209 703	1.17	1.5
23	Plasma 0.25-5µg/ml x6_20160613_024.lcd	4	7.83	226 675	1.26	1.5
24	Plasma 0.25-5µg/ml x6_20160613_025.lcd	5	7.824	588 442	3.22	3

25	Plasma 0.25-5µg/ml x6_20160613_026.lcd	5	7.829	617 340	3.38	3
26	Plasma 0.25-5µg/ml x6_20160613_027.lcd	5	7.823	635 086	3.48	3
27	Plasma 0.25-5µg/ml x6_20160613_028.lcd	5	7.826	601 362	3.29	3
28	Plasma 0.25-5µg/ml x6_20160613_029.lcd	5	7.822	640 184	3.5	3
29	Plasma 0.25-5µg/ml x6_20160613_030.lcd	5	7.828	632 589	3.46	3
30	Plasma 0.25-5µg/ml x6_20160613_031.lcd	6	7.817	824 345	4.5	5
31	Plasma 0.25-5µg/ml x6_20160613_032.lcd	6	7.816	860 499	4.7	5
32	Plasma free 0.25-5µg/ml x6_20160613_033.lcd	6	7.816	888 503	4.85	5
33	Plasma 0.25-5µg/ml x6_20160613_034.lcd	6	7.816	904 489	4.94	5
34	Plasma 0.25-5µg/ml x6_20160613_035.lcd	6	7.829	903 090	4.93	5
35	Plasma 0.25-5µg/ml x6_20160613_036.lcd	6	7.832	952 138	5.19	5
	Average		**7.825**	**348 485**	**1.92**	
	%RSD		**0.219**	**89.973269**	**88.3**	
	Maximum		**7.841**	**952 138**	**5.19**	
	Minimum		**7.76**	**10 937**	**0.1**	
	Std. Dev.		**0.017**	**313 543.591029**	**1.7**	

Addendum B: Chapter 3

Part B: Karl Fischer experimental data

3.5 Karl Fischer auto-titrator method parameters

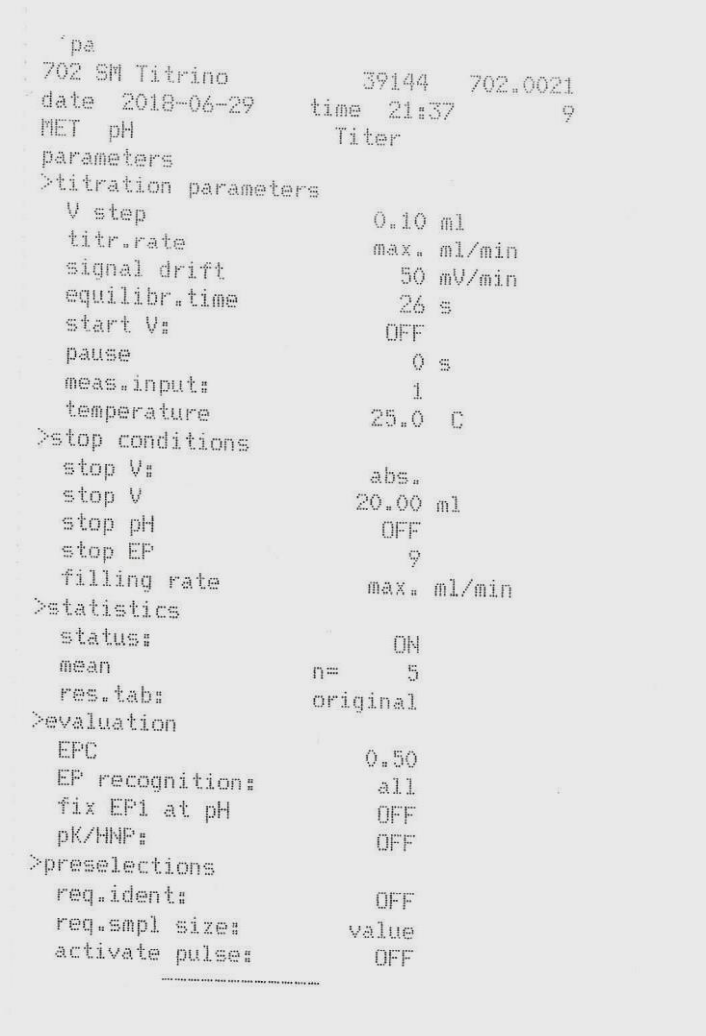

```
 'pa
702 SM Titrino          39144   702.0021
date  2018-06-29    time  21:37        9
MET  pH                 Titer
parameters
>titration parameters
  V step                 0.10 ml
  titr.rate              max. ml/min
  signal drift             50 mV/min
  equilibr.time            26 s
  start V:                 OFF
  pause                     0 s
  meas.input:               1
  temperature            25.0  C
>stop conditions
  stop V:                abs.
  stop V                20.00 ml
  stop pH                  OFF
  stop EP                    9
  filling rate           max. ml/min
>statistics
  status:                   ON
  mean                n=     5
  res.tab:            original
>evaluation
  EPC                      0.50
  EP recognition:           all
  fix EP1 at pH            OFF
  pK/HNP:                  OFF
>preselections
  req.ident:               OFF
  req.smpl size:         value
  activate pulse:          OFF
        ----------
```

Figure 1: Karl Fischer method parameters: volume step of titrant 1ml, signal drift (Signal before the next increment of titrant can be released for further titrant requirment) of 50 mV/min, equilibrium time of 26s, temperature at 273.15K, Stop volume 20ml.

Sample analysis 1

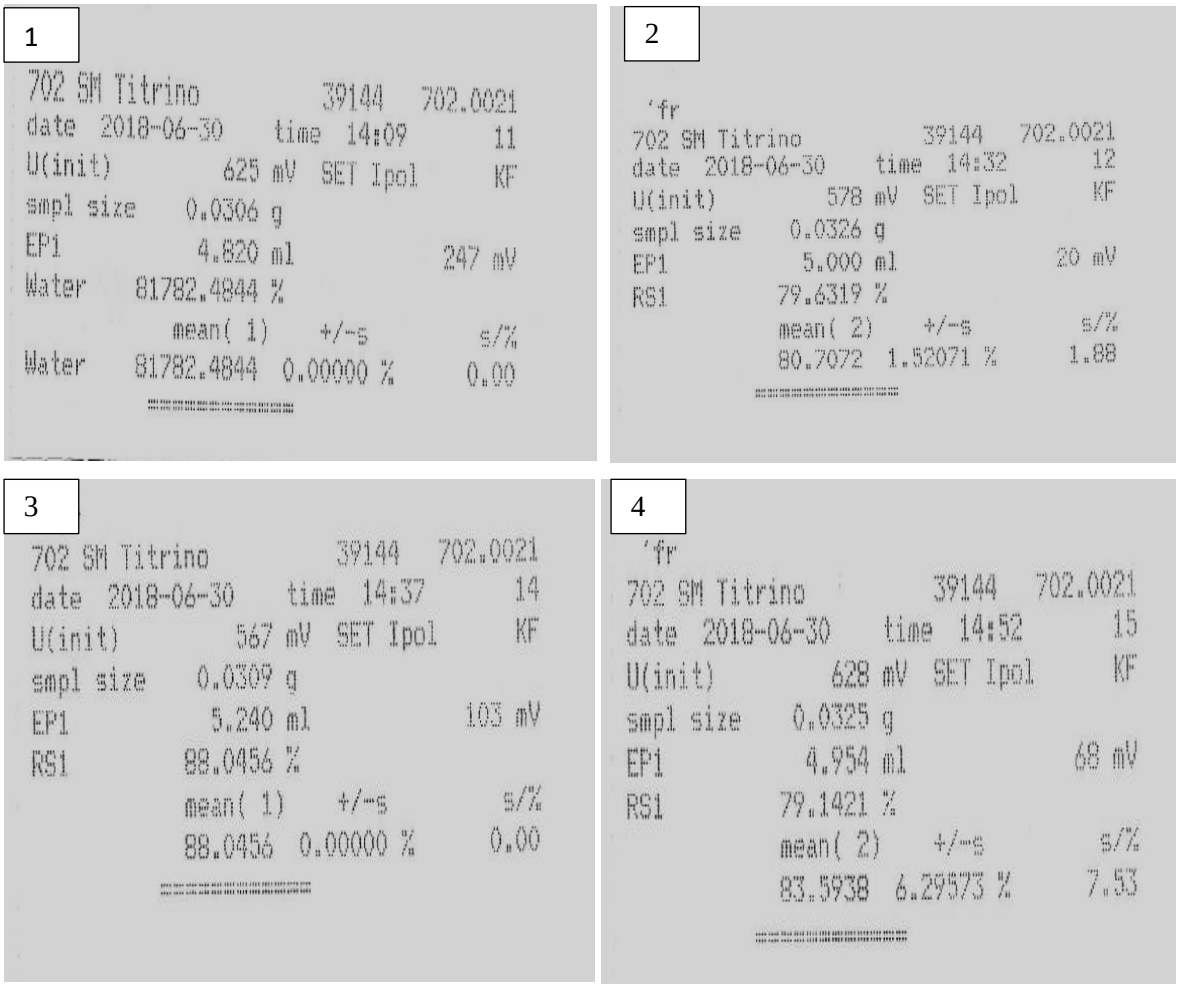

Figure 2: Sample analysis 1: Standing Plasma sample 1 runs 1-4

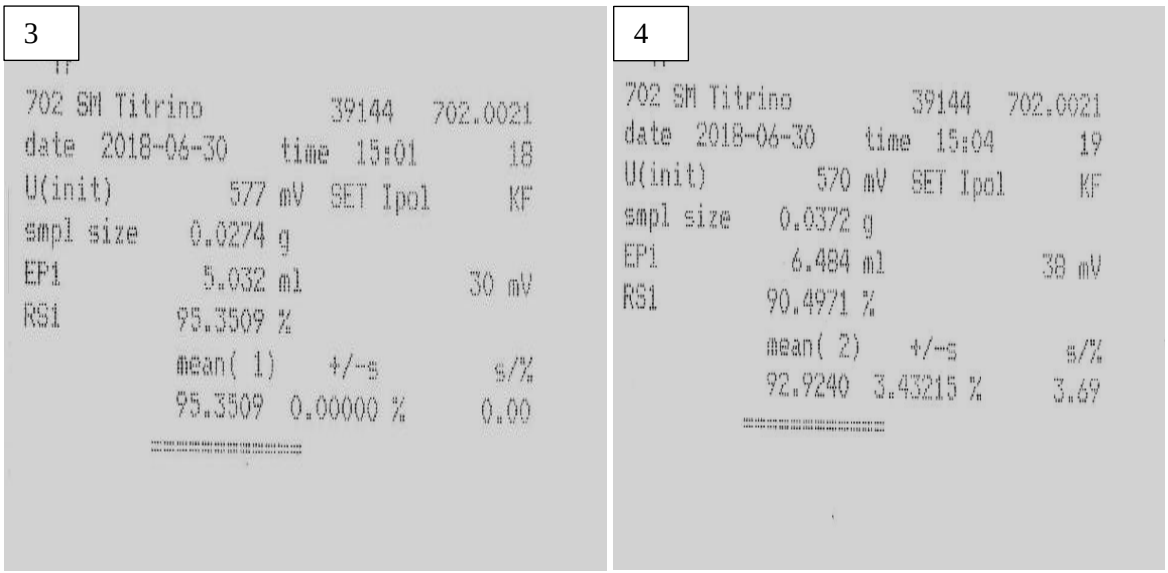

Figure 3: Sample analysis 1: Standing Plasma sample 2 runs 1-4

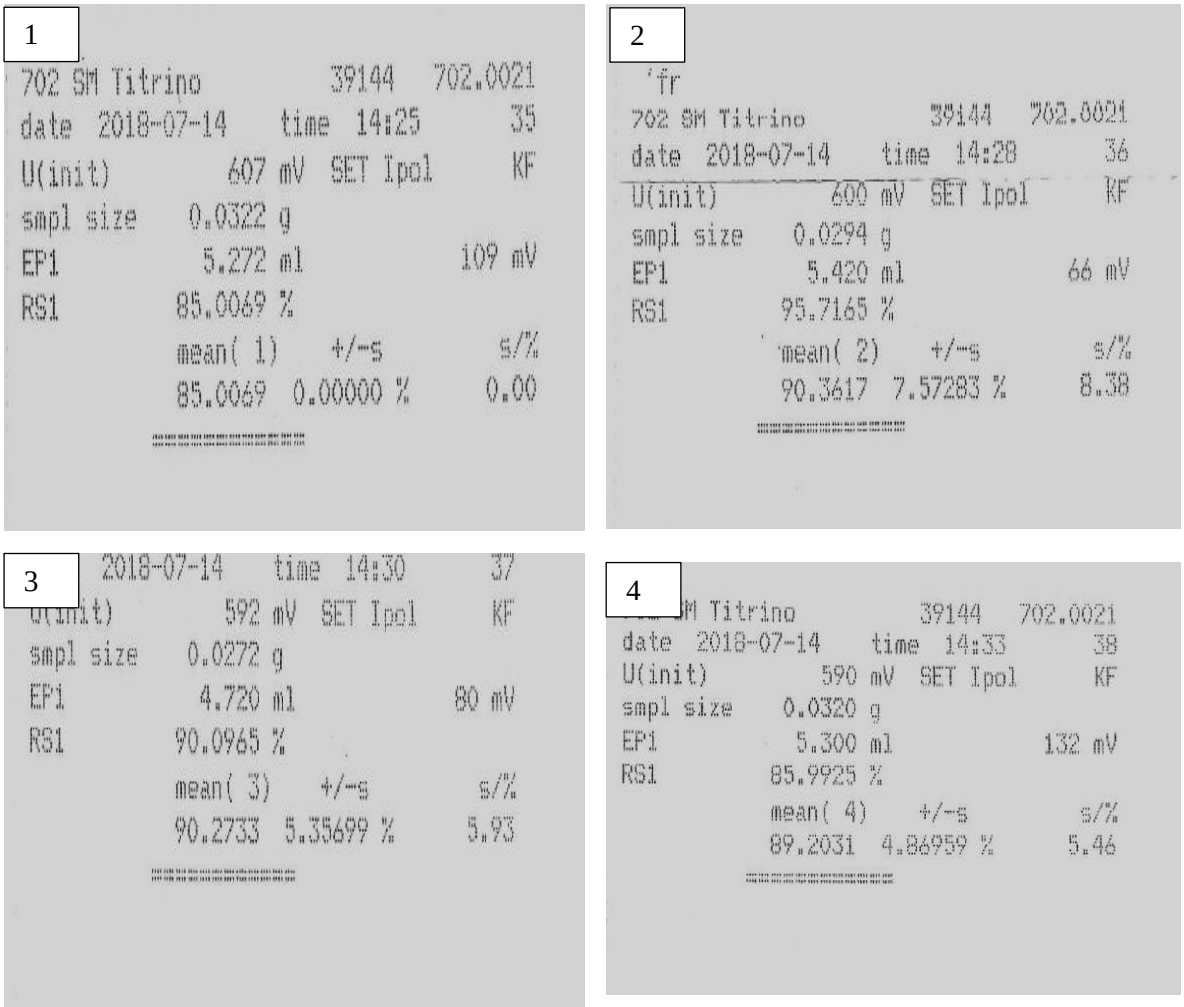

Figure 4: Sample analysis 1: Standing Plasma sample 3 runs 1-4

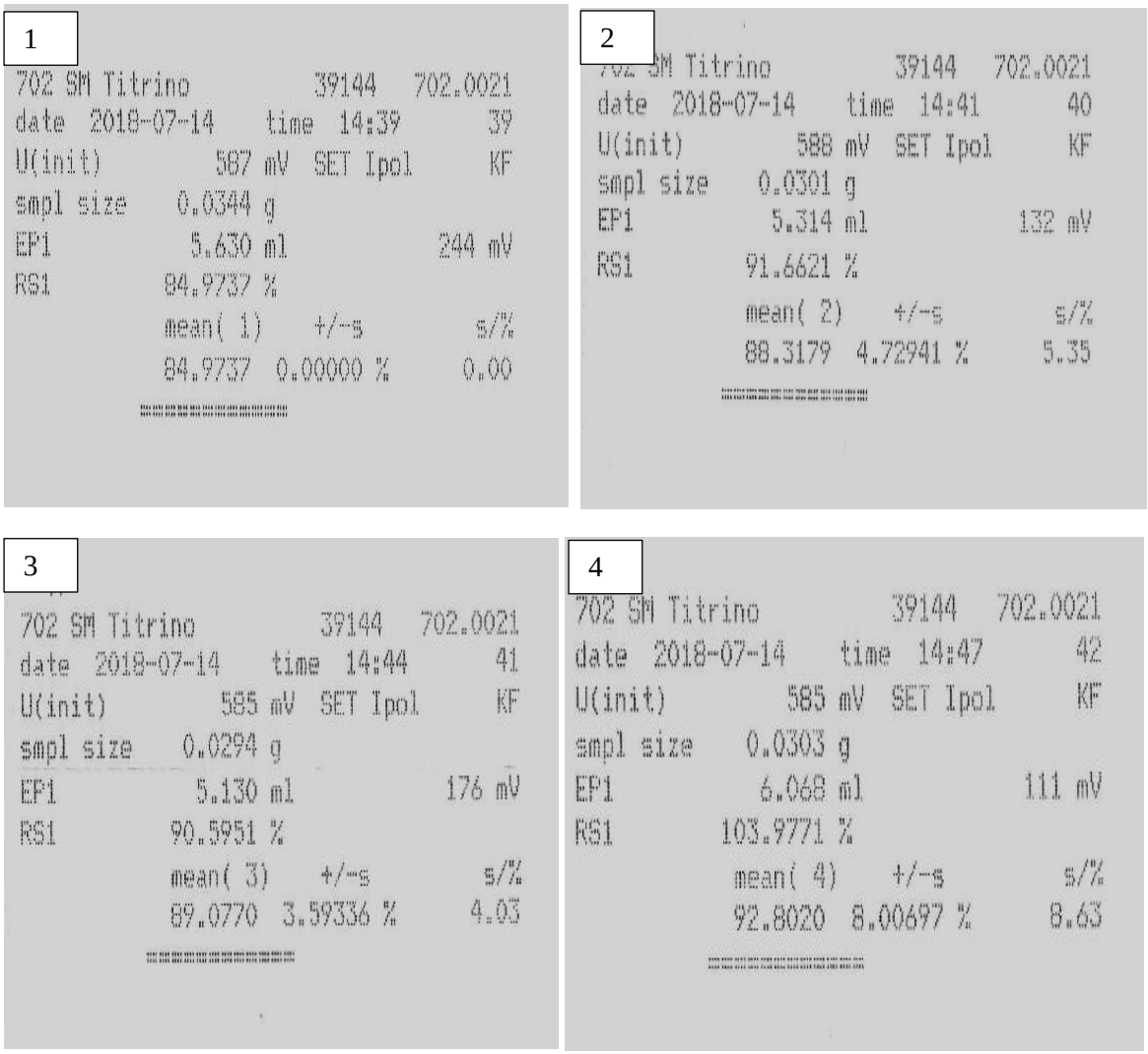

Figure 5: Sample analysis 1: Standing Plasma Sample 4 runs 1-4

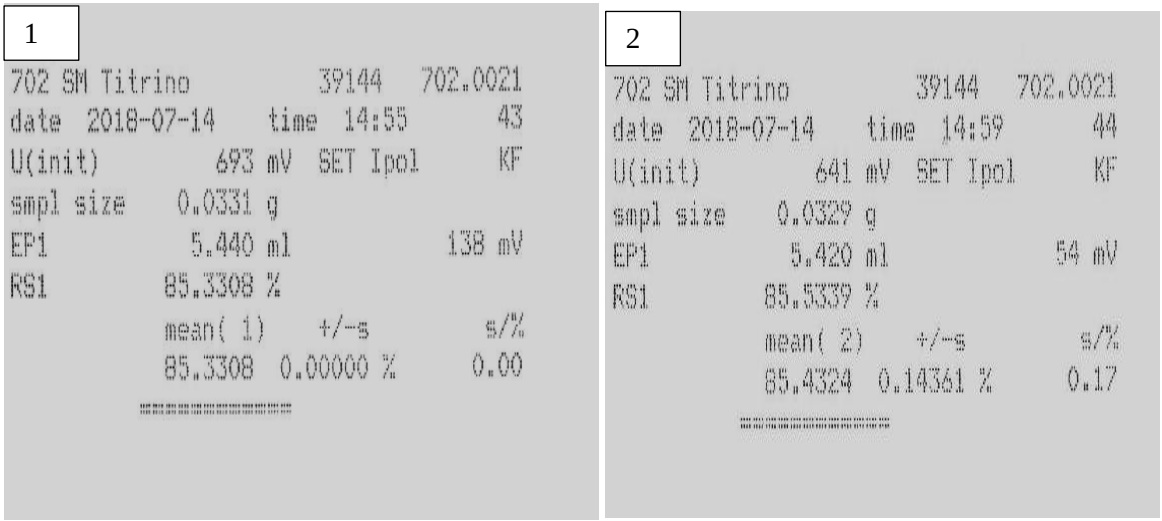

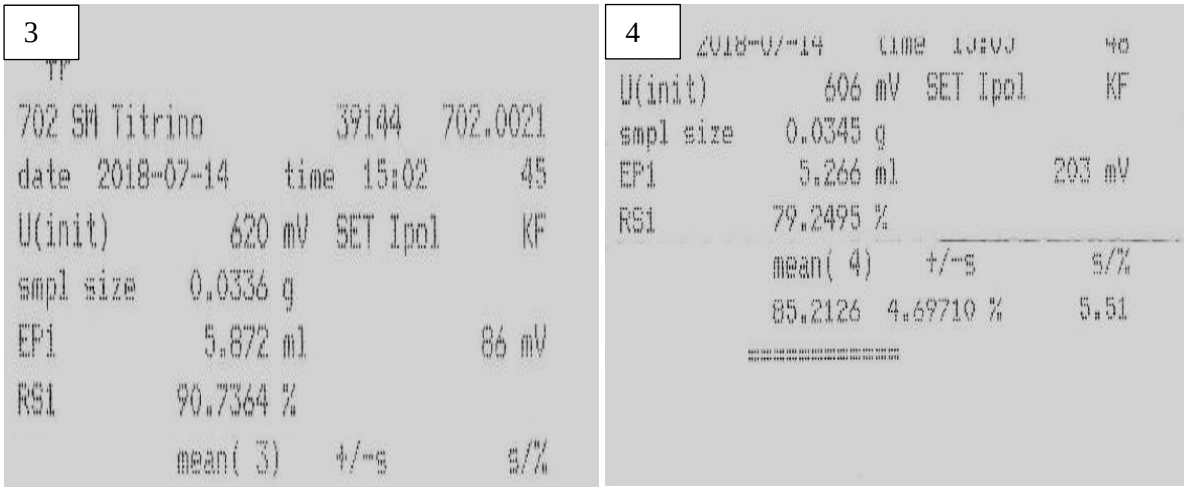

Figure 6: Sample analysis 1: Standing Plasma sample 5 runs 1-4

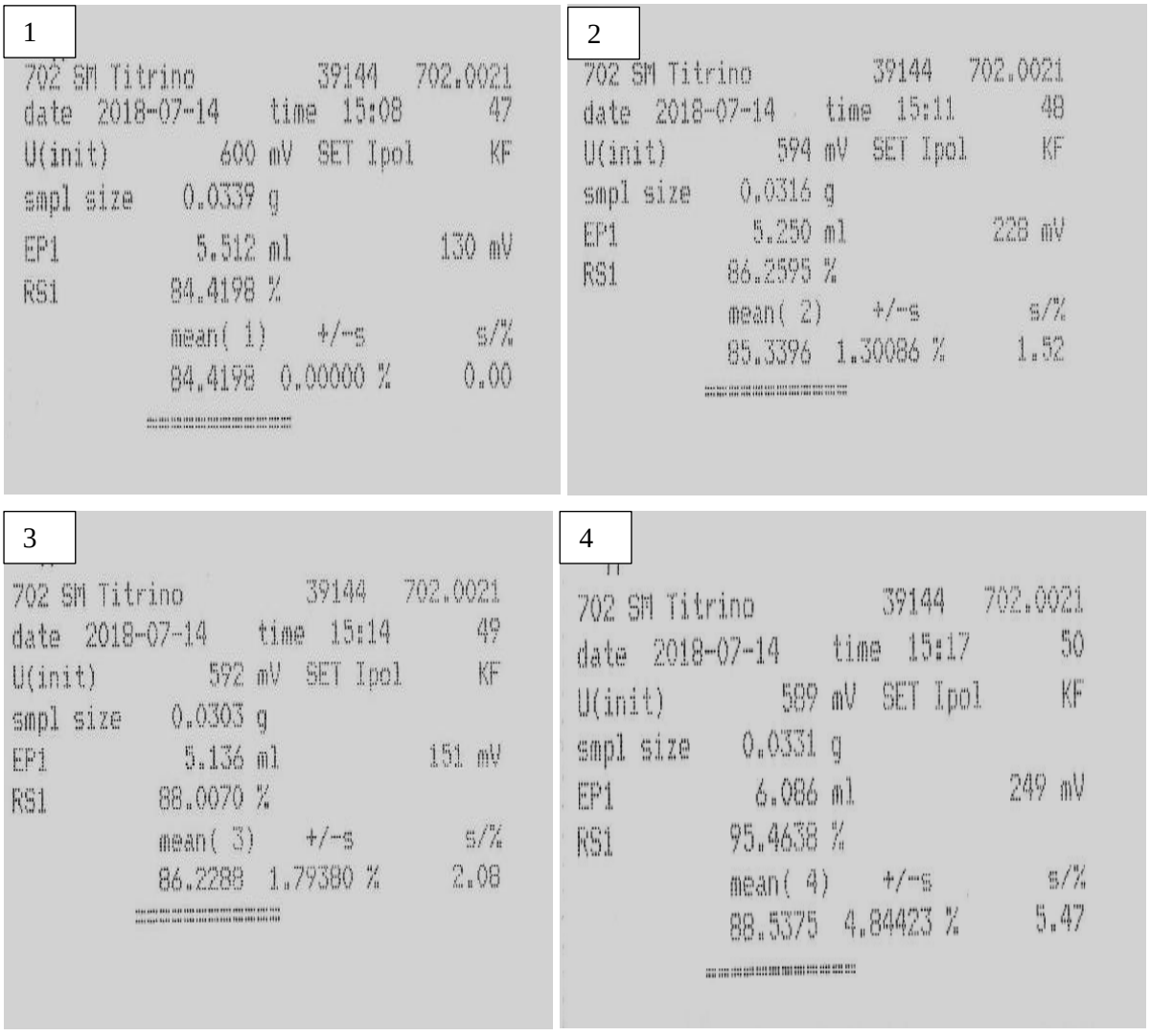

Figure 7: Sample analysis 1: Standing Plasma sample 6 runs 1-4

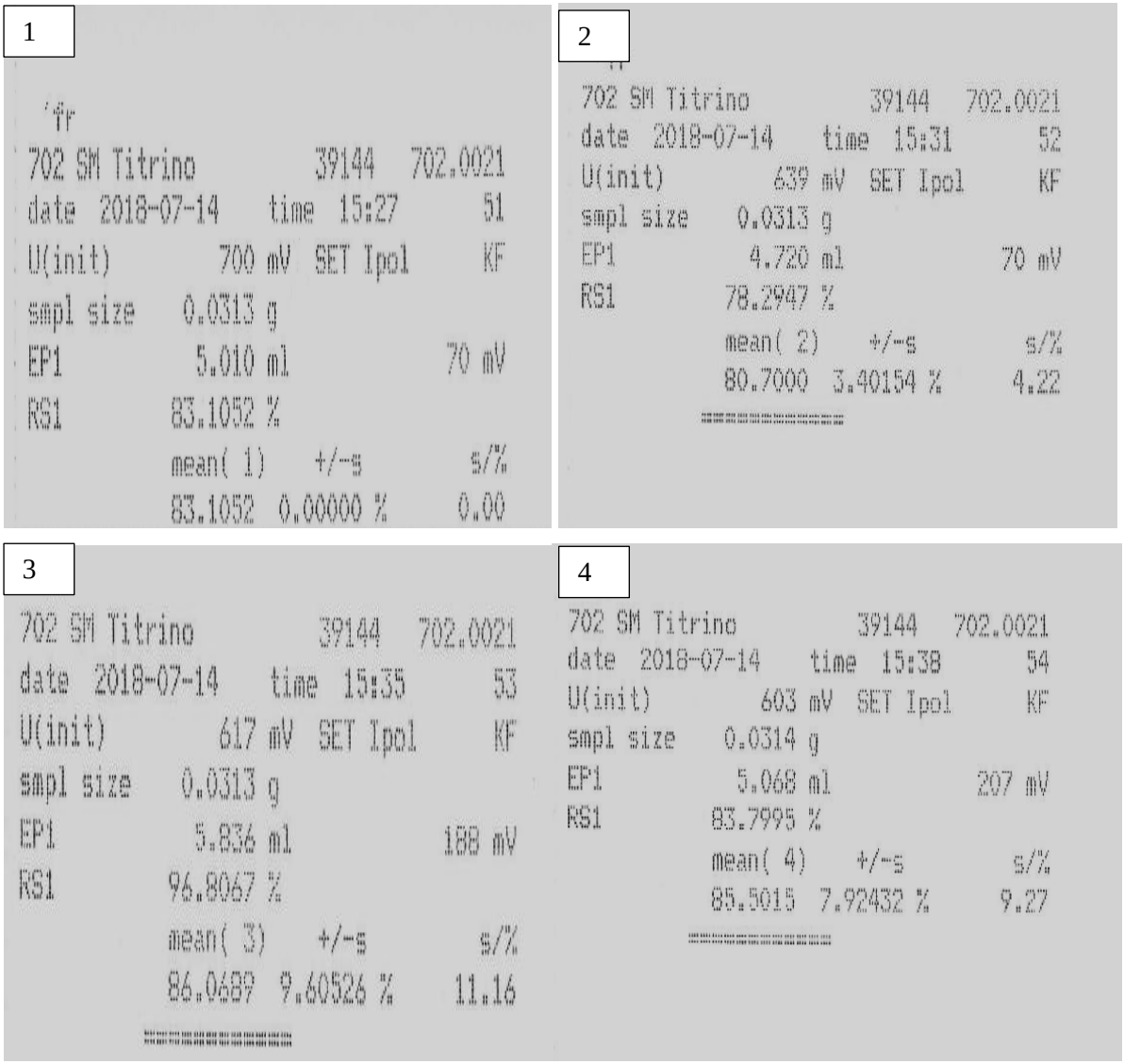

Figure 8: Sample analysis 1: Standing Plasma sample 7 runs 1-4

Table 1: Plasma standing samples analysis 1: Sample 1 Percentages rounded off to second decimal

	Plasma sample 1:(Patient ID)1098435		
Runs	**Mass in grams(g)**	**Water%**	**Protein%**
1	0.0306	81.78	18.22
2	0.0326	79.63	20.37
3	0.0390	88.04	11.96
4	0.0325	79.14	20.86
Average	0.0337	82.15	17.85
RSD%	9.43	4.31	19.85

4 runs table (water content present in plasma analysis 1 sample 1) at 200µL of plasma sample per run illustrated in table 3.7, with a mean mass value of 0.0337. The highest water content % detected was 88.04 and the lowest water content % was 79.14 with an RSD% for all 4 runs of 4.31%.

Table 2: Plasma standing samples analysis 1: Sample 2 Percentages rounded off to second decimal

	Plasma sample 2: (Patient ID)11127901		
Runs	**Mass in grams**	**Water%**	**Protein%**
1	0.0316	77.06	22.94
2	0.0281	94.64	5.36
3	0.0274	95.35	4.65
4	0.0372	94.50	5.50
Average	0.0311	90.39	9.61
RSD%	12.47	8.52	80.12

4 runs (water content present in plasma analysis 1 sample 2) at 200µL of plasma sample per run, illustrated in table 3.8, with a mean mass value of 0.0311. The highest water content % detected was 95.35 and the lowest water content % was 77.06 with an RSD% for all 4 runs of 8.52%.

Table 3: Plasma standing samples analysis 1: Sample 3 Percentages rounded off to second decimal

	Plasma sample 3: (Patient ID)11127901		
Runs	**Mass in grams**	**Water%**	**Protein%**
1	0.0322	85.01	14.99
2	0.0294	95.72	4.28
3	0.0272	90.10	9.90
4	0.0320	85.99	14.01
Average	0.0302	89.21	10.79
RSD%	6.02	4.73	39.08

4 runs (water content present in plasma analysis 1 sample 3) at 200µL of plasma sample per run, illustrated in table 3.9, with a mean mass value of 0.0302. The highest water content % detected was 95.72 and the lowest water content % was 85.01 with an RSD% for all 4 runs of 4.73%.

Table 4: Plasma standing samples analysis 1: Sample 4 Percentages rounded off to second decimal

	Plasma sample 4: (Patient ID)11114623		
Runs	**Mass in grams**	**Water%**	**Protein%**
1	0.0344	84.97	15.03
2	0.0301	91.66	8.34
3	0.0294	90.60	9.40
4	0.0303	103.97	0
Average	0.0311	92.80	7.20
RSD%	6.32	7.40	65.55

4 runs (water content present in plasma analysis 1) at 200µL of plasma sample per run, illustrated in table 3.10, with a mean mass value of 0.0311. The highest water content % detected was 103.97% and the lowest water content % was 84.97% with an RSD% for all 4 runs of 7.40%.

Table 5: Plasma standing samples analysis 1: Sample 5 Percentages rounded off to second decimal

	Plasma sample 5: (Patient ID)10984359		
Runs	**Mass in grams**	**Water%**	**Protein%**
1	0.0331	85.33	14.67
2	0.0329	85.53	14.47
3	0.0336	90.73	9.27
4	0.0345	79.25	20.75
Average	0.0335	85.21	14.79
RSD%	1.84	4.77	27.49

4 runs (water content present in plasma analysis 1, sample 5) at 200µL of plasma sample per run, illustrated in table 3.11 with a mean mass value of 0.0335g. The highest water content % detected was 90.73% and the lowest water content % was 79.25% with an RSD% for all 4 runs of 4.77%.

Table 6: Plasma standing samples analysis 1: Sample 6 Percentages rounded off to second decimal

	Plasma sample 6: (Patient ID)10984359		
Runs	**Mass in grams**	**Water%**	**Protein%**
1	0.0339	84.42	15.58
2	0.0316	86.26	13.74
3	0.0303	88.01	11.99
4	0.0331	95.46	4.54
Average	0.0322	88.53	11.47
RSD%	4.30	4.74	36.58

4 runs (water content present in plasma analysis 1, sample 6) at 200µL of plasma sample per run, illustrated in table 3.12, with a mean mass value of 0.0322. The highest water content % detected was 95.46 % and the lowest water content % was 84.42% with an RSD% for all 4 runs of 4.74%.

Table 7: Plasma standing samples analysis 1: Sample 7 Percentages rounded off to second decimal

	Plasma sample 7: (Patient ID)1114623		
Runs	**Mass in grams**	**Water%**	**Protein%**
1	0.0313	83.10	16.90
2	0.0313	78.29	21.71
3	0.0313	96.81	3.19
4	0.0314	83.80	16.20
Average	0.0313	85.50	14.50
RSD%	0.14	8.03	47.35

4 runs (water content present in plasma analysis 1, sample 7) at 200µL of plasma sample per run, illustrated in table 3.13, with a mean mass value of 0.0313g. The highest water content % detected was 96.81% and the lowest water content % was 78.29% with an RSD% for all 4 runs of 8.03%.

Sample analysis 2

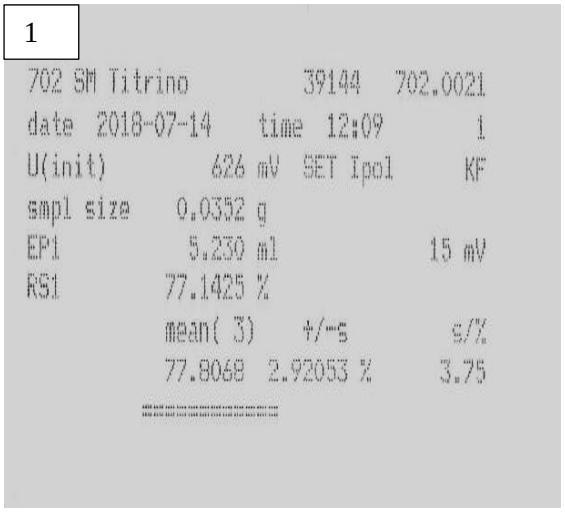

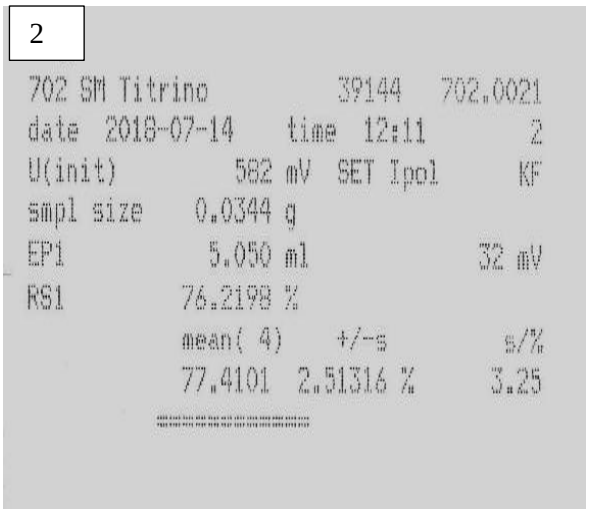

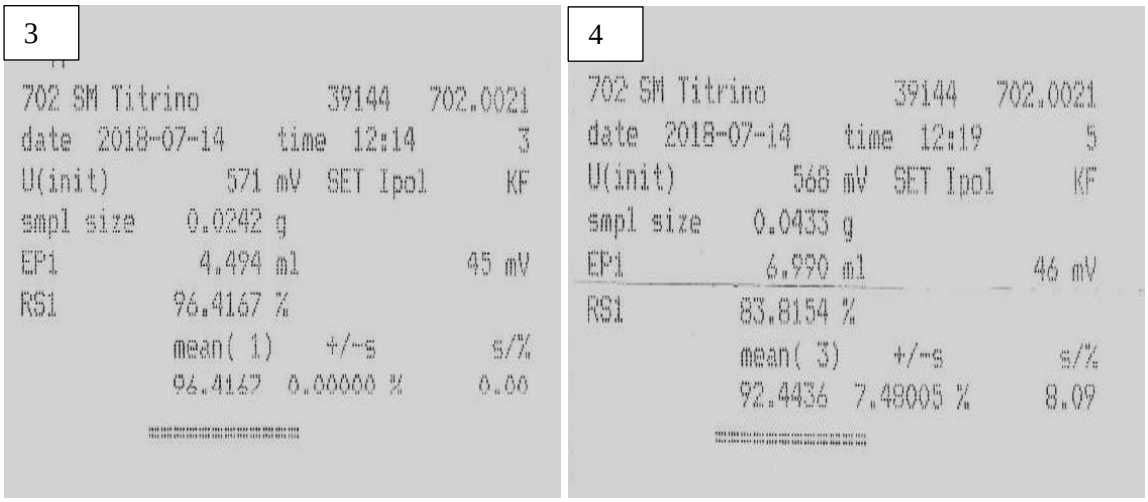

Figure 9: Sample analysis 2: Shaken Plasma Sample 1 runs 1-4

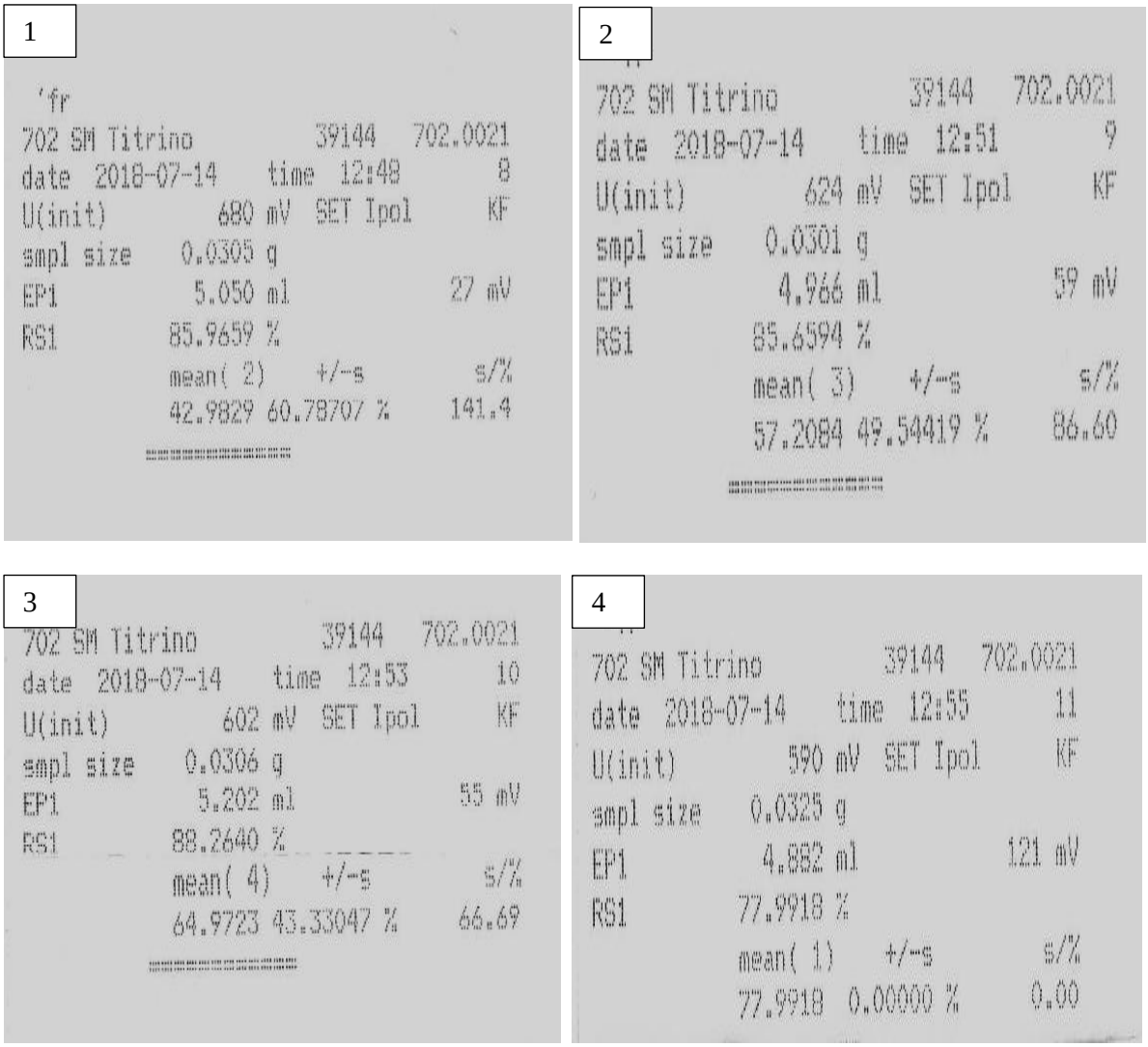

Figure 10: Sample analysis 2: Shaken Plasma Sample 2 runs1-4

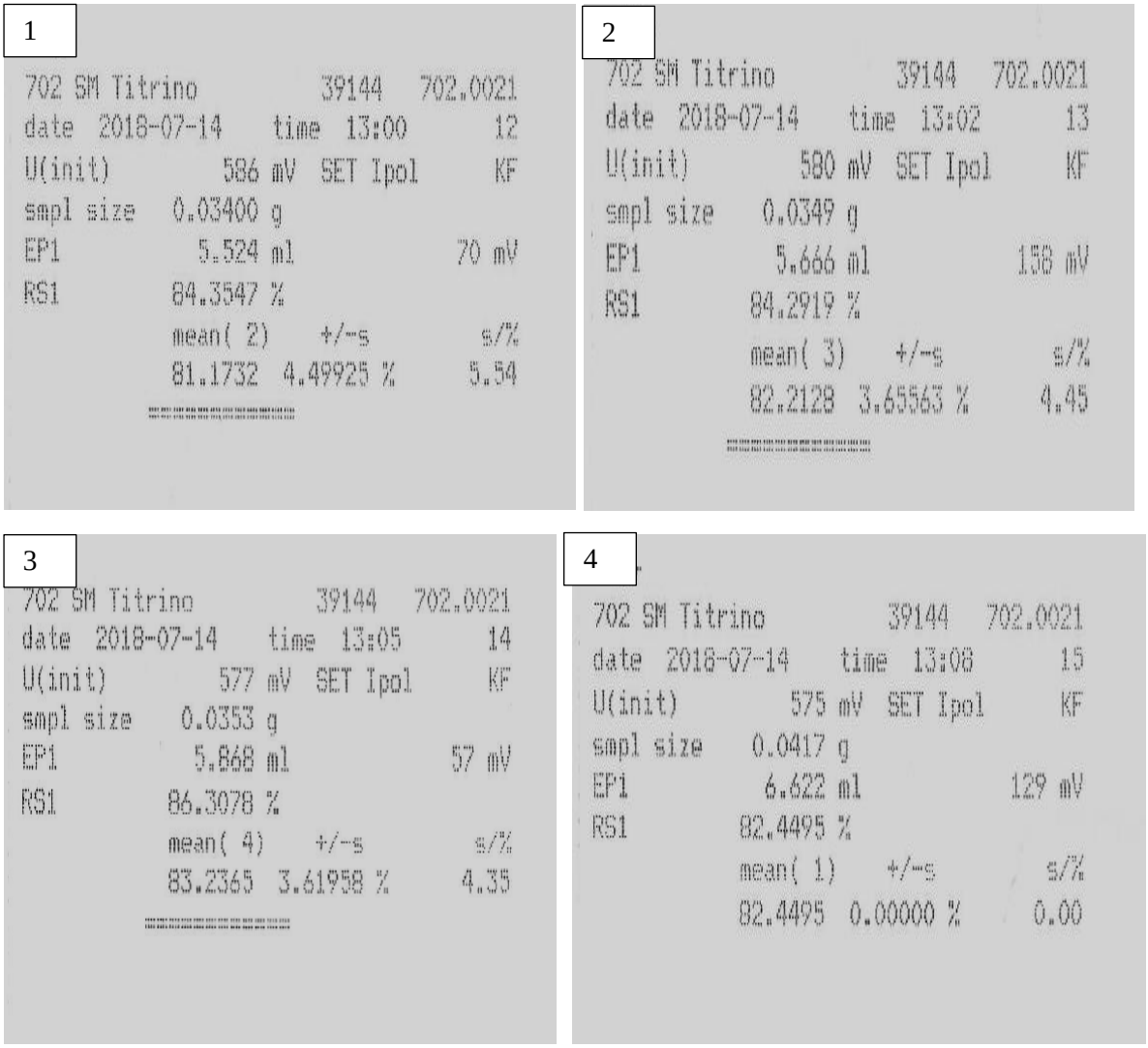

Figure 11: Sample analysis 2: Shaken Plasma sample 3 runs 1-4

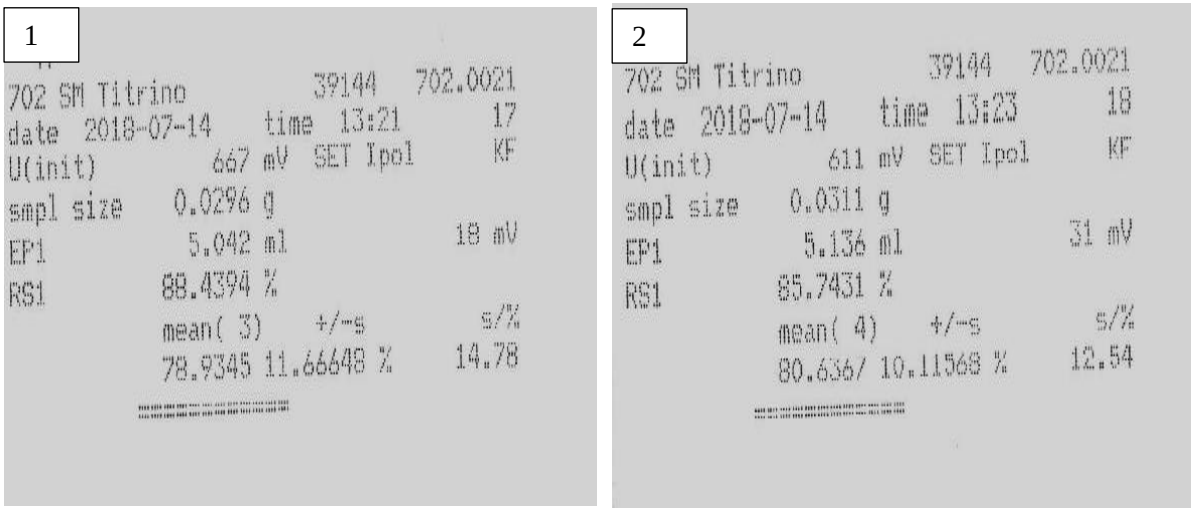

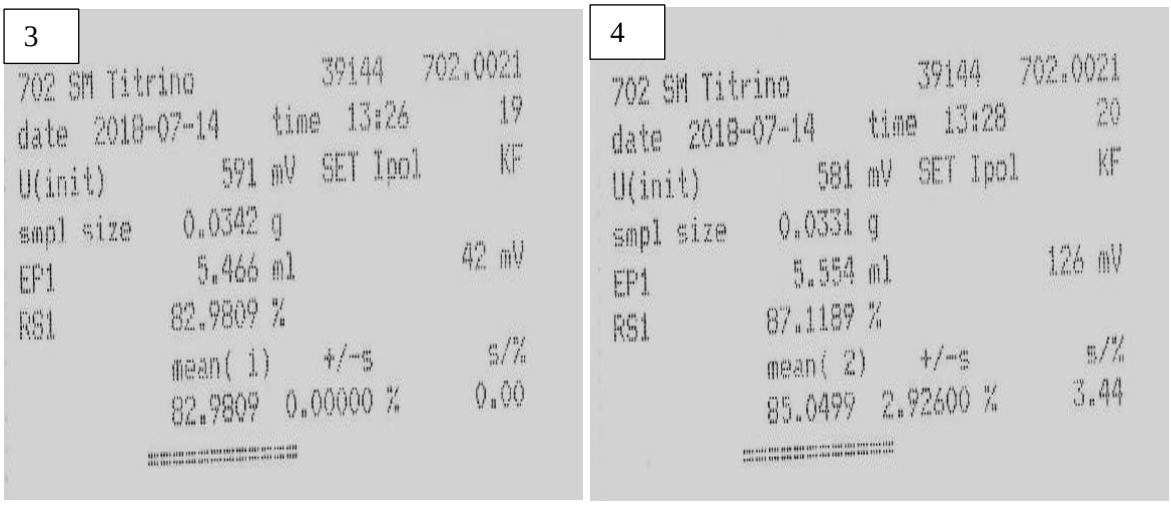

Figure 12: Sample analysis 2: Shaken Plasma Sample 4 runs 1-4

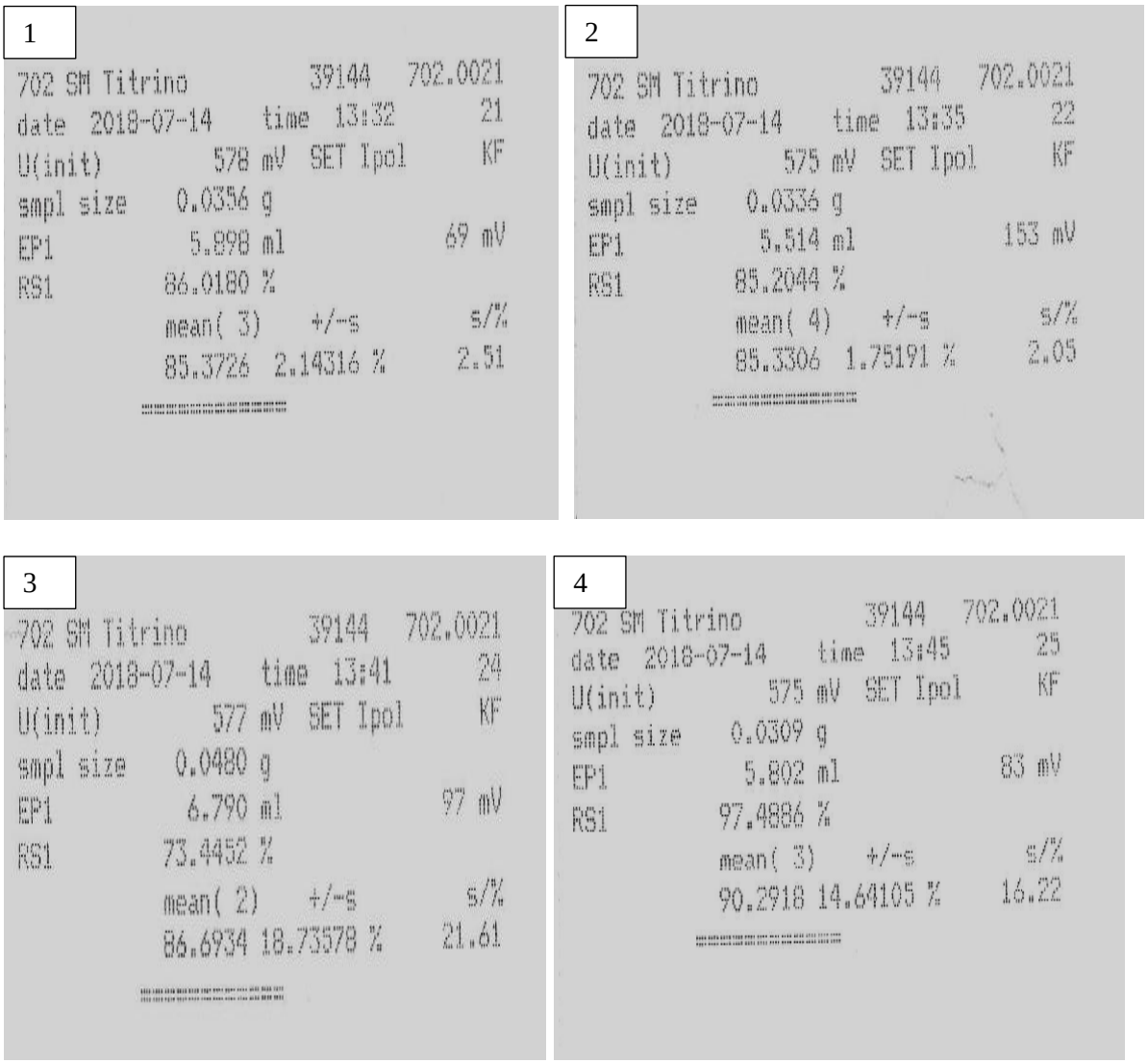

Figure 13: Sample analysis 2: Shaken Plasma sample 5 runs 1-4

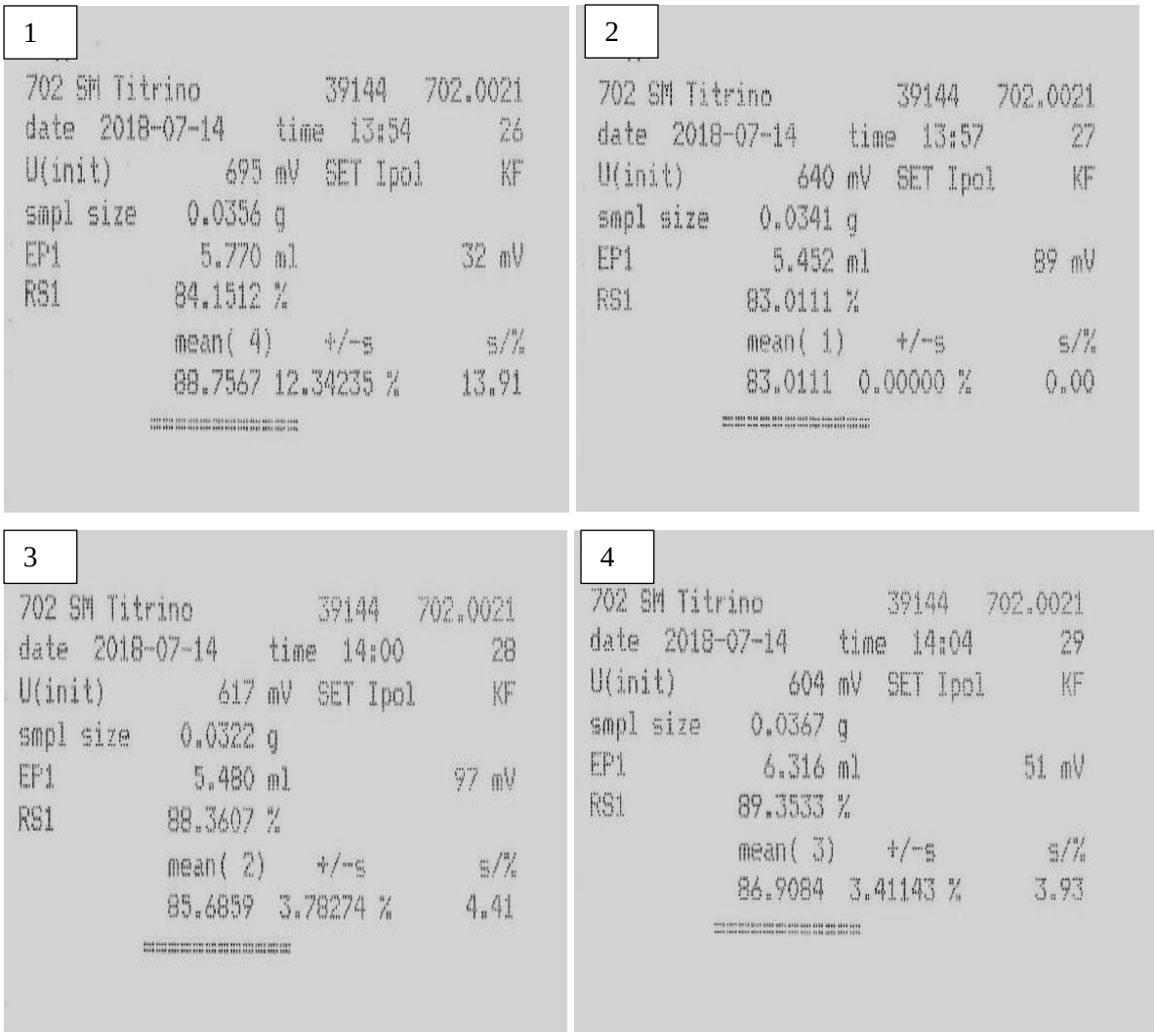

Figure 14: Sample analysis 2: Shaken Plasma sample 6 runs 1-4

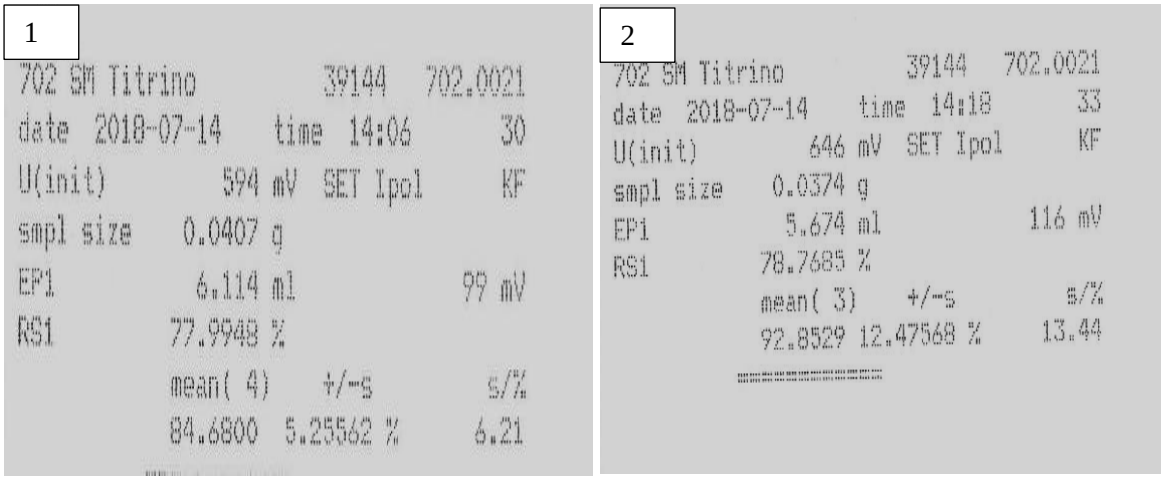

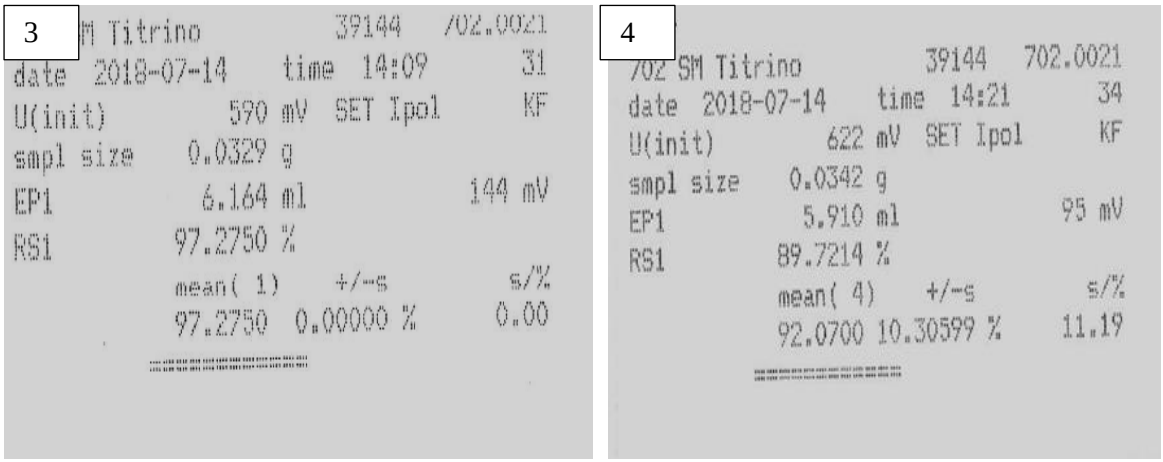

Figure 15: Sample analysis 2: Shaken Plasma sample 7 runs 1-4

Table 8: Plasma shaken samples analysis 2: Sample 1 Percentage rounded off to 2 decimals

	Plasma sample 1: (Patient ID)11127901		
Runs	**Mass in grams**	**Water%**	**Protein%**
1	0.0352	77.14	22.86
2	0.0344	76.21	23.79
3	0.0275	96.90	3.10
4	0.0433	83.82	16.18
Average	0.0351	83.52	16.48
RSD%	15.96	9.90	50.14

4 runs (water content present in plasma analysis 2, sample 1) at 200µL of plasma sample per run, illustrated in table 3.14 with a mean mass value of 0.0351g. The highest water content % detected was 96.90% and the lowest water content % was 77.14% with an RSD% for all 4 runs of 9.90%.

Table 9: Plasma shaken samples analysis 2: Sample 2 Percentage rounded off to 2 decimals

	Plasma sample 2: (Patient ID)11114623		
Runs	**Mass in grams**	**Water%**	**Protein%**
1	0.0305	85.97	14.03
2	0.0301	85.67	14.33
3	0.0306	88.26	11.33
4	0.0325	77.99	22.01
Average	0.0309	84.47	15.53
RSD%	3.00	4.59	25.78

4 runs (water content present in plasma analysis 2) at 200µL of plasma sample per run, illustrated in table 3.15 with a mean mass value of 0.0309g. The highest water content % detected was 88.26% and the lowest water content % was 77.99% with an RSD% for all 4 runs of 4.59%.

Table 10: Plasma shaken samples analysis 2: Sample 3 Percentage rounded of to 2 decimals

	Plasma sample 3: (Patient ID)10984359		
Runs	**Mass in grams**	**Water%**	**Protein%**
1	0.0340	84.35	15.65
2	0.0349	84.29	15.71
3	0.0353	86.30	13.70
4	0.0417	82.45	17.55
Average	0.0365	84.35	15.65
RSD%	8.37	1.61	8.70

4 runs (water content present in plasma analysis 2, sample 3) at 200µL of plasma sample per run, illustrated in table 3.16 with a mean mass value of 0.0365g. The highest water content % detected was 86.30% and the lowest water content % was 82.45% with an RSD% for all 4 runs of 1.61%.

Table 11: Plasma shaken samples analysis 2: Sample 4 Percentage rounded off to 2 decimals.

	Plasma sample 4:10984359		
Runs	**Mass in grams**	**Water%**	**Protein%**
1	0.0296	88.44	11.56
2	0.0311	85.74	14.26
3	0.0342	82.98	17.02
4	0.0331	87.12	12.88
Average	0.0320	86.07	13.93
	5.55	2.35	14.52

4 runs (water content present in plasma analysis 2, sample 4) at 200µL of plasma sample per run, illustrate in table 3.17, with a mean mass value of 0.0320. The highest water content % detected was 88.44% and the lowest water content % was 82.29% with an RSD% for all 4 runs of 2.35%.

Table 12: Plasma shaken samples analysis 2: Sample 5 Percentage rounded off to 2 decimals

	Plasma sample 5: (Patient ID)11114623		
Runs	**Mass in grams**	**Water%**	**Protein%**
1	0.0356	86.02	13.98
2	0.0336	85.20	14.80
3	0.0480	73.45	26.55
4	0.0309	97.49	2.51
Average	0.0370	85.54	14.46
RSD%	17.69	9.94	58.82

4 runs (water content present in plasma analysis 2, sample 5) at 200µL of plasma sample per run, illustrated in table 3.18 with a mean mass value of 0.0370. The highest water content % detected was 97.49% and the lowest water content % was 73.45% with an RSD% for all 4 runs of 9.94%.

Table 13: Plasma shaken samples analysis 2: Sample 6 Percentage rounded off to 2 decimals

	Plasma sample 6: (Patient ID)11114623		
Runs	**Mass in grams**	**Water%**	**Protein%**
1	0.0356	84.15	15.85
2	0.0341	83.01	16.99
3	0.0322	88.36	11.64
4	0.0367	89.35	10.65
Average	0.0347	86.22	13.78
RSD%	4.87	3.12	19.52

4 runs (water content present in plasma analysis 2, sample 6) at 200µL of plasma sample per run, illustrated in table 3.19 with a mean mass value of 0.0347g. The highest water content % detected was 89.35% and the lowest water content % was 83.01% with an RSD% for all 4 runs of 3.12%.

Table 14: Plasma shaken samples analysis 2: Sample 7 Percentage rounded off to 2 decimals

	Plasma sample 7: (Patient ID)11114623		
Runs	**Mass in grams**	**Water%**	**Protein%**
1	0.0407	77.99	22.01
2	0.0374	97.28	2.72
3	0.0329	89.72	10.28
4	0.0342	78.77	21.23
Average	0.0363	85.94	14.06
RSD%	8.33	9.34	57.65

4 runs (water content present in plasma analysis 2, sample 7) at 200µL of plasma sample per run, illustrated in table 3.20 with a mean mass value of 0.0363g. The highest water content % detected was 97.28% and the lowest water content % was 77.99% with an RSD% for all 4 runs of 9.34%.

***Table* 4.5** One way Anova detailed statistical comparison of the [plasma protein] in sample pairs using Bonferonni's multiple comparison test

Bonferroni's Multiple Comparison Test	Mean Diff.	t	Significant? P < 0.05?	Summary	95% CI of diff
CL13 vs CL14	-9.2	3.62	No	ns	-20.3 to 1.91
CL13 vs CL15	-5.41	2.13	No	ns	-16.5 to 5.70
CL13 vs CL16	13.6	5.34	Yes	***	2.44 to 24.7
CL13 vs CL17	3.65	1.44	No	ns	-7.47 to 14.8
CL13 vs CL18	-28.1	11.1	Yes	***	-39.2 to -17.0
CL13 vs CL19	31.2	12.3	Yes	***	20.1 to 42.3
CL13 vs CL20	-32.4	12.8	Yes	***	-43.5 to -21.3
CL13 vs CL21	-39.3	15.5	Yes	***	-50.4 to -28.1
CL13 vs CL22	-39.2	15.4	Yes	***	-50.3 to -28.1
CL13 vs CL23	-39.4	15.5	Yes	***	-50.5 to -28.2
CL13 vs CL24	-12	4.73	Yes	*	-23.1 to -0.894
CL13 vs CL25	-11.1	4.35	No	ns	-22.2 to 0.0594
CL13 vs CL26	-66.2	26.1	Yes	***	-77.3 to -55.1
CL13 vs CL27	-13.2	5.2	Yes	**	-24.3 to -2.09
CL13 vs LCR54	-50.1	19.7	Yes	***	-61.2 to -39.0
CL13 vs LCR55	9.9	3.9	No	ns	-1.21 to 21.0
CL13 vs LCR56	-3.51	1.38	No	ns	-14.6 to 7.60
CL13 vs LCR57	10.3	4.04	No	ns	-0.859 to 21.4
CL13 vs LCR58	1.24	0.488	No	ns	-9.87 to 12.4
CL13 vs LCR59	-3.89	1.53	No	ns	-15.0 to 7.22
CL13 vs LCR60	12.8	5.06	Yes	**	1.73 to 24.0
CL13 vs LCR63	-11.3	4.44	Yes	*	-22.4 to -0.154
CL13 vs LCR65	-1.82	0.717	No	ns	-12.9 to 9.29

CL13 vs LCR66	13.2	5.19	Yes	**	2.06 to 24.3
CL13 vs LCR67	27.5	10.8	Yes	***	16.4 to 38.6
CL13 vs LCR68	12	4.72	Yes	*	0.881 to 23.1
CL13 vs LCR70	-3.09	1.22	No	ns	-14.2 to 8.02
CL13 vs LCR43	4.53	1.78	No	ns	-6.59 to 15.6
CL13 vs LCR64	-1.35	0.533	No	ns	-12.5 to 9.76
CL13 vs LCR71	24.4	9.62	Yes	***	13.3 to 35.5
CL13 vs LCR72	-6.09	2.4	No	ns	-17.2 to 5.02
CL13 vs LCR73	-3.26	1.28	No	ns	-14.4 to 7.85
CL13 vs LCR74	13.6	5.35	Yes	***	2.48 to 24.7
CL13 vs LCR75	13.1	5.14	Yes	**	1.95 to 24.2
CL13 vs LCR76	0.12	0.0473	No	ns	-11.0 to 11.2
CL13 vs LCR77	1.63	0.641	No	ns	-9.49 to 12.7
CL13 vs LCR78	0.367	0.144	No	ns	-10.7 to 11.5
CL13 vs LCR131	-14.9	5.88	Yes	***	-26.1 to -3.83
CL13 vs LCR135	-11	4.35	No	ns	-22.2 to 0.0660
CL13 vs LV134	11.7	4.63	Yes	*	0.634 to 22.9
CL13 vs LV136	11.5	4.54	Yes	*	0.421 to 22.6
CL13 vs LV138	18.8	7.41	Yes	***	7.69 to 29.9
CL13 vs LV139	9.44	3.72	No	ns	-1.67 to 20.6
CL13 vs LV140	7.52	2.96	No	ns	-3.59 to 18.6
CL13 vs LV141	16.9	6.67	Yes	***	5.82 to 28.0
CL13 vs LV142	26.3	10.3	Yes	***	15.2 to 37.4
CL13 vs LV143	3.81	1.5	No	ns	-7.31 to 14.9
CL13 vs LV144	6.8	2.68	No	ns	-4.31 to 17.9
CL13 vs LV145	-3.75	1.48	No	ns	-14.9 to 7.36
CL13 vs LV146	36.4	14.3	Yes	***	25.3 to 47.5

CL13 vs LV161	11	4.32	No	ns	-0.146 to 22.1
CL13 vs LV163	2.76	1.09	No	ns	-8.35 to 13.9
CL13 vs LV162	29.7	11.7	Yes	***	18.6 to 40.8
CL13 vs LV164	27.9	11	Yes	***	16.8 to 39.0
CL13 vs LV165	19.5	7.68	Yes	***	8.38 to 30.6
CL13 vs LV167	10.3	4.04	No	ns	-0.853 to 21.4
CL13 vs LV168	24.3	9.58	Yes	***	13.2 to 35.4
CL13 vs LV176	-13.1	5.14	Yes	**	-24.2 to -1.95
CL13 vs CV125(L)	-9.61	3.78	No	ns	-20.7 to 1.51
CL13 vs CV126(L)	15.8	6.23	Yes	***	4.71 to 26.9
CL13 vs CV130	-3.88	1.53	No	ns	-15.0 to 7.23
CL13 vs LV180	5.18	2.04	No	ns	-5.93 to 16.3
CL13 vs LV183	6.35	2.5	No	ns	-4.77 to 17.5
CL14 vs CL15	3.79	1.49	No	ns	-7.33 to 14.9
CL14 vs CL16	22.8	8.96	Yes	***	11.6 to 33.9
CL14 vs CL17	12.8	5.06	Yes	**	1.73 to 24.0
CL14 vs CL18	-18.9	7.44	Yes	***	-30.0 to -7.79
CL14 vs CL19	40.4	15.9	Yes	***	29.3 to 51.5
CL14 vs CL20	-23.2	9.14	Yes	***	-34.3 to -12.1
CL14 vs CL21	-30.1	11.8	Yes	***	-41.2 to -18.9
CL14 vs CL22	-30	11.8	Yes	***	-41.1 to -18.9
CL14 vs CL23	-30.2	11.9	Yes	***	-41.3 to -19.0
CL14 vs CL24	-2.81	1.11	No	ns	-13.9 to 8.31
CL14 vs CL25	-1.85	0.73	No	ns	-13.0 to 9.26
CL14 vs CL26	-57	22.4	Yes	***	-68.1 to -45.9
CL14 vs CL27	-4	1.58	No	ns	-15.1 to 7.11
CL14 vs LCR54	-40.9	16.1	Yes	***	-52.0 to -29.8

CL14 vs LCR55	19.1	7.52	Yes	***	7.99 to 30.2
CL14 vs LCR56	5.69	2.24	No	ns	-5.43 to 16.8
CL14 vs LCR57	19.5	7.66	Yes	***	8.34 to 30.6
CL14 vs LCR58	10.4	4.11	No	ns	-0.673 to 21.6
CL14 vs LCR59	5.31	2.09	No	ns	-5.81 to 16.4
CL14 vs LCR60	22	8.68	Yes	***	10.9 to 33.2
CL14 vs LCR63	-2.07	0.814	No	ns	-13.2 to 9.05
CL14 vs LCR65	7.38	2.91	No	ns	-3.73 to 18.5
CL14 vs LCR66	22.4	8.81	Yes	***	11.3 to 33.5
CL14 vs LCR67	36.7	14.4	Yes	***	25.6 to 47.8
CL14 vs LCR68	21.2	8.35	Yes	***	10.1 to 32.3
CL14 vs LCR70	6.11	2.4	No	ns	-5.01 to 17.2
CL14 vs LCR43	13.7	5.41	Yes	***	2.61 to 24.8
CL14 vs LCR64	7.85	3.09	No	ns	-3.27 to 19.0
CL14 vs LCR71	33.6	13.2	Yes	***	22.5 to 44.7
CL14 vs LCR72	3.11	1.22	No	ns	-8.01 to 14.2
CL14 vs LCR73	5.94	2.34	No	ns	-5.17 to 17.1
CL14 vs LCR74	22.8	8.98	Yes	***	11.7 to 33.9
CL14 vs LCR75	22.3	8.77	Yes	***	11.1 to 33.4
CL14 vs LCR76	9.32	3.67	No	ns	-1.79 to 20.4
CL14 vs LCR77	10.8	4.26	No	ns	-0.286 to 21.9
CL14 vs LCR78	9.57	3.77	No	ns	-1.55 to 20.7
CL14 vs LCR131	-5.74	2.26	No	ns	-16.9 to 5.37
CL14 vs LCR135	-1.85	0.727	No	ns	-13.0 to 9.27
CL14 vs LV134	20.9	8.25	Yes	***	9.83 to 32.1
CL14 vs LV136	20.7	8.17	Yes	***	9.62 to 31.8
CL14 vs LV138	28	11	Yes	***	16.9 to 39.1

CL14 vs LV139	18.6	7.34	Yes	***	7.53 to 29.8
CL14 vs LV140	16.7	6.58	Yes	***	5.61 to 27.8
CL14 vs LV141	26.1	10.3	Yes	***	15.0 to 37.2
CL14 vs LV142	35.5	14	Yes	***	24.4 to 46.6
CL14 vs LV143	13	5.12	Yes	**	1.89 to 24.1
CL14 vs LV144	16	6.3	Yes	***	4.89 to 27.1
CL14 vs LV145	5.45	2.15	No	ns	-5.67 to 16.6
CL14 vs LV146	45.6	18	Yes	***	34.5 to 56.7
CL14 vs LV161	20.2	7.94	Yes	***	9.05 to 31.3
CL14 vs LV163	12	4.71	Yes	*	0.847 to 23.1
CL14 vs LV162	38.9	15.3	Yes	***	27.8 to 50.0
CL14 vs LV164	37.1	14.6	Yes	***	26.0 to 48.2
CL14 vs LV165	28.7	11.3	Yes	***	17.6 to 39.8
CL14 vs LV167	19.5	7.66	Yes	***	8.35 to 30.6
CL14 vs LV168	33.5	13.2	Yes	***	22.4 to 44.6
CL14 vs LV176	-3.86	1.52	No	ns	-15.0 to 7.25
CL14 vs CV125(L)	-0.407	0.16	No	ns	-11.5 to 10.7
CL14 vs CV126(L)	25	9.86	Yes	***	13.9 to 36.1
CL14 vs CV130	5.32	2.1	No	ns	-5.79 to 16.4
CL14 vs LV180	14.4	5.66	Yes	***	3.27 to 25.5
CL14 vs LV183	15.5	6.12	Yes	***	4.43 to 26.7
CL15 vs CL16	19	7.47	Yes	***	7.85 to 30.1
CL15 vs CL17	9.06	3.57	No	ns	-2.05 to 20.2
CL15 vs CL18	-22.7	8.93	Yes	***	-33.8 to -11.6
CL15 vs CL19	36.6	14.4	Yes	***	25.5 to 47.7
CL15 vs CL20	-27	10.6	Yes	***	-38.1 to -15.9
CL15 vs CL21	-33.8	13.3	Yes	***	-45.0 to -22.7

CL15 vs CL22	-33.8	13.3	Yes	***	-44.9 to -22.7
CL15 vs CL23	-33.9	13.4	Yes	***	-45.1 to -22.8
CL15 vs CL24	-6.59	2.6	No	ns	-17.7 to 4.52
CL15 vs CL25	-5.64	2.22	No	ns	-16.8 to 5.47
CL15 vs CL26	-60.8	23.9	Yes	***	-71.9 to -49.6
CL15 vs CL27	-7.79	3.07	No	ns	-18.9 to 3.33
CL15 vs LCR54	-44.7	17.6	Yes	***	-55.8 to -33.6
CL15 vs LCR55	15.3	6.03	Yes	***	4.20 to 26.4
CL15 vs LCR56	1.9	0.748	No	ns	-9.21 to 13.0
CL15 vs LCR57	15.7	6.17	Yes	***	4.55 to 26.8
CL15 vs LCR58	6.65	2.62	No	ns	-4.46 to 17.8
CL15 vs LCR59	1.52	0.599	No	ns	-9.59 to 12.6
CL15 vs LCR60	18.3	7.19	Yes	***	7.15 to 29.4
CL15 vs LCR63	-5.85	2.31	No	ns	-17.0 to 5.26
CL15 vs LCR65	3.59	1.42	No	ns	-7.52 to 14.7
CL15 vs LCR66	18.6	7.32	Yes	***	7.47 to 29.7
CL15 vs LCR67	32.9	12.9	Yes	***	21.8 to 44.0
CL15 vs LCR68	17.4	6.86	Yes	***	6.29 to 28.5
CL15 vs LCR70	2.32	0.914	No	ns	-8.79 to 13.4
CL15 vs LCR43	9.94	3.91	No	ns	-1.17 to 21.1
CL15 vs LCR64	4.06	1.6	No	ns	-7.05 to 15.2
CL15 vs LCR71	29.8	11.8	Yes	***	18.7 to 41.0
CL15 vs LCR72	-0.68	0.268	No	ns	-11.8 to 10.4
CL15 vs LCR73	2.15	0.848	No	ns	-8.96 to 13.3
CL15 vs LCR74	19	7.49	Yes	***	7.89 to 30.1
CL15 vs LCR75	18.5	7.28	Yes	***	7.36 to 29.6
CL15 vs LCR76	5.53	2.18	No	ns	-5.58 to 16.6

CL15 vs LCR77	7.04	2.77	No	ns	-4.07 to 18.2
CL15 vs LCR78	5.78	2.28	No	ns	-5.33 to 16.9
CL15 vs LCR131	-9.53	3.75	No	ns	-20.6 to 1.59
CL15 vs LCR135	-5.63	2.22	No	ns	-16.7 to 5.48
CL15 vs LV134	17.2	6.76	Yes	***	6.05 to 28.3
CL15 vs LV136	16.9	6.67	Yes	***	5.83 to 28.1
CL15 vs LV138	24.2	9.54	Yes	***	13.1 to 35.3
CL15 vs LV139	14.9	5.85	Yes	***	3.74 to 26.0
CL15 vs LV140	12.9	5.09	Yes	**	1.82 to 24.0
CL15 vs LV141	22.3	8.8	Yes	***	11.2 to 33.5
CL15 vs LV142	31.7	12.5	Yes	***	20.6 to 42.8
CL15 vs LV143	9.22	3.63	No	ns	-1.89 to 20.3
CL15 vs LV144	12.2	4.81	Yes	**	1.10 to 23.3
CL15 vs LV145	1.66	0.654	No	ns	-9.45 to 12.8
CL15 vs LV146	41.8	16.5	Yes	***	30.7 to 52.9
CL15 vs LV161	16.4	6.45	Yes	***	5.27 to 27.5
CL15 vs LV163	8.17	3.22	No	ns	-2.94 to 19.3
CL15 vs LV162	35.1	13.8	Yes	***	24.0 to 46.2
CL15 vs LV164	33.3	13.1	Yes	***	22.2 to 44.4
CL15 vs LV165	24.9	9.81	Yes	***	13.8 to 36.0
CL15 vs LV167	15.7	6.17	Yes	***	4.56 to 26.8
CL15 vs LV168	29.7	11.7	Yes	***	18.6 to 40.9
CL15 vs LV176	-7.65	3.01	No	ns	-18.8 to 3.47
CL15 vs CV125(L)	-4.19	1.65	No	ns	-15.3 to 6.92
CL15 vs CV126(L)	21.2	8.36	Yes	***	10.1 to 32.4
CL15 vs CV130	1.53	0.604	No	ns	-9.58 to 12.6
CL15 vs LV180	10.6	4.17	No	ns	-0.519 to 21.7

CL15 vs LV183	11.8	4.63	Yes	*	0.647 to 22.9
CL16 vs CL17	-9.91	3.9	No	ns	-21.0 to 1.21
CL16 vs CL18	-41.7	16.4	Yes	***	-52.8 to -30.5
CL16 vs CL19	17.6	6.94	Yes	***	6.52 to 28.7
CL16 vs CL20	-46	18.1	Yes	***	-57.1 to -34.8
CL16 vs CL21	-52.8	20.8	Yes	***	-63.9 to -41.7
CL16 vs CL22	-52.8	20.8	Yes	***	-63.9 to -41.7
CL16 vs CL23	-52.9	20.8	Yes	***	-64.0 to -41.8
CL16 vs CL24	-25.6	10.1	Yes	***	-36.7 to -14.4
CL16 vs CL25	-24.6	9.69	Yes	***	-35.7 to -13.5
CL16 vs CL26	-79.7	31.4	Yes	***	-90.8 to -68.6
CL16 vs CL27	-26.8	10.5	Yes	***	-37.9 to -15.6
CL16 vs LCR54	-63.7	25.1	Yes	***	-74.8 to -52.6
CL16 vs LCR55	-3.65	1.44	No	ns	-14.8 to 7.46
CL16 vs LCR56	-17.1	6.72	Yes	***	-28.2 to -5.95
CL16 vs LCR57	-3.3	1.3	No	ns	-14.4 to 7.81
CL16 vs LCR58	-12.3	4.85	Yes	**	-23.4 to -1.20
CL16 vs LCR59	-17.4	6.87	Yes	***	-28.6 to -6.33
CL16 vs LCR60	-0.707	0.278	No	ns	-11.8 to 10.4
CL16 vs LCR63	-24.8	9.77	Yes	***	-35.9 to -13.7
CL16 vs LCR65	-15.4	6.05	Yes	***	-26.5 to -4.26
CL16 vs LCR66	-0.38	0.15	No	ns	-11.5 to 10.7
CL16 vs LCR67	13.9	5.48	Yes	***	2.80 to 25.0
CL16 vs LCR68	-1.56	0.614	No	ns	-12.7 to 9.55
CL16 vs LCR70	-16.6	6.56	Yes	***	-27.8 to -5.53
CL16 vs LCR43	-9.03	3.55	No	ns	-20.1 to 2.09
CL16 vs LCR64	-14.9	5.87	Yes	***	-26.0 to -3.79

CL16 vs LCR71	10.9	4.28	No	ns	-0.239 to 22.0
CL16 vs LCR72	-19.6	7.74	Yes	***	-30.8 to -8.53
CL16 vs LCR73	-16.8	6.62	Yes	***	-27.9 to -5.70
CL16 vs LCR74	0.04	0.0158	No	ns	-11.1 to 11.2
CL16 vs LCR75	-0.493	0.194	No	ns	-11.6 to 10.6
CL16 vs LCR76	-13.4	5.29	Yes	**	-24.5 to -2.32
CL16 vs LCR77	-11.9	4.7	Yes	*	-23.0 to -0.814
CL16 vs LCR78	-13.2	5.19	Yes	**	-24.3 to -2.07
CL16 vs LCR131	-28.5	11.2	Yes	***	-39.6 to -17.4
CL16 vs LCR135	-24.6	9.69	Yes	***	-35.7 to -13.5
CL16 vs LV134	-1.81	0.712	No	ns	-12.9 to 9.31
CL16 vs LV136	-2.02	0.796	No	ns	-13.1 to 9.09
CL16 vs LV138	5.25	2.07	No	ns	-5.86 to 16.4
CL16 vs LV139	-4.11	1.62	No	ns	-15.2 to 7.00
CL16 vs LV140	-6.03	2.38	No	ns	-17.1 to 5.08
CL16 vs LV141	3.38	1.33	No	ns	-7.73 to 14.5
CL16 vs LV142	12.7	5.01	Yes	**	1.60 to 23.8
CL16 vs LV143	-9.75	3.84	No	ns	-20.9 to 1.37
CL16 vs LV144	-6.75	2.66	No	ns	-17.9 to 4.36
CL16 vs LV145	-17.3	6.82	Yes	***	-28.4 to -6.19
CL16 vs LV146	22.8	8.99	Yes	***	11.7 to 34.0
CL16 vs LV161	-2.59	1.02	No	ns	-13.7 to 8.53
CL16 vs LV163	-10.8	4.25	No	ns	-21.9 to 0.319
CL16 vs LV162	16.2	6.36	Yes	***	5.04 to 27.3
CL16 vs LV164	14.3	5.65	Yes	***	3.23 to 25.5
CL16 vs LV165	5.94	2.34	No	ns	-5.17 to 17.1
CL16 vs LV167	-3.29	1.3	No	ns	-14.4 to 7.82

CL16 vs LV168	10.8	4.25	No	ns	-0.333 to 21.9
CL16 vs LV176	-26.6	10.5	Yes	***	-37.7 to -15.5
CL16 vs CV125(L)	-23.2	9.12	Yes	***	-34.3 to -12.0
CL16 vs CV126(L)	2.27	0.895	No	ns	-8.84 to 13.4
CL16 vs CV130	-17.4	6.87	Yes	***	-28.5 to -6.32
CL16 vs LV180	-8.37	3.3	No	ns	-19.5 to 2.74
CL16 vs LV183	-7.21	2.84	No	ns	-18.3 to 3.91
CL17 vs CL18	-31.7	12.5	Yes	***	-42.9 to -20.6
CL17 vs CL19	27.5	10.8	Yes	***	16.4 to 38.7
CL17 vs CL20	-36.1	14.2	Yes	***	-47.2 to -24.9
CL17 vs CL21	-42.9	16.9	Yes	***	-54.0 to -31.8
CL17 vs CL22	-42.9	16.9	Yes	***	-54.0 to -31.7
CL17 vs CL23	-43	16.9	Yes	***	-54.1 to -31.9
CL17 vs CL24	-15.7	6.16	Yes	***	-26.8 to -4.54
CL17 vs CL25	-14.7	5.79	Yes	***	-25.8 to -3.59
CL17 vs CL26	-69.8	27.5	Yes	***	-80.9 to -58.7
CL17 vs CL27	-16.8	6.63	Yes	***	-28.0 to -5.73
CL17 vs LCR54	-53.8	21.2	Yes	***	-64.9 to -42.7
CL17 vs LCR55	6.25	2.46	No	ns	-4.86 to 17.4
CL17 vs LCR56	-7.16	2.82	No	ns	-18.3 to 3.95
CL17 vs LCR57	6.61	2.6	No	ns	-4.51 to 17.7
CL17 vs LCR58	-2.41	0.948	No	ns	-13.5 to 8.71
CL17 vs LCR59	-7.54	2.97	No	ns	-18.7 to 3.57
CL17 vs LCR60	9.2	3.62	No	ns	-1.91 to 20.3
CL17 vs LCR63	-14.9	5.87	Yes	***	-26.0 to -3.80
CL17 vs LCR65	-5.47	2.15	No	ns	-16.6 to 5.65
CL17 vs LCR66	9.53	3.75	No	ns	-1.59 to 20.6

CL17 vs LCR67	23.8	9.38	Yes	***	12.7 to 34.9
CL17 vs LCR68	8.35	3.29	No	ns	-2.77 to 19.5
CL17 vs LCR70	-6.74	2.65	No	ns	-17.9 to 4.37
CL17 vs LCR43	0.88	0.347	No	ns	-10.2 to 12.0
CL17 vs LCR64	-5	1.97	No	ns	-16.1 to 6.11
CL17 vs LCR71	20.8	8.18	Yes	***	9.67 to 31.9
CL17 vs LCR72	-9.74	3.84	No	ns	-20.9 to 1.37
CL17 vs LCR73	-6.91	2.72	No	ns	-18.0 to 4.21
CL17 vs LCR74	9.95	3.92	No	ns	-1.17 to 21.1
CL17 vs LCR75	9.41	3.71	No	ns	-1.70 to 20.5
CL17 vs LCR76	-3.53	1.39	No	ns	-14.6 to 7.59
CL17 vs LCR77	-2.02	0.796	No	ns	-13.1 to 9.09
CL17 vs LCR78	-3.28	1.29	No	ns	-14.4 to 7.83
CL17 vs LCR131	-18.6	7.32	Yes	***	-29.7 to -7.47
CL17 vs LCR135	-14.7	5.79	Yes	***	-25.8 to -3.58
CL17 vs LV134	8.1	3.19	No	ns	-3.01 to 19.2
CL17 vs LV136	7.89	3.11	No	ns	-3.23 to 19.0
CL17 vs LV138	15.2	5.97	Yes	***	4.05 to 26.3
CL17 vs LV139	5.79	2.28	No	ns	-5.32 to 16.9
CL17 vs LV140	3.87	1.53	No	ns	-7.24 to 15.0
CL17 vs LV141	13.3	5.23	Yes	**	2.17 to 24.4
CL17 vs LV142	22.6	8.91	Yes	***	11.5 to 33.7
CL17 vs LV143	0.16	0.063	No	ns	-11.0 to 11.3
CL17 vs LV144	3.15	1.24	No	ns	-7.96 to 14.3
CL17 vs LV145	-7.4	2.91	No	ns	-18.5 to 3.71
CL17 vs LV146	32.7	12.9	Yes	***	21.6 to 43.9
CL17 vs LV161	7.32	2.88	No	ns	-3.79 to 18.4

CL17 vs LV163	-0.887	0.349	No	ns	-12.0 to 10.2
CL17 vs LV162	26.1	10.3	Yes	***	14.9 to 37.2
CL17 vs LV164	24.2	9.55	Yes	***	13.1 to 35.4
CL17 vs LV165	15.8	6.24	Yes	***	4.73 to 27.0
CL17 vs LV167	6.61	2.6	No	ns	-4.50 to 17.7
CL17 vs LV168	20.7	8.15	Yes	***	9.57 to 31.8
CL17 vs LV176	-16.7	6.58	Yes	***	-27.8 to -5.59
CL17 vs CV125(L)	-13.3	5.22	Yes	**	-24.4 to -2.14
CL17 vs CV126(L)	12.2	4.8	Yes	**	1.07 to 23.3
CL17 vs CV130	-7.53	2.96	No	ns	-18.6 to 3.59
CL17 vs LV180	1.53	0.604	No	ns	-9.58 to 12.6
CL17 vs LV183	2.7	1.06	No	ns	-8.41 to 13.8
CL18 vs CL19	59.3	23.3	Yes	***	48.2 to 70.4
CL18 vs CL20	-4.31	1.7	No	ns	-15.4 to 6.81
CL18 vs CL21	-11.2	4.39	Yes	*	-22.3 to -0.0406
CL18 vs CL22	-11.1	4.38	Yes	*	-22.2 to -0.000617
CL18 vs CL23	-11.3	4.43	Yes	*	-22.4 to -0.147
CL18 vs CL24	16.1	6.34	Yes	***	4.98 to 27.2
CL18 vs CL25	17	6.71	Yes	***	5.93 to 28.2
CL18 vs CL26	-38.1	15	Yes	***	-49.2 to -27.0
CL18 vs CL27	14.9	5.87	Yes	***	3.79 to 26.0
CL18 vs LCR54	-22	8.67	Yes	***	-33.1 to -10.9
CL18 vs LCR55	38	15	Yes	***	26.9 to 49.1
CL18 vs LCR56	24.6	9.68	Yes	***	13.5 to 35.7
CL18 vs LCR57	38.4	15.1	Yes	***	27.2 to 49.5
CL18 vs LCR58	29.3	11.6	Yes	***	18.2 to 40.5
CL18 vs LCR59	24.2	9.53	Yes	***	13.1 to 35.3

CL18 vs LCR60	40.9	16.1	Yes	***	29.8 to 52.1
CL18 vs LCR63	16.8	6.63	Yes	***	5.72 to 27.9
CL18 vs LCR65	26.3	10.3	Yes	***	15.2 to 37.4
CL18 vs LCR66	41.3	16.3	Yes	***	30.2 to 52.4
CL18 vs LCR67	55.6	21.9	Yes	***	44.5 to 66.7
CL18 vs LCR68	40.1	15.8	Yes	***	29.0 to 51.2
CL18 vs LCR70	25	9.85	Yes	***	13.9 to 36.1
CL18 vs LCR43	32.6	12.8	Yes	***	21.5 to 43.7
CL18 vs LCR64	26.7	10.5	Yes	***	15.6 to 37.9
CL18 vs LCR71	52.5	20.7	Yes	***	41.4 to 63.6
CL18 vs LCR72	22	8.67	Yes	***	10.9 to 33.1
CL18 vs LCR73	24.8	9.78	Yes	***	13.7 to 36.0
CL18 vs LCR74	41.7	16.4	Yes	***	30.6 to 52.8
CL18 vs LCR75	41.2	16.2	Yes	***	30.0 to 52.3
CL18 vs LCR76	28.2	11.1	Yes	***	17.1 to 39.3
CL18 vs LCR77	29.7	11.7	Yes	***	18.6 to 40.8
CL18 vs LCR78	28.5	11.2	Yes	***	17.4 to 39.6
CL18 vs LCR131	13.2	5.18	Yes	**	2.05 to 24.3
CL18 vs LCR135	17.1	6.72	Yes	***	5.94 to 28.2
CL18 vs LV134	39.8	15.7	Yes	***	28.7 to 51.0
CL18 vs LV136	39.6	15.6	Yes	***	28.5 to 50.7
CL18 vs LV138	46.9	18.5	Yes	***	35.8 to 58.0
CL18 vs LV139	37.5	14.8	Yes	***	26.4 to 48.7
CL18 vs LV140	35.6	14	Yes	***	24.5 to 46.7
CL18 vs LV141	45	17.7	Yes	***	33.9 to 56.1
CL18 vs LV142	54.4	21.4	Yes	***	43.3 to 65.5
CL18 vs LV143	31.9	12.6	Yes	***	20.8 to 43.0

CL18 vs LV144	34.9	13.7	Yes	***	23.8 to 46.0
CL18 vs LV145	24.3	9.59	Yes	***	13.2 to 35.5
CL18 vs LV146	64.5	25.4	Yes	***	53.4 to 75.6
CL18 vs LV161	39.1	15.4	Yes	***	28.0 to 50.2
CL18 vs LV163	30.9	12.2	Yes	***	19.7 to 42.0
CL18 vs LV162	57.8	22.8	Yes	***	46.7 to 68.9
CL18 vs LV164	56	22.1	Yes	***	44.9 to 67.1
CL18 vs LV165	47.6	18.7	Yes	***	36.5 to 58.7
CL18 vs LV167	38.4	15.1	Yes	***	27.2 to 49.5
CL18 vs LV168	52.4	20.6	Yes	***	41.3 to 63.5
CL18 vs LV176	15	5.92	Yes	***	3.93 to 26.2
CL18 vs CV125(L)	18.5	7.28	Yes	***	7.38 to 29.6
CL18 vs CV126(L)	43.9	17.3	Yes	***	32.8 to 55.0
CL18 vs CV130	24.2	9.54	Yes	***	13.1 to 35.3
CL18 vs LV180	33.3	13.1	Yes	***	22.2 to 44.4
CL18 vs LV183	34.4	13.6	Yes	***	23.3 to 45.6
CL19 vs CL20	-63.6	25	Yes	***	-74.7 to -52.5
CL19 vs CL21	-70.4	27.7	Yes	***	-81.6 to -59.3
CL19 vs CL22	-70.4	27.7	Yes	***	-81.5 to -59.3
CL19 vs CL23	-70.5	27.8	Yes	***	-81.7 to -59.4
CL19 vs CL24	-43.2	17	Yes	***	-54.3 to -32.1
CL19 vs CL25	-42.2	16.6	Yes	***	-53.4 to -31.1
CL19 vs CL26	-97.4	38.3	Yes	***	-108 to -86.2
CL19 vs CL27	-44.4	17.5	Yes	***	-55.5 to -33.3
CL19 vs LCR54	-81.3	32	Yes	***	-92.4 to -70.2
CL19 vs LCR55	-21.3	8.38	Yes	***	-32.4 to -10.2
CL19 vs LCR56	-34.7	13.7	Yes	***	-45.8 to -23.6

CL19 vs LCR57	-20.9	8.24	Yes	***	-32.0 to -9.82
CL19 vs LCR58	-29.9	11.8	Yes	***	-41.1 to -18.8
CL19 vs LCR59	-35.1	13.8	Yes	***	-46.2 to -24.0
CL19 vs LCR60	-18.3	7.22	Yes	***	-29.5 to -7.23
CL19 vs LCR63	-42.5	16.7	Yes	***	-53.6 to -31.3
CL19 vs LCR65	-33	13	Yes	***	-44.1 to -21.9
CL19 vs LCR66	-18	7.09	Yes	***	-29.1 to -6.90
CL19 vs LCR67	-3.72	1.47	No	ns	-14.8 to 7.39
CL19 vs LCR68	-19.2	7.56	Yes	***	-30.3 to -8.08
CL19 vs LCR70	-34.3	13.5	Yes	***	-45.4 to -23.2
CL19 vs LCR43	-26.7	10.5	Yes	***	-37.8 to -15.5
CL19 vs LCR64	-32.5	12.8	Yes	***	-43.7 to -21.4
CL19 vs LCR71	-6.76	2.66	No	ns	-17.9 to 4.35
CL19 vs LCR72	-37.3	14.7	Yes	***	-48.4 to -26.2
CL19 vs LCR73	-34.4	13.6	Yes	***	-45.6 to -23.3
CL19 vs LCR74	-17.6	6.93	Yes	***	-28.7 to -6.48
CL19 vs LCR75	-18.1	7.14	Yes	***	-29.2 to -7.01
CL19 vs LCR76	-31.1	12.2	Yes	***	-42.2 to -20.0
CL19 vs LCR77	-29.6	11.6	Yes	***	-40.7 to -18.4
CL19 vs LCR78	-30.8	12.1	Yes	***	-41.9 to -19.7
CL19 vs LCR131	-46.1	18.2	Yes	***	-57.2 to -35.0
CL19 vs LCR135	-42.2	16.6	Yes	***	-53.3 to -31.1
CL19 vs LV134	-19.4	7.66	Yes	***	-30.6 to -8.33
CL19 vs LV136	-19.7	7.74	Yes	***	-30.8 to -8.54
CL19 vs LV138	-12.4	4.88	Yes	**	-23.5 to -1.27
CL19 vs LV139	-21.7	8.56	Yes	***	-32.9 to -10.6
CL19 vs LV140	-23.7	9.32	Yes	***	-34.8 to -12.6

CL19 vs LV141	-14.3	5.61	Yes	***	-25.4 to -3.14
CL19 vs LV142	-4.92	1.94	No	ns	-16.0 to 6.19
CL19 vs LV143	-27.4	10.8	Yes	***	-38.5 to -16.3
CL19 vs LV144	-24.4	9.6	Yes	***	-35.5 to -13.3
CL19 vs LV145	-34.9	13.8	Yes	***	-46.1 to -23.8
CL19 vs LV146	5.21	2.05	No	ns	-5.91 to 16.3
CL19 vs LV161	-20.2	7.96	Yes	***	-31.3 to -9.11
CL19 vs LV163	-28.4	11.2	Yes	***	-39.5 to -17.3
CL19 vs LV162	-1.48	0.584	No	ns	-12.6 to 9.63
CL19 vs LV164	-3.29	1.3	No	ns	-14.4 to 7.82
CL19 vs LV165	-11.7	4.61	Yes	*	-22.8 to -0.581
CL19 vs LV167	-20.9	8.24	Yes	***	-32.0 to -9.81
CL19 vs LV168	-6.85	2.7	No	ns	-18.0 to 4.26
CL19 vs LV176	-44.2	17.4	Yes	***	-55.4 to -33.1
CL19 vs CV125(L)	-40.8	16.1	Yes	***	-51.9 to -29.7
CL19 vs CV126(L)	-15.4	6.05	Yes	***	-26.5 to -4.25
CL19 vs CV130	-35.1	13.8	Yes	***	-46.2 to -24.0
CL19 vs LV180	-26	10.2	Yes	***	-37.1 to -14.9
CL19 vs LV183	-24.8	9.78	Yes	***	-36.0 to -13.7
CL20 vs CL21	-6.85	2.7	No	ns	-18.0 to 4.27
CL20 vs CL22	-6.81	2.68	No	ns	-17.9 to 4.31
CL20 vs CL23	-6.95	2.74	No	ns	-18.1 to 4.16
CL20 vs CL24	20.4	8.03	Yes	***	9.29 to 31.5
CL20 vs CL25	21.4	8.41	Yes	***	10.2 to 32.5
CL20 vs CL26	-33.8	13.3	Yes	***	-44.9 to -22.6
CL20 vs CL27	19.2	7.56	Yes	***	8.09 to 30.3
CL20 vs LCR54	-17.7	6.98	Yes	***	-28.8 to -6.61

CL20 vs LCR55	42.3	16.7	Yes	***	31.2 to 53.4
CL20 vs LCR56	28.9	11.4	Yes	***	17.8 to 40.0
CL20 vs LCR57	42.7	16.8	Yes	***	31.5 to 53.8
CL20 vs LCR58	33.6	13.3	Yes	***	22.5 to 44.8
CL20 vs LCR59	28.5	11.2	Yes	***	17.4 to 39.6
CL20 vs LCR60	45.3	17.8	Yes	***	34.1 to 56.4
CL20 vs LCR63	21.1	8.33	Yes	***	10.0 to 32.3
CL20 vs LCR65	30.6	12	Yes	***	19.5 to 41.7
CL20 vs LCR66	45.6	18	Yes	***	34.5 to 56.7
CL20 vs LCR67	59.9	23.6	Yes	***	48.8 to 71.0
CL20 vs LCR68	44.4	17.5	Yes	***	33.3 to 55.5
CL20 vs LCR70	29.3	11.5	Yes	***	18.2 to 40.4
CL20 vs LCR43	36.9	14.5	Yes	***	25.8 to 48.0
CL20 vs LCR64	31.1	12.2	Yes	***	19.9 to 42.2
CL20 vs LCR71	56.8	22.4	Yes	***	45.7 to 67.9
CL20 vs LCR72	26.3	10.4	Yes	***	15.2 to 37.4
CL20 vs LCR73	29.1	11.5	Yes	***	18.0 to 40.3
CL20 vs LCR74	46	18.1	Yes	***	34.9 to 57.1
CL20 vs LCR75	45.5	17.9	Yes	***	34.4 to 56.6
CL20 vs LCR76	32.5	12.8	Yes	***	21.4 to 43.6
CL20 vs LCR77	34	13.4	Yes	***	22.9 to 45.1
CL20 vs LCR78	32.8	12.9	Yes	***	21.7 to 43.9
CL20 vs LCR131	17.5	6.88	Yes	***	6.35 to 28.6
CL20 vs LCR135	21.4	8.41	Yes	***	10.2 to 32.5
CL20 vs LV134	44.2	17.4	Yes	***	33.0 to 55.3
CL20 vs LV136	43.9	17.3	Yes	***	32.8 to 55.1
CL20 vs LV138	51.2	20.2	Yes	***	40.1 to 62.3

CL20 vs LV139	41.8	16.5	Yes	***	30.7 to 53.0
CL20 vs LV140	39.9	15.7	Yes	***	28.8 to 51.0
CL20 vs LV141	49.3	19.4	Yes	***	38.2 to 60.5
CL20 vs LV142	58.7	23.1	Yes	***	47.6 to 69.8
CL20 vs LV143	36.2	14.3	Yes	***	25.1 to 47.3
CL20 vs LV144	39.2	15.4	Yes	***	28.1 to 50.3
CL20 vs LV145	28.7	11.3	Yes	***	17.5 to 39.8
CL20 vs LV146	68.8	27.1	Yes	***	57.7 to 79.9
CL20 vs LV161	43.4	17.1	Yes	***	32.3 to 54.5
CL20 vs LV163	35.2	13.8	Yes	***	24.1 to 46.3
CL20 vs LV162	62.1	24.5	Yes	***	51.0 to 73.2
CL20 vs LV164	60.3	23.7	Yes	***	49.2 to 71.4
CL20 vs LV165	51.9	20.4	Yes	***	40.8 to 63.0
CL20 vs LV167	42.7	16.8	Yes	***	31.6 to 53.8
CL20 vs LV168	56.7	22.3	Yes	***	45.6 to 67.9
CL20 vs LV176	19.3	7.62	Yes	***	8.23 to 30.5
CL20 vs CV125(L)	22.8	8.98	Yes	***	11.7 to 33.9
CL20 vs CV126(L)	48.2	19	Yes	***	37.1 to 59.3
CL20 vs CV130	28.5	11.2	Yes	***	17.4 to 39.6
CL20 vs LV180	37.6	14.8	Yes	***	26.5 to 48.7
CL20 vs LV183	38.8	15.3	Yes	***	27.6 to 49.9
CL21 vs CL22	0.04	0.0158	No	ns	-11.1 to 11.2
CL21 vs CL23	-0.107	0.042	No	ns	-11.2 to 11.0
CL21 vs CL24	27.2	10.7	Yes	***	16.1 to 38.4
CL21 vs CL25	28.2	11.1	Yes	***	17.1 to 39.3
CL21 vs CL26	-26.9	10.6	Yes	***	-38.0 to -15.8
CL21 vs CL27	26.1	10.3	Yes	***	14.9 to 37.2

CL21 vs LCR54	-10.9	4.28	No	ns	-22.0 to 0.239
CL21 vs LCR55	49.2	19.4	Yes	***	38.0 to 60.3
CL21 vs LCR56	35.7	14.1	Yes	***	24.6 to 46.9
CL21 vs LCR57	49.5	19.5	Yes	***	38.4 to 60.6
CL21 vs LCR58	40.5	15.9	Yes	***	29.4 to 51.6
CL21 vs LCR59	35.4	13.9	Yes	***	24.2 to 46.5
CL21 vs LCR60	52.1	20.5	Yes	***	41.0 to 63.2
CL21 vs LCR63	28	11	Yes	***	16.9 to 39.1
CL21 vs LCR65	37.4	14.7	Yes	***	26.3 to 48.5
CL21 vs LCR66	52.4	20.6	Yes	***	41.3 to 63.5
CL21 vs LCR67	66.7	26.3	Yes	***	55.6 to 77.8
CL21 vs LCR68	51.2	20.2	Yes	***	40.1 to 62.4
CL21 vs LCR70	36.2	14.2	Yes	***	25.0 to 47.3
CL21 vs LCR43	43.8	17.2	Yes	***	32.7 to 54.9
CL21 vs LCR64	37.9	14.9	Yes	***	26.8 to 49.0
CL21 vs LCR71	63.7	25.1	Yes	***	52.6 to 74.8
CL21 vs LCR72	33.2	13.1	Yes	***	22.0 to 44.3
CL21 vs LCR73	36	14.2	Yes	***	24.9 to 47.1
CL21 vs LCR74	52.8	20.8	Yes	***	41.7 to 64.0
CL21 vs LCR75	52.3	20.6	Yes	***	41.2 to 63.4
CL21 vs LCR76	39.4	15.5	Yes	***	28.3 to 50.5
CL21 vs LCR77	40.9	16.1	Yes	***	29.8 to 52.0
CL21 vs LCR78	39.6	15.6	Yes	***	28.5 to 50.7
CL21 vs LCR131	24.3	9.58	Yes	***	13.2 to 35.4
CL21 vs LCR135	28.2	11.1	Yes	***	17.1 to 39.3
CL21 vs LV134	51	20.1	Yes	***	39.9 to 62.1
CL21 vs LV136	50.8	20	Yes	***	39.7 to 61.9

CL21 vs LV138	58.1	22.9	Yes	***	46.9 to 69.2
CL21 vs LV139	48.7	19.2	Yes	***	37.6 to 59.8
CL21 vs LV140	46.8	18.4	Yes	***	35.7 to 57.9
CL21 vs LV141	56.2	22.1	Yes	***	45.1 to 67.3
CL21 vs LV142	65.5	25.8	Yes	***	54.4 to 76.6
CL21 vs LV143	43.1	17	Yes	***	31.9 to 54.2
CL21 vs LV144	46.1	18.1	Yes	***	34.9 to 57.2
CL21 vs LV145	35.5	14	Yes	***	24.4 to 46.6
CL21 vs LV146	75.6	29.8	Yes	***	64.5 to 86.8
CL21 vs LV161	50.2	19.8	Yes	***	39.1 to 61.3
CL21 vs LV163	42	16.5	Yes	***	30.9 to 53.1
CL21 vs LV162	69	27.2	Yes	***	57.8 to 80.1
CL21 vs LV164	67.1	26.4	Yes	***	56.0 to 78.3
CL21 vs LV165	58.7	23.1	Yes	***	47.6 to 69.9
CL21 vs LV167	49.5	19.5	Yes	***	38.4 to 60.6
CL21 vs LV168	63.6	25	Yes	***	52.5 to 74.7
CL21 vs LV176	26.2	10.3	Yes	***	15.1 to 37.3
CL21 vs CV125(L)	29.6	11.7	Yes	***	18.5 to 40.8
CL21 vs CV126(L)	55.1	21.7	Yes	***	44.0 to 66.2
CL21 vs CV130	35.4	13.9	Yes	***	24.3 to 46.5
CL21 vs LV180	44.4	17.5	Yes	***	33.3 to 55.5
CL21 vs LV183	45.6	18	Yes	***	34.5 to 56.7
CL22 vs CL23	-0.147	0.0578	No	ns	-11.3 to 11.0
CL22 vs CL24	27.2	10.7	Yes	***	16.1 to 38.3
CL22 vs CL25	28.2	11.1	Yes	***	17.0 to 39.3
CL22 vs CL26	-27	10.6	Yes	***	-38.1 to -15.8
CL22 vs CL27	26	10.2	Yes	***	14.9 to 37.1

CL22 vs LCR54	-10.9	4.3	No	ns	-22.0 to 0.199
CL22 vs LCR55	49.1	19.3	Yes	***	38.0 to 60.2
CL22 vs LCR56	35.7	14.1	Yes	***	24.6 to 46.8
CL22 vs LCR57	49.5	19.5	Yes	***	38.4 to 60.6
CL22 vs LCR58	40.5	15.9	Yes	***	29.3 to 51.6
CL22 vs LCR59	35.3	13.9	Yes	***	24.2 to 46.4
CL22 vs LCR60	52.1	20.5	Yes	***	40.9 to 63.2
CL22 vs LCR63	27.9	11	Yes	***	16.8 to 39.1
CL22 vs LCR65	37.4	14.7	Yes	***	26.3 to 48.5
CL22 vs LCR66	52.4	20.6	Yes	***	41.3 to 63.5
CL22 vs LCR67	66.7	26.3	Yes	***	55.6 to 77.8
CL22 vs LCR68	51.2	20.2	Yes	***	40.1 to 62.3
CL22 vs LCR70	36.1	14.2	Yes	***	25.0 to 47.2
CL22 vs LCR43	43.7	17.2	Yes	***	32.6 to 54.9
CL22 vs LCR64	37.9	14.9	Yes	***	26.7 to 49.0
CL22 vs LCR71	63.6	25.1	Yes	***	52.5 to 74.8
CL22 vs LCR72	33.1	13	Yes	***	22.0 to 44.2
CL22 vs LCR73	36	14.2	Yes	***	24.8 to 47.1
CL22 vs LCR74	52.8	20.8	Yes	***	41.7 to 63.9
CL22 vs LCR75	52.3	20.6	Yes	***	41.2 to 63.4
CL22 vs LCR76	39.3	15.5	Yes	***	28.2 to 50.4
CL22 vs LCR77	40.8	16.1	Yes	***	29.7 to 52.0
CL22 vs LCR78	39.6	15.6	Yes	***	28.5 to 50.7
CL22 vs LCR131	24.3	9.56	Yes	***	13.2 to 35.4
CL22 vs LCR135	28.2	11.1	Yes	***	17.1 to 39.3
CL22 vs LV134	51	20.1	Yes	***	39.8 to 62.1
CL22 vs LV136	50.7	20	Yes	***	39.6 to 61.9

CL22 vs LV138	58	22.8	Yes	***	46.9 to 69.1
CL22 vs LV139	48.7	19.2	Yes	***	37.5 to 59.8
CL22 vs LV140	46.7	18.4	Yes	***	35.6 to 57.8
CL22 vs LV141	56.1	22.1	Yes	***	45.0 to 67.3
CL22 vs LV142	65.5	25.8	Yes	***	54.4 to 76.6
CL22 vs LV143	43	16.9	Yes	***	31.9 to 54.1
CL22 vs LV144	46	18.1	Yes	***	34.9 to 57.1
CL22 vs LV145	35.5	14	Yes	***	24.3 to 46.6
CL22 vs LV146	75.6	29.8	Yes	***	64.5 to 86.7
CL22 vs LV161	50.2	19.8	Yes	***	39.1 to 61.3
CL22 vs LV163	42	16.5	Yes	***	30.9 to 53.1
CL22 vs LV162	68.9	27.1	Yes	***	57.8 to 80.0
CL22 vs LV164	67.1	26.4	Yes	***	56.0 to 78.2
CL22 vs LV165	58.7	23.1	Yes	***	47.6 to 69.8
CL22 vs LV167	49.5	19.5	Yes	***	38.4 to 60.6
CL22 vs LV168	63.5	25	Yes	***	52.4 to 74.7
CL22 vs LV176	26.2	10.3	Yes	***	15.0 to 37.3
CL22 vs CV125(L)	29.6	11.7	Yes	***	18.5 to 40.7
CL22 vs CV126(L)	55	21.7	Yes	***	43.9 to 66.2
CL22 vs CV130	35.3	13.9	Yes	***	24.2 to 46.4
CL22 vs LV180	44.4	17.5	Yes	***	33.3 to 55.5
CL22 vs LV183	45.6	17.9	Yes	***	34.4 to 56.7
CL23 vs CL24	27.4	10.8	Yes	***	16.2 to 38.5
CL23 vs CL25	28.3	11.1	Yes	***	17.2 to 39.4
CL23 vs CL26	-26.8	10.6	Yes	***	-37.9 to -15.7
CL23 vs CL27	26.2	10.3	Yes	***	15.0 to 37.3
CL23 vs LCR54	-10.8	4.24	No	ns	-21.9 to 0.346

CL23 vs LCR55	49.3	19.4	Yes	***	38.1 to 60.4
CL23 vs LCR56	35.8	14.1	Yes	***	24.7 to 47.0
CL23 vs LCR57	49.6	19.5	Yes	***	38.5 to 60.7
CL23 vs LCR58	40.6	16	Yes	***	29.5 to 51.7
CL23 vs LCR59	35.5	14	Yes	***	24.4 to 46.6
CL23 vs LCR60	52.2	20.6	Yes	***	41.1 to 63.3
CL23 vs LCR63	28.1	11.1	Yes	***	17.0 to 39.2
CL23 vs LCR65	37.5	14.8	Yes	***	26.4 to 48.7
CL23 vs LCR66	52.5	20.7	Yes	***	41.4 to 63.6
CL23 vs LCR67	66.8	26.3	Yes	***	55.7 to 77.9
CL23 vs LCR68	51.4	20.2	Yes	***	40.2 to 62.5
CL23 vs LCR70	36.3	14.3	Yes	***	25.2 to 47.4
CL23 vs LCR43	43.9	17.3	Yes	***	32.8 to 55.0
CL23 vs LCR64	38	15	Yes	***	26.9 to 49.1
CL23 vs LCR71	63.8	25.1	Yes	***	52.7 to 74.9
CL23 vs LCR72	33.3	13.1	Yes	***	22.2 to 44.4
CL23 vs LCR73	36.1	14.2	Yes	***	25.0 to 47.2
CL23 vs LCR74	53	20.9	Yes	***	41.8 to 64.1
CL23 vs LCR75	52.4	20.6	Yes	***	41.3 to 63.5
CL23 vs LCR76	39.5	15.5	Yes	***	28.4 to 50.6
CL23 vs LCR77	41	16.1	Yes	***	29.9 to 52.1
CL23 vs LCR78	39.7	15.6	Yes	***	28.6 to 50.8
CL23 vs LCR131	24.4	9.62	Yes	***	13.3 to 35.5
CL23 vs LCR135	28.3	11.2	Yes	***	17.2 to 39.4
CL23 vs LV134	51.1	20.1	Yes	***	40.0 to 62.2
CL23 vs LV136	50.9	20	Yes	***	39.8 to 62.0
CL23 vs LV138	58.2	22.9	Yes	***	47.1 to 69.3

CL23 vs LV139	48.8	19.2	Yes	***	37.7 to 59.9
CL23 vs LV140	46.9	18.5	Yes	***	35.8 to 58.0
CL23 vs LV141	56.3	22.2	Yes	***	45.2 to 67.4
CL23 vs LV142	65.6	25.8	Yes	***	54.5 to 76.7
CL23 vs LV143	43.2	17	Yes	***	32.1 to 54.3
CL23 vs LV144	46.2	18.2	Yes	***	35.0 to 57.3
CL23 vs LV145	35.6	14	Yes	***	24.5 to 46.7
CL23 vs LV146	75.8	29.8	Yes	***	64.6 to 86.9
CL23 vs LV161	50.3	19.8	Yes	***	39.2 to 61.4
CL23 vs LV163	42.1	16.6	Yes	***	31.0 to 53.2
CL23 vs LV162	69.1	27.2	Yes	***	58.0 to 80.2
CL23 vs LV164	67.3	26.5	Yes	***	56.1 to 78.4
CL23 vs LV165	58.9	23.2	Yes	***	47.7 to 70.0
CL23 vs LV167	49.6	19.5	Yes	***	38.5 to 60.7
CL23 vs LV168	63.7	25.1	Yes	***	52.6 to 74.8
CL23 vs LV176	26.3	10.4	Yes	***	15.2 to 37.4
CL23 vs CV125(L)	29.8	11.7	Yes	***	18.6 to 40.9
CL23 vs CV126(L)	55.2	21.7	Yes	***	44.1 to 66.3
CL23 vs CV130	35.5	14	Yes	***	24.4 to 46.6
CL23 vs LV180	44.5	17.5	Yes	***	33.4 to 55.7
CL23 vs LV183	45.7	18	Yes	***	34.6 to 56.8
CL24 vs CL25	0.953	0.375	No	ns	-10.2 to 12.1
CL24 vs CL26	-54.2	21.3	Yes	***	-65.3 to -43.0
CL24 vs CL27	-1.19	0.47	No	ns	-12.3 to 9.92
CL24 vs LCR54	-38.1	15	Yes	***	-49.2 to -27.0
CL24 vs LCR55	21.9	8.63	Yes	***	10.8 to 33.0
CL24 vs LCR56	8.49	3.34	No	ns	-2.62 to 19.6

CL24 vs LCR57	22.3	8.77	Yes	***	11.1 to 33.4
CL24 vs LCR58	13.2	5.22	Yes	**	2.13 to 24.4
CL24 vs LCR59	8.11	3.2	No	ns	-3.00 to 19.2
CL24 vs LCR60	24.9	9.79	Yes	***	13.7 to 36.0
CL24 vs LCR63	0.74	0.291	No	ns	-10.4 to 11.9
CL24 vs LCR65	10.2	4.01	No	ns	-0.926 to 21.3
CL24 vs LCR66	25.2	9.92	Yes	***	14.1 to 36.3
CL24 vs LCR67	39.5	15.5	Yes	***	28.4 to 50.6
CL24 vs LCR68	24	9.45	Yes	***	12.9 to 35.1
CL24 vs LCR70	8.91	3.51	No	ns	-2.20 to 20.0
CL24 vs LCR43	16.5	6.51	Yes	***	5.42 to 27.6
CL24 vs LCR64	10.7	4.2	No	ns	-0.459 to 21.8
CL24 vs LCR71	36.4	14.3	Yes	***	25.3 to 47.5
CL24 vs LCR72	5.91	2.33	No	ns	-5.20 to 17.0
CL24 vs LCR73	8.75	3.44	No	ns	-2.37 to 19.9
CL24 vs LCR74	25.6	10.1	Yes	***	14.5 to 36.7
CL24 vs LCR75	25.1	9.87	Yes	***	14.0 to 36.2
CL24 vs LCR76	12.1	4.78	Yes	**	1.01 to 23.2
CL24 vs LCR77	13.6	5.37	Yes	***	2.52 to 24.7
CL24 vs LCR78	12.4	4.87	Yes	**	1.26 to 23.5
CL24 vs LCR131	-2.93	1.16	No	ns	-14.0 to 8.18
CL24 vs LCR135	0.96	0.378	No	ns	-10.2 to 12.1
CL24 vs LV134	23.8	9.35	Yes	***	12.6 to 34.9
CL24 vs LV136	23.5	9.27	Yes	***	12.4 to 34.7
CL24 vs LV138	30.8	12.1	Yes	***	19.7 to 41.9
CL24 vs LV139	21.4	8.45	Yes	***	10.3 to 32.6
CL24 vs LV140	19.5	7.69	Yes	***	8.41 to 30.6

CL24 vs LV141	28.9	11.4	Yes	***	17.8 to 40.1
CL24 vs LV142	38.3	15.1	Yes	***	27.2 to 49.4
CL24 vs LV143	15.8	6.23	Yes	***	4.70 to 26.9
CL24 vs LV144	18.8	7.41	Yes	***	7.69 to 29.9
CL24 vs LV145	8.25	3.25	No	ns	-2.86 to 19.4
CL24 vs LV146	48.4	19.1	Yes	***	37.3 to 59.5
CL24 vs LV161	23	9.05	Yes	***	11.9 to 34.1
CL24 vs LV163	14.8	5.82	Yes	***	3.65 to 25.9
CL24 vs LV162	41.7	16.4	Yes	***	30.6 to 52.8
CL24 vs LV164	39.9	15.7	Yes	***	28.8 to 51.0
CL24 vs LV165	31.5	12.4	Yes	***	20.4 to 42.6
CL24 vs LV167	22.3	8.77	Yes	***	11.2 to 33.4
CL24 vs LV168	36.3	14.3	Yes	***	25.2 to 47.5
CL24 vs LV176	-1.05	0.415	No	ns	-12.2 to 10.1
CL24 vs CV125(L)	2.4	0.945	No	ns	-8.71 to 13.5
CL24 vs CV126(L)	27.8	11	Yes	***	16.7 to 38.9
CL24 vs CV130	8.13	3.2	No	ns	-2.99 to 19.2
CL24 vs LV180	17.2	6.77	Yes	***	6.07 to 28.3
CL24 vs LV183	18.4	7.23	Yes	***	7.24 to 29.5
CL25 vs CL26	-55.1	21.7	Yes	***	-66.2 to -44.0
CL25 vs CL27	-2.15	0.845	No	ns	-13.3 to 8.97
CL25 vs LCR54	-39.1	15.4	Yes	***	-50.2 to -28.0
CL25 vs LCR55	21	8.25	Yes	***	9.84 to 32.1
CL25 vs LCR56	7.54	2.97	No	ns	-3.57 to 18.7
CL25 vs LCR57	21.3	8.39	Yes	***	10.2 to 32.4
CL25 vs LCR58	12.3	4.84	Yes	**	1.18 to 23.4
CL25 vs LCR59	7.16	2.82	No	ns	-3.95 to 18.3

CL25 vs LCR60	23.9	9.41	Yes	***	12.8 to 35.0
CL25 vs LCR63	-0.213	0.084	No	ns	-11.3 to 10.9
CL25 vs LCR65	9.23	3.64	No	ns	-1.88 to 20.3
CL25 vs LCR66	24.2	9.54	Yes	***	13.1 to 35.3
CL25 vs LCR67	38.5	15.2	Yes	***	27.4 to 49.6
CL25 vs LCR68	23	9.08	Yes	***	11.9 to 34.2
CL25 vs LCR70	7.96	3.13	No	ns	-3.15 to 19.1
CL25 vs LCR43	15.6	6.14	Yes	***	4.47 to 26.7
CL25 vs LCR64	9.7	3.82	No	ns	-1.41 to 20.8
CL25 vs LCR71	35.5	14	Yes	***	24.4 to 46.6
CL25 vs LCR72	4.96	1.95	No	ns	-6.15 to 16.1
CL25 vs LCR73	7.79	3.07	No	ns	-3.32 to 18.9
CL25 vs LCR74	24.6	9.71	Yes	***	13.5 to 35.8
CL25 vs LCR75	24.1	9.5	Yes	***	13.0 to 35.2
CL25 vs LCR76	11.2	4.4	Yes	*	0.0606 to 22.3
CL25 vs LCR77	12.7	4.99	Yes	**	1.57 to 23.8
CL25 vs LCR78	11.4	4.5	Yes	*	0.307 to 22.5
CL25 vs LCR131	-3.89	1.53	No	ns	-15.0 to 7.23
CL25 vs LCR135	0.00667	0.00263	No	ns	-11.1 to 11.1
CL25 vs LV134	22.8	8.98	Yes	***	11.7 to 33.9
CL25 vs LV136	22.6	8.9	Yes	***	11.5 to 33.7
CL25 vs LV138	29.9	11.8	Yes	***	18.7 to 41.0
CL25 vs LV139	20.5	8.07	Yes	***	9.38 to 31.6
CL25 vs LV140	18.6	7.31	Yes	***	7.46 to 29.7
CL25 vs LV141	28	11	Yes	***	16.9 to 39.1
CL25 vs LV142	37.3	14.7	Yes	***	26.2 to 48.4
CL25 vs LV143	14.9	5.85	Yes	***	3.75 to 26.0

CL25 vs LV144	17.9	7.03	Yes	***	6.74 to 29.0
CL25 vs LV145	7.3	2.87	No	ns	-3.81 to 18.4
CL25 vs LV146	47.4	18.7	Yes	***	36.3 to 58.6
CL25 vs LV161	22	8.67	Yes	***	10.9 to 33.1
CL25 vs LV163	13.8	5.44	Yes	***	2.70 to 24.9
CL25 vs LV162	40.8	16.1	Yes	***	29.6 to 51.9
CL25 vs LV164	38.9	15.3	Yes	***	27.8 to 50.1
CL25 vs LV165	30.5	12	Yes	***	19.4 to 41.7
CL25 vs LV167	21.3	8.39	Yes	***	10.2 to 32.4
CL25 vs LV168	35.4	13.9	Yes	***	24.3 to 46.5
CL25 vs LV176	-2.01	0.79	No	ns	-13.1 to 9.11
CL25 vs CV125(L)	1.45	0.57	No	ns	-9.67 to 12.6
CL25 vs CV126(L)	26.9	10.6	Yes	***	15.8 to 38.0
CL25 vs CV130	7.17	2.83	No	ns	-3.94 to 18.3
CL25 vs LV180	16.2	6.39	Yes	***	5.12 to 27.3
CL25 vs LV183	17.4	6.85	Yes	***	6.29 to 28.5
CL26 vs CL27	53	20.9	Yes	***	41.9 to 64.1
CL26 vs LCR54	16	6.32	Yes	***	4.93 to 27.2
CL26 vs LCR55	76.1	30	Yes	***	65.0 to 87.2
CL26 vs LCR56	62.7	24.7	Yes	***	51.5 to 73.8
CL26 vs LCR57	76.4	30.1	Yes	***	65.3 to 87.5
CL26 vs LCR58	67.4	26.5	Yes	***	56.3 to 78.5
CL26 vs LCR59	62.3	24.5	Yes	***	51.2 to 73.4
CL26 vs LCR60	79	31.1	Yes	***	67.9 to 90.1
CL26 vs LCR63	54.9	21.6	Yes	***	43.8 to 66.0
CL26 vs LCR65	64.3	25.3	Yes	***	53.2 to 75.5
CL26 vs LCR66	79.3	31.2	Yes	***	68.2 to 90.5

CL26 vs LCR67	93.6	36.9	Yes	***	82.5 to 105
CL26 vs LCR68	78.2	30.8	Yes	***	67.0 to 89.3
CL26 vs LCR70	63.1	24.8	Yes	***	52.0 to 74.2
CL26 vs LCR43	70.7	27.8	Yes	***	59.6 to 81.8
CL26 vs LCR64	64.8	25.5	Yes	***	53.7 to 75.9
CL26 vs LCR71	90.6	35.7	Yes	***	79.5 to 102
CL26 vs LCR72	60.1	23.7	Yes	***	49.0 to 71.2
CL26 vs LCR73	62.9	24.8	Yes	***	51.8 to 74.0
CL26 vs LCR74	79.8	31.4	Yes	***	68.6 to 90.9
CL26 vs LCR75	79.2	31.2	Yes	***	68.1 to 90.3
CL26 vs LCR76	66.3	26.1	Yes	***	55.2 to 77.4
CL26 vs LCR77	67.8	26.7	Yes	***	56.7 to 78.9
CL26 vs LCR78	66.5	26.2	Yes	***	55.4 to 77.6
CL26 vs LCR131	51.2	20.2	Yes	***	40.1 to 62.3
CL26 vs LCR135	55.1	21.7	Yes	***	44.0 to 66.2
CL26 vs LV134	77.9	30.7	Yes	***	66.8 to 89.0
CL26 vs LV136	77.7	30.6	Yes	***	66.6 to 88.8
CL26 vs LV138	85	33.5	Yes	***	73.9 to 96.1
CL26 vs LV139	75.6	29.8	Yes	***	64.5 to 86.7
CL26 vs LV140	73.7	29	Yes	***	62.6 to 84.8
CL26 vs LV141	83.1	32.7	Yes	***	72.0 to 94.2
CL26 vs LV142	92.4	36.4	Yes	***	81.3 to 104
CL26 vs LV143	70	27.6	Yes	***	58.9 to 81.1
CL26 vs LV144	73	28.7	Yes	***	61.9 to 84.1
CL26 vs LV145	62.4	24.6	Yes	***	51.3 to 73.5
CL26 vs LV146	103	40.4	Yes	***	91.4 to 114
CL26 vs LV161	77.1	30.4	Yes	***	66.0 to 88.2

CL26 vs LV163	68.9	27.1	Yes	***	57.8 to 80.0
CL26 vs LV162	95.9	37.8	Yes	***	84.8 to 107
CL26 vs LV164	94.1	37	Yes	***	82.9 to 105
CL26 vs LV165	85.7	33.7	Yes	***	74.5 to 96.8
CL26 vs LV167	76.4	30.1	Yes	***	65.3 to 87.5
CL26 vs LV168	90.5	35.6	Yes	***	79.4 to 102
CL26 vs LV176	53.1	20.9	Yes	***	42.0 to 64.2
CL26 vs CV125(L)	56.6	22.3	Yes	***	45.4 to 67.7
CL26 vs CV126(L)	82	32.3	Yes	***	70.9 to 93.1
CL26 vs CV130	62.3	24.5	Yes	***	51.2 to 73.4
CL26 vs LV180	71.3	28.1	Yes	***	60.2 to 82.5
CL26 vs LV183	72.5	28.6	Yes	***	61.4 to 83.6
CL27 vs LCR54	-36.9	14.5	Yes	***	-48.0 to -25.8
CL27 vs LCR55	23.1	9.1	Yes	***	12.0 to 34.2
CL27 vs LCR56	9.69	3.81	No	ns	-1.43 to 20.8
CL27 vs LCR57	23.5	9.24	Yes	***	12.3 to 34.6
CL27 vs LCR58	14.4	5.69	Yes	***	3.33 to 25.6
CL27 vs LCR59	9.31	3.67	No	ns	-1.81 to 20.4
CL27 vs LCR60	26	10.3	Yes	***	14.9 to 37.2
CL27 vs LCR63	1.93	0.761	No	ns	-9.18 to 13.0
CL27 vs LCR65	11.4	4.48	Yes	*	0.267 to 22.5
CL27 vs LCR66	26.4	10.4	Yes	***	15.3 to 37.5
CL27 vs LCR67	40.7	16	Yes	***	29.6 to 51.8
CL27 vs LCR68	25.2	9.92	Yes	***	14.1 to 36.3
CL27 vs LCR70	10.1	3.98	No	ns	-1.01 to 21.2
CL27 vs LCR43	17.7	6.98	Yes	***	6.61 to 28.8
CL27 vs LCR64	11.8	4.67	Yes	*	0.734 to 23.0

CL27 vs LCR71	37.6	14.8	Yes	***	26.5 to 48.7
CL27 vs LCR72	7.11	2.8	No	ns	-4.01 to 18.2
CL27 vs LCR73	9.94	3.91	No	ns	-1.17 to 21.1
CL27 vs LCR74	26.8	10.6	Yes	***	15.7 to 37.9
CL27 vs LCR75	26.3	10.3	Yes	***	15.1 to 37.4
CL27 vs LCR76	13.3	5.25	Yes	**	2.21 to 24.4
CL27 vs LCR77	14.8	5.84	Yes	***	3.71 to 25.9
CL27 vs LCR78	13.6	5.34	Yes	***	2.45 to 24.7
CL27 vs LCR131	-1.74	0.685	No	ns	-12.9 to 9.37
CL27 vs LCR135	2.15	0.848	No	ns	-8.96 to 13.3
CL27 vs LV134	24.9	9.82	Yes	***	13.8 to 36.1
CL27 vs LV136	24.7	9.74	Yes	***	13.6 to 35.8
CL27 vs LV138	32	12.6	Yes	***	20.9 to 43.1
CL27 vs LV139	22.6	8.92	Yes	***	11.5 to 33.8
CL27 vs LV140	20.7	8.16	Yes	***	9.61 to 31.8
CL27 vs LV141	30.1	11.9	Yes	***	19.0 to 41.2
CL27 vs LV142	39.5	15.5	Yes	***	28.4 to 50.6
CL27 vs LV143	17	6.7	Yes	***	5.89 to 28.1
CL27 vs LV144	20	7.88	Yes	***	8.89 to 31.1
CL27 vs LV145	9.45	3.72	No	ns	-1.67 to 20.6
CL27 vs LV146	49.6	19.5	Yes	***	38.5 to 60.7
CL27 vs LV161	24.2	9.52	Yes	***	13.1 to 35.3
CL27 vs LV163	16	6.29	Yes	***	4.85 to 27.1
CL27 vs LV162	42.9	16.9	Yes	***	31.8 to 54.0
CL27 vs LV164	41.1	16.2	Yes	***	30.0 to 52.2
CL27 vs LV165	32.7	12.9	Yes	***	21.6 to 43.8
CL27 vs LV167	23.5	9.24	Yes	***	12.3 to 34.6

CL27 vs LV168	37.5	14.8	Yes	***	26.4 to 48.6
CL27 vs LV176	0.14	0.0551	No	ns	-11.0 to 11.3
CL27 vs CV125(L)	3.59	1.42	No	ns	-7.52 to 14.7
CL27 vs CV126(L)	29	11.4	Yes	***	17.9 to 40.1
CL27 vs CV130	9.32	3.67	No	ns	-1.79 to 20.4
CL27 vs LV180	18.4	7.24	Yes	***	7.27 to 29.5
CL27 vs LV183	19.5	7.7	Yes	***	8.43 to 30.7
LCR54 vs LCR55	60	23.6	Yes	***	48.9 to 71.1
LCR54 vs LCR56	46.6	18.4	Yes	***	35.5 to 57.7
LCR54 vs LCR57	60.4	23.8	Yes	***	49.3 to 71.5
LCR54 vs LCR58	51.4	20.2	Yes	***	40.3 to 62.5
LCR54 vs LCR59	46.2	18.2	Yes	***	35.1 to 57.3
LCR54 vs LCR60	63	24.8	Yes	***	51.9 to 74.1
LCR54 vs LCR63	38.9	15.3	Yes	***	27.7 to 50.0
LCR54 vs LCR65	48.3	19	Yes	***	37.2 to 59.4
LCR54 vs LCR66	63.3	24.9	Yes	***	52.2 to 74.4
LCR54 vs LCR67	77.6	30.6	Yes	***	66.5 to 88.7
LCR54 vs LCR68	62.1	24.5	Yes	***	51.0 to 73.2
LCR54 vs LCR70	47	18.5	Yes	***	35.9 to 58.1
LCR54 vs LCR43	54.7	21.5	Yes	***	43.5 to 65.8
LCR54 vs LCR64	48.8	19.2	Yes	***	37.7 to 59.9
LCR54 vs LCR71	74.6	29.4	Yes	***	63.4 to 85.7
LCR54 vs LCR72	44	17.3	Yes	***	32.9 to 55.1
LCR54 vs LCR73	46.9	18.5	Yes	***	35.8 to 58.0
LCR54 vs LCR74	63.7	25.1	Yes	***	52.6 to 74.8
LCR54 vs LCR75	63.2	24.9	Yes	***	52.1 to 74.3
LCR54 vs LCR76	50.2	19.8	Yes	***	39.1 to 61.4

LCR54 vs LCR77	51.8	20.4	Yes	***	40.6 to 62.9
LCR54 vs LCR78	50.5	19.9	Yes	***	39.4 to 61.6
LCR54 vs LCR131	35.2	13.9	Yes	***	24.1 to 46.3
LCR54 vs LCR135	39.1	15.4	Yes	***	28.0 to 50.2
LCR54 vs LV134	61.9	24.4	Yes	***	50.8 to 73.0
LCR54 vs LV136	61.7	24.3	Yes	***	50.5 to 72.8
LCR54 vs LV138	68.9	27.1	Yes	***	57.8 to 80.0
LCR54 vs LV139	59.6	23.5	Yes	***	48.5 to 70.7
LCR54 vs LV140	57.6	22.7	Yes	***	46.5 to 68.8
LCR54 vs LV141	67.1	26.4	Yes	***	55.9 to 78.2
LCR54 vs LV142	76.4	30.1	Yes	***	65.3 to 87.5
LCR54 vs LV143	53.9	21.2	Yes	***	42.8 to 65.0
LCR54 vs LV144	56.9	22.4	Yes	***	45.8 to 68.0
LCR54 vs LV145	46.4	18.3	Yes	***	35.3 to 57.5
LCR54 vs LV146	86.5	34.1	Yes	***	75.4 to 97.6
LCR54 vs LV161	61.1	24.1	Yes	***	50.0 to 72.2
LCR54 vs LV163	52.9	20.8	Yes	***	41.8 to 64.0
LCR54 vs LV162	79.8	31.4	Yes	***	68.7 to 90.9
LCR54 vs LV164	78	30.7	Yes	***	66.9 to 89.1
LCR54 vs LV165	69.6	27.4	Yes	***	58.5 to 80.7
LCR54 vs LV167	60.4	23.8	Yes	***	49.3 to 71.5
LCR54 vs LV168	74.5	29.3	Yes	***	63.3 to 85.6
LCR54 vs LV176	37.1	14.6	Yes	***	26.0 to 48.2
LCR54 vs CV125(L)	40.5	16	Yes	***	29.4 to 51.6
LCR54 vs CV126(L)	66	26	Yes	***	54.8 to 77.1
LCR54 vs CV130	46.2	18.2	Yes	***	35.1 to 57.4
LCR54 vs LV180	55.3	21.8	Yes	***	44.2 to 66.4

LCR54 vs LV183	56.5	22.2	Yes	***	45.4 to 67.6
LCR55 vs LCR56	-13.4	5.28	Yes	**	-24.5 to -2.30
LCR55 vs LCR57	0.353	0.139	No	ns	-10.8 to 11.5
LCR55 vs LCR58	-8.66	3.41	No	ns	-19.8 to 2.45
LCR55 vs LCR59	-13.8	5.43	Yes	***	-24.9 to -2.68
LCR55 vs LCR60	2.95	1.16	No	ns	-8.17 to 14.1
LCR55 vs LCR63	-21.2	8.34	Yes	***	-32.3 to -10.1
LCR55 vs LCR65	-11.7	4.62	Yes	*	-22.8 to -0.607
LCR55 vs LCR66	3.27	1.29	No	ns	-7.84 to 14.4
LCR55 vs LCR67	17.6	6.92	Yes	***	6.45 to 28.7
LCR55 vs LCR68	2.09	0.824	No	ns	-9.02 to 13.2
LCR55 vs LCR70	-13	5.12	Yes	**	-24.1 to -1.88
LCR55 vs LCR43	-5.37	2.12	No	ns	-16.5 to 5.74
LCR55 vs LCR64	-11.3	4.43	Yes	*	-22.4 to -0.141
LCR55 vs LCR71	14.5	5.72	Yes	***	3.41 to 25.6
LCR55 vs LCR72	-16	6.3	Yes	***	-27.1 to -4.88
LCR55 vs LCR73	-13.2	5.18	Yes	**	-24.3 to -2.05
LCR55 vs LCR74	3.69	1.45	No	ns	-7.42 to 14.8
LCR55 vs LCR75	3.16	1.24	No	ns	-7.95 to 14.3
LCR55 vs LCR76	-9.78	3.85	No	ns	-20.9 to 1.33
LCR55 vs LCR77	-8.27	3.26	No	ns	-19.4 to 2.84
LCR55 vs LCR78	-9.53	3.75	No	ns	-20.6 to 1.58
LCR55 vs LCR131	-24.8	9.78	Yes	***	-36.0 to -13.7
LCR55 vs LCR135	-20.9	8.25	Yes	***	-32.1 to -9.83
LCR55 vs LV134	1.85	0.727	No	ns	-9.27 to 13.0
LCR55 vs LV136	1.63	0.643	No	ns	-9.48 to 12.7
LCR55 vs LV138	8.91	3.51	No	ns	-2.21 to 20.0

LCR55 vs LV139	-0.46	0.181	No	ns	-11.6 to 10.7
LCR55 vs LV140	-2.38	0.937	No	ns	-13.5 to 8.73
LCR55 vs LV141	7.03	2.77	No	ns	-4.08 to 18.1
LCR55 vs LV142	16.4	6.45	Yes	***	5.25 to 27.5
LCR55 vs LV143	-6.09	2.4	No	ns	-17.2 to 5.02
LCR55 vs LV144	-3.1	1.22	No	ns	-14.2 to 8.01
LCR55 vs LV145	-13.7	5.38	Yes	***	-24.8 to -2.54
LCR55 vs LV146	26.5	10.4	Yes	***	15.4 to 37.6
LCR55 vs LV161	1.07	0.42	No	ns	-10.0 to 12.2
LCR55 vs LV163	-7.14	2.81	No	ns	-18.3 to 3.97
LCR55 vs LV162	19.8	7.8	Yes	***	8.69 to 30.9
LCR55 vs LV164	18	7.09	Yes	***	6.88 to 29.1
LCR55 vs LV165	9.59	3.78	No	ns	-1.52 to 20.7
LCR55 vs LV167	0.36	0.142	No	ns	-10.8 to 11.5
LCR55 vs LV168	14.4	5.68	Yes	***	3.32 to 25.5
LCR55 vs LV176	-23	9.04	Yes	***	-34.1 to -11.8
LCR55 vs CV125(L)	-19.5	7.68	Yes	***	-30.6 to -8.39
LCR55 vs CV126(L)	5.93	2.33	No	ns	-5.19 to 17.0
LCR55 vs CV130	-13.8	5.43	Yes	***	-24.9 to -2.67
LCR55 vs LV180	-4.72	1.86	No	ns	-15.8 to 6.39
LCR55 vs LV183	-3.55	1.4	No	ns	-14.7 to 7.56
LCR56 vs LCR57	13.8	5.42	Yes	***	2.65 to 24.9
LCR56 vs LCR58	4.75	1.87	No	ns	-6.36 to 15.9
LCR56 vs LCR59	-0.38	0.15	No	ns	-11.5 to 10.7
LCR56 vs LCR60	16.4	6.44	Yes	***	5.25 to 27.5
LCR56 vs LCR63	-7.75	3.05	No	ns	-18.9 to 3.36
LCR56 vs LCR65	1.69	0.667	No	ns	-9.42 to 12.8

LCR56 vs LCR66	16.7	6.57	Yes	***	5.57 to 27.8
LCR56 vs LCR67	31	12.2	Yes	***	19.9 to 42.1
LCR56 vs LCR68	15.5	6.11	Yes	***	4.39 to 26.6
LCR56 vs LCR70	0.42	0.165	No	ns	-10.7 to 11.5
LCR56 vs LCR43	8.04	3.17	No	ns	-3.07 to 19.2
LCR56 vs LCR64	2.16	0.851	No	ns	-8.95 to 13.3
LCR56 vs LCR71	27.9	11	Yes	***	16.8 to 39.1
LCR56 vs LCR72	-2.58	1.02	No	ns	-13.7 to 8.53
LCR56 vs LCR73	0.253	0.0998	No	ns	-10.9 to 11.4
LCR56 vs LCR74	17.1	6.74	Yes	***	5.99 to 28.2
LCR56 vs LCR75	16.6	6.53	Yes	***	5.46 to 27.7
LCR56 vs LCR76	3.63	1.43	No	ns	-7.48 to 14.7
LCR56 vs LCR77	5.14	2.02	No	ns	-5.97 to 16.3
LCR56 vs LCR78	3.88	1.53	No	ns	-7.23 to 15.0
LCR56 vs LCR131	-11.4	4.5	Yes	*	-22.5 to -0.314
LCR56 vs LCR135	-7.53	2.97	No	ns	-18.6 to 3.58
LCR56 vs LV134	15.3	6.01	Yes	***	4.15 to 26.4
LCR56 vs LV136	15	5.93	Yes	***	3.93 to 26.2
LCR56 vs LV138	22.3	8.79	Yes	***	11.2 to 33.4
LCR56 vs LV139	13	5.1	Yes	**	1.84 to 24.1
LCR56 vs LV140	11	4.35	No	ns	-0.0794 to 22.1
LCR56 vs LV141	20.4	8.05	Yes	***	9.33 to 31.6
LCR56 vs LV142	29.8	11.7	Yes	***	18.7 to 40.9
LCR56 vs LV143	7.32	2.88	No	ns	-3.79 to 18.4
LCR56 vs LV144	10.3	4.06	No	ns	-0.799 to 21.4
LCR56 vs LV145	-0.24	0.0945	No	ns	-11.4 to 10.9
LCR56 vs LV146	39.9	15.7	Yes	***	28.8 to 51.0

LCR56 vs LV161	14.5	5.7	Yes	***	3.37 to 25.6
LCR56 vs LV163	6.27	2.47	No	ns	-4.84 to 17.4
LCR56 vs LV162	33.2	13.1	Yes	***	22.1 to 44.3
LCR56 vs LV164	31.4	12.4	Yes	***	20.3 to 42.5
LCR56 vs LV165	23	9.06	Yes	***	11.9 to 34.1
LCR56 vs LV167	13.8	5.42	Yes	***	2.66 to 24.9
LCR56 vs LV168	27.8	11	Yes	***	16.7 to 39.0
LCR56 vs LV176	-9.55	3.76	No	ns	-20.7 to 1.57
LCR56 vs CV125(L)	-6.09	2.4	No	ns	-17.2 to 5.02
LCR56 vs CV126(L)	19.3	7.62	Yes	***	8.23 to 30.5
LCR56 vs CV130	-0.367	0.144	No	ns	-11.5 to 10.7
LCR56 vs LV180	8.69	3.42	No	ns	-2.42 to 19.8
LCR56 vs LV183	9.86	3.88	No	ns	-1.25 to 21.0
LCR57 vs LCR58	-9.01	3.55	No	ns	-20.1 to 2.10
LCR57 vs LCR59	-14.1	5.57	Yes	***	-25.3 to -3.03
LCR57 vs LCR60	2.59	1.02	No	ns	-8.52 to 13.7
LCR57 vs LCR63	-21.5	8.48	Yes	***	-32.6 to -10.4
LCR57 vs LCR65	-12.1	4.75	Yes	*	-23.2 to -0.961
LCR57 vs LCR66	2.92	1.15	No	ns	-8.19 to 14.0
LCR57 vs LCR67	17.2	6.78	Yes	***	6.10 to 28.3
LCR57 vs LCR68	1.74	0.685	No	ns	-9.37 to 12.9
LCR57 vs LCR70	-13.3	5.26	Yes	**	-24.5 to -2.23
LCR57 vs LCR43	-5.73	2.26	No	ns	-16.8 to 5.39
LCR57 vs LCR64	-11.6	4.57	Yes	*	-22.7 to -0.494
LCR57 vs LCR71	14.2	5.58	Yes	***	3.06 to 25.3
LCR57 vs LCR72	-16.3	6.44	Yes	***	-27.5 to -5.23
LCR57 vs LCR73	-13.5	5.32	Yes	***	-24.6 to -2.40

LCR57 vs LCR74	3.34	1.32	No	ns	-7.77 to 14.5
LCR57 vs LCR75	2.81	1.11	No	ns	-8.31 to 13.9
LCR57 vs LCR76	-10.1	3.99	No	ns	-21.2 to 0.979
LCR57 vs LCR77	-8.63	3.4	No	ns	-19.7 to 2.49
LCR57 vs LCR78	-9.89	3.89	No	ns	-21.0 to 1.23
LCR57 vs LCR131	-25.2	9.92	Yes	***	-36.3 to -14.1
LCR57 vs LCR135	-21.3	8.39	Yes	***	-32.4 to -10.2
LCR57 vs LV134	1.49	0.588	No	ns	-9.62 to 12.6
LCR57 vs LV136	1.28	0.504	No	ns	-9.83 to 12.4
LCR57 vs LV138	8.55	3.37	No	ns	-2.56 to 19.7
LCR57 vs LV139	-0.813	0.32	No	ns	-11.9 to 10.3
LCR57 vs LV140	-2.73	1.08	No	ns	-13.8 to 8.38
LCR57 vs LV141	6.68	2.63	No	ns	-4.43 to 17.8
LCR57 vs LV142	16	6.31	Yes	***	4.90 to 27.1
LCR57 vs LV143	-6.45	2.54	No	ns	-17.6 to 4.67
LCR57 vs LV144	-3.45	1.36	No	ns	-14.6 to 7.66
LCR57 vs LV145	-14	5.52	Yes	***	-25.1 to -2.89
LCR57 vs LV146	26.1	10.3	Yes	***	15.0 to 37.3
LCR57 vs LV161	0.713	0.281	No	ns	-10.4 to 11.8
LCR57 vs LV163	-7.49	2.95	No	ns	-18.6 to 3.62
LCR57 vs LV162	19.5	7.66	Yes	***	8.34 to 30.6
LCR57 vs LV164	17.6	6.95	Yes	***	6.53 to 28.8
LCR57 vs LV165	9.24	3.64	No	ns	-1.87 to 20.4
LCR57 vs LV167	0.00667	0.00263	No	ns	-11.1 to 11.1
LCR57 vs LV168	14.1	5.54	Yes	***	2.97 to 25.2
LCR57 vs LV176	-23.3	9.18	Yes	***	-34.4 to -12.2
LCR57 vs CV125(L)	-19.9	7.82	Yes	***	-31.0 to -8.75

LCR57 vs CV126(L)	5.57	2.19	No	ns	-5.54 to 16.7
LCR57 vs CV130	-14.1	5.57	Yes	***	-25.2 to -3.02
LCR57 vs LV180	-5.07	2	No	ns	-16.2 to 6.04
LCR57 vs LV183	-3.91	1.54	No	ns	-15.0 to 7.21
LCR58 vs LCR59	-5.13	2.02	No	ns	-16.2 to 5.98
LCR58 vs LCR60	11.6	4.57	Yes	*	0.494 to 22.7
LCR58 vs LCR63	-12.5	4.93	Yes	**	-23.6 to -1.39
LCR58 vs LCR65	-3.06	1.21	No	ns	-14.2 to 8.05
LCR58 vs LCR66	11.9	4.7	Yes	*	0.821 to 23.0
LCR58 vs LCR67	26.2	10.3	Yes	***	15.1 to 37.3
LCR58 vs LCR68	10.8	4.23	No	ns	-0.359 to 21.9
LCR58 vs LCR70	-4.33	1.71	No	ns	-15.4 to 6.78
LCR58 vs LCR43	3.29	1.29	No	ns	-7.83 to 14.4
LCR58 vs LCR64	-2.59	1.02	No	ns	-13.7 to 8.52
LCR58 vs LCR71	23.2	9.13	Yes	***	12.1 to 34.3
LCR58 vs LCR72	-7.33	2.89	No	ns	-18.4 to 3.78
LCR58 vs LCR73	-4.5	1.77	No	ns	-15.6 to 6.61
LCR58 vs LCR74	12.4	4.86	Yes	**	1.24 to 23.5
LCR58 vs LCR75	11.8	4.65	Yes	*	0.707 to 22.9
LCR58 vs LCR76	-1.12	0.441	No	ns	-12.2 to 9.99
LCR58 vs LCR77	0.387	0.152	No	ns	-10.7 to 11.5
LCR58 vs LCR78	-0.873	0.344	No	ns	-12.0 to 10.2
LCR58 vs LCR131	-16.2	6.37	Yes	***	-27.3 to -5.07
LCR58 vs LCR135	-12.3	4.84	Yes	**	-23.4 to -1.17
LCR58 vs LV134	10.5	4.14	No	ns	-0.606 to 21.6
LCR58 vs LV136	10.3	4.05	No	ns	-0.819 to 21.4
LCR58 vs LV138	17.6	6.92	Yes	***	6.45 to 28.7

LCR58 vs LV139	8.2	3.23	No	ns	-2.91 to 19.3
LCR58 vs LV140	6.28	2.47	No	ns	-4.83 to 17.4
LCR58 vs LV141	15.7	6.18	Yes	***	4.58 to 26.8
LCR58 vs LV142	25	9.86	Yes	***	13.9 to 36.1
LCR58 vs LV143	2.57	1.01	No	ns	-8.55 to 13.7
LCR58 vs LV144	5.56	2.19	No	ns	-5.55 to 16.7
LCR58 vs LV145	-4.99	1.97	No	ns	-16.1 to 6.12
LCR58 vs LV146	35.2	13.8	Yes	***	24.0 to 46.3
LCR58 vs LV161	9.73	3.83	No	ns	-1.39 to 20.8
LCR58 vs LV163	1.52	0.599	No	ns	-9.59 to 12.6
LCR58 vs LV162	28.5	11.2	Yes	***	17.4 to 39.6
LCR58 vs LV164	26.7	10.5	Yes	***	15.5 to 37.8
LCR58 vs LV165	18.3	7.19	Yes	***	7.14 to 29.4
LCR58 vs LV167	9.02	3.55	No	ns	-2.09 to 20.1
LCR58 vs LV168	23.1	9.09	Yes	***	12.0 to 34.2
LCR58 vs LV176	-14.3	5.63	Yes	***	-25.4 to -3.19
LCR58 vs CV125(L)	-10.8	4.27	No	ns	-22.0 to 0.266
LCR58 vs CV126(L)	14.6	5.74	Yes	***	3.47 to 25.7
LCR58 vs CV130	-5.12	2.02	No	ns	-16.2 to 5.99
LCR58 vs LV180	3.94	1.55	No	ns	-7.17 to 15.1
LCR58 vs LV183	5.11	2.01	No	ns	-6.01 to 16.2
LCR59 vs LCR60	16.7	6.59	Yes	***	5.63 to 27.9
LCR59 vs LCR63	-7.37	2.9	No	ns	-18.5 to 3.74
LCR59 vs LCR65	2.07	0.817	No	ns	-9.04 to 13.2
LCR59 vs LCR66	17.1	6.72	Yes	***	5.95 to 28.2
LCR59 vs LCR67	31.4	12.4	Yes	***	20.2 to 42.5
LCR59 vs LCR68	15.9	6.26	Yes	***	4.77 to 27.0

LCR59 vs LCR70	0.8	0.315	No	ns	-10.3 to 11.9
LCR59 vs LCR43	8.42	3.32	No	ns	-2.69 to 19.5
LCR59 vs LCR64	2.54	1	No	ns	-8.57 to 13.7
LCR59 vs LCR71	28.3	11.2	Yes	***	17.2 to 39.4
LCR59 vs LCR72	-2.2	0.866	No	ns	-13.3 to 8.91
LCR59 vs LCR73	0.633	0.249	No	ns	-10.5 to 11.7
LCR59 vs LCR74	17.5	6.89	Yes	***	6.37 to 28.6
LCR59 vs LCR75	17	6.68	Yes	***	5.84 to 28.1
LCR59 vs LCR76	4.01	1.58	No	ns	-7.10 to 15.1
LCR59 vs LCR77	5.52	2.17	No	ns	-5.59 to 16.6
LCR59 vs LCR78	4.26	1.68	No	ns	-6.85 to 15.4
LCR59 vs LCR131	-11	4.35	No	ns	-22.2 to 0.0661
LCR59 vs LCR135	-7.15	2.82	No	ns	-18.3 to 3.96
LCR59 vs LV134	15.6	6.16	Yes	***	4.53 to 26.8
LCR59 vs LV136	15.4	6.08	Yes	***	4.31 to 26.5
LCR59 vs LV138	22.7	8.94	Yes	***	11.6 to 33.8
LCR59 vs LV139	13.3	5.25	Yes	**	2.22 to 24.4
LCR59 vs LV140	11.4	4.49	Yes	*	0.301 to 22.5
LCR59 vs LV141	20.8	8.2	Yes	***	9.71 to 31.9
LCR59 vs LV142	30.2	11.9	Yes	***	19.0 to 41.3
LCR59 vs LV143	7.7	3.03	No	ns	-3.41 to 18.8
LCR59 vs LV144	10.7	4.21	No	ns	-0.419 to 21.8
LCR59 vs LV145	0.14	0.0551	No	ns	-11.0 to 11.3
LCR59 vs LV146	40.3	15.9	Yes	***	29.2 to 51.4
LCR59 vs LV161	14.9	5.85	Yes	***	3.75 to 26.0
LCR59 vs LV163	6.65	2.62	No	ns	-4.46 to 17.8
LCR59 vs LV162	33.6	13.2	Yes	***	22.5 to 44.7

LCR59 vs LV164	31.8	12.5	Yes	***	20.7 to 42.9
LCR59 vs LV165	23.4	9.21	Yes	***	12.3 to 34.5
LCR59 vs LV167	14.2	5.57	Yes	***	3.04 to 25.3
LCR59 vs LV168	28.2	11.1	Yes	***	17.1 to 39.3
LCR59 vs LV176	-9.17	3.61	No	ns	-20.3 to 1.95
LCR59 vs CV125(L)	-5.71	2.25	No	ns	-16.8 to 5.40
LCR59 vs CV126(L)	19.7	7.77	Yes	***	8.61 to 30.8
LCR59 vs CV130	0.0133	0.00525	No	ns	-11.1 to 11.1
LCR59 vs LV180	9.07	3.57	No	ns	-2.04 to 20.2
LCR59 vs LV183	10.2	4.03	No	ns	-0.873 to 21.4
LCR60 vs LCR63	-24.1	9.5	Yes	***	-35.2 to -13.0
LCR60 vs LCR65	-14.7	5.78	Yes	***	-25.8 to -3.55
LCR60 vs LCR66	0.327	0.129	No	ns	-10.8 to 11.4
LCR60 vs LCR67	14.6	5.76	Yes	***	3.51 to 25.7
LCR60 vs LCR68	-0.853	0.336	No	ns	-12.0 to 10.3
LCR60 vs LCR70	-15.9	6.28	Yes	***	-27.1 to -4.83
LCR60 vs LCR43	-8.32	3.28	No	ns	-19.4 to 2.79
LCR60 vs LCR64	-14.2	5.59	Yes	***	-25.3 to -3.09
LCR60 vs LCR71	11.6	4.56	Yes	*	0.467 to 22.7
LCR60 vs LCR72	-18.9	7.46	Yes	***	-30.1 to -7.83
LCR60 vs LCR73	-16.1	6.34	Yes	***	-27.2 to -4.99
LCR60 vs LCR74	0.747	0.294	No	ns	-10.4 to 11.9
LCR60 vs LCR75	0.213	0.084	No	ns	-10.9 to 11.3
LCR60 vs LCR76	-12.7	5.01	Yes	**	-23.8 to -1.61
LCR60 vs LCR77	-11.2	4.42	Yes	*	-22.3 to -0.107
LCR60 vs LCR78	-12.5	4.91	Yes	**	-23.6 to -1.37
LCR60 vs LCR131	-27.8	10.9	Yes	***	-38.9 to -16.7

LCR60 vs LCR135	-23.9	9.41	Yes	***	-35.0 to -12.8
LCR60 vs LV134	-1.1	0.433	No	ns	-12.2 to 10.0
LCR60 vs LV136	-1.31	0.517	No	ns	-12.4 to 9.80
LCR60 vs LV138	5.96	2.35	No	ns	-5.15 to 17.1
LCR60 vs LV139	-3.41	1.34	No	ns	-14.5 to 7.71
LCR60 vs LV140	-5.33	2.1	No	ns	-16.4 to 5.79
LCR60 vs LV141	4.09	1.61	No	ns	-7.03 to 15.2
LCR60 vs LV142	13.4	5.29	Yes	**	2.31 to 24.5
LCR60 vs LV143	-9.04	3.56	No	ns	-20.2 to 2.07
LCR60 vs LV144	-6.05	2.38	No	ns	-17.2 to 5.07
LCR60 vs LV145	-16.6	6.54	Yes	***	-27.7 to -5.49
LCR60 vs LV146	23.5	9.27	Yes	***	12.4 to 34.7
LCR60 vs LV161	-1.88	0.74	No	ns	-13.0 to 9.23
LCR60 vs LV163	-10.1	3.97	No	ns	-21.2 to 1.03
LCR60 vs LV162	16.9	6.64	Yes	***	5.74 to 28.0
LCR60 vs LV164	15	5.93	Yes	***	3.93 to 26.2
LCR60 vs LV165	6.65	2.62	No	ns	-4.47 to 17.8
LCR60 vs LV167	-2.59	1.02	No	ns	-13.7 to 8.53
LCR60 vs LV168	11.5	4.52	Yes	*	0.374 to 22.6
LCR60 vs LV176	-25.9	10.2	Yes	***	-37.0 to -14.8
LCR60 vs CV125(L)	-22.5	8.84	Yes	***	-33.6 to -11.3
LCR60 vs CV126(L)	2.98	1.17	No	ns	-8.13 to 14.1
LCR60 vs CV130	-16.7	6.59	Yes	***	-27.8 to -5.61
LCR60 vs LV180	-7.67	3.02	No	ns	-18.8 to 3.45
LCR60 vs LV183	-6.5	2.56	No	ns	-17.6 to 4.61
LCR63 vs LCR65	9.45	3.72	No	ns	-1.67 to 20.6
LCR63 vs LCR66	24.4	9.62	Yes	***	13.3 to 35.6

LCR63 vs LCR67	38.7	15.3	Yes	***	27.6 to 49.8
LCR63 vs LCR68	23.3	9.16	Yes	***	12.1 to 34.4
LCR63 vs LCR70	8.17	3.22	No	ns	-2.94 to 19.3
LCR63 vs LCR43	15.8	6.22	Yes	***	4.68 to 26.9
LCR63 vs LCR64	9.91	3.9	No	ns	-1.20 to 21.0
LCR63 vs LCR71	35.7	14.1	Yes	***	24.6 to 46.8
LCR63 vs LCR72	5.17	2.04	No	ns	-5.94 to 16.3
LCR63 vs LCR73	8.01	3.15	No	ns	-3.11 to 19.1
LCR63 vs LCR74	24.9	9.79	Yes	***	13.7 to 36.0
LCR63 vs LCR75	24.3	9.58	Yes	***	13.2 to 35.4
LCR63 vs LCR76	11.4	4.48	Yes	*	0.274 to 22.5
LCR63 vs LCR77	12.9	5.08	Yes	**	1.78 to 24.0
LCR63 vs LCR78	11.6	4.58	Yes	*	0.521 to 22.7
LCR63 vs LCR131	-3.67	1.45	No	ns	-14.8 to 7.44
LCR63 vs LCR135	0.22	0.0866	No	ns	-10.9 to 11.3
LCR63 vs LV134	23	9.06	Yes	***	11.9 to 34.1
LCR63 vs LV136	22.8	8.98	Yes	***	11.7 to 33.9
LCR63 vs LV138	30.1	11.8	Yes	***	19.0 to 41.2
LCR63 vs LV139	20.7	8.15	Yes	***	9.59 to 31.8
LCR63 vs LV140	18.8	7.4	Yes	***	7.67 to 29.9
LCR63 vs LV141	28.2	11.1	Yes	***	17.1 to 39.3
LCR63 vs LV142	37.5	14.8	Yes	***	26.4 to 48.6
LCR63 vs LV143	15.1	5.94	Yes	***	3.96 to 26.2
LCR63 vs LV144	18.1	7.12	Yes	***	6.95 to 29.2
LCR63 vs LV145	7.51	2.96	No	ns	-3.60 to 18.6
LCR63 vs LV146	47.7	18.8	Yes	***	36.5 to 58.8
LCR63 vs LV161	22.2	8.76	Yes	***	11.1 to 33.3

LCR63 vs LV163	14	5.52	Yes	***	2.91 to 25.1
LCR63 vs LV162	41	16.1	Yes	***	29.9 to 52.1
LCR63 vs LV164	39.2	15.4	Yes	***	28.0 to 50.3
LCR63 vs LV165	30.8	12.1	Yes	***	19.6 to 41.9
LCR63 vs LV167	21.5	8.48	Yes	***	10.4 to 32.6
LCR63 vs LV168	35.6	14	Yes	***	24.5 to 46.7
LCR63 vs LV176	-1.79	0.706	No	ns	-12.9 to 9.32
LCR63 vs CV125(L)	1.66	0.654	No	ns	-9.45 to 12.8
LCR63 vs CV126(L)	27.1	10.7	Yes	***	16.0 to 38.2
LCR63 vs CV130	7.39	2.91	No	ns	-3.73 to 18.5
LCR63 vs LV180	16.4	6.48	Yes	***	5.33 to 27.6
LCR63 vs LV183	17.6	6.94	Yes	***	6.50 to 28.7
LCR65 vs LCR66	15	5.9	Yes	***	3.88 to 26.1
LCR65 vs LCR67	29.3	11.5	Yes	***	18.2 to 40.4
LCR65 vs LCR68	13.8	5.44	Yes	***	2.70 to 24.9
LCR65 vs LCR70	-1.27	0.501	No	ns	-12.4 to 9.84
LCR65 vs LCR43	6.35	2.5	No	ns	-4.77 to 17.5
LCR65 vs LCR64	0.467	0.184	No	ns	-10.6 to 11.6
LCR65 vs LCR71	26.2	10.3	Yes	***	15.1 to 37.4
LCR65 vs LCR72	-4.27	1.68	No	ns	-15.4 to 6.84
LCR65 vs LCR73	-1.44	0.567	No	ns	-12.6 to 9.67
LCR65 vs LCR74	15.4	6.07	Yes	***	4.30 to 26.5
LCR65 vs LCR75	14.9	5.86	Yes	***	3.77 to 26.0
LCR65 vs LCR76	1.94	0.764	No	ns	-9.17 to 13.1
LCR65 vs LCR77	3.45	1.36	No	ns	-7.67 to 14.6
LCR65 vs LCR78	2.19	0.861	No	ns	-8.93 to 13.3
LCR65 vs LCR131	-13.1	5.17	Yes	**	-24.2 to -2.01

LCR65 vs LCR135	-9.23	3.63	No	ns	-20.3 to 1.89
LCR65 vs LV134	13.6	5.34	Yes	***	2.45 to 24.7
LCR65 vs LV136	13.4	5.26	Yes	**	2.24 to 24.5
LCR65 vs LV138	20.6	8.12	Yes	***	9.51 to 31.7
LCR65 vs LV139	11.3	4.43	Yes	*	0.147 to 22.4
LCR65 vs LV140	9.34	3.68	No	ns	-1.77 to 20.5
LCR65 vs LV141	18.8	7.39	Yes	***	7.64 to 29.9
LCR65 vs LV142	28.1	11.1	Yes	***	17.0 to 39.2
LCR65 vs LV143	5.63	2.22	No	ns	-5.49 to 16.7
LCR65 vs LV144	8.62	3.39	No	ns	-2.49 to 19.7
LCR65 vs LV145	-1.93	0.761	No	ns	-13.0 to 9.18
LCR65 vs LV146	38.2	15	Yes	***	27.1 to 49.3
LCR65 vs LV161	12.8	5.04	Yes	**	1.67 to 23.9
LCR65 vs LV163	4.58	1.8	No	ns	-6.53 to 15.7
LCR65 vs LV162	31.5	12.4	Yes	***	20.4 to 42.6
LCR65 vs LV164	29.7	11.7	Yes	***	18.6 to 40.8
LCR65 vs LV165	21.3	8.39	Yes	***	10.2 to 32.4
LCR65 vs LV167	12.1	4.76	Yes	*	0.967 to 23.2
LCR65 vs LV168	26.2	10.3	Yes	***	15.0 to 37.3
LCR65 vs LV176	-11.2	4.43	Yes	*	-22.4 to -0.127
LCR65 vs CV125(L)	-7.79	3.07	No	ns	-18.9 to 3.33
LCR65 vs CV126(L)	17.6	6.95	Yes	***	6.53 to 28.8
LCR65 vs CV130	-2.06	0.811	No	ns	-13.2 to 9.05
LCR65 vs LV180	7	2.76	No	ns	-4.11 to 18.1
LCR65 vs LV183	8.17	3.22	No	ns	-2.95 to 19.3
LCR66 vs LCR67	14.3	5.63	Yes	***	3.18 to 25.4
LCR66 vs LCR68	-1.18	0.465	No	ns	-12.3 to 9.93

LCR66 vs LCR70	-16.3	6.41	Yes	***	-27.4 to -5.15
LCR66 vs LCR43	-8.65	3.41	No	ns	-19.8 to 2.47
LCR66 vs LCR64	-14.5	5.72	Yes	***	-25.6 to -3.41
LCR66 vs LCR71	11.3	4.43	Yes	*	0.141 to 22.4
LCR66 vs LCR72	-19.3	7.59	Yes	***	-30.4 to -8.15
LCR66 vs LCR73	-16.4	6.47	Yes	***	-27.5 to -5.32
LCR66 vs LCR74	0.42	0.165	No	ns	-10.7 to 11.5
LCR66 vs LCR75	-0.113	0.0446	No	ns	-11.2 to 11.0
LCR66 vs LCR76	-13.1	5.14	Yes	**	-24.2 to -1.94
LCR66 vs LCR77	-11.5	4.55	Yes	*	-22.7 to -0.434
LCR66 vs LCR78	-12.8	5.04	Yes	**	-23.9 to -1.69
LCR66 vs LCR131	-28.1	11.1	Yes	***	-39.2 to -17.0
LCR66 vs LCR135	-24.2	9.54	Yes	***	-35.3 to -13.1
LCR66 vs LV134	-1.43	0.562	No	ns	-12.5 to 9.69
LCR66 vs LV136	-1.64	0.646	No	ns	-12.8 to 9.47
LCR66 vs LV138	5.63	2.22	No	ns	-5.48 to 16.7
LCR66 vs LV139	-3.73	1.47	No	ns	-14.8 to 7.38
LCR66 vs LV140	-5.65	2.23	No	ns	-16.8 to 5.46
LCR66 vs LV141	3.76	1.48	No	ns	-7.35 to 14.9
LCR66 vs LV142	13.1	5.16	Yes	**	1.98 to 24.2
LCR66 vs LV143	-9.37	3.69	No	ns	-20.5 to 1.75
LCR66 vs LV144	-6.37	2.51	No	ns	-17.5 to 4.74
LCR66 vs LV145	-16.9	6.67	Yes	***	-28.0 to -5.81
LCR66 vs LV146	23.2	9.14	Yes	***	12.1 to 34.3
LCR66 vs LV161	-2.21	0.869	No	ns	-13.3 to 8.91
LCR66 vs LV163	-10.4	4.1	No	ns	-21.5 to 0.699
LCR66 vs LV162	16.5	6.51	Yes	***	5.42 to 27.6

LCR66 vs LV164	14.7	5.8	Yes	***	3.61 to 25.8
LCR66 vs LV165	6.32	2.49	No	ns	-4.79 to 17.4
LCR66 vs LV167	-2.91	1.15	No	ns	-14.0 to 8.20
LCR66 vs LV168	11.2	4.4	Yes	*	0.0473 to 22.3
LCR66 vs LV176	-26.2	10.3	Yes	***	-37.3 to -15.1
LCR66 vs CV125(L)	-22.8	8.97	Yes	***	-33.9 to -11.7
LCR66 vs CV126(L)	2.65	1.04	No	ns	-8.46 to 13.8
LCR66 vs CV130	-17.1	6.72	Yes	***	-28.2 to -5.94
LCR66 vs LV180	-7.99	3.15	No	ns	-19.1 to 3.12
LCR66 vs LV183	-6.83	2.69	No	ns	-17.9 to 4.29
LCR67 vs LCR68	-15.5	6.09	Yes	***	-26.6 to -4.36
LCR67 vs LCR70	-30.6	12	Yes	***	-41.7 to -19.4
LCR67 vs LCR43	-22.9	9.03	Yes	***	-34.1 to -11.8
LCR67 vs LCR64	-28.8	11.3	Yes	***	-39.9 to -17.7
LCR67 vs LCR71	-3.04	1.2	No	ns	-14.2 to 8.07
LCR67 vs LCR72	-33.6	13.2	Yes	***	-44.7 to -22.4
LCR67 vs LCR73	-30.7	12.1	Yes	***	-41.8 to -19.6
LCR67 vs LCR74	-13.9	5.46	Yes	***	-25.0 to -2.76
LCR67 vs LCR75	-14.4	5.67	Yes	***	-25.5 to -3.29
LCR67 vs LCR76	-27.3	10.8	Yes	***	-38.5 to -16.2
LCR67 vs LCR77	-25.8	10.2	Yes	***	-37.0 to -14.7
LCR67 vs LCR78	-27.1	10.7	Yes	***	-38.2 to -16.0
LCR67 vs LCR131	-42.4	16.7	Yes	***	-53.5 to -31.3
LCR67 vs LCR135	-38.5	15.2	Yes	***	-49.6 to -27.4
LCR67 vs LV134	-15.7	6.19	Yes	***	-26.8 to -4.61
LCR67 vs LV136	-15.9	6.27	Yes	***	-27.0 to -4.82
LCR67 vs LV138	-8.66	3.41	No	ns	-19.8 to 2.45

LCR67 vs LV139	-18	7.1	Yes	***	-29.1 to -6.91
LCR67 vs LV140	-19.9	7.86	Yes	***	-31.1 to -8.83
LCR67 vs LV141	-10.5	4.15	No	ns	-21.6 to 0.579
LCR67 vs LV142	-1.2	0.473	No	ns	-12.3 to 9.91
LCR67 vs LV143	-23.7	9.32	Yes	***	-34.8 to -12.5
LCR67 vs LV144	-20.7	8.14	Yes	***	-31.8 to -9.55
LCR67 vs LV145	-31.2	12.3	Yes	***	-42.3 to -20.1
LCR67 vs LV146	8.93	3.52	No	ns	-2.19 to 20.0
LCR67 vs LV161	-16.5	6.5	Yes	***	-27.6 to -5.39
LCR67 vs LV163	-24.7	9.73	Yes	***	-35.8 to -13.6
LCR67 vs LV162	2.24	0.881	No	ns	-8.88 to 13.4
LCR67 vs LV164	0.427	0.168	No	ns	-10.7 to 11.5
LCR67 vs LV165	-7.97	3.14	No	ns	-19.1 to 3.14
LCR67 vs LV167	-17.2	6.78	Yes	***	-28.3 to -6.09
LCR67 vs LV168	-3.13	1.23	No	ns	-14.2 to 7.98
LCR67 vs LV176	-40.5	16	Yes	***	-51.6 to -29.4
LCR67 vs CV125(L)	-37.1	14.6	Yes	***	-48.2 to -26.0
LCR67 vs CV126(L)	-11.6	4.58	Yes	*	-22.8 to -0.527
LCR67 vs CV130	-31.3	12.3	Yes	***	-42.5 to -20.2
LCR67 vs LV180	-22.3	8.78	Yes	***	-33.4 to -11.2
LCR67 vs LV183	-21.1	8.32	Yes	***	-32.2 to -10.0
LCR68 vs LCR70	-15.1	5.94	Yes	***	-26.2 to -3.97
LCR68 vs LCR43	-7.47	2.94	No	ns	-18.6 to 3.65
LCR68 vs LCR64	-13.3	5.26	Yes	**	-24.5 to -2.23
LCR68 vs LCR71	12.4	4.9	Yes	**	1.32 to 23.5
LCR68 vs LCR72	-18.1	7.12	Yes	***	-29.2 to -6.97
LCR68 vs LCR73	-15.3	6.01	Yes	***	-26.4 to -4.14

LCR68 vs LCR74	1.6	0.63	No	ns	-9.51 to 12.7
LCR68 vs LCR75	1.07	0.42	No	ns	-10.0 to 12.2
LCR68 vs LCR76	-11.9	4.68	Yes	*	-23.0 to -0.761
LCR68 vs LCR77	-10.4	4.08	No	ns	-21.5 to 0.746
LCR68 vs LCR78	-11.6	4.58	Yes	*	-22.7 to -0.514
LCR68 vs LCR131	-26.9	10.6	Yes	***	-38.0 to -15.8
LCR68 vs LCR135	-23	9.07	Yes	***	-34.2 to -11.9
LCR68 vs LV134	-0.247	0.0971	No	ns	-11.4 to 10.9
LCR68 vs LV136	-0.46	0.181	No	ns	-11.6 to 10.7
LCR68 vs LV138	6.81	2.68	No	ns	-4.30 to 17.9
LCR68 vs LV139	-2.55	1.01	No	ns	-13.7 to 8.56
LCR68 vs LV140	-4.47	1.76	No	ns	-15.6 to 6.64
LCR68 vs LV141	4.94	1.95	No	ns	-6.17 to 16.1
LCR68 vs LV142	14.3	5.62	Yes	***	3.16 to 25.4
LCR68 vs LV143	-8.19	3.22	No	ns	-19.3 to 2.93
LCR68 vs LV144	-5.19	2.05	No	ns	-16.3 to 5.92
LCR68 vs LV145	-15.7	6.2	Yes	***	-26.9 to -4.63
LCR68 vs LV146	24.4	9.61	Yes	***	13.3 to 35.5
LCR68 vs LV161	-1.03	0.404	No	ns	-12.1 to 10.1
LCR68 vs LV163	-9.23	3.64	No	ns	-20.3 to 1.88
LCR68 vs LV162	17.7	6.97	Yes	***	6.60 to 28.8
LCR68 vs LV164	15.9	6.26	Yes	***	4.79 to 27.0
LCR68 vs LV165	7.5	2.95	No	ns	-3.61 to 18.6
LCR68 vs LV167	-1.73	0.683	No	ns	-12.8 to 9.38
LCR68 vs LV168	12.3	4.86	Yes	**	1.23 to 23.5
LCR68 vs LV176	-25.1	9.87	Yes	***	-36.2 to -13.9
LCR68 vs CV125(L)	-21.6	8.51	Yes	***	-32.7 to -10.5

LCR68 vs CV126(L)	3.83	1.51	No	ns	-7.28 to 14.9
LCR68 vs CV130	-15.9	6.25	Yes	***	-27.0 to -4.76
LCR68 vs LV180	-6.81	2.68	No	ns	-17.9 to 4.30
LCR68 vs LV183	-5.65	2.22	No	ns	-16.8 to 5.47
LCR70 vs LCR43	7.62	3	No	ns	-3.49 to 18.7
LCR70 vs LCR64	1.74	0.685	No	ns	-9.37 to 12.9
LCR70 vs LCR71	27.5	10.8	Yes	***	16.4 to 38.6
LCR70 vs LCR72	-3	1.18	No	ns	-14.1 to 8.11
LCR70 vs LCR73	-0.167	0.0656	No	ns	-11.3 to 10.9
LCR70 vs LCR74	16.7	6.57	Yes	***	5.57 to 27.8
LCR70 vs LCR75	16.2	6.36	Yes	***	5.04 to 27.3
LCR70 vs LCR76	3.21	1.27	No	ns	-7.90 to 14.3
LCR70 vs LCR77	4.72	1.86	No	ns	-6.39 to 15.8
LCR70 vs LCR78	3.46	1.36	No	ns	-7.65 to 14.6
LCR70 vs LCR131	-11.8	4.67	Yes	*	-23.0 to -0.734
LCR70 vs LCR135	-7.95	3.13	No	ns	-19.1 to 3.16
LCR70 vs LV134	14.8	5.84	Yes	***	3.73 to 26.0
LCR70 vs LV136	14.6	5.76	Yes	***	3.51 to 25.7
LCR70 vs LV138	21.9	8.62	Yes	***	10.8 to 33.0
LCR70 vs LV139	12.5	4.94	Yes	**	1.42 to 23.6
LCR70 vs LV140	10.6	4.18	No	ns	-0.499 to 21.7
LCR70 vs LV141	20	7.89	Yes	***	8.91 to 31.1
LCR70 vs LV142	29.4	11.6	Yes	***	18.2 to 40.5
LCR70 vs LV143	6.9	2.72	No	ns	-4.21 to 18.0
LCR70 vs LV144	9.89	3.9	No	ns	-1.22 to 21.0
LCR70 vs LV145	-0.66	0.26	No	ns	-11.8 to 10.5
LCR70 vs LV146	39.5	15.6	Yes	***	28.4 to 50.6

LCR70 vs LV161	14.1	5.54	Yes	***	2.95 to 25.2
LCR70 vs LV163	5.85	2.31	No	ns	-5.26 to 17.0
LCR70 vs LV162	32.8	12.9	Yes	***	21.7 to 43.9
LCR70 vs LV164	31	12.2	Yes	***	19.9 to 42.1
LCR70 vs LV165	22.6	8.9	Yes	***	11.5 to 33.7
LCR70 vs LV167	13.4	5.26	Yes	**	2.24 to 24.5
LCR70 vs LV168	27.4	10.8	Yes	***	16.3 to 38.5
LCR70 vs LV176	-9.97	3.93	No	ns	-21.1 to 1.15
LCR70 vs CV125(L)	-6.51	2.57	No	ns	-17.6 to 4.60
LCR70 vs CV126(L)	18.9	7.45	Yes	***	7.81 to 30.0
LCR70 vs CV130	-0.787	0.31	No	ns	-11.9 to 10.3
LCR70 vs LV180	8.27	3.26	No	ns	-2.84 to 19.4
LCR70 vs LV183	9.44	3.72	No	ns	-1.67 to 20.6
LCR43 vs LCR64	-5.88	2.32	No	ns	-17.0 to 5.23
LCR43 vs LCR71	19.9	7.84	Yes	***	8.79 to 31.0
LCR43 vs LCR72	-10.6	4.18	No	ns	-21.7 to 0.493
LCR43 vs LCR73	-7.79	3.07	No	ns	-18.9 to 3.33
LCR43 vs LCR74	9.07	3.57	No	ns	-2.05 to 20.2
LCR43 vs LCR75	8.53	3.36	No	ns	-2.58 to 19.6
LCR43 vs LCR76	-4.41	1.74	No	ns	-15.5 to 6.71
LCR43 vs LCR77	-2.9	1.14	No	ns	-14.0 to 8.21
LCR43 vs LCR78	-4.16	1.64	No	ns	-15.3 to 6.95
LCR43 vs LCR131	-19.5	7.67	Yes	***	-30.6 to -8.35
LCR43 vs LCR135	-15.6	6.13	Yes	***	-26.7 to -4.46
LCR43 vs LV134	7.22	2.84	No	ns	-3.89 to 18.3
LCR43 vs LV136	7.01	2.76	No	ns	-4.11 to 18.1
LCR43 vs LV138	14.3	5.62	Yes	***	3.17 to 25.4

LCR43 vs LV139	4.91	1.93	No	ns	-6.20 to 16.0
LCR43 vs LV140	2.99	1.18	No	ns	-8.12 to 14.1
LCR43 vs LV141	12.4	4.89	Yes	**	1.29 to 23.5
LCR43 vs LV142	21.7	8.56	Yes	***	10.6 to 32.9
LCR43 vs LV143	-0.72	0.284	No	ns	-11.8 to 10.4
LCR43 vs LV144	2.27	0.895	No	ns	-8.84 to 13.4
LCR43 vs LV145	-8.28	3.26	No	ns	-19.4 to 2.83
LCR43 vs LV146	31.9	12.5	Yes	***	20.8 to 43.0
LCR43 vs LV161	6.44	2.54	No	ns	-4.67 to 17.6
LCR43 vs LV163	-1.77	0.696	No	ns	-12.9 to 9.35
LCR43 vs LV162	25.2	9.92	Yes	***	14.1 to 36.3
LCR43 vs LV164	23.4	9.2	Yes	***	12.3 to 34.5
LCR43 vs LV165	15	5.89	Yes	***	3.85 to 26.1
LCR43 vs LV167	5.73	2.26	No	ns	-5.38 to 16.8
LCR43 vs LV168	19.8	7.8	Yes	***	8.69 to 30.9
LCR43 vs LV176	-17.6	6.93	Yes	***	-28.7 to -6.47
LCR43 vs CV125(L)	-14.1	5.57	Yes	***	-25.2 to -3.02
LCR43 vs CV126(L)	11.3	4.45	Yes	*	0.187 to 22.4
LCR43 vs CV130	-8.41	3.31	No	ns	-19.5 to 2.71
LCR43 vs LV180	0.653	0.257	No	ns	-10.5 to 11.8
LCR43 vs LV183	1.82	0.717	No	ns	-9.29 to 12.9
LCR64 vs LCR71	25.8	10.2	Yes	***	14.7 to 36.9
LCR64 vs LCR72	-4.74	1.87	No	ns	-15.9 to 6.37
LCR64 vs LCR73	-1.91	0.751	No	ns	-13.0 to 9.21
LCR64 vs LCR74	14.9	5.89	Yes	***	3.83 to 26.1
LCR64 vs LCR75	14.4	5.68	Yes	***	3.30 to 25.5
LCR64 vs LCR76	1.47	0.58	No	ns	-9.64 to 12.6

LCR64 vs LCR77	2.98	1.17	No	ns	-8.13 to 14.1
LCR64 vs LCR78	1.72	0.677	No	ns	-9.39 to 12.8
LCR64 vs LCR131	-13.6	5.35	Yes	***	-24.7 to -2.47
LCR64 vs LCR135	-9.69	3.82	No	ns	-20.8 to 1.42
LCR64 vs LV134	13.1	5.16	Yes	**	1.99 to 24.2
LCR64 vs LV136	12.9	5.08	Yes	**	1.77 to 24.0
LCR64 vs LV138	20.2	7.94	Yes	***	9.05 to 31.3
LCR64 vs LV139	10.8	4.25	No	ns	-0.319 to 21.9
LCR64 vs LV140	8.87	3.49	No	ns	-2.24 to 20.0
LCR64 vs LV141	18.3	7.2	Yes	***	7.17 to 29.4
LCR64 vs LV142	27.6	10.9	Yes	***	16.5 to 38.7
LCR64 vs LV143	5.16	2.03	No	ns	-5.95 to 16.3
LCR64 vs LV144	8.15	3.21	No	ns	-2.96 to 19.3
LCR64 vs LV145	-2.4	0.945	No	ns	-13.5 to 8.71
LCR64 vs LV146	37.7	14.9	Yes	***	26.6 to 48.9
LCR64 vs LV161	12.3	4.85	Yes	**	1.21 to 23.4
LCR64 vs LV163	4.11	1.62	No	ns	-7.00 to 15.2
LCR64 vs LV162	31.1	12.2	Yes	***	19.9 to 42.2
LCR64 vs LV164	29.2	11.5	Yes	***	18.1 to 40.4
LCR64 vs LV165	20.8	8.21	Yes	***	9.73 to 32.0
LCR64 vs LV167	11.6	4.57	Yes	*	0.501 to 22.7
LCR64 vs LV168	25.7	10.1	Yes	***	14.6 to 36.8
LCR64 vs LV176	-11.7	4.61	Yes	*	-22.8 to -0.594
LCR64 vs CV125(L)	-8.25	3.25	No	ns	-19.4 to 2.86
LCR64 vs CV126(L)	17.2	6.77	Yes	***	6.07 to 28.3
LCR64 vs CV130	-2.53	0.995	No	ns	-13.6 to 8.59
LCR64 vs LV180	6.53	2.57	No	ns	-4.58 to 17.6

LCR64 vs LV183	7.7	3.03	No	ns	-3.41 to 18.8
LCR71 vs LCR72	-30.5	12	Yes	***	-41.6 to -19.4
LCR71 vs LCR73	-27.7	10.9	Yes	***	-38.8 to -16.6
LCR71 vs LCR74	-10.8	4.27	No	ns	-21.9 to 0.279
LCR71 vs LCR75	-11.4	4.48	Yes	*	-22.5 to -0.254
LCR71 vs LCR76	-24.3	9.57	Yes	***	-35.4 to -13.2
LCR71 vs LCR77	-22.8	8.98	Yes	***	-33.9 to -11.7
LCR71 vs LCR78	-24.1	9.48	Yes	***	-35.2 to -12.9
LCR71 vs LCR131	-39.4	15.5	Yes	***	-50.5 to -28.3
LCR71 vs LCR135	-35.5	14	Yes	***	-46.6 to -24.4
LCR71 vs LV134	-12.7	4.99	Yes	**	-23.8 to -1.57
LCR71 vs LV136	-12.9	5.08	Yes	**	-24.0 to -1.78
LCR71 vs LV138	-5.62	2.21	No	ns	-16.7 to 5.49
LCR71 vs LV139	-15	5.9	Yes	***	-26.1 to -3.87
LCR71 vs LV140	-16.9	6.66	Yes	***	-28.0 to -5.79
LCR71 vs LV141	-7.49	2.95	No	ns	-18.6 to 3.62
LCR71 vs LV142	1.84	0.725	No	ns	-9.27 to 13.0
LCR71 vs LV143	-20.6	8.12	Yes	***	-31.7 to -9.51
LCR71 vs LV144	-17.6	6.94	Yes	***	-28.7 to -6.51
LCR71 vs LV145	-28.2	11.1	Yes	***	-39.3 to -17.1
LCR71 vs LV146	12	4.71	Yes	*	0.854 to 23.1
LCR71 vs LV161	-13.5	5.3	Yes	***	-24.6 to -2.35
LCR71 vs LV163	-21.7	8.53	Yes	***	-32.8 to -10.6
LCR71 vs LV162	5.28	2.08	No	ns	-5.84 to 16.4
LCR71 vs LV164	3.47	1.37	No	ns	-7.65 to 14.6
LCR71 vs LV165	-4.93	1.94	No	ns	-16.0 to 6.18
LCR71 vs LV167	-14.2	5.58	Yes	***	-25.3 to -3.05

LCR71 vs LV168	-0.0933	0.0368	No	ns	-11.2 to 11.0
LCR71 vs LV176	-37.5	14.8	Yes	***	-48.6 to -26.4
LCR71 vs CV125(L)	-34	13.4	Yes	***	-45.1 to -22.9
LCR71 vs CV126(L)	-8.6	3.39	No	ns	-19.7 to 2.51
LCR71 vs CV130	-28.3	11.1	Yes	***	-39.4 to -17.2
LCR71 vs LV180	-19.2	7.58	Yes	***	-30.4 to -8.13
LCR71 vs LV183	-18.1	7.12	Yes	***	-29.2 to -6.97
LCR72 vs LCR73	2.83	1.12	No	ns	-8.28 to 13.9
LCR72 vs LCR74	19.7	7.75	Yes	***	8.57 to 30.8
LCR72 vs LCR75	19.2	7.54	Yes	***	8.04 to 30.3
LCR72 vs LCR76	6.21	2.45	No	ns	-4.90 to 17.3
LCR72 vs LCR77	7.72	3.04	No	ns	-3.39 to 18.8
LCR72 vs LCR78	6.46	2.54	No	ns	-4.65 to 17.6
LCR72 vs LCR131	-8.85	3.48	No	ns	-20.0 to 2.27
LCR72 vs LCR135	-4.95	1.95	No	ns	-16.1 to 6.16
LCR72 vs LV134	17.8	7.03	Yes	***	6.73 to 29.0
LCR72 vs LV136	17.6	6.94	Yes	***	6.51 to 28.7
LCR72 vs LV138	24.9	9.81	Yes	***	13.8 to 36.0
LCR72 vs LV139	15.5	6.12	Yes	***	4.42 to 26.6
LCR72 vs LV140	13.6	5.36	Yes	***	2.50 to 24.7
LCR72 vs LV141	23	9.07	Yes	***	11.9 to 34.1
LCR72 vs LV142	32.4	12.7	Yes	***	21.2 to 43.5
LCR72 vs LV143	9.9	3.9	No	ns	-1.21 to 21.0
LCR72 vs LV144	12.9	5.08	Yes	**	1.78 to 24.0
LCR72 vs LV145	2.34	0.922	No	ns	-8.77 to 13.5
LCR72 vs LV146	42.5	16.7	Yes	***	31.4 to 53.6
LCR72 vs LV161	17.1	6.72	Yes	***	5.95 to 28.2

LCR72 vs LV163	8.85	3.49	No	ns	-2.26 to 20.0
LCR72 vs LV162	35.8	14.1	Yes	***	24.7 to 46.9
LCR72 vs LV164	34	13.4	Yes	***	22.9 to 45.1
LCR72 vs LV165	25.6	10.1	Yes	***	14.5 to 36.7
LCR72 vs LV167	16.4	6.44	Yes	***	5.24 to 27.5
LCR72 vs LV168	30.4	12	Yes	***	19.3 to 41.5
LCR72 vs LV176	-6.97	2.74	No	ns	-18.1 to 4.15
LCR72 vs CV125(L)	-3.51	1.38	No	ns	-14.6 to 7.60
LCR72 vs CV126(L)	21.9	8.63	Yes	***	10.8 to 33.0
LCR72 vs CV130	2.21	0.872	No	ns	-8.90 to 13.3
LCR72 vs LV180	11.3	4.44	Yes	*	0.161 to 22.4
LCR72 vs LV183	12.4	4.9	Yes	**	1.33 to 23.6
LCR73 vs LCR74	16.9	6.64	Yes	***	5.74 to 28.0
LCR73 vs LCR75	16.3	6.43	Yes	***	5.21 to 27.4
LCR73 vs LCR76	3.38	1.33	No	ns	-7.73 to 14.5
LCR73 vs LCR77	4.89	1.92	No	ns	-6.23 to 16.0
LCR73 vs LCR78	3.63	1.43	No	ns	-7.49 to 14.7
LCR73 vs LCR131	-11.7	4.6	Yes	*	-22.8 to -0.567
LCR73 vs LCR135	-7.79	3.07	No	ns	-18.9 to 3.33
LCR73 vs LV134	15	5.91	Yes	***	3.89 to 26.1
LCR73 vs LV136	14.8	5.83	Yes	***	3.68 to 25.9
LCR73 vs LV138	22.1	8.69	Yes	***	11.0 to 33.2
LCR73 vs LV139	12.7	5	Yes	**	1.59 to 23.8
LCR73 vs LV140	10.8	4.25	No	ns	-0.333 to 21.9
LCR73 vs LV141	20.2	7.95	Yes	***	9.08 to 31.3
LCR73 vs LV142	29.5	11.6	Yes	***	18.4 to 40.6
LCR73 vs LV143	7.07	2.78	No	ns	-4.05 to 18.2

LCR73 vs LV144	10.1	3.96	No	ns	-1.05 to 21.2
LCR73 vs LV145	-0.493	0.194	No	ns	-11.6 to 10.6
LCR73 vs LV146	39.7	15.6	Yes	***	28.5 to 50.8
LCR73 vs LV161	14.2	5.6	Yes	***	3.11 to 25.3
LCR73 vs LV163	6.02	2.37	No	ns	-5.09 to 17.1
LCR73 vs LV162	33	13	Yes	***	21.9 to 44.1
LCR73 vs LV164	31.2	12.3	Yes	***	20.0 to 42.3
LCR73 vs LV165	22.8	8.96	Yes	***	11.6 to 33.9
LCR73 vs LV167	13.5	5.32	Yes	***	2.41 to 24.6
LCR73 vs LV168	27.6	10.9	Yes	***	16.5 to 38.7
LCR73 vs LV176	-9.8	3.86	No	ns	-20.9 to 1.31
LCR73 vs CV125(L)	-6.35	2.5	No	ns	-17.5 to 4.77
LCR73 vs CV126(L)	19.1	7.52	Yes	***	7.97 to 30.2
LCR73 vs CV130	-0.62	0.244	No	ns	-11.7 to 10.5
LCR73 vs LV180	8.44	3.32	No	ns	-2.67 to 19.6
LCR73 vs LV183	9.61	3.78	No	ns	-1.51 to 20.7
LCR74 vs LCR75	-0.533	0.21	No	ns	-11.6 to 10.6
LCR74 vs LCR76	-13.5	5.31	Yes	***	-24.6 to -2.36
LCR74 vs LCR77	-12	4.71	Yes	*	-23.1 to -0.854
LCR74 vs LCR78	-13.2	5.21	Yes	**	-24.3 to -2.11
LCR74 vs LCR131	-28.5	11.2	Yes	***	-39.6 to -17.4
LCR74 vs LCR135	-24.6	9.7	Yes	***	-35.8 to -13.5
LCR74 vs LV134	-1.85	0.727	No	ns	-13.0 to 9.27
LCR74 vs LV136	-2.06	0.811	No	ns	-13.2 to 9.05
LCR74 vs LV138	5.21	2.05	No	ns	-5.90 to 16.3
LCR74 vs LV139	-4.15	1.64	No	ns	-15.3 to 6.96
LCR74 vs LV140	-6.07	2.39	No	ns	-17.2 to 5.04

LCR74 vs LV141	3.34	1.32	No	ns	-7.77 to 14.5
LCR74 vs LV142	12.7	4.99	Yes	**	1.56 to 23.8
LCR74 vs LV143	-9.79	3.85	No	ns	-20.9 to 1.33
LCR74 vs LV144	-6.79	2.68	No	ns	-17.9 to 4.32
LCR74 vs LV145	-17.3	6.83	Yes	***	-28.5 to -6.23
LCR74 vs LV146	22.8	8.98	Yes	***	11.7 to 33.9
LCR74 vs LV161	-2.63	1.03	No	ns	-13.7 to 8.49
LCR74 vs LV163	-10.8	4.27	No	ns	-21.9 to 0.279
LCR74 vs LV162	16.1	6.34	Yes	***	5.00 to 27.2
LCR74 vs LV164	14.3	5.63	Yes	***	3.19 to 25.4
LCR74 vs LV165	5.9	2.32	No	ns	-5.21 to 17.0
LCR74 vs LV167	-3.33	1.31	No	ns	-14.4 to 7.78
LCR74 vs LV168	10.7	4.23	No	ns	-0.373 to 21.9
LCR74 vs LV176	-26.7	10.5	Yes	***	-37.8 to -15.5
LCR74 vs CV125(L)	-23.2	9.14	Yes	***	-34.3 to -12.1
LCR74 vs CV126(L)	2.23	0.88	No	ns	-8.88 to 13.3
LCR74 vs CV130	-17.5	6.88	Yes	***	-28.6 to -6.36
LCR74 vs LV180	-8.41	3.31	No	ns	-19.5 to 2.70
LCR74 vs LV183	-7.25	2.85	No	ns	-18.4 to 3.87
LCR75 vs LCR76	-12.9	5.1	Yes	**	-24.1 to -1.83
LCR75 vs LCR77	-11.4	4.5	Yes	*	-22.5 to -0.321
LCR75 vs LCR78	-12.7	5	Yes	**	-23.8 to -1.58
LCR75 vs LCR131	-28	11	Yes	***	-39.1 to -16.9
LCR75 vs LCR135	-24.1	9.49	Yes	***	-35.2 to -13.0
LCR75 vs LV134	-1.31	0.517	No	ns	-12.4 to 9.80
LCR75 vs LV136	-1.53	0.601	No	ns	-12.6 to 9.59
LCR75 vs LV138	5.75	2.26	No	ns	-5.37 to 16.9

LCR75 vs LV139	-3.62	1.43	No	ns	-14.7 to 7.49
LCR75 vs LV140	-5.54	2.18	No	ns	-16.7 to 5.57
LCR75 vs LV141	3.87	1.53	No	ns	-7.24 to 15.0
LCR75 vs LV142	13.2	5.2	Yes	**	2.09 to 24.3
LCR75 vs LV143	-9.25	3.64	No	ns	-20.4 to 1.86
LCR75 vs LV144	-6.26	2.47	No	ns	-17.4 to 4.85
LCR75 vs LV145	-16.8	6.62	Yes	***	-27.9 to -5.70
LCR75 vs LV146	23.3	9.19	Yes	***	12.2 to 34.4
LCR75 vs LV161	-2.09	0.824	No	ns	-13.2 to 9.02
LCR75 vs LV163	-10.3	4.06	No	ns	-21.4 to 0.813
LCR75 vs LV162	16.6	6.55	Yes	***	5.53 to 27.8
LCR75 vs LV164	14.8	5.84	Yes	***	3.72 to 25.9
LCR75 vs LV165	6.43	2.53	No	ns	-4.68 to 17.5
LCR75 vs LV167	-2.8	1.1	No	ns	-13.9 to 8.31
LCR75 vs LV168	11.3	4.44	Yes	*	0.161 to 22.4
LCR75 vs LV176	-26.1	10.3	Yes	***	-37.2 to -15.0
LCR75 vs CV125(L)	-22.7	8.93	Yes	***	-33.8 to -11.6
LCR75 vs CV126(L)	2.77	1.09	No	ns	-8.35 to 13.9
LCR75 vs CV130	-16.9	6.67	Yes	***	-28.1 to -5.83
LCR75 vs LV180	-7.88	3.1	No	ns	-19.0 to 3.23
LCR75 vs LV183	-6.71	2.64	No	ns	-17.8 to 4.40
LCR76 vs LCR77	1.51	0.593	No	ns	-9.61 to 12.6
LCR76 vs LCR78	0.247	0.0971	No	ns	-10.9 to 11.4
LCR76 vs LCR131	-15.1	5.93	Yes	***	-26.2 to -3.95
LCR76 vs LCR135	-11.2	4.4	Yes	*	-22.3 to -0.0540
LCR76 vs LV134	11.6	4.58	Yes	*	0.514 to 22.7
LCR76 vs LV136	11.4	4.49	Yes	*	0.301 to 22.5

LCR76 vs LV138	18.7	7.36	Yes	***	7.57 to 29.8
LCR76 vs LV139	9.32	3.67	No	ns	-1.79 to 20.4
LCR76 vs LV140	7.4	2.91	No	ns	-3.71 to 18.5
LCR76 vs LV141	16.8	6.62	Yes	***	5.70 to 27.9
LCR76 vs LV142	26.1	10.3	Yes	***	15.0 to 37.3
LCR76 vs LV143	3.69	1.45	No	ns	-7.43 to 14.8
LCR76 vs LV144	6.68	2.63	No	ns	-4.43 to 17.8
LCR76 vs LV145	-3.87	1.53	No	ns	-15.0 to 7.24
LCR76 vs LV146	36.3	14.3	Yes	***	25.2 to 47.4
LCR76 vs LV161	10.8	4.27	No	ns	-0.266 to 22.0
LCR76 vs LV163	2.64	1.04	No	ns	-8.47 to 13.8
LCR76 vs LV162	29.6	11.7	Yes	***	18.5 to 40.7
LCR76 vs LV164	27.8	10.9	Yes	***	16.7 to 38.9
LCR76 vs LV165	19.4	7.63	Yes	***	8.26 to 30.5
LCR76 vs LV167	10.1	3.99	No	ns	-0.973 to 21.3
LCR76 vs LV168	24.2	9.54	Yes	***	13.1 to 35.3
LCR76 vs LV176	-13.2	5.19	Yes	**	-24.3 to -2.07
LCR76 vs CV125(L)	-9.73	3.83	No	ns	-20.8 to 1.39
LCR76 vs CV126(L)	15.7	6.19	Yes	***	4.59 to 26.8
LCR76 vs CV130	-4	1.58	No	ns	-15.1 to 7.11
LCR76 vs LV180	5.06	1.99	No	ns	-6.05 to 16.2
LCR76 vs LV183	6.23	2.45	No	ns	-4.89 to 17.3
LCR77 vs LCR78	-1.26	0.496	No	ns	-12.4 to 9.85
LCR77 vs LCR131	-16.6	6.52	Yes	***	-27.7 to -5.45
LCR77 vs LCR135	-12.7	4.99	Yes	**	-23.8 to -1.56
LCR77 vs LV134	10.1	3.99	No	ns	-0.993 to 21.2
LCR77 vs LV136	9.91	3.9	No	ns	-1.21 to 21.0

LCR77 vs LV138	17.2	6.77	Yes	***	6.07 to 28.3
LCR77 vs LV139	7.81	3.08	No	ns	-3.30 to 18.9
LCR77 vs LV140	5.89	2.32	No	ns	-5.22 to 17.0
LCR77 vs LV141	15.3	6.03	Yes	***	4.19 to 26.4
LCR77 vs LV142	24.6	9.7	Yes	***	13.5 to 35.8
LCR77 vs LV143	2.18	0.859	No	ns	-8.93 to 13.3
LCR77 vs LV144	5.17	2.04	No	ns	-5.94 to 16.3
LCR77 vs LV145	-5.38	2.12	No	ns	-16.5 to 5.73
LCR77 vs LV146	34.8	13.7	Yes	***	23.7 to 45.9
LCR77 vs LV161	9.34	3.68	No	ns	-1.77 to 20.5
LCR77 vs LV163	1.13	0.446	No	ns	-9.98 to 12.2
LCR77 vs LV162	28.1	11.1	Yes	***	17.0 to 39.2
LCR77 vs LV164	26.3	10.3	Yes	***	15.2 to 37.4
LCR77 vs LV165	17.9	7.04	Yes	***	6.75 to 29.0
LCR77 vs LV167	8.63	3.4	No	ns	-2.48 to 19.7
LCR77 vs LV168	22.7	8.94	Yes	***	11.6 to 33.8
LCR77 vs LV176	-14.7	5.78	Yes	***	-25.8 to -3.57
LCR77 vs CV125(L)	-11.2	4.42	Yes	*	-22.3 to -0.121
LCR77 vs CV126(L)	14.2	5.59	Yes	***	3.09 to 25.3
LCR77 vs CV130	-5.51	2.17	No	ns	-16.6 to 5.61
LCR77 vs LV180	3.55	1.4	No	ns	-7.56 to 14.7
LCR77 vs LV183	4.72	1.86	No	ns	-6.39 to 15.8
LCR78 vs LCR131	-15.3	6.03	Yes	***	-26.4 to -4.19
LCR78 vs LCR135	-11.4	4.49	Yes	*	-22.5 to -0.301
LCR78 vs LV134	11.4	4.48	Yes	*	0.267 to 22.5
LCR78 vs LV136	11.2	4.4	Yes	*	0.0539 to 22.3
LCR78 vs LV138	18.4	7.26	Yes	***	7.33 to 29.6

LCR78 vs LV139	9.07	3.57	No	ns	-2.04 to 20.2
LCR78 vs LV140	7.15	2.82	No	ns	-3.96 to 18.3
LCR78 vs LV141	16.6	6.52	Yes	***	5.45 to 27.7
LCR78 vs LV142	25.9	10.2	Yes	***	14.8 to 37.0
LCR78 vs LV143	3.44	1.35	No	ns	-7.67 to 14.6
LCR78 vs LV144	6.43	2.53	No	ns	-4.68 to 17.5
LCR78 vs LV145	-4.12	1.62	No	ns	-15.2 to 6.99
LCR78 vs LV146	36	14.2	Yes	***	24.9 to 47.1
LCR78 vs LV161	10.6	4.17	No	ns	-0.513 to 21.7
LCR78 vs LV163	2.39	0.943	No	ns	-8.72 to 13.5
LCR78 vs LV162	29.3	11.6	Yes	***	18.2 to 40.5
LCR78 vs LV164	27.5	10.8	Yes	***	16.4 to 38.6
LCR78 vs LV165	19.1	7.53	Yes	***	8.01 to 30.2
LCR78 vs LV167	9.89	3.9	No	ns	-1.22 to 21.0
LCR78 vs LV168	24	9.44	Yes	***	12.9 to 35.1
LCR78 vs LV176	-13.4	5.29	Yes	**	-24.5 to -2.31
LCR78 vs CV125(L)	-9.97	3.93	No	ns	-21.1 to 1.14
LCR78 vs CV126(L)	15.5	6.09	Yes	***	4.35 to 26.6
LCR78 vs CV130	-4.25	1.67	No	ns	-15.4 to 6.87
LCR78 vs LV180	4.81	1.9	No	ns	-6.30 to 15.9
LCR78 vs LV183	5.98	2.36	No	ns	-5.13 to 17.1
LCR131 vs LCR135	3.89	1.53	No	ns	-7.22 to 15.0
LCR131 vs LV134	26.7	10.5	Yes	***	15.6 to 37.8
LCR131 vs LV136	26.5	10.4	Yes	***	15.4 to 37.6
LCR131 vs LV138	33.7	13.3	Yes	***	22.6 to 44.9
LCR131 vs LV139	24.4	9.6	Yes	***	13.3 to 35.5
LCR131 vs LV140	22.5	8.85	Yes	***	11.3 to 33.6

LCR131 vs LV141	31.9	12.6	Yes	***	20.8 to 43.0
LCR131 vs LV142	41.2	16.2	Yes	***	30.1 to 52.3
LCR131 vs LV143	18.7	7.38	Yes	***	7.63 to 29.9
LCR131 vs LV144	21.7	8.56	Yes	***	10.6 to 32.9
LCR131 vs LV145	11.2	4.41	Yes	*	0.0739 to 22.3
LCR131 vs LV146	51.3	20.2	Yes	***	40.2 to 62.4
LCR131 vs LV161	25.9	10.2	Yes	***	14.8 to 37.0
LCR131 vs LV163	17.7	6.97	Yes	***	6.59 to 28.8
LCR131 vs LV162	44.6	17.6	Yes	***	33.5 to 55.8
LCR131 vs LV164	42.8	16.9	Yes	***	31.7 to 53.9
LCR131 vs LV165	34.4	13.6	Yes	***	23.3 to 45.5
LCR131 vs LV167	25.2	9.92	Yes	***	14.1 to 36.3
LCR131 vs LV168	39.3	15.5	Yes	***	28.2 to 50.4
LCR131 vs LV176	1.88	0.74	No	ns	-9.23 to 13.0
LCR131 vs CV125(L)	5.33	2.1	No	ns	-5.78 to 16.4
LCR131 vs CV126(L)	30.8	12.1	Yes	***	19.7 to 41.9
LCR131 vs CV130	11.1	4.36	No	ns	-0.0527 to 22.2
LCR131 vs LV180	20.1	7.92	Yes	***	9.01 to 31.2
LCR131 vs LV183	21.3	8.38	Yes	***	10.2 to 32.4
LCR135 vs LV134	22.8	8.98	Yes	***	11.7 to 33.9
LCR135 vs LV136	22.6	8.89	Yes	***	11.5 to 33.7
LCR135 vs LV138	29.9	11.8	Yes	***	18.7 to 41.0
LCR135 vs LV139	20.5	8.07	Yes	***	9.37 to 31.6
LCR135 vs LV140	18.6	7.31	Yes	***	7.45 to 29.7
LCR135 vs LV141	28	11	Yes	***	16.9 to 39.1
LCR135 vs LV142	37.3	14.7	Yes	***	26.2 to 48.4
LCR135 vs LV143	14.9	5.85	Yes	***	3.74 to 26.0

LCR135 vs LV144	17.8	7.03	Yes	***	6.73 to 29.0
LCR135 vs LV145	7.29	2.87	No	ns	-3.82 to 18.4
LCR135 vs LV146	47.4	18.7	Yes	***	36.3 to 58.6
LCR135 vs LV161	22	8.67	Yes	***	10.9 to 33.1
LCR135 vs LV163	13.8	5.44	Yes	***	2.69 to 24.9
LCR135 vs LV162	40.8	16	Yes	***	29.6 to 51.9
LCR135 vs LV164	38.9	15.3	Yes	***	27.8 to 50.1
LCR135 vs LV165	30.5	12	Yes	***	19.4 to 41.7
LCR135 vs LV167	21.3	8.39	Yes	***	10.2 to 32.4
LCR135 vs LV168	35.4	13.9	Yes	***	24.3 to 46.5
LCR135 vs LV176	-2.01	0.793	No	ns	-13.1 to 9.10
LCR135 vs CV125(L)	1.44	0.567	No	ns	-9.67 to 12.6
LCR135 vs CV126(L)	26.9	10.6	Yes	***	15.8 to 38.0
LCR135 vs CV130	7.17	2.82	No	ns	-3.95 to 18.3
LCR135 vs LV180	16.2	6.39	Yes	***	5.11 to 27.3
LCR135 vs LV183	17.4	6.85	Yes	***	6.28 to 28.5
LV134 vs LV136	-0.213	0.084	No	ns	-11.3 to 10.9
LV134 vs LV138	7.06	2.78	No	ns	-4.05 to 18.2
LV134 vs LV139	-2.31	0.908	No	ns	-13.4 to 8.81
LV134 vs LV140	-4.23	1.66	No	ns	-15.3 to 6.89
LV134 vs LV141	5.19	2.04	No	ns	-5.93 to 16.3
LV134 vs LV142	14.5	5.72	Yes	***	3.41 to 25.6
LV134 vs LV143	-7.94	3.13	No	ns	-19.1 to 3.17
LV134 vs LV144	-4.95	1.95	No	ns	-16.1 to 6.17
LV134 vs LV145	-15.5	6.1	Yes	***	-26.6 to -4.39
LV134 vs LV146	24.6	9.71	Yes	***	13.5 to 35.8
LV134 vs LV161	-0.78	0.307	No	ns	-11.9 to 10.3

LV134 vs LV163	-8.99	3.54	No	ns	-20.1 to 2.13
LV134 vs LV162	18	7.07	Yes	***	6.84 to 29.1
LV134 vs LV164	16.1	6.36	Yes	***	5.03 to 27.3
LV134 vs LV165	7.75	3.05	No	ns	-3.37 to 18.9
LV134 vs LV167	-1.49	0.585	No	ns	-12.6 to 9.63
LV134 vs LV168	12.6	4.96	Yes	**	1.47 to 23.7
LV134 vs LV176	-24.8	9.77	Yes	***	-35.9 to -13.7
LV134 vs CV125(L)	-21.4	8.41	Yes	***	-32.5 to -10.2
LV134 vs CV126(L)	4.08	1.61	No	ns	-7.03 to 15.2
LV134 vs CV130	-15.6	6.15	Yes	***	-26.7 to -4.51
LV134 vs LV180	-6.57	2.59	No	ns	-17.7 to 4.55
LV134 vs LV183	-5.4	2.13	No	ns	-16.5 to 5.71
LV136 vs LV138	7.27	2.86	No	ns	-3.84 to 18.4
LV136 vs LV139	-2.09	0.824	No	ns	-13.2 to 9.02
LV136 vs LV140	-4.01	1.58	No	ns	-15.1 to 7.10
LV136 vs LV141	5.4	2.13	No	ns	-5.71 to 16.5
LV136 vs LV142	14.7	5.8	Yes	***	3.62 to 25.8
LV136 vs LV143	-7.73	3.04	No	ns	-18.8 to 3.39
LV136 vs LV144	-4.73	1.86	No	ns	-15.8 to 6.38
LV136 vs LV145	-15.3	6.02	Yes	***	-26.4 to -4.17
LV136 vs LV146	24.9	9.79	Yes	***	13.7 to 36.0
LV136 vs LV161	-0.567	0.223	No	ns	-11.7 to 10.5
LV136 vs LV163	-8.77	3.46	No	ns	-19.9 to 2.34
LV136 vs LV162	18.2	7.16	Yes	***	7.06 to 29.3
LV136 vs LV164	16.4	6.44	Yes	***	5.25 to 27.5
LV136 vs LV165	7.96	3.13	No	ns	-3.15 to 19.1
LV136 vs LV167	-1.27	0.501	No	ns	-12.4 to 9.84

LV136 vs LV168	12.8	5.04	Yes	**	1.69 to 23.9
LV136 vs LV176	-24.6	9.69	Yes	***	-35.7 to -13.5
LV136 vs CV125(L)	-21.1	8.33	Yes	***	-32.3 to -10.0
LV136 vs CV126(L)	4.29	1.69	No	ns	-6.82 to 15.4
LV136 vs CV130	-15.4	6.07	Yes	***	-26.5 to -4.30
LV136 vs LV180	-6.35	2.5	No	ns	-17.5 to 4.76
LV136 vs LV183	-5.19	2.04	No	ns	-16.3 to 5.93
LV138 vs LV139	-9.37	3.69	No	ns	-20.5 to 1.75
LV138 vs LV140	-11.3	4.44	Yes	*	-22.4 to -0.174
LV138 vs LV141	-1.87	0.738	No	ns	-13.0 to 9.24
LV138 vs LV142	7.46	2.94	No	ns	-3.65 to 18.6
LV138 vs LV143	-15	5.91	Yes	***	-26.1 to -3.89
LV138 vs LV144	-12	4.73	Yes	*	-23.1 to -0.894
LV138 vs LV145	-22.6	8.88	Yes	***	-33.7 to -11.4
LV138 vs LV146	17.6	6.93	Yes	***	6.47 to 28.7
LV138 vs LV161	-7.84	3.09	No	ns	-19.0 to 3.27
LV138 vs LV163	-16	6.32	Yes	***	-27.2 to -4.93
LV138 vs LV162	10.9	4.29	No	ns	-0.215 to 22.0
LV138 vs LV164	9.09	3.58	No	ns	-2.03 to 20.2
LV138 vs LV165	0.687	0.27	No	ns	-10.4 to 11.8
LV138 vs LV167	-8.55	3.37	No	ns	-19.7 to 2.57
LV138 vs LV168	5.53	2.18	No	ns	-5.59 to 16.6
LV138 vs LV176	-31.9	12.5	Yes	***	-43.0 to -20.8
LV138 vs CV125(L)	-28.4	11.2	Yes	***	-39.5 to -17.3
LV138 vs CV126(L)	-2.98	1.17	No	ns	-14.1 to 8.13
LV138 vs CV130	-22.7	8.93	Yes	***	-33.8 to -11.6
LV138 vs LV180	-13.6	5.37	Yes	***	-24.7 to -2.51

LV138 vs LV183	-12.5	4.91	Yes	**	-23.6 to -1.35
LV139 vs LV140	-1.92	0.756	No	ns	-13.0 to 9.19
LV139 vs LV141	7.49	2.95	No	ns	-3.62 to 18.6
LV139 vs LV142	16.8	6.63	Yes	***	5.71 to 27.9
LV139 vs LV143	-5.63	2.22	No	ns	-16.7 to 5.48
LV139 vs LV144	-2.64	1.04	No	ns	-13.8 to 8.47
LV139 vs LV145	-13.2	5.2	Yes	**	-24.3 to -2.08
LV139 vs LV146	27	10.6	Yes	***	15.8 to 38.1
LV139 vs LV161	1.53	0.601	No	ns	-9.59 to 12.6
LV139 vs LV163	-6.68	2.63	No	ns	-17.8 to 4.43
LV139 vs LV162	20.3	7.98	Yes	***	9.15 to 31.4
LV139 vs LV164	18.5	7.27	Yes	***	7.34 to 29.6
LV139 vs LV165	10.1	3.96	No	ns	-1.06 to 21.2
LV139 vs LV167	0.82	0.323	No	ns	-10.3 to 11.9
LV139 vs LV168	14.9	5.87	Yes	***	3.78 to 26.0
LV139 vs LV176	-22.5	8.86	Yes	***	-33.6 to -11.4
LV139 vs CV125(L)	-19	7.5	Yes	***	-30.2 to -7.93
LV139 vs CV126(L)	6.39	2.52	No	ns	-4.73 to 17.5
LV139 vs CV130	-13.3	5.25	Yes	**	-24.4 to -2.21
LV139 vs LV180	-4.26	1.68	No	ns	-15.4 to 6.85
LV139 vs LV183	-3.09	1.22	No	ns	-14.2 to 8.02
LV140 vs LV141	9.41	3.71	No	ns	-1.70 to 20.5
LV140 vs LV142	18.7	7.38	Yes	***	7.63 to 29.9
LV140 vs LV143	-3.71	1.46	No	ns	-14.8 to 7.40
LV140 vs LV144	-0.72	0.284	No	ns	-11.8 to 10.4
LV140 vs LV145	-11.3	4.44	Yes	*	-22.4 to -0.161
LV140 vs LV146	28.9	11.4	Yes	***	17.8 to 40.0

LV140 vs LV161	3.45	1.36	No	ns	-7.67 to 14.6
LV140 vs LV163	-4.76	1.87	No	ns	-15.9 to 6.35
LV140 vs LV162	22.2	8.74	Yes	***	11.1 to 33.3
LV140 vs LV164	20.4	8.02	Yes	***	9.26 to 31.5
LV140 vs LV165	12	4.72	Yes	*	0.861 to 23.1
LV140 vs LV167	2.74	1.08	No	ns	-8.37 to 13.9
LV140 vs LV168	16.8	6.62	Yes	***	5.70 to 27.9
LV140 vs LV176	-20.6	8.1	Yes	***	-31.7 to -9.47
LV140 vs CV125(L)	-17.1	6.74	Yes	***	-28.2 to -6.01
LV140 vs CV126(L)	8.31	3.27	No	ns	-2.81 to 19.4
LV140 vs CV130	-11.4	4.49	Yes	*	-22.5 to -0.287
LV140 vs LV180	-2.34	0.922	No	ns	-13.5 to 8.77
LV140 vs LV183	-1.17	0.462	No	ns	-12.3 to 9.94
LV141 vs LV142	9.33	3.68	No	ns	-1.78 to 20.4
LV141 vs LV143	-13.1	5.17	Yes	**	-24.2 to -2.01
LV141 vs LV144	-10.1	3.99	No	ns	-21.2 to 0.979
LV141 vs LV145	-20.7	8.15	Yes	***	-31.8 to -9.57
LV141 vs LV146	19.5	7.66	Yes	***	8.35 to 30.6
LV141 vs LV161	-5.97	2.35	No	ns	-17.1 to 5.15
LV141 vs LV163	-14.2	5.58	Yes	***	-25.3 to -3.06
LV141 vs LV162	12.8	5.03	Yes	**	1.66 to 23.9
LV141 vs LV164	11	4.32	No	ns	-0.153 to 22.1
LV141 vs LV165	2.56	1.01	No	ns	-8.55 to 13.7
LV141 vs LV167	-6.67	2.63	No	ns	-17.8 to 4.44
LV141 vs LV168	7.4	2.91	No	ns	-3.71 to 18.5
LV141 vs LV176	-30	11.8	Yes	***	-41.1 to -18.9
LV141 vs CV125(L)	-26.5	10.5	Yes	***	-37.7 to -15.4

LV141 vs CV126(L)	-1.11	0.436	No	ns	-12.2 to 10.0
LV141 vs CV130	-20.8	8.2	Yes	***	-31.9 to -9.70
LV141 vs LV180	-11.8	4.63	Yes	*	-22.9 to -0.641
LV141 vs LV183	-10.6	4.17	No	ns	-21.7 to 0.526
LV142 vs LV143	-22.5	8.85	Yes	***	-33.6 to -11.3
LV142 vs LV144	-19.5	7.67	Yes	***	-30.6 to -8.35
LV142 vs LV145	-30	11.8	Yes	***	-41.1 to -18.9
LV142 vs LV146	10.1	3.99	No	ns	-0.986 to 21.2
LV142 vs LV161	-15.3	6.03	Yes	***	-26.4 to -4.19
LV142 vs LV163	-23.5	9.26	Yes	***	-34.6 to -12.4
LV142 vs LV162	3.44	1.35	No	ns	-7.68 to 14.6
LV142 vs LV164	1.63	0.641	No	ns	-9.49 to 12.7
LV142 vs LV165	-6.77	2.67	No	ns	-17.9 to 4.34
LV142 vs LV167	-16	6.3	Yes	***	-27.1 to -4.89
LV142 vs LV168	-1.93	0.761	No	ns	-13.0 to 9.18
LV142 vs LV176	-39.3	15.5	Yes	***	-50.4 to -28.2
LV142 vs CV125(L)	-35.9	14.1	Yes	***	-47.0 to -24.8
LV142 vs CV126(L)	-10.4	4.11	No	ns	-21.6 to 0.673
LV142 vs CV130	-30.1	11.9	Yes	***	-41.3 to -19.0
LV142 vs LV180	-21.1	8.3	Yes	***	-32.2 to -9.97
LV142 vs LV183	-19.9	7.84	Yes	***	-31.0 to -8.81
LV143 vs LV144	2.99	1.18	No	ns	-8.12 to 14.1
LV143 vs LV145	-7.56	2.98	No	ns	-18.7 to 3.55
LV143 vs LV146	32.6	12.8	Yes	***	21.5 to 43.7
LV143 vs LV161	7.16	2.82	No	ns	-3.95 to 18.3
LV143 vs LV163	-1.05	0.412	No	ns	-12.2 to 10.1
LV143 vs LV162	25.9	10.2	Yes	***	14.8 to 37.0

LV143 vs LV164	24.1	9.49	Yes	***	13.0 to 35.2
LV143 vs LV165	15.7	6.18	Yes	***	4.57 to 26.8
LV143 vs LV167	6.45	2.54	No	ns	-4.66 to 17.6
LV143 vs LV168	20.5	8.08	Yes	***	9.41 to 31.6
LV143 vs LV176	-16.9	6.64	Yes	***	-28.0 to -5.75
LV143 vs CV125(L)	-13.4	5.28	Yes	**	-24.5 to -2.30
LV143 vs CV126(L)	12	4.73	Yes	*	0.907 to 23.1
LV143 vs CV130	-7.69	3.03	No	ns	-18.8 to 3.43
LV143 vs LV180	1.37	0.541	No	ns	-9.74 to 12.5
LV143 vs LV183	2.54	1	No	ns	-8.57 to 13.7
LV144 vs LV145	-10.6	4.16	No	ns	-21.7 to 0.559
LV144 vs LV146	29.6	11.7	Yes	***	18.5 to 40.7
LV144 vs LV161	4.17	1.64	No	ns	-6.95 to 15.3
LV144 vs LV163	-4.04	1.59	No	ns	-15.2 to 7.07
LV144 vs LV162	22.9	9.02	Yes	***	11.8 to 34.0
LV144 vs LV164	21.1	8.31	Yes	***	9.98 to 32.2
LV144 vs LV165	12.7	5	Yes	**	1.58 to 23.8
LV144 vs LV167	3.46	1.36	No	ns	-7.65 to 14.6
LV144 vs LV168	17.5	6.9	Yes	***	6.42 to 28.6
LV144 vs LV176	-19.9	7.82	Yes	***	-31.0 to -8.75
LV144 vs CV125(L)	-16.4	6.46	Yes	***	-27.5 to -5.29
LV144 vs CV126(L)	9.03	3.55	No	ns	-2.09 to 20.1
LV144 vs CV130	-10.7	4.21	No	ns	-21.8 to 0.433
LV144 vs LV180	-1.62	0.638	No	ns	-12.7 to 9.49
LV144 vs LV183	-0.453	0.179	No	ns	-11.6 to 10.7
LV145 vs LV146	40.1	15.8	Yes	***	29.0 to 51.3
LV145 vs LV161	14.7	5.8	Yes	***	3.61 to 25.8

LV145 vs LV163	6.51	2.57	No	ns	-4.60 to 17.6
LV145 vs LV162	33.5	13.2	Yes	***	22.3 to 44.6
LV145 vs LV164	31.6	12.5	Yes	***	20.5 to 42.8
LV145 vs LV165	23.2	9.16	Yes	***	12.1 to 34.4
LV145 vs LV167	14	5.52	Yes	***	2.90 to 25.1
LV145 vs LV168	28.1	11.1	Yes	***	17.0 to 39.2
LV145 vs LV176	-9.31	3.67	No	ns	-20.4 to 1.81
LV145 vs CV125(L)	-5.85	2.31	No	ns	-17.0 to 5.26
LV145 vs CV126(L)	19.6	7.71	Yes	***	8.47 to 30.7
LV145 vs CV130	-0.127	0.0499	No	ns	-11.2 to 11.0
LV145 vs LV180	8.93	3.52	No	ns	-2.18 to 20.0
LV145 vs LV183	10.1	3.98	No	ns	-1.01 to 21.2
LV146 vs LV161	-25.4	10	Yes	***	-36.5 to -14.3
LV146 vs LV163	-33.6	13.2	Yes	***	-44.7 to -22.5
LV146 vs LV162	-6.69	2.63	No	ns	-17.8 to 4.42
LV146 vs LV164	-8.5	3.35	No	ns	-19.6 to 2.61
LV146 vs LV165	-16.9	6.66	Yes	***	-28.0 to -5.79
LV146 vs LV167	-26.1	10.3	Yes	***	-37.2 to -15.0
LV146 vs LV168	-12.1	4.75	Yes	*	-23.2 to -0.947
LV146 vs LV176	-49.5	19.5	Yes	***	-60.6 to -38.3
LV146 vs CV125(L)	-46	18.1	Yes	***	-57.1 to -34.9
LV146 vs CV126(L)	-20.6	8.1	Yes	***	-31.7 to -9.45
LV146 vs CV130	-40.3	15.9	Yes	***	-51.4 to -29.2
LV146 vs LV180	-31.2	12.3	Yes	***	-42.3 to -20.1
LV146 vs LV183	-30	11.8	Yes	***	-41.2 to -18.9
LV161 vs LV163	-8.21	3.23	No	ns	-19.3 to 2.91
LV161 vs LV162	18.7	7.38	Yes	***	7.62 to 29.9

LV161 vs LV164	16.9	6.67	Yes	***	5.81 to 28.0
LV161 vs LV165	8.53	3.36	No	ns	-2.59 to 19.6
LV161 vs LV167	-0.707	0.278	No	ns	-11.8 to 10.4
LV161 vs LV168	13.4	5.26	Yes	**	2.25 to 24.5
LV161 vs LV176	-24	9.46	Yes	***	-35.1 to -12.9
LV161 vs CV125(L)	-20.6	8.1	Yes	***	-31.7 to -9.46
LV161 vs CV126(L)	4.86	1.91	No	ns	-6.25 to 16.0
LV161 vs CV130	-14.8	5.85	Yes	***	-26.0 to -3.73
LV161 vs LV180	-5.79	2.28	No	ns	-16.9 to 5.33
LV161 vs LV183	-4.62	1.82	No	ns	-15.7 to 6.49
LV163 vs LV162	26.9	10.6	Yes	***	15.8 to 38.1
LV163 vs LV164	25.1	9.9	Yes	***	14.0 to 36.2
LV163 vs LV165	16.7	6.59	Yes	***	5.62 to 27.8
LV163 vs LV167	7.5	2.95	No	ns	-3.61 to 18.6
LV163 vs LV168	21.6	8.5	Yes	***	10.5 to 32.7
LV163 vs LV176	-15.8	6.23	Yes	***	-26.9 to -4.71
LV163 vs CV125(L)	-12.4	4.87	Yes	**	-23.5 to -1.25
LV163 vs CV126(L)	13.1	5.15	Yes	**	1.95 to 24.2
LV163 vs CV130	-6.64	2.61	No	ns	-17.8 to 4.47
LV163 vs LV180	2.42	0.953	No	ns	-8.69 to 13.5
LV163 vs LV183	3.59	1.41	No	ns	-7.53 to 14.7
LV162 vs LV164	-1.81	0.713	No	ns	-12.9 to 9.30
LV162 vs LV165	-10.2	4.02	No	ns	-21.3 to 0.902
LV162 vs LV167	-19.4	7.66	Yes	***	-30.6 to -8.33
LV162 vs LV168	-5.37	2.12	No	ns	-16.5 to 5.74
LV162 vs LV176	-42.8	16.8	Yes	***	-53.9 to -31.7
LV162 vs CV125(L)	-39.3	15.5	Yes	***	-50.4 to -28.2

LV162 vs CV126(L)	-13.9	5.47	Yes	***	-25.0 to -2.76
LV162 vs CV130	-33.6	13.2	Yes	***	-44.7 to -22.5
LV162 vs LV180	-24.5	9.66	Yes	***	-35.6 to -13.4
LV162 vs LV183	-23.4	9.2	Yes	***	-34.5 to -12.2
LV164 vs LV165	-8.4	3.31	No	ns	-19.5 to 2.71
LV164 vs LV167	-17.6	6.94	Yes	***	-28.7 to -6.52
LV164 vs LV168	-3.56	1.4	No	ns	-14.7 to 7.55
LV164 vs LV176	-41	16.1	Yes	***	-52.1 to -29.8
LV164 vs CV125(L)	-37.5	14.8	Yes	***	-48.6 to -26.4
LV164 vs CV126(L)	-12.1	4.75	Yes	*	-23.2 to -0.954
LV164 vs CV130	-31.8	12.5	Yes	***	-42.9 to -20.7
LV164 vs LV180	-22.7	8.94	Yes	***	-33.8 to -11.6
LV164 vs LV183	-21.5	8.49	Yes	***	-32.7 to -10.4
LV165 vs LV167	-9.23	3.64	No	ns	-20.3 to 1.88
LV165 vs LV168	4.84	1.91	No	ns	-6.27 to 16.0
LV165 vs LV176	-32.6	12.8	Yes	***	-43.7 to -21.4
LV165 vs CV125(L)	-29.1	11.5	Yes	***	-40.2 to -18.0
LV165 vs CV126(L)	-3.67	1.44	No	ns	-14.8 to 7.45
LV165 vs CV130	-23.4	9.2	Yes	***	-34.5 to -12.3
LV165 vs LV180	-14.3	5.64	Yes	***	-25.4 to -3.20
LV165 vs LV183	-13.1	5.18	Yes	**	-24.3 to -2.03
LV167 vs LV168	14.1	5.54	Yes	***	2.96 to 25.2
LV167 vs LV176	-23.3	9.18	Yes	***	-34.4 to -12.2
LV167 vs CV125(L)	-19.9	7.82	Yes	***	-31.0 to -8.75
LV167 vs CV126(L)	5.57	2.19	No	ns	-5.55 to 16.7
LV167 vs CV130	-14.1	5.57	Yes	***	-25.3 to -3.03
LV167 vs LV180	-5.08	2	No	ns	-16.2 to 6.03

LV167 vs LV183	-3.91	1.54	No	ns	-15.0 to 7.20
LV168 vs LV176	-37.4	14.7	Yes	***	-48.5 to -26.3
LV168 vs CV125(L)	-33.9	13.4	Yes	***	-45.1 to -22.8
LV168 vs CV126(L)	-8.51	3.35	No	ns	-19.6 to 2.61
LV168 vs CV130	-28.2	11.1	Yes	***	-39.3 to -17.1
LV168 vs LV180	-19.2	7.54	Yes	***	-30.3 to -8.04
LV168 vs LV183	-18	7.08	Yes	***	-29.1 to -6.87
LV176 vs CV125(L)	3.45	1.36	No	ns	-7.66 to 14.6
LV176 vs CV126(L)	28.9	11.4	Yes	***	17.8 to 40.0
LV176 vs CV130	9.18	3.62	No	ns	-1.93 to 20.3
LV176 vs LV180	18.2	7.18	Yes	***	7.13 to 29.4
LV176 vs LV183	19.4	7.64	Yes	***	8.29 to 30.5
CV125(L) vs CV126(L)	25.4	10	Yes	***	14.3 to 36.5
CV125(L) vs CV130	5.73	2.26	No	ns	-5.39 to 16.8
CV125(L) vs LV180	14.8	5.82	Yes	***	3.67 to 25.9
CV125(L) vs LV183	16	6.28	Yes	***	4.84 to 27.1
CV126(L) vs CV130	-19.7	7.76	Yes	***	-30.8 to -8.59
CV126(L) vs LV180	-10.6	4.19	No	ns	-21.8 to 0.466
CV126(L) vs LV183	-9.48	3.73	No	ns	-20.6 to 1.63
CV130 vs LV180	9.06	3.57	No	ns	-2.05 to 20.2
CV130 vs LV183	10.2	4.03	No	ns	-0.886 to 21.3
LV180 vs LV183	1.17	0.459	No	ns	-9.95 to 12.3

Addendum C: Chapter 5 supporting data tables for Fluorescence and UV graphs

4. Fluorescence data of Plasma and Plasma containing drug with concentrations of 30-1 µg/ml with increments of 5 µg/ml.

4.1. Rifampicin

Wavelength	**plasma**	**1 µg/ml**	**5 µg/ml**	**10 µg/ml**	**15 µg/ml**	**20 µg/ml**	**25 µg/ml**	**30 µg/ml**
300	39597	37843	37866	34462	33695	31023	23698	26824
310	45012	42281	42983	38514	37343	34654	29152	29208
320	46028	43431	43292	39273	37298	35007	30712	29588
330	44984	42175	42214	37987	36304	33346	30035	28220
340	40923	38709	38511	34653	32948	30698	27193	25810
350	32997	31227	31408	28367	27058	25269	21893	21392
360	25106	23653	23831	21747	20859	19537	16119	16617
370	17831	16865	17156	15669	14971	14196	11465	12121
380	12054	11419	11637	10663	10319	9643	7681	8300
390	7854	7525	7591	7014	6734	6379	4987	5479
400	5134	4855	4964	4554	4414	4159	3237	3630
410	3226	3075	3109	2869	2792	2618	2033	2271
420	2067	1953	1981	1837	1795	1680	1312	1456
430	1312	1250	1255	1154	1144	1066	849	905
440	880	823	837	760	756	683	573	610
450	595	577	606	526	516	473	433	423
460	437	379	421	391	376	338	306	300
470	290	302	306	267	257	235	234	228
480	251	240	230	216	218	200	185	180
490	207	186	195	182	180	169	170	144
500	171	160	163	147	162	146	161	115
510	152	143	135	146	145	130	137	109
520	143	129	136	129	124	111	129	98
530	104	89	109	101	113	101	105	86
540	107	79	104	95	85	78	98	80
550	84	75	66	81	75	78	94	73

560	64	56	54	56	74	62	72	69
570	62	57	67	56	47	61	47	52
580	58	49	49	41	50	62	56	54
590	34	31	30	42	36	48	47	56
600	23	44	48	48	29	47	29	41
610	23	31	25	31	31	31	31	54
620	36	24	14	36	23	18	30	20
630	18	17	32	12	37	8	22	21
640	4	0	12	43	25	0	0	39
650	0	33	12	6	25	29	0	52
660	18	0	19	0	13	26	21	0
670	13	7	0	0	0	0	35	9
680	26	11	35	18	3	64	0	0
690	57	47	0	0	0	39	0	7
700	10	0	10	12	0	26	0	0

4.2. 25-desacetyl rifampicin

Wavelength	**PLASMA**	**1 µg/ml**	**5 µg/ml**	**10 µg/ml**	**15 µg/ml**	**20 µg/ml**	**25 µg/ml**	**30 µg/ml**
300	39186	25029	23982	23698	22956	22230	22415	20200
310	49771	28141	26560	26232	25682	25328	24821	22496
320	53168	28931	27184	27040	26642	25704	25613	22957
330	51647	28226	26579	26600	25762	24946	24850	22326
340	47162	25647	24471	24186	23669	22975	22744	20621
350	37194	20981	19611	19737	19146	18863	18576	16767
360	27731	15832	14887	15123	14620	14386	14276	12899
370	19479	11239	10663	10686	10384	10331	10248	9281
380	12987	7616	7137	7218	7106	6975	6880	6247
390	8387	4991	4669	4757	4639	4586	4539	4129
400	5391	3241	3134	3138	3093	3001	2987	2694
410	3391	2063	1945	1962	1914	1897	1877	1711
420	2172	1319	1285	1246	1241	1234	1222	1089
430	1369	837	800	799	776	780	785	724
440	955	568	562	536	539	531	530	468

450	683	412	387	377	380	376	359	356
460	493	273	282	278	270	284	268	230
470	376	193	199	189	193	191	191	195
480	298	169	169	156	157	157	156	160
490	266	135	123	132	141	130	129	123
500	246	117	108	113	118	122	113	127
510	220	96	90	98	102	112	109	108
520	174	86	89	85	96	85	119	94
530	149	76	68	78	90	90	91	94
540	138	73	62	62	76	84	61	78
550	127	54	51	74	73	81	65	64
560	110	38	34	50	63	70	65	64
570	90	20	21	34	37	48	52	62
580	74	37	11	32	43	39	54	43
590	57	23	20	31	32	39	36	26
600	42	18	16	21	29	46	33	50
610	46	6	15	22	39	52	48	26
620	47	0	12	13	12	25	36	28
630	32	22	27	15	14	44	27	0
640	16	5	43	12	0	9	33	15
650	16	17	8	41	0	0	48	23
660	15	0	36	9	10	6	34	0
670	0	0	17	22	9	0	23	8
680	28	0	7	0	11	0	22	15
690	15	0	4	34	25	0	9	0
700	0	0	25	0	37	0	0	0

4.3. Isoniazid

wavelength	**plasma**	**1 µg/ml**	**5 µg/ml**	**10 µg/ml**	**15 µg/ml**	**20 µg/ml**	**25 µg/ml**	**30 µg/ml**
300	38752	24185	23010	21562	19243	18903	17050	14759
310	47757	26938	25910	24332	21864	21060	19257	16481
320	50481	27607	26830	25167	22661	21981	19972	17314
330	49023	27141	26446	24848	22140	21549	19772	17067

340	44619	24746	24091	22707	20537	19763	17945	15708
350	35433	19962	19443	18513	16375	16050	14618	12549
360	26474	14895	14727	13641	12385	12056	10997	9404
370	18602	10680	10379	9749	8721	8493	7774	6808
380	12489	7309	7140	6579	5913	5799	5292	4551
390	8075	4741	4606	4288	3947	3799	3423	3022
400	5302	3122	3033	2814	2537	2495	2247	1997
410	3279	1944	1901	1775	1583	1581	1383	1273
420	2089	1241	1236	1151	1044	1015	913	848
430	1348	794	787	728	663	653	598	549
440	931	548	530	495	459	454	398	370
450	666	372	343	340	329	319	289	278
460	488	259	259	248	251	216	190	193
470	355	181	181	158	163	162	148	139
480	300	141	162	141	137	126	106	119
490	256	129	127	107	112	106	90	94
500	235	109	93	93	97	74	86	71
510	212	91	86	85	75	62	56	58
520	166	78	73	70	73	59	67	48
530	163	62	77	69	58	53	49	29
540	136	55	50	50	59	40	46	37
550	120	33	45	55	37	48	36	42
560	99	46	35	33	36	48	26	30
570	86	40	28	35	32	20	23	24
580	76	36	19	12	30	28	27	15
590	61	41	19	6	17	21	11	12
600	38	36	13	16	6	20	17	17
610	28	18	16	26	0	9	28	10
620	42	12	39	20	16	13	10	34
630	0	17	22	19	35	27	7	0
640	9	0	10	5	5	33	44	9
650	24	0	24	0	0	19	0	23
660	30	0	0	27	0	6	23	0
670	2	19	0	29	26	0	0	50
680	39	0	0	0	0	0	15	0

690	22	0	0	13	34	19	0	7
700	5	0	0	100	0	28	27	43

4.4. Ethambutol

wavelength	**plasma**	**1 µg/ml**	**5 µg/ml**	**10 µg/ml**	**15 µg/ml**	**20 µg/ml**	**25 µg/ml**	**30 µg/ml**
300	31098	28219	25373	25738	25188	24548	23456	23356
310	39084	32457	28693	28726	28564	28063	26545	26200
320	41906	33072	29769	29678	29245	28803	27224	27023
330	41206	32438	28851	29092	28276	28099	26470	26249
340	36939	29693	26564	26644	25890	25582	24173	24044
350	29466	24183	21286	21428	21083	20676	19517	19478
360	21805	17845	15944	16197	15720	15556	14695	14676
370	15442	12903	11372	11478	11248	11108	10512	10459
380	10307	8711	7702	7742	7642	7614	7138	7105
390	6677	5638	5050	5104	4961	4949	4675	4631
400	4337	3717	3308	3318	3241	3243	3057	3057
410	2693	2352	2081	2115	2066	2013	1901	1939
420	1737	1510	1344	1363	1327	1313	1244	1224
430	1127	954	866	853	856	852	806	790
440	760	645	566	591	557	559	540	517
450	539	471	434	384	400	398	369	362
460	412	330	263	279	271	278	264	269
470	294	227	209	206	198	190	184	194
480	256	186	163	174	150	157	157	145
490	221	149	127	140	132	129	125	127
500	193	120	107	115	121	103	105	106
510	175	107	94	94	94	103	89	85
520	166	90	97	88	92	80	76	78
530	138	70	74	57	67	72	62	68
540	120	66	56	50	63	59	42	66
550	82	60	58	48	50	55	50	55
560	92	54	43	45	16	39	36	52
570	73	51	37	36	29	36	34	27

580	57	41	40	31	34	36	24	33
590	42	10	12	5	35	19	44	23
600	44	45	14	43	28	9	15	35
610	27	7	10	19	31	15	15	34
620	48	23	34	19	0	4	39	5
630	42	6	28	1	0	0	13	1
640	20	8	3	9	9	20	24	4
650	0	20	0	0	7	0	15	8
660	0	29	48	22	26	14	40	5
670	14	0	34	0	32	4	0	30
680	8	55	6	34	9	43	4	8
690	17	0	20	0	0	0	4	21
700	21	12	0	63	31	21	0	15

4.5. Pyrazinamide

wavelength	**plasma**	**1 µg/ml**	**5 µg/ml**	**10 µg/ml**	**15 µg/ml**	**20 µg/ml**	**25 µg/ml**	**30 µg/ml**
300	33410	31435	25642	25559	22741	22356	20644	19064
310	38286	35099	32205	29109	25804	24706	23327	21231
320	38986	36346	34815	29651	26284	25809	23996	21778
330	38115	35720	33874	29196	25668	25276	23559	21209
340	34863	32612	30775	26818	23541	23191	21536	19457
350	28236	26358	24331	21428	18867	18844	17299	15644
360	21139	19865	18057	16290	14161	14058	13048	11828
370	15034	14098	12704	11463	10028	10030	9309	8347
380	10193	9604	8488	7805	6818	6808	6308	5704
390	6606	6264	5538	5107	4446	4420	4132	3710
400	4365	4131	3584	3323	2949	2898	2728	2434
410	2777	2553	2231	2110	1861	1829	1709	1548
420	1725	1674	1452	1372	1211	1191	1119	995
430	1132	1072	919	881	781	755	718	642
440	739	707	663	619	525	545	473	450
450	512	524	469	437	366	374	332	303
460	378	364	355	299	260	269	235	218

470	268	253	286	222	199	194	183	160
480	218	217	222	180	171	167	135	131
490	174	174	194	155	126	129	129	113
500	140	140	177	126	121	109	106	90
510	140	127	153	117	91	100	93	87
520	122	103	144	87	70	88	63	74
530	96	93	122	75	70	69	68	73
540	70	69	116	57	53	77	50	44
550	69	62	91	61	48	45	35	24
560	49	68	90	44	39	36	27	39
570	52	36	78	50	31	41	20	54
580	41	38	48	16	29	29	33	14
590	43	41	66	28	18	31	30	18
600	43	30	44	17	6	39	26	21
610	42	25	41	23	30	5	28	12
620	6	22	36	26	22	32	0	22
630	18	18	19	1	0	7	10	11
640	47	43	32	30	18	23	32	0
650	35	39	29	31	11	14	34	21
660	0	1	52	0	22	0	30	12
670	0	12	7	19	0	17	4	0
680	0	21	2	29	17	25	0	0
690	20	58	28	0	0	21	43	2
700	0	0	10	40	0	8	0	0

4.5. RIF-4 (combination of INH, RIF, ETH and PYR)

wavelength	**plasma**	**1 µg/ml**	**5 µg/ml**	**10 µg/ml**	**15 µg/ml**	**20 µg/ml**	**25 µg/ml**	**30 µg/ml**
300	35339	33386	32165	31237	29202	28586	24398	20631
310	43334	38006	35976	34894	32497	32131	27235	22930
320	45812	38763	37205	35816	33900	33069	27851	23529
330	44629	37972	36068	34824	32848	32243	27523	22981
340	40598	34609	33040	31991	30038	29483	25237	21017
350	32073	28034	26706	25954	24321	23708	20285	17040

360	24069	21077	20041	19696	18240	17812	15310	12893
370	16890	15041	14402	14027	13119	12745	10873	9180
380	11293	10163	9789	9525	8847	8635	7386	6296
390	7323	6645	6401	6240	5807	5699	4847	4134
400	4726	4333	4169	4087	3783	3675	3164	2694
410	2943	2769	2603	2602	2397	2339	1991	1697
420	1918	1779	1697	1633	1511	1529	1271	1115
430	1236	1113	1075	1058	985	948	819	686
440	853	756	739	697	659	652	554	489
450	621	524	507	486	475	454	384	366
460	458	373	366	360	332	313	265	236
470	354	263	253	245	235	218	204	164
480	293	207	200	192	185	178	156	137
490	247	180	165	172	155	158	132	119
500	221	150	146	128	122	120	96	96
510	205	134	116	117	118	112	92	88
520	188	106	110	102	97	89	79	69
530	155	84	78	82	83	80	81	64
540	134	90	77	67	78	77	47	46
550	119	80	60	71	55	56	54	41
560	101	52	56	47	41	44	35	37
570	81	47	33	55	31	62	33	28
580	65	34	32	44	38	50	24	25
590	53	33	31	40	38	34	12	22
600	56	31	10	12	15	31	16	24
610	38	3	8	23	28	7	25	17
620	40	27	6	26	25	32	29	25
630	0	29	11	21	0	7	12	9
640	25	13	0	12	12	7	10	0
650	13	7	4	4	4	13	0	26
660	0	0	0	0	18	5	0	33
670	32	31	6	30	18	0	15	34
680	0	14	0	0	0	0	22	3
690	92	56	7	16	12	37	0	4
700	0	0	27	0	8	15	0	1

4.2 Preparation of in-vitro drug sample to human plasma protein for UV spectroscopy analysis

Table 1: Absorbance spectroscopy data of Plasma, INH and Plasma with INH at different concentrations ranging from 30 µg/ml-1 µg/ml by increments of 5 µg/ml

wavelength [nm]	plasma	inh	inh 1µg/ml	inh 5µg/ml	inh 10µg/ml	inh 15µg/ml	inh 20µg/ml	inh 25µg/ml	inh 30µg/ml
220	0.647	-1.253	-0.929	-1.002	-1.321	0.647	-0.33	-1.406	-0.44
222	0.856	-0.972	-0.316	-0.697	-1.157	-0.647	0.425	-1.022	0.856
224	-0.9	0.114	-1.168	-1.701	-1.405	-1.201	-1.224	-1.182	-0.983
226	-0.522	-0.586	0.323	0.323	0.323	0.323	0.323	-0.955	0.323
228	-0.35	-0.993	-0.333	-0.208	-0.397	0.14	-0.377	-0.651	-0.265
230	0.134	-0.173	0.134	-0.096	0.134	0.134	0.134	-0.345	0.134
232	0.226	-0.486	0.226	-0.24	0.226	0.226	0.226	-0.194	0.226
234	0	-1.05	0	-0.572	0	0	0	0	0
236	0.064	-0.293	0.064	0.064	-0.231	0.064	0.064	0.064	0.064
238	0.354	0.261	0.354	0.132	-0.055	0.354	0.354	-0.25	0.354
240	0.169	0.124	0.386	-0.233	0.275	0.033	-0.182	-0.306	-0.179
242	0.025	0.025	-0.004	0.025	0.025	0.025	0.025	0.025	-0.01
244	0	-0.294	0	-0.504	-0.287	0	0	0	0
246	0	0	0	0	0	0	0	0	0
248	0	-0.113	0	-0.053	0	0	0	0	0
250	-0.165	0	0	-0.282	0	0	0	0	0
252	0.206	-0.086	-0.067	0.049	0.03	0.001	0.055	0.425	0.425
254	0.043	-0.07	0.032	0.043	-0.11	0.043	0.043	0.043	0.043

256	0	-0.08	0	0	0	0	0	0	0
258	-0.091	-0.153	0	-0.033	-0.008	0	0	-0.213	-0.507
260	0	0	0	-0.229	0	0	0	-0.314	-0.145
262	0.092	0.134	0.135	0.061	0.135	0.135	0.077	0.135	0.135
264	0	0	0	0	0	0	0	0	0
266	-0.264	0	0	0	-0.428	0	0	0	0
268	0	-0.323	0	0	-0.274	0	0	0	0
270	0	0	0	0	0	0	0	0	0
272	0	0	0	0	0	0	0	0	0
274	0.153	-0.324	0.153	0.153	-0.255	0.153	0.153	0.153	0.152
276	0	0	0	0	0	0	0	-0.239	0
278	0.024	-0.358	0.024	0.024	-0.084	0.024	0.024	0.024	-0.109
280	0.248	0.095	0.248	0.232	0.248	-0.032	0.248	0.248	0.248
282	0.871	0.35	0.871	0.538	0.593	0.341	0.457	0.594	0.59
284	1.34	1.34	1.34	1.34	1.34	1.34	1.34	1.34	1.34
286	1.809	1.649	1.809	1.809	1.809	1.809	1.809	1.809	1.809
288	2.147	1.482	2.147	1.991	2.147	2.147	2.147	1.743	1.87
290	1.878	1.719	2.103	1.746	2.172	2.364	1.936	1.743	2.364
292	2.481	2.022	2.003	1.887	2.265	2.481	2.138	2.112	2.481
294	2.611	2.417	2.611	2.568	2.611	2.611	2.611	2.597	2.611
296	2.791	1.94	2.791	2.791	2.791	2.791	2.791	2.791	2.791
298	2.938	1.638	2.938	2.938	2.938	2.839	2.938	2.938	2.938
300	2.555	1.424	2.578	2.885	2.841	2.567	3.033	2.849	2.624
302	2.592	1.194	2.414	2.424	2.482	2.712	2.638	2.378	2.45
304	3.142	1.076	2.431	2.389	2.455	2.69	2.827	2.893	2.804
306	2.869	0.96	2.244	2.248	2.993	2.195	2.866	2.57	2.821
308	2.673	0.828	2.002	2.005	2.474	2.052	2.236	2.367	2.249
310	2.929	0.713	1.809	1.853	2.295	1.985	2.387	2.466	2.077
312	2.35	0.613	1.606	1.703	1.972	1.801	2.032	1.897	1.974
314	2.084	0.527	1.474	1.503	1.922	1.666	1.818	1.892	1.837
316	2.191	0.451	1.337	1.388	1.695	1.536	1.721	1.694	1.657

318	2.233	0.385	1.266	1.306	1.59	1.458	1.628	1.6	1.574
320	2.062	0.325	1.19	1.245	1.513	1.411	1.535	1.53	1.464
322	2.091	0.27	1.132	1.175	1.474	1.333	1.486	1.542	1.479
324	2.056	0.223	1.091	1.147	1.415	1.284	1.399	1.429	1.423
326	1.881	0.186	1.029	1.095	1.379	1.257	1.335	1.388	1.365
328	1.949	0.158	0.998	1.066	1.353	1.265	1.329	1.403	1.379
330	1.868	0.136	0.967	1.031	1.3	1.197	1.278	1.318	1.311
332	1.794	0.115	0.922	1.001	1.285	1.151	1.237	1.273	1.278
334	1.867	0.094	0.896	0.989	1.228	1.163	1.227	1.26	1.267
336	1.888	0.073	0.874	0.961	1.236	1.149	1.205	1.217	1.266
338	1.82	0.06	0.851	0.939	1.209	1.116	1.2	1.219	1.25
340	1.748	0.048	0.844	0.913	1.176	1.1	1.177	1.183	1.254
342	1.779	0.039	0.82	0.88	1.148	1.088	1.156	1.155	1.228
344	1.692	0.03	0.797	0.874	1.136	1.076	1.107	1.138	1.191
346	1.659	0.023	0.777	0.865	1.11	1.048	1.084	1.128	1.182
348	1.697	0.02	0.778	0.851	1.09	1.046	1.062	1.117	1.19
350	1.726	0.015	0.76	0.84	1.098	1.047	1.08	1.117	1.195
352	1.665	0.01	0.741	0.815	1.061	1.006	1.046	1.081	1.133
354	1.651	0.006	0.73	0.821	1.04	0.994	1.062	1.084	1.151
356	1.647	0.005	0.715	0.794	1.037	0.989	1.029	1.075	1.126
358	1.636	0.003	0.711	0.788	1.027	0.976	1.02	1.061	1.123
360	1.561	-0.002	0.7	0.772	1.003	0.953	0.983	1.039	1.09
362	1.662	-0.004	0.692	0.768	1.004	0.963	0.984	1.046	1.109
364	1.652	-0.004	0.679	0.754	0.968	0.946	0.964	1.028	1.085
366	1.536	-0.005	0.664	0.739	0.941	0.916	0.951	0.994	1.071
368	1.528	-0.004	0.662	0.72	0.945	0.906	0.939	0.998	1.061
370	1.518	-0.004	0.653	0.708	0.93	0.908	0.917	0.97	1.048
372	1.538	-0.006	0.643	0.715	0.932	0.901	0.931	0.972	1.049

374	1.489	-0.008	0.636	0.699	0.917	0.892	0.931	0.964	1.025
376	1.522	-0.008	0.634	0.693	0.914	0.889	0.923	0.963	1.029
378	1.504	-0.008	0.624	0.682	0.901	0.883	0.907	0.945	1.022
380	1.46	-0.007	0.615	0.673	0.889	0.871	0.894	0.937	1.004
382	1.524	-0.009	0.612	0.671	0.882	0.873	0.902	0.935	1.002
384	1.502	-0.011	0.611	0.668	0.88	0.875	0.894	0.93	1
386	1.479	-0.01	0.611	0.664	0.878	0.868	0.894	0.922	0.995
388	1.528	-0.011	0.606	0.664	0.88	0.867	0.897	0.926	1.002
390	1.509	-0.012	0.603	0.665	0.876	0.859	0.888	0.923	0.995
392	1.483	-0.012	0.601	0.661	0.866	0.863	0.886	0.924	0.994
394	1.482	-0.011	0.597	0.659	0.86	0.851	0.879	0.917	0.989
396	1.481	-0.011	0.594	0.656	0.855	0.847	0.872	0.911	0.979
398	1.485	-0.012	0.6	0.659	0.862	0.85	0.881	0.911	0.985
400	1.479	-0.012	0.599	0.66	0.863	0.855	0.881	0.916	0.991
402	1.494	-0.013	0.602	0.666	0.861	0.857	0.883	0.923	1.004
404	1.48	-0.012	0.604	0.665	0.861	0.862	0.886	0.925	0.993
406	1.491	-0.012	0.606	0.672	0.861	0.864	0.885	0.92	0.982
408	1.489	-0.011	0.604	0.674	0.861	0.859	0.883	0.917	0.987
410	1.508	-	0.607	0.675	0.862	0.866	0.888	0.924	0.989

		0.012							
412	1.529	-0.013	0.607	0.675	0.865	0.873	0.893	0.929	0.995
414	1.531	-0.014	0.609	0.675	0.867	0.868	0.893	0.927	0.992
416	1.54	-0.015	0.611	0.678	0.866	0.872	0.896	0.93	0.993
418	1.55	-0.015	0.609	0.681	0.865	0.876	0.901	0.934	0.99
420	1.54	-0.017	0.612	0.68	0.868	0.872	0.9	0.931	0.997
422	1.544	-0.016	0.612	0.679	0.867	0.868	0.9	0.935	1.001
424	1.542	-0.016	0.61	0.68	0.865	0.868	0.897	0.928	0.998
426	1.548	-0.016	0.608	0.677	0.861	0.869	0.895	0.927	0.989
428	1.521	-0.015	0.605	0.674	0.852	0.864	0.891	0.924	0.985
430	1.527	-0.016	0.607	0.676	0.857	0.865	0.894	0.923	0.983
432	1.552	-0.016	0.609	0.679	0.86	0.868	0.897	0.926	0.988
434	1.558	-0.016	0.61	0.68	0.859	0.869	0.897	0.927	0.986
436	1.541	-0.015	0.607	0.68	0.855	0.866	0.896	0.928	0.987
438	1.542	-0.016	0.609	0.679	0.855	0.866	0.894	0.925	0.983
440	1.551	-0.016	0.608	0.68	0.857	0.869	0.898	0.928	0.989
442	1.553	-0.016	0.607	0.681	0.853	0.868	0.895	0.924	0.984
444	1.558	-0.015	0.606	0.678	0.848	0.866	0.892	0.921	0.983
446	1.564	-	0.608	0.682	0.852	0.866	0.897	0.926	0.986

		0.016							
448	1.579	-0.015	0.61	0.684	0.853	0.871	0.896	0.924	0.99
450	1.558	-0.015	0.607	0.681	0.852	0.866	0.894	0.923	0.983
452	1.565	-0.016	0.61	0.686	0.853	0.868	0.899	0.928	0.985
454	1.574	-0.016	0.611	0.686	0.854	0.872	0.9	0.928	0.986
456	1.581	-0.016	0.613	0.69	0.855	0.872	0.903	0.931	0.989
458	1.59	-0.017	0.615	0.691	0.859	0.877	0.906	0.935	0.991
460	1.59	-0.018	0.62	0.693	0.86	0.878	0.909	0.937	0.995
462	1.579	-0.017	0.61	0.687	0.85	0.87	0.899	0.928	0.985
464	1.555	-0.016	0.603	0.682	0.843	0.865	0.891	0.919	0.978
466	1.551	-0.018	0.603	0.678	0.841	0.862	0.89	0.917	0.975
468	1.56	-0.017	0.6	0.675	0.838	0.858	0.887	0.913	0.973
470	1.541	-0.018	0.593	0.667	0.829	0.85	0.88	0.906	0.961
472	1.534	-0.019	0.589	0.663	0.822	0.845	0.875	0.9	0.957
474	1.538	-0.018	0.587	0.66	0.82	0.844	0.87	0.896	0.953
476	1.523	-0.019	0.581	0.655	0.812	0.837	0.863	0.889	0.949
478	1.517	-0.019	0.578	0.651	0.809	0.831	0.862	0.888	0.948
480	1.523	-0.019	0.575	0.647	0.805	0.828	0.856	0.886	0.947
482	1.509	-	0.574	0.646	0.802	0.828	0.857	0.883	0.941

		0.021							
484	1.498	-0.021	0.575	0.643	0.801	0.828	0.858	0.885	0.939
486	1.472	-0.017	0.559	0.628	0.782	0.808	0.837	0.863	0.919
488	1.448	-0.018	0.547	0.617	0.769	0.794	0.824	0.849	0.908
490	1.426	-0.017	0.538	0.605	0.756	0.781	0.809	0.835	0.894
492	1.418	-0.018	0.532	0.598	0.749	0.774	0.805	0.832	0.89
494	1.38	-0.015	0.515	0.582	0.73	0.757	0.785	0.812	0.87
496	1.362	-0.016	0.507	0.57	0.717	0.746	0.774	0.801	0.856
498	1.352	-0.017	0.501	0.561	0.712	0.739	0.766	0.795	0.851
500	1.324	-0.016	0.488	0.547	0.697	0.723	0.752	0.781	0.837
502	1.3	-0.017	0.478	0.535	0.683	0.71	0.739	0.767	0.825
504	1.274	-0.018	0.471	0.524	0.673	0.699	0.729	0.756	0.815
506	1.256	-0.018	0.462	0.513	0.663	0.69	0.719	0.746	0.807
508	1.236	-0.019	0.454	0.505	0.651	0.679	0.709	0.736	0.795
510	1.222	-0.019	0.447	0.497	0.643	0.671	0.699	0.727	0.786
512	1.207	-0.019	0.441	0.487	0.635	0.663	0.692	0.719	0.777
514	1.19	-0.019	0.432	0.478	0.625	0.653	0.684	0.71	0.766
516	1.175	-0.019	0.426	0.471	0.617	0.646	0.675	0.705	0.76
518	1.17	-	0.425	0.468	0.612	0.641	0.672	0.7	0.759

		0.021							
520	1.154	-0.019	0.418	0.461	0.602	0.633	0.662	0.691	0.749
522	1.138	-0.019	0.412	0.453	0.594	0.624	0.654	0.682	0.74
524	1.132	-0.021	0.409	0.45	0.591	0.621	0.652	0.68	0.738
526	1.128	-0.021	0.408	0.448	0.59	0.62	0.65	0.679	0.736
528	1.124	-0.022	0.406	0.444	0.587	0.616	0.648	0.676	0.734
530	1.104	-0.02	0.396	0.434	0.575	0.605	0.635	0.664	0.72
532	1.084	-0.019	0.386	0.425	0.564	0.593	0.623	0.65	0.707
534	1.075	-0.02	0.384	0.422	0.56	0.591	0.621	0.649	0.705
536	1.066	-0.018	0.38	0.417	0.555	0.587	0.617	0.644	0.7
538	1.058	-0.019	0.377	0.414	0.551	0.584	0.613	0.64	0.696
540	1.054	-0.021	0.378	0.413	0.55	0.581	0.613	0.64	0.696
542	1.056	-0.021	0.38	0.413	0.551	0.584	0.614	0.643	0.698
544	1.038	-0.018	0.369	0.405	0.541	0.573	0.602	0.631	0.685
546	1.033	-0.019	0.366	0.402	0.536	0.57	0.599	0.627	0.682
548	1.035	-0.019	0.367	0.401	0.535	0.569	0.598	0.627	0.682
550	1.026	-0.018	0.364	0.398	0.532	0.565	0.595	0.622	0.678
552	1.028	-0.02	0.365	0.399	0.533	0.566	0.596	0.623	0.679
554	1.026	-0.02	0.365	0.397	0.533	0.565	0.596	0.622	0.681
556	1.022	-0.02	0.363	0.396	0.529	0.563	0.593	0.62	0.676
558	1.019	-0.02	0.362	0.394	0.527	0.563	0.59	0.618	0.675
560	1.019	-0.02	0.362	0.394	0.527	0.561	0.589	0.618	0.674

562	1.016	-0.021	0.361	0.392	0.525	0.559	0.589	0.617	0.673
564	1.014	-0.022	0.359	0.392	0.523	0.558	0.587	0.615	0.67
566	1.015	-0.022	0.358	0.393	0.523	0.558	0.589	0.615	0.669
568	1.008	-0.022	0.357	0.389	0.519	0.554	0.584	0.612	0.666
570	1.004	-0.021	0.354	0.387	0.517	0.553	0.583	0.609	0.665
572	1.004	-0.022	0.355	0.388	0.516	0.552	0.584	0.609	0.663
574	1.001	-0.021	0.352	0.386	0.515	0.549	0.582	0.607	0.661
576	0.997	-0.02	0.35	0.383	0.512	0.547	0.577	0.605	0.657
578	0.992	-0.02	0.348	0.381	0.51	0.545	0.575	0.6	0.653
580	0.985	-0.02	0.346	0.379	0.506	0.543	0.572	0.597	0.652
582	0.988	-0.02	0.347	0.379	0.506	0.543	0.572	0.599	0.652
584	0.991	-0.02	0.348	0.379	0.507	0.543	0.574	0.599	0.653
586	0.986	-0.02	0.348	0.38	0.507	0.542	0.572	0.6	0.653
588	0.985	-0.02	0.347	0.378	0.505	0.542	0.572	0.598	0.651
590	0.988	-0.019	0.347	0.378	0.503	0.54	0.571	0.597	0.651
592	0.986	-0.019	0.345	0.377	0.503	0.538	0.569	0.597	0.65
594	0.981	-0.02	0.344	0.376	0.501	0.538	0.568	0.596	0.648
596	0.984	-0.02	0.345	0.376	0.501	0.539	0.568	0.596	0.648
598	0.98	-0.019	0.344	0.375	0.5	0.537	0.568	0.595	0.648
600	0.974	-0.018	0.341	0.373	0.496	0.534	0.564	0.59	0.641
602	0.976	-0.019	0.341	0.373	0.496	0.534	0.564	0.591	0.642
604	0.979	-0.02	0.343	0.375	0.498	0.536	0.568	0.593	0.646
606	0.978	-0.02	0.342	0.373	0.496	0.534	0.567	0.591	0.643
608	0.972	-	0.338	0.371	0.493	0.53	0.561	0.586	0.637

		0.019							
610	0.97	-0.021	0.338	0.37	0.492	0.53	0.562	0.586	0.638
612	0.967	-0.019	0.337	0.369	0.491	0.53	0.56	0.586	0.637
614	0.962	-0.019	0.336	0.367	0.488	0.526	0.558	0.582	0.633
616	0.966	-0.02	0.336	0.366	0.487	0.526	0.558	0.582	0.634
618	0.967	-0.02	0.337	0.367	0.488	0.526	0.558	0.583	0.635
620	0.968	-0.02	0.337	0.368	0.488	0.527	0.559	0.585	0.636
622	0.965	-0.021	0.336	0.366	0.486	0.526	0.558	0.584	0.636
624	0.964	-0.021	0.335	0.366	0.486	0.527	0.557	0.583	0.633
626	0.966	-0.021	0.337	0.367	0.487	0.527	0.557	0.584	0.633
628	0.96	-0.021	0.335	0.366	0.484	0.525	0.555	0.581	0.633
630	0.956	-0.021	0.332	0.364	0.482	0.522	0.552	0.578	0.63
632	0.955	-0.021	0.331	0.362	0.479	0.52	0.55	0.576	0.628
634	0.954	-0.021	0.331	0.361	0.479	0.521	0.55	0.575	0.628
636	0.952	-0.02	0.331	0.36	0.476	0.518	0.548	0.575	0.626
638	0.947	-0.021	0.328	0.358	0.474	0.516	0.547	0.572	0.623
640	0.945	-0.02	0.326	0.357	0.471	0.513	0.544	0.569	0.621
642	0.94	-0.02	0.325	0.356	0.47	0.512	0.542	0.567	0.621
644	0.938	-0.019	0.323	0.354	0.468	0.51	0.541	0.567	0.616
646	0.938	-0.019	0.323	0.354	0.467	0.509	0.54	0.567	0.615
648	0.936	-0.019	0.322	0.353	0.467	0.508	0.539	0.565	0.615
650	0.938	-	0.322	0.354	0.465	0.508	0.539	0.564	0.615

		0.019							

Table 2: Absorbance spectroscopy data of Plasma, Rifampicin and Plasma with Rifampicin at different concentrations ranging from 30 µg/ml-1 µg/ml by increments of 5 µg/ml

Wavelength [nm]	**plasma**	**Rif without plasma**	**RIF 1µg/ml**	**RIF 5µg/ml**	**RIF 10µg/ml**	**RIF 15µg/ml**	**RIF 20µg/ml**	**RIF 25µg/ml**	**RIF 30µg/ml**
220	-0.975	-1.325	-1.005	-1.303	0.288	-0.592	-0.967	-0.887	-1.074
222	-0.834	-0.644	-1.078	-0.817	-0.494	-0.907	-0.826	0.856	-0.786
224	-1.052	-1.04	-1.792	-1.566	-1.635	-1.566	-1.423	-1.284	-1.644
226	0.323	-0.781	-0.806	-1.083	-1.127	-0.744	-1.132	-1.199	-1.201
228	-0.707	-0.653	-0.768	-0.966	-0.776	-0.936	-0.815	-1.09	-0.652
230	0.134	-0.398	-0.58	-0.202	0.134	-0.458	0.134	0.134	0.134
232	-0.241	-0.656	-0.579	-0.577	0.226	-0.403	-0.383	0.226	-0.273
234	-0.787	-0.763	0	-0.957	0	-0.708	-0.773	0	-0.724
236	-0.692	0.064	-0.114	0.064	-0.582	0.064	0.064	-0.763	-0.686
238	-0.111	-0.454	-0.252	0.125	0.003	-0.406	0.285	-0.272	-0.435
240	0.369	0.07	-0.346	-0.061	-0.336	-0.31	-0.138	-0.321	-0.389
242	0.025	0.025	-0.021	0.025	-0.333	-0.194	0.025	0.025	-0.155
244	0	0	0	-0.136	-0.189	-0.517	0	0	-0.383
246	0	0	0	-0.474	-0.597	-0.645	0	0	0
248	-0.174	0	0	-0.003	-0.067	0	0	0	0
250	0	0	-0.311	-0.141	0	-0.344	-0.15	-0.21	0
252	0.136	-0.335	-0.232	-0.274	0.217	-0.265	-0.172	-0.039	-0.161
254	0.043	-0.312	-0.25	-0.352	0.043	-0.066	-0.167	0.007	-0.536
256	0	-0.236	0	-0.207	0	-0.541	0	-0.129	-0.702
258	0	-0.175	0	-0.292	0	-0.28	-0.208	-0.168	-0.36
260	0	-0.102	0	-0.499	0	0	-0.282	-0.143	-0.174
262	-0.002	0.135	0.135	-0.183	0.135	0.135	-0.356	-0.239	0.135
264	0	0	0	0	0	0	-0.138	0	0
266	-0.376	-0.189	-0.485	-0.236	-0.023	0	-0.54	-0.441	-0.345
268	0	-0.422	0	-0.396	0	0	-0.613	-0.357	-0.029
270	0	0	0	-0.438	0	0	0	0	0
272	0	0	0	0	0	0	-0.142	0	0

274	0.153	0.068	-0.172	-0.095	-0.431	-0.513	0.153	0.002	0.114
276	-0.042	0	0	-0.421	0	0	-0.261	0	-0.424
278	-0.154	-0.438	-0.108	-0.431	0.024	0.024	-0.274	-0.335	-0.019
280	0.248	0.248	0.181	-0.148	0.17	0.248	-0.279	0.132	0.172
282	0.866	0.831	0.588	0.231	0.428	0.658	0.571	0.257	0.318
284	1.34	1.068	1.34	1.012	1.34	1.102	1.34	1.067	1.254
286	1.809	1.543	1.809	1.585	1.809	1.809	1.809	1.592	1.673
288	2.058	1.324	1.622	1.473	2.147	2.147	1.707	1.759	1.332
290	1.801	1.448	2.035	2.104	2.364	1.727	1.765	2.053	1.749
292	1.931	1.469	2.481	2.266	2.481	2.153	2.444	2.258	2.404
294	2.611	1.494	2.611	2.611	2.611	2.611	2.303	2.611	2.611
296	2.791	1.45	2.791	2.791	2.791	2.791	2.791	2.791	2.791
298	2.938	1.355	2.813	2.447	2.624	2.938	2.602	2.846	2.588
300	2.414	1.322	2.277	2.081	2.713	3.033	2.353	2.203	2.457
302	2.863	1.308	2.451	2.07	2.34	2.369	2.359	2.257	2.168
304	3.111	1.352	2.626	2.171	2.237	2.379	3.142	2.289	2.189
306	2.629	1.393	1.986	1.916	2.057	2.129	2.131	2.265	1.946
308	2.691	1.397	1.602	1.693	1.751	1.926	1.786	1.785	1.719
310	2.537	1.517	1.444	1.573	1.598	1.73	1.679	1.685	1.581
312	2.293	1.543	1.311	1.445	1.417	1.529	1.546	1.521	1.469
314	2.05	1.657	1.175	1.325	1.31	1.417	1.426	1.416	1.366
316	1.716	1.7	1.089	1.24	1.224	1.361	1.351	1.348	1.289
318	1.614	1.715	1.035	1.213	1.181	1.286	1.339	1.306	1.264
320	1.563	1.749	0.994	1.196	1.125	1.235	1.32	1.284	1.238
322	1.549	2.074	0.958	1.186	1.1	1.211	1.247	1.319	1.257
324	1.443	1.967	0.935	1.137	1.099	1.21	1.24	1.292	1.24
326	1.432	1.918	0.919	1.155	1.061	1.192	1.232	1.263	1.223
328	1.47	2.044	0.896	1.161	1.064	1.195	1.253	1.296	1.257
330	1.395	1.908	0.873	1.129	1.028	1.185	1.23	1.299	1.245
332	1.392	1.994	0.86	1.118	1.01	1.175	1.247	1.272	1.276
334	1.396	2.135	0.855	1.102	1.005	1.142	1.227	1.237	1.283
336	1.334	2.156	0.856	1.104	1.023	1.148	1.251	1.284	1.262
338	1.34	2.168	0.843	1.097	1.005	1.156	1.27	1.332	1.267
340	1.31	2.178	0.829	1.057	0.999	1.135	1.267	1.295	1.291
342	1.322	1.985	0.82	1.074	0.979	1.136	1.267	1.282	1.238

344	1.279	1.844	0.798	1.05	0.962	1.122	1.197	1.251	1.212
346	1.271	1.718	0.795	1.031	0.959	1.095	1.172	1.237	1.175
348	1.272	1.596	0.778	1.021	0.948	1.054	1.15	1.238	1.168
350	1.27	1.519	0.778	1.002	0.936	1.06	1.164	1.229	1.145
352	1.218	1.281	0.765	0.96	0.901	1.025	1.083	1.116	1.077
354	1.204	1.156	0.761	0.935	0.901	1.004	1.058	1.081	1.041
356	1.22	1.023	0.742	0.921	0.884	0.982	1.024	1.042	0.989
358	1.203	0.914	0.739	0.887	0.871	0.961	0.992	1.008	0.954
360	1.172	0.798	0.73	0.848	0.854	0.931	0.969	0.948	0.904
362	1.18	0.725	0.726	0.832	0.849	0.922	0.953	0.939	0.871
364	1.153	0.661	0.71	0.814	0.828	0.903	0.91	0.895	0.833
366	1.137	0.595	0.696	0.788	0.816	0.88	0.874	0.864	0.801
368	1.124	0.541	0.682	0.766	0.8	0.859	0.855	0.829	0.775
370	1.099	0.498	0.672	0.744	0.787	0.84	0.833	0.802	0.744
372	1.122	0.463	0.673	0.744	0.788	0.841	0.822	0.79	0.734
374	1.113	0.434	0.671	0.739	0.788	0.839	0.8	0.771	0.709
376	1.089	0.411	0.673	0.73	0.79	0.833	0.797	0.758	0.691
378	1.085	0.388	0.662	0.72	0.777	0.819	0.784	0.742	0.675
380	1.075	0.37	0.655	0.7	0.764	0.809	0.764	0.723	0.649
382	1.088	0.359	0.654	0.695	0.764	0.807	0.757	0.718	0.648
384	1.078	0.346	0.649	0.691	0.764	0.801	0.755	0.706	0.638
386	1.068	0.336	0.645	0.681	0.755	0.792	0.745	0.701	0.629
388	1.07	0.327	0.648	0.683	0.757	0.792	0.737	0.693	0.619
390	1.072	0.32	0.651	0.679	0.754	0.791	0.737	0.687	0.615
392	1.075	0.317	0.648	0.679	0.758	0.793	0.734	0.686	0.608
394	1.064	0.314	0.639	0.675	0.751	0.779	0.726	0.678	0.608
396	1.058	0.312	0.639	0.67	0.75	0.779	0.718	0.675	0.603
398	1.068	0.314	0.64	0.674	0.753	0.781	0.719	0.673	0.604
400	1.072	0.317	0.642	0.675	0.756	0.781	0.722	0.673	0.605
402	1.083	0.323	0.647	0.678	0.759	0.79	0.727	0.679	0.608
404	1.084	0.329	0.652	0.684	0.76	0.786	0.729	0.682	0.61
406	1.093	0.338	0.653	0.681	0.761	0.786	0.728	0.682	0.613
408	1.092	0.349	0.653	0.681	0.763	0.787	0.733	0.683	0.615
410	1.104	0.362	0.658	0.686	0.77	0.79	0.736	0.691	0.62
412	1.108	0.378	0.662	0.691	0.769	0.793	0.739	0.694	0.625

414	1.113	0.396	0.66	0.688	0.77	0.795	0.745	0.7	0.628
416	1.116	0.416	0.662	0.692	0.777	0.797	0.753	0.704	0.636
418	1.132	0.437	0.663	0.698	0.782	0.803	0.755	0.711	0.643
420	1.123	0.46	0.665	0.699	0.781	0.804	0.76	0.717	0.649
422	1.126	0.485	0.667	0.703	0.782	0.806	0.765	0.725	0.656
424	1.128	0.51	0.667	0.704	0.783	0.808	0.766	0.727	0.661
426	1.128	0.537	0.664	0.705	0.781	0.812	0.77	0.732	0.666
428	1.123	0.566	0.66	0.703	0.778	0.804	0.771	0.734	0.671
430	1.13	0.594	0.663	0.708	0.778	0.806	0.777	0.743	0.678
432	1.135	0.624	0.665	0.712	0.784	0.814	0.785	0.753	0.688
434	1.136	0.654	0.666	0.717	0.788	0.818	0.791	0.762	0.698
436	1.133	0.687	0.666	0.721	0.787	0.819	0.797	0.767	0.706
438	1.139	0.719	0.666	0.726	0.79	0.822	0.802	0.777	0.715
440	1.146	0.752	0.668	0.729	0.796	0.829	0.813	0.786	0.726
442	1.139	0.783	0.667	0.732	0.794	0.829	0.816	0.793	0.737
444	1.139	0.813	0.666	0.734	0.793	0.83	0.821	0.798	0.743
446	1.145	0.846	0.668	0.74	0.799	0.837	0.833	0.811	0.756
448	1.152	0.885	0.67	0.745	0.802	0.841	0.843	0.824	0.768
450	1.142	0.913	0.67	0.744	0.801	0.841	0.846	0.829	0.775
452	1.152	0.941	0.671	0.753	0.806	0.846	0.852	0.841	0.786
454	1.161	0.967	0.673	0.758	0.808	0.85	0.863	0.849	0.797
456	1.169	0.991	0.676	0.763	0.811	0.855	0.873	0.858	0.807
458	1.174	1.013	0.681	0.77	0.815	0.861	0.883	0.873	0.818
460	1.178	1.03	0.684	0.776	0.819	0.865	0.892	0.884	0.83
462	1.163	1.047	0.675	0.77	0.813	0.858	0.888	0.881	0.831
464	1.149	1.062	0.67	0.768	0.806	0.853	0.884	0.88	0.831
466	1.147	1.073	0.67	0.769	0.808	0.856	0.889	0.885	0.837
468	1.145	1.085	0.667	0.767	0.805	0.856	0.891	0.888	0.84
470	1.126	1.091	0.659	0.762	0.799	0.849	0.887	0.885	0.838
472	1.121	1.096	0.654	0.76	0.794	0.845	0.886	0.884	0.839
474	1.111	1.099	0.654	0.758	0.792	0.844	0.885	0.884	0.839
476	1.107	1.093	0.648	0.753	0.787	0.839	0.882	0.884	0.836
478	1.103	1.092	0.646	0.752	0.786	0.839	0.88	0.885	0.837
480	1.1	1.086	0.643	0.75	0.784	0.836	0.883	0.882	0.835
482	1.092	1.071	0.643	0.749	0.783	0.836	0.882	0.883	0.836

484	1.092	1.053	0.644	0.751	0.785	0.835	0.881	0.883	0.836
486	1.062	1.038	0.624	0.732	0.764	0.815	0.862	0.864	0.819
488	1.042	1.009	0.614	0.72	0.752	0.804	0.849	0.851	0.804
490	1.023	0.983	0.602	0.708	0.739	0.791	0.834	0.838	0.791
492	1.009	0.95	0.597	0.7	0.734	0.784	0.825	0.827	0.783
494	0.979	0.92	0.581	0.681	0.716	0.763	0.805	0.804	0.76
496	0.961	0.88	0.571	0.671	0.706	0.751	0.791	0.79	0.745
498	0.945	0.845	0.566	0.664	0.701	0.744	0.78	0.779	0.733
500	0.92	0.802	0.553	0.646	0.685	0.728	0.761	0.759	0.712
502	0.899	0.756	0.541	0.632	0.674	0.714	0.743	0.736	0.69
504	0.879	0.714	0.533	0.621	0.663	0.701	0.726	0.72	0.67
506	0.86	0.673	0.526	0.609	0.653	0.688	0.71	0.703	0.651
508	0.843	0.633	0.516	0.595	0.642	0.675	0.694	0.685	0.632
510	0.828	0.592	0.509	0.584	0.636	0.665	0.678	0.667	0.614
512	0.813	0.553	0.501	0.572	0.626	0.654	0.661	0.647	0.593
514	0.799	0.511	0.492	0.558	0.617	0.642	0.644	0.625	0.57
516	0.786	0.474	0.486	0.548	0.61	0.633	0.627	0.608	0.551
518	0.78	0.44	0.484	0.542	0.605	0.625	0.615	0.595	0.536
520	0.766	0.411	0.477	0.53	0.595	0.613	0.599	0.576	0.518
522	0.751	0.383	0.469	0.517	0.585	0.601	0.585	0.559	0.499
524	0.746	0.349	0.467	0.511	0.582	0.595	0.573	0.546	0.485
526	0.741	0.321	0.465	0.506	0.581	0.591	0.564	0.536	0.472
528	0.736	0.297	0.464	0.501	0.579	0.586	0.555	0.527	0.461
530	0.717	0.282	0.453	0.487	0.566	0.573	0.538	0.507	0.442
532	0.697	0.264	0.442	0.472	0.554	0.559	0.52	0.488	0.423
534	0.691	0.241	0.441	0.467	0.551	0.554	0.512	0.479	0.412
536	0.682	0.226	0.436	0.46	0.545	0.547	0.502	0.467	0.401
538	0.675	0.211	0.432	0.455	0.54	0.541	0.494	0.457	0.391
540	0.674	0.197	0.433	0.453	0.54	0.54	0.49	0.453	0.386
542	0.675	0.185	0.435	0.453	0.543	0.541	0.488	0.451	0.383
544	0.657	0.176	0.424	0.441	0.53	0.527	0.473	0.435	0.366
546	0.651	0.166	0.42	0.435	0.526	0.522	0.466	0.427	0.36
548	0.65	0.158	0.42	0.433	0.525	0.521	0.463	0.424	0.355
550	0.644	0.151	0.417	0.428	0.521	0.515	0.458	0.418	0.349
552	0.645	0.141	0.418	0.429	0.522	0.515	0.456	0.417	0.346

554	0.643	0.134	0.418	0.427	0.521	0.514	0.454	0.413	0.343
556	0.64	0.129	0.416	0.424	0.518	0.51	0.45	0.409	0.339
558	0.638	0.123	0.414	0.422	0.516	0.508	0.445	0.406	0.336
560	0.637	0.117	0.415	0.421	0.515	0.508	0.443	0.404	0.333
562	0.635	0.112	0.413	0.42	0.515	0.506	0.441	0.402	0.331
564	0.631	0.108	0.412	0.416	0.513	0.503	0.438	0.398	0.328
566	0.634	0.105	0.413	0.416	0.514	0.504	0.439	0.398	0.327
568	0.629	0.101	0.409	0.414	0.51	0.501	0.435	0.394	0.323
570	0.625	0.097	0.408	0.411	0.507	0.498	0.432	0.392	0.321
572	0.625	0.093	0.407	0.41	0.508	0.498	0.432	0.391	0.321
574	0.622	0.09	0.406	0.408	0.507	0.496	0.43	0.388	0.318
576	0.617	0.088	0.403	0.403	0.503	0.491	0.425	0.384	0.315
578	0.613	0.085	0.399	0.4	0.5	0.487	0.423	0.381	0.31
580	0.611	0.082	0.398	0.399	0.498	0.485	0.419	0.378	0.307
582	0.61	0.078	0.398	0.397	0.496	0.484	0.419	0.378	0.308
584	0.61	0.075	0.398	0.398	0.498	0.486	0.419	0.378	0.307
586	0.611	0.073	0.399	0.397	0.498	0.485	0.418	0.377	0.307
588	0.61	0.069	0.398	0.396	0.497	0.483	0.417	0.377	0.306
590	0.609	0.066	0.397	0.396	0.498	0.484	0.417	0.376	0.305
592	0.607	0.064	0.396	0.393	0.495	0.482	0.415	0.375	0.303
594	0.606	0.062	0.397	0.392	0.494	0.481	0.414	0.374	0.302
596	0.606	0.058	0.398	0.393	0.495	0.481	0.416	0.373	0.302
598	0.604	0.056	0.394	0.392	0.495	0.48	0.413	0.372	0.301
600	0.597	0.054	0.391	0.386	0.491	0.475	0.409	0.368	0.297
602	0.597	0.051	0.391	0.386	0.491	0.475	0.409	0.369	0.298
604	0.602	0.047	0.395	0.39	0.494	0.479	0.413	0.372	0.3
606	0.6	0.045	0.393	0.388	0.492	0.476	0.411	0.369	0.298
608	0.593	0.043	0.389	0.382	0.487	0.471	0.406	0.365	0.294
610	0.594	0.039	0.389	0.381	0.487	0.471	0.405	0.365	0.294
612	0.593	0.038	0.388	0.38	0.485	0.47	0.404	0.363	0.292
614	0.587	0.036	0.386	0.377	0.483	0.466	0.401	0.361	0.289
616	0.589	0.032	0.386	0.378	0.484	0.466	0.401	0.361	0.289
618	0.591	0.029	0.387	0.378	0.484	0.467	0.401	0.362	0.29
620	0.59	0.027	0.387	0.377	0.485	0.468	0.402	0.362	0.29
622	0.589	0.025	0.387	0.376	0.483	0.466	0.4	0.361	0.29

624	0.588	0.023	0.386	0.375	0.484	0.465	0.4	0.362	0.289
626	0.589	0.021	0.387	0.376	0.485	0.467	0.401	0.362	0.291
628	0.587	0.018	0.386	0.375	0.482	0.465	0.399	0.361	0.289
630	0.583	0.016	0.384	0.371	0.48	0.463	0.396	0.358	0.286
632	0.58	0.015	0.382	0.37	0.479	0.461	0.395	0.356	0.283
634	0.581	0.012	0.38	0.369	0.478	0.46	0.394	0.355	0.283
636	0.578	0.011	0.379	0.366	0.476	0.457	0.392	0.354	0.281
638	0.575	0.009	0.378	0.364	0.473	0.454	0.39	0.352	0.279
640	0.572	0.007	0.375	0.363	0.472	0.451	0.387	0.349	0.278
642	0.568	0.006	0.373	0.36	0.469	0.45	0.385	0.348	0.277
644	0.568	0.006	0.372	0.358	0.467	0.449	0.384	0.346	0.277
646	0.566	0.005	0.371	0.358	0.467	0.449	0.383	0.346	0.275
648	0.565	0.003	0.37	0.357	0.466	0.448	0.383	0.345	0.273
650	0.564	0.002	0.371	0.356	0.466	0.447	0.382	0.345	0.274

Table 3: Absorbance spectroscopy data of Plasma, 25-desacetyl rifampicin and Plasma with 25-desacetyl rifampicin at different concentrations ranging from 30 µg/ml-1 µg/ml by increments of 5 µg/ml

Wavelength [nm]	**D-RIF**	**D-RIF 1 µg/ml**	**D-RIF 5µg/ml**	**D-RIF 10 µg/ml**	**D-RIF 15µg/ml**	**D-RIF 20µg/ml**	**D-RIF 25 µg/ml**	**D-RIF 30 µg/ml**	**plasma**
220	-0.952	-1.088	0.647	-0.466	-0.901	-0.426	-1.098	-0.554	-0.803
222	-0.474	0.856	0.856	-1.034	-0.478	-0.091	-0.753	-0.36	-0.327
224	-0.993	0.114	-1.408	-1.459	-1.579	-1.126	-1.798	-0.888	-1.127
226	-0.368	-0.946	0.323	-1.189	-0.943	0.323	-0.185	0.323	0.323
228	-0.311	-1.022	-0.499	-1.066	0.237	-0.032	-0.55	0.237	0.237
230	0.134	-0.549	-0.009	-0.32	0.134	0.134	0.134	-0.204	0.134
232	-0.284	-0.517	0.196	-0.613	0.226	-0.443	0.21	-0.604	0.226
234	-0.118	-0.549	0	0	0	-0.958	-0.577	-0.268	0
236	0.064	-0.181	-0.377	-0.473	0.064	0.064	-0.547	0.064	0.034
238	0.354	-0.293	-0.097	-0.011	0.354	0.353	-0.413	0.354	0.164
240	0.403	-0.213	-0.216	-0.306	-0.292	0.517	0.517	-0.268	-0.112
242	0.025	0.025	-0.554	-0.252	-0.069	0.025	0.025	-0.028	0.025
244	0	-0.227	0	0	0	0	-0.252	0	0

246	0	0	0	0	0	0	0	0	0
248	0	0	0	0	0	0	0	0	0
250	0	-0.208	0	-0.276	0	-0.406	0	0	0
252	-0.033	-0.167	-0.157	-0.228	0.033	-0.052	-0.1	-0.152	0.126
254	0.043	-0.279	-0.226	0.043	0.043	-0.105	-0.099	-0.281	-0.133
256	0	-0.263	0	-0.13	0	0	0	-0.467	0
258	0	0	0	-0.312	0	-0.287	-0.171	-0.177	0
260	0	0	0	0	0	0	0	0	0
262	0.135	0.015	-0.023	0.135	0.135	0.135	0.135	0.135	0.135
264	0	0	0	-0.007	0	0	0	0	0
266	-0.023	-0.429	0	0	-0.28	0	0	0	-0.13
268	0	-0.076	0	0	0	0	0	-0.148	0
270	0	0	0	0	0	0	0	0	0
272	0	0	0	0	0	0	0	0	0
274	0.153	0.153	0.153	-0.062	0.113	0.06	0.153	-0.055	0.025
276	0	0	0	0	0	0	0	0	0
278	0.024	0.024	0.024	0.024	0.024	0.024	0.024	0.024	0.024
280	0.246	0.248	0.248	0.155	-0.009	0.248	0.11	0.248	0.248
282	0.351	0.871	0.871	0.504	0.871	0.446	0.424	0.7	0.871
284	1.34	1.34	1.34	1.34	1.34	1.193	1.318	1.34	1.34
286	1.781	1.809	1.782	1.809	1.809	1.809	1.809	1.809	1.809
288	1.275	1.865	1.51	1.808	1.996	1.63	1.745	1.975	1.791
290	1.206	1.842	2.08	2.364	2.364	2.364	1.928	2.364	2.361
292	1.264	2.481	2.408	2.387	2.481	2.481	2.102	2.481	2.181
294	1.304	2.611	2.611	2.611	2.611	2.611	2.611	2.611	2.611
296	1.225	2.791	2.791	2.791	2.791	2.791	2.791	2.791	2.791
298	1.151	2.512	2.938	2.604	2.707	2.938	2.938	2.938	2.634
300	1.114	2.606	2.639	2.351	2.592	2.796	3.033	2.464	2.353
302	1.088	2.268	2.474	2.312	2.576	2.504	2.344	2.439	2.372
304	1.092	2.305	2.364	2.442	2.348	2.653	2.243	2.218	2.383
306	1.098	1.984	2.003	2.105	2.152	2.124	2.204	2.312	2.651
308	1.114	1.628	1.812	1.72	1.833	1.762	1.76	1.972	2.357
310	1.14	1.485	1.671	1.594	1.645	1.609	1.65	1.846	3.215
312	1.173	1.327	1.498	1.365	1.516	1.483	1.479	1.615	2.541
314	1.219	1.209	1.411	1.298	1.376	1.379	1.392	1.492	2.39

316	1.282	1.111	1.309	1.205	1.324	1.314	1.287	1.386	2.351
318	1.331	1.09	1.294	1.175	1.32	1.276	1.247	1.312	2.236
320	1.338	1.041	1.243	1.154	1.277	1.242	1.195	1.251	2.166
322	1.486	1.008	1.245	1.115	1.252	1.205	1.189	1.258	2.083
324	1.476	0.972	1.227	1.084	1.215	1.2	1.183	1.208	1.974
326	1.493	0.949	1.229	1.077	1.217	1.195	1.18	1.192	1.94
328	1.621	0.955	1.262	1.077	1.25	1.199	1.17	1.181	1.991
330	1.603	0.94	1.221	1.047	1.205	1.155	1.143	1.11	1.882
332	1.572	0.932	1.231	1.033	1.216	1.161	1.147	1.122	1.776
334	1.589	0.908	1.211	1.014	1.2	1.137	1.142	1.117	1.901
336	1.516	0.903	1.206	1.027	1.185	1.171	1.151	1.097	1.955
338	1.517	0.881	1.191	1.01	1.19	1.168	1.122	1.11	1.92
340	1.513	0.89	1.149	0.997	1.181	1.148	1.09	1.08	1.949
342	1.489	0.86	1.159	0.999	1.161	1.125	1.076	1.056	1.885
344	1.293	0.844	1.15	0.983	1.14	1.102	1.069	1.051	1.814
346	1.182	0.828	1.139	0.948	1.111	1.076	1.041	1.065	1.687
348	1.088	0.821	1.08	0.93	1.074	1.061	1.019	1.036	1.714
350	0.986	0.809	1.057	0.913	1.084	1.048	1.017	1.039	1.892
352	0.853	0.794	1.006	0.89	1.015	0.981	0.972	1.011	1.764
354	0.756	0.788	0.983	0.898	0.984	0.957	0.958	0.996	1.744
356	0.669	0.769	0.933	0.873	0.947	0.935	0.926	0.984	1.691
358	0.607	0.759	0.901	0.848	0.916	0.914	0.919	0.968	1.746
360	0.544	0.744	0.86	0.822	0.885	0.884	0.885	0.962	1.699
362	0.505	0.742	0.839	0.821	0.876	0.869	0.876	0.962	1.773
364	0.469	0.725	0.814	0.811	0.855	0.851	0.862	0.951	1.706
366	0.439	0.716	0.789	0.788	0.822	0.824	0.833	0.929	1.689
368	0.416	0.703	0.764	0.776	0.809	0.804	0.823	0.914	1.626
370	0.397	0.708	0.75	0.768	0.799	0.782	0.804	0.9	1.574
372	0.386	0.706	0.737	0.774	0.797	0.784	0.796	0.904	1.593
374	0.375	0.69	0.728	0.758	0.779	0.773	0.802	0.898	1.604
376	0.368	0.687	0.718	0.748	0.768	0.77	0.798	0.904	1.623
378	0.362	0.691	0.707	0.745	0.751	0.755	0.781	0.898	1.592
380	0.356	0.676	0.699	0.737	0.743	0.743	0.775	0.884	1.53
382	0.358	0.678	0.69	0.741	0.745	0.74	0.771	0.89	1.589
384	0.354	0.679	0.683	0.74	0.738	0.74	0.765	0.886	1.586

386	0.35	0.672	0.682	0.73	0.735	0.737	0.754	0.871	1.562
388	0.348	0.672	0.675	0.729	0.724	0.732	0.76	0.877	1.579
390	0.343	0.672	0.672	0.727	0.728	0.735	0.762	0.875	1.573
392	0.339	0.669	0.668	0.727	0.727	0.729	0.762	0.88	1.566
394	0.337	0.665	0.663	0.725	0.718	0.721	0.753	0.871	1.53
396	0.332	0.666	0.66	0.716	0.714	0.725	0.75	0.87	1.518
398	0.328	0.666	0.664	0.724	0.713	0.726	0.749	0.868	1.561
400	0.322	0.669	0.663	0.727	0.715	0.722	0.75	0.875	1.559
402	0.314	0.676	0.668	0.726	0.719	0.725	0.76	0.871	1.57
404	0.308	0.676	0.67	0.732	0.725	0.727	0.76	0.872	1.566
406	0.303	0.675	0.669	0.732	0.721	0.728	0.759	0.872	1.555
408	0.299	0.674	0.668	0.732	0.723	0.727	0.757	0.871	1.565
410	0.293	0.679	0.672	0.737	0.728	0.731	0.761	0.876	1.577
412	0.289	0.681	0.673	0.741	0.73	0.735	0.766	0.878	1.581
414	0.282	0.683	0.676	0.739	0.729	0.736	0.767	0.875	1.586
416	0.277	0.686	0.681	0.743	0.732	0.738	0.772	0.882	1.62
418	0.273	0.689	0.687	0.749	0.739	0.743	0.772	0.884	1.617
420	0.268	0.686	0.688	0.745	0.741	0.744	0.773	0.88	1.607
422	0.267	0.687	0.692	0.747	0.74	0.745	0.774	0.88	1.608
424	0.266	0.687	0.692	0.746	0.741	0.747	0.774	0.877	1.616
426	0.266	0.685	0.692	0.745	0.74	0.747	0.773	0.873	1.605
428	0.266	0.683	0.693	0.742	0.738	0.744	0.77	0.869	1.59
430	0.265	0.684	0.698	0.745	0.743	0.747	0.773	0.873	1.588
432	0.264	0.687	0.704	0.75	0.749	0.751	0.778	0.871	1.618
434	0.266	0.687	0.708	0.749	0.751	0.756	0.781	0.874	1.611
436	0.269	0.687	0.712	0.751	0.753	0.757	0.782	0.871	1.606
438	0.269	0.687	0.715	0.753	0.755	0.759	0.784	0.872	1.61
440	0.269	0.69	0.72	0.755	0.761	0.763	0.787	0.873	1.611
442	0.27	0.688	0.724	0.756	0.762	0.763	0.786	0.871	1.604
444	0.272	0.688	0.726	0.755	0.766	0.767	0.787	0.867	1.6
446	0.272	0.692	0.733	0.758	0.77	0.772	0.792	0.869	1.613
448	0.274	0.693	0.739	0.76	0.776	0.776	0.794	0.872	1.615
450	0.276	0.69	0.742	0.761	0.776	0.774	0.795	0.868	1.606
452	0.277	0.694	0.748	0.766	0.782	0.781	0.799	0.871	1.617
454	0.279	0.696	0.753	0.767	0.786	0.785	0.802	0.874	1.621

456	0.281	0.697	0.758	0.769	0.791	0.789	0.805	0.875	1.637
458	0.281	0.7	0.764	0.775	0.796	0.796	0.811	0.877	1.635
460	0.282	0.702	0.772	0.777	0.801	0.8	0.814	0.878	1.636
462	0.286	0.696	0.768	0.77	0.794	0.793	0.809	0.869	1.619
464	0.288	0.691	0.765	0.765	0.792	0.789	0.805	0.863	1.598
466	0.288	0.691	0.766	0.764	0.794	0.791	0.804	0.861	1.6
468	0.29	0.687	0.766	0.763	0.791	0.789	0.804	0.857	1.592
470	0.292	0.68	0.76	0.756	0.788	0.783	0.797	0.848	1.58
472	0.292	0.677	0.759	0.753	0.786	0.782	0.792	0.844	1.57
474	0.293	0.673	0.757	0.751	0.782	0.778	0.791	0.842	1.568
476	0.294	0.67	0.753	0.747	0.779	0.775	0.787	0.838	1.555
478	0.295	0.668	0.751	0.745	0.778	0.773	0.784	0.832	1.554
480	0.296	0.664	0.75	0.741	0.775	0.77	0.781	0.832	1.55
482	0.294	0.662	0.751	0.739	0.774	0.771	0.781	0.833	1.546
484	0.294	0.663	0.75	0.739	0.773	0.771	0.781	0.832	1.54
486	0.299	0.647	0.73	0.722	0.757	0.751	0.763	0.813	1.507
488	0.299	0.637	0.718	0.71	0.744	0.74	0.752	0.802	1.485
490	0.3	0.627	0.706	0.7	0.733	0.728	0.74	0.79	1.464
492	0.298	0.623	0.701	0.694	0.728	0.722	0.735	0.783	1.457
494	0.301	0.606	0.681	0.678	0.712	0.704	0.716	0.767	1.416
496	0.299	0.597	0.669	0.667	0.701	0.694	0.706	0.757	1.397
498	0.297	0.591	0.661	0.661	0.694	0.688	0.7	0.752	1.387
500	0.298	0.578	0.647	0.648	0.679	0.673	0.687	0.737	1.353
502	0.298	0.568	0.631	0.636	0.667	0.661	0.674	0.725	1.331
504	0.297	0.559	0.619	0.626	0.655	0.647	0.662	0.716	1.311
506	0.297	0.55	0.606	0.618	0.644	0.638	0.652	0.706	1.294
508	0.295	0.541	0.595	0.608	0.633	0.628	0.643	0.699	1.274
510	0.295	0.534	0.583	0.598	0.625	0.618	0.634	0.69	1.258
512	0.294	0.529	0.57	0.591	0.614	0.607	0.625	0.683	1.238
514	0.295	0.521	0.557	0.582	0.604	0.596	0.615	0.675	1.222
516	0.295	0.515	0.547	0.574	0.594	0.588	0.607	0.668	1.208
518	0.294	0.512	0.54	0.57	0.587	0.583	0.6	0.664	1.203
520	0.295	0.504	0.528	0.561	0.578	0.573	0.591	0.656	1.189
522	0.295	0.496	0.516	0.553	0.567	0.562	0.583	0.648	1.172
524	0.294	0.494	0.509	0.55	0.562	0.558	0.579	0.646	1.165

526	0.293	0.493	0.504	0.548	0.559	0.555	0.577	0.645	1.163
528	0.292	0.49	0.499	0.546	0.554	0.55	0.575	0.644	1.158
530	0.295	0.481	0.486	0.536	0.542	0.537	0.562	0.631	1.135
532	0.296	0.471	0.471	0.525	0.531	0.525	0.549	0.619	1.11
534	0.295	0.469	0.466	0.521	0.526	0.522	0.546	0.618	1.102
536	0.296	0.465	0.458	0.517	0.52	0.516	0.54	0.613	1.093
538	0.295	0.462	0.454	0.514	0.515	0.511	0.537	0.608	1.086
540	0.293	0.461	0.452	0.512	0.513	0.511	0.536	0.61	1.084
542	0.291	0.462	0.451	0.512	0.512	0.511	0.537	0.61	1.085
544	0.293	0.453	0.438	0.503	0.503	0.499	0.525	0.599	1.067
546	0.293	0.451	0.434	0.5	0.499	0.495	0.521	0.595	1.058
548	0.291	0.451	0.432	0.499	0.497	0.494	0.52	0.594	1.056
550	0.291	0.448	0.428	0.496	0.494	0.49	0.516	0.591	1.05
552	0.287	0.447	0.427	0.495	0.493	0.49	0.516	0.591	1.05
554	0.284	0.446	0.425	0.494	0.492	0.489	0.515	0.591	1.047
556	0.282	0.444	0.423	0.492	0.488	0.486	0.512	0.588	1.044
558	0.279	0.443	0.42	0.49	0.487	0.483	0.511	0.586	1.041
560	0.276	0.443	0.419	0.489	0.485	0.481	0.509	0.585	1.042
562	0.273	0.442	0.417	0.489	0.482	0.481	0.507	0.583	1.038
564	0.27	0.44	0.414	0.488	0.48	0.479	0.506	0.583	1.034
566	0.265	0.44	0.414	0.487	0.48	0.479	0.505	0.583	1.034
568	0.262	0.438	0.411	0.485	0.476	0.476	0.504	0.581	1.028
570	0.259	0.436	0.407	0.48	0.474	0.473	0.5	0.577	1.025
572	0.254	0.436	0.405	0.481	0.473	0.472	0.5	0.576	1.025
574	0.25	0.435	0.404	0.48	0.472	0.47	0.497	0.576	1.022
576	0.245	0.432	0.4	0.477	0.468	0.467	0.495	0.573	1.015
578	0.242	0.43	0.397	0.474	0.466	0.463	0.491	0.569	1.01
580	0.238	0.427	0.394	0.472	0.462	0.461	0.489	0.565	1.007
582	0.23	0.427	0.393	0.471	0.461	0.46	0.487	0.566	1.004
584	0.225	0.428	0.394	0.472	0.462	0.46	0.488	0.566	1.01
586	0.22	0.427	0.393	0.472	0.46	0.46	0.486	0.566	1.007
588	0.213	0.426	0.391	0.47	0.459	0.458	0.485	0.564	1.005
590	0.208	0.424	0.39	0.469	0.458	0.457	0.485	0.564	1.002
592	0.202	0.425	0.387	0.467	0.456	0.455	0.483	0.562	1
594	0.196	0.423	0.386	0.467	0.455	0.454	0.481	0.561	0.999

596	0.187	0.423	0.385	0.466	0.454	0.454	0.481	0.562	0.999
598	0.182	0.422	0.384	0.466	0.452	0.453	0.479	0.56	0.996
600	0.178	0.418	0.38	0.462	0.448	0.448	0.475	0.556	0.988
602	0.169	0.418	0.379	0.462	0.447	0.447	0.477	0.557	0.992
604	0.162	0.421	0.38	0.463	0.45	0.45	0.478	0.559	0.994
606	0.156	0.419	0.378	0.462	0.447	0.448	0.476	0.557	0.99
608	0.149	0.415	0.374	0.458	0.443	0.443	0.472	0.552	0.985
610	0.142	0.415	0.373	0.458	0.442	0.443	0.471	0.551	0.982
612	0.137	0.415	0.37	0.456	0.441	0.441	0.469	0.551	0.981
614	0.131	0.412	0.366	0.453	0.436	0.437	0.467	0.548	0.972
616	0.124	0.411	0.366	0.452	0.435	0.438	0.465	0.547	0.974
618	0.117	0.411	0.366	0.452	0.436	0.437	0.466	0.547	0.978
620	0.111	0.41	0.366	0.451	0.435	0.437	0.466	0.548	0.978
622	0.105	0.411	0.365	0.45	0.432	0.435	0.464	0.547	0.976
624	0.098	0.41	0.363	0.452	0.432	0.435	0.463	0.546	0.976
626	0.093	0.41	0.364	0.451	0.432	0.435	0.464	0.547	0.977
628	0.087	0.408	0.361	0.449	0.43	0.432	0.461	0.544	0.973
630	0.082	0.406	0.357	0.446	0.427	0.429	0.459	0.54	0.969
632	0.078	0.404	0.354	0.444	0.425	0.427	0.457	0.54	0.965
634	0.072	0.403	0.354	0.444	0.423	0.426	0.455	0.539	0.965
636	0.067	0.402	0.352	0.441	0.421	0.424	0.453	0.537	0.961
638	0.063	0.4	0.349	0.44	0.419	0.421	0.45	0.535	0.956
640	0.058	0.398	0.347	0.436	0.417	0.42	0.448	0.532	0.949
642	0.055	0.397	0.345	0.435	0.416	0.417	0.447	0.529	0.947
644	0.05	0.395	0.344	0.434	0.413	0.415	0.445	0.527	0.946
646	0.047	0.395	0.342	0.433	0.413	0.414	0.444	0.527	0.947
648	0.044	0.394	0.341	0.432	0.411	0.413	0.443	0.526	0.944
650	0.04	0.393	0.34	0.432	0.411	0.412	0.442	0.525	0.942

Table 4: Absorbance spectroscopy data of Plasma, Pyrazinamide and Plasma with Pyrazinamide at different concentrations ranging from 30 µg/ml-1 µg/ml by increments of 5 µg/ml

Wavelength [nm]	Plasma	PYR	PYR 1µg/ml	PYR 5 µg/ml	PYR 10 µg/ml	PYR 15 µg/ml	PYR 20 µg/ml	PYR 25 µg/ml	PYR 30 µg/ml
220	-0.383	-1.02	-1.087	0.647	-0.57	-0.248	-0.942	-0.962	-1.269
222	-0.048	-0.884	-0.581	-0.087	-0.235	-0.696	-0.596	-0.235	-0.638
224	-1.394	0.114	-1.518	-1.131	-1.083	-1.639	-0.794	-1.042	0.114
226	-0.74	-1.096	-0.618	-1.089	-0.539	0.323	-0.661	0.323	0.323
228	-1.205	-0.908	-0.211	-0.455	-0.852	-0.605	0.237	0.237	0.237
230	-0.25	-0.491	0.134	0.134	-0.498	-0.187	-0.075	-0.393	0.134
232	-0.317	-0.269	0.226	0.226	-0.459	-0.084	-0.296	-0.333	0.226
234	-0.533	-0.65	-0.063	0	-0.134	0	-0.685	0	0
236	0.064	-0.135	0.064	0.064	-0.664	0.064	0.064	0.064	0.064
238	0.104	-0.396	0.354	0.354	-0.055	0.229	-0.198	0.354	0.354
240	-0.356	-0.431	0.238	0.517	0.222	0.517	0.251	-0.068	0.517
242	0.025	-0.153	0.025	0.025	-0.06	0.025	0.025	-0.139	0.025
244	0	0	0	0	0	0	0	0	-0.514
246	0	0	0	0	0	0	0	0	0
248	0	0	-0.074	0	0	0	0	0	0
250	-0.034	-0.021	-0.057	0	0	-0.158	0	0	0
252	0.387	-0.173	0.077	-0.072	0.425	-0.007	-0.134	0.212	0.425
254	-0.029	-0.295	0.043	-0.349	0.043	-0.16	-0.178	0.043	0.043
256	0	0	0	-0.357	0	-0.145	0	-0.33	-0.072
258	0	0	0	0	0	0	0	0	0
260	0	0	0	0	0	0	0	0	0
262	-0.052	-0.059	0.135	0.135	0.135	0.135	0.135	-0.093	0.135
264	0	0	0	0	0	0	-0.259	0	-0.349
266	0	0	0	0	0	-0.249	-0.327	0	-0.023
268	0	-0.231	0	0	0	0	0	0	0
270	0	0	0	0	0	0	0	0	0
272	0	0	0	0	0	0	0	0	0
274	0.153	0.153	0.153	0.035	0.153	0.153	0.153	0.153	0.153
276	0	-0.411	0	0	0	0	0	0	0
278	0.024	-0.461	-0.421	0.024	0.024	0.024	-0.048	0.024	0.024

280	0.248	0.206	0.248	0.248	0.248	0.248	0.248	0.248	0.248
282	0.871	0.218	0.457	0.871	0.413	0.146	0.759	0.585	0.375
284	1.34	0.67	1	1.34	1.013	1.238	1.34	1.34	1.34
286	1.809	0.58	1.809	1.809	1.809	1.809	1.809	1.809	1.809
288	1.969	0.432	2.05	1.672	2.147	2.147	2.147	1.55	1.844
290	1.989	0.359	1.973	2.243	2.179	2.364	2.364	2.061	1.999
292	2.245	0.305	2.481	1.948	2.481	2.481	2.481	2.481	2.481
294	2.611	0.295	2.611	2.611	2.611	2.611	2.611	2.611	2.611
296	2.791	0.289	2.791	2.791	2.791	2.791	2.791	2.791	2.791
298	2.938	0.279	2.885	2.938	2.517	2.851	2.938	2.604	2.686
300	2.542	0.286	2.512	2.439	2.539	2.843	2.674	2.687	2.36
302	3.1	0.298	2.132	2.343	2.403	2.529	2.493	2.482	2.951
304	3.142	0.309	2.009	2.492	2.18	2.948	2.606	2.573	2.294
306	2.577	0.318	1.72	1.935	1.911	2.266	2.075	2.069	2.115
308	2.569	0.328	1.424	1.606	1.776	1.748	1.656	1.802	1.878
310	2.565	0.339	1.266	1.456	1.588	1.558	1.542	1.713	1.746
312	2.475	0.34	1.13	1.311	1.41	1.357	1.369	1.517	1.456
314	2.578	0.341	1.004	1.202	1.259	1.275	1.232	1.361	1.332
316	2.374	0.335	0.936	1.117	1.181	1.17	1.143	1.272	1.258
318	2.229	0.32	0.9	1.066	1.14	1.117	1.1	1.211	1.209
320	2.031	0.303	0.871	1.002	1.1	1.082	1.047	1.177	1.158
322	2.1	0.275	0.85	0.972	1.046	1.041	1.013	1.118	1.149
324	1.993	0.242	0.826	0.939	1.011	0.996	0.997	1.074	1.095
326	1.844	0.213	0.799	0.908	1	0.987	0.953	1.047	1.079
328	1.964	0.188	0.787	0.89	0.98	0.968	0.938	1.038	1.063
330	1.92	0.164	0.764	0.868	0.964	0.931	0.925	1.004	1.017
332	1.916	0.136	0.754	0.844	0.941	0.904	0.914	0.976	0.998
334	1.932	0.109	0.724	0.82	0.915	0.911	0.891	0.96	0.976
336	1.942	0.086	0.715	0.805	0.893	0.909	0.874	0.932	0.956
338	1.945	0.066	0.715	0.787	0.89	0.884	0.86	0.925	0.937
340	1.878	0.049	0.705	0.776	0.867	0.868	0.85	0.918	0.927
342	2.007	0.036	0.696	0.764	0.854	0.865	0.842	0.917	0.904
344	1.859	0.022	0.679	0.738	0.844	0.848	0.835	0.898	0.891
346	1.805	0.013	0.67	0.736	0.829	0.845	0.819	0.877	0.887
348	1.729	0.007	0.668	0.737	0.822	0.838	0.808	0.861	0.875

350	1.813	0.006	0.665	0.722	0.819	0.827	0.814	0.858	0.869
352	1.714	0.0007	0.648	0.697	0.794	0.798	0.8	0.832	0.837
354	1.705	-0.003	0.65	0.692	0.788	0.791	0.798	0.827	0.845
356	1.712	-0.005	0.639	0.684	0.784	0.789	0.784	0.822	0.837
358	1.669	-0.005	0.627	0.675	0.773	0.789	0.775	0.821	0.83
360	1.658	-0.007	0.616	0.662	0.755	0.771	0.756	0.804	0.817
362	1.703	-0.008	0.617	0.657	0.763	0.775	0.767	0.805	0.819
364	1.661	-0.006	0.607	0.652	0.745	0.76	0.753	0.793	0.808
366	1.569	-0.007	0.594	0.638	0.726	0.748	0.739	0.775	0.8
368	1.589	-0.006	0.588	0.628	0.729	0.736	0.743	0.776	0.782
370	1.571	-0.005	0.584	0.626	0.721	0.734	0.722	0.771	0.769
372	1.612	-0.007	0.587	0.629	0.723	0.736	0.725	0.771	0.774
374	1.599	-0.005	0.582	0.624	0.717	0.728	0.727	0.762	0.77
376	1.589	-0.006	0.58	0.62	0.712	0.726	0.718	0.755	0.774
378	1.567	-0.007	0.57	0.614	0.707	0.719	0.714	0.747	0.763
380	1.505	-0.005	0.566	0.604	0.695	0.717	0.709	0.744	0.756
382	1.525	-0.006	0.564	0.608	0.697	0.716	0.715	0.745	0.755
384	1.548	-0.01	0.56	0.604	0.697	0.712	0.708	0.743	0.751
386	1.525	-0.009	0.561	0.601	0.688	0.701	0.704	0.74	0.752
388	1.523	-0.009	0.559	0.6	0.692	0.705	0.706	0.738	0.753
390	1.528	-0.009	0.558	0.598	0.693	0.704	0.701	0.737	0.749
392	1.52	-0.01	0.56	0.6	0.688	0.706	0.702	0.737	0.746
394	1.507	-0.008	0.555	0.594	0.685	0.7	0.698	0.73	0.742
396	1.509	-0.007	0.554	0.591	0.685	0.699	0.696	0.726	0.739
398	1.531	-0.01	0.555	0.594	0.686	0.698	0.698	0.729	0.746
400	1.53	-0.008	0.555	0.599	0.685	0.698	0.699	0.734	0.74
402	1.565	-0.009	0.559	0.602	0.689	0.71	0.707	0.738	0.749
404	1.551	-0.009	0.559	0.601	0.691	0.707	0.705	0.74	0.747
406	1.544	-0.008	0.556	0.603	0.693	0.705	0.706	0.736	0.749
408	1.537	-0.009	0.556	0.602	0.69	0.71	0.707	0.733	0.75
410	1.549	-0.009	0.56	0.604	0.692	0.711	0.709	0.738	0.752
412	1.565	-0.009	0.561	0.608	0.696	0.712	0.708	0.742	0.753
414	1.567	-0.009	0.559	0.608	0.695	0.711	0.709	0.739	0.75
416	1.567	-0.011	0.562	0.606	0.694	0.712	0.711	0.742	0.754
418	1.597	-0.011	0.562	0.607	0.698	0.712	0.716	0.743	0.757

420	1.575	-0.012	0.563	0.61	0.697	0.714	0.713	0.744	0.756
422	1.583	-0.012	0.563	0.609	0.694	0.713	0.711	0.739	0.756
424	1.592	-0.012	0.56	0.607	0.692	0.708	0.709	0.739	0.754
426	1.579	-0.012	0.558	0.605	0.69	0.708	0.707	0.737	0.751
428	1.56	-0.011	0.554	0.602	0.688	0.705	0.704	0.734	0.745
430	1.566	-0.012	0.553	0.602	0.689	0.707	0.706	0.734	0.747
432	1.583	-0.012	0.556	0.604	0.69	0.708	0.708	0.737	0.752
434	1.586	-0.012	0.556	0.605	0.69	0.709	0.707	0.737	0.75
436	1.581	-0.012	0.555	0.604	0.689	0.708	0.708	0.735	0.75
438	1.566	-0.012	0.554	0.605	0.69	0.707	0.708	0.735	0.749
440	1.574	-0.012	0.554	0.606	0.691	0.709	0.708	0.736	0.751
442	1.572	-0.013	0.554	0.606	0.688	0.707	0.706	0.735	0.748
444	1.566	-0.011	0.551	0.603	0.686	0.704	0.704	0.732	0.746
446	1.582	-0.013	0.552	0.605	0.689	0.707	0.707	0.735	0.749
448	1.598	-0.012	0.552	0.607	0.69	0.708	0.708	0.735	0.75
450	1.583	-0.012	0.549	0.605	0.687	0.706	0.705	0.732	0.75
452	1.597	-0.013	0.551	0.608	0.69	0.708	0.708	0.733	0.75
454	1.61	-0.012	0.552	0.608	0.691	0.708	0.71	0.735	0.752
456	1.608	-0.013	0.552	0.61	0.694	0.71	0.711	0.738	0.754
458	1.618	-0.014	0.556	0.613	0.694	0.714	0.713	0.74	0.758
460	1.617	-0.015	0.558	0.614	0.696	0.717	0.715	0.743	0.759
462	1.594	-0.013	0.55	0.607	0.691	0.708	0.707	0.736	0.752
464	1.577	-0.013	0.545	0.603	0.683	0.703	0.702	0.729	0.745
466	1.572	-0.014	0.545	0.601	0.681	0.702	0.701	0.726	0.741
468	1.574	-0.014	0.543	0.598	0.679	0.698	0.699	0.724	0.74
470	1.554	-0.014	0.537	0.592	0.673	0.692	0.691	0.718	0.734
472	1.537	-0.015	0.535	0.588	0.668	0.687	0.688	0.713	0.729
474	1.541	-0.016	0.531	0.586	0.665	0.685	0.685	0.711	0.725
476	1.531	-0.015	0.527	0.581	0.662	0.678	0.681	0.707	0.722
478	1.536	-0.016	0.527	0.579	0.657	0.677	0.678	0.704	0.72
480	1.53	-0.016	0.524	0.578	0.655	0.676	0.677	0.701	0.719
482	1.532	-0.018	0.524	0.576	0.655	0.674	0.676	0.699	0.718
484	1.518	-0.018	0.526	0.577	0.654	0.673	0.675	0.699	0.717
486	1.482	-0.014	0.51	0.561	0.639	0.657	0.658	0.682	0.7
488	1.465	-0.015	0.5	0.55	0.628	0.646	0.647	0.673	0.689

490	1.432	-0.014	0.491	0.54	0.619	0.638	0.638	0.662	0.68
492	1.426	-0.015	0.488	0.537	0.613	0.632	0.633	0.658	0.675
494	1.389	-0.012	0.473	0.521	0.6	0.616	0.618	0.642	0.66
496	1.371	-0.013	0.467	0.513	0.59	0.608	0.608	0.634	0.65
498	1.361	-0.015	0.465	0.508	0.584	0.602	0.604	0.63	0.645
500	1.328	-0.014	0.454	0.497	0.572	0.591	0.592	0.616	0.634
502	1.307	-0.014	0.445	0.486	0.561	0.58	0.581	0.606	0.624
504	1.282	-0.014	0.439	0.479	0.554	0.571	0.574	0.598	0.615
506	1.267	-0.015	0.432	0.471	0.545	0.562	0.564	0.589	0.607
508	1.244	-0.015	0.426	0.464	0.538	0.555	0.559	0.582	0.6
510	1.231	-0.016	0.422	0.457	0.532	0.547	0.552	0.575	0.593
512	1.213	-0.017	0.415	0.451	0.525	0.541	0.543	0.568	0.585
514	1.193	-0.016	0.409	0.444	0.516	0.532	0.535	0.559	0.577
516	1.182	-0.016	0.405	0.439	0.512	0.527	0.531	0.554	0.572
518	1.178	-0.017	0.404	0.437	0.507	0.524	0.528	0.551	0.57
520	1.16	-0.017	0.398	0.429	0.5	0.516	0.52	0.544	0.562
522	1.141	-0.016	0.39	0.423	0.494	0.51	0.513	0.536	0.554
524	1.136	-0.017	0.391	0.421	0.493	0.507	0.512	0.534	0.553
526	1.132	-0.019	0.39	0.421	0.49	0.506	0.511	0.534	0.553
528	1.127	-0.02	0.389	0.42	0.487	0.504	0.508	0.532	0.551
530	1.105	-0.017	0.379	0.409	0.479	0.495	0.498	0.522	0.541
532	1.085	-0.015	0.369	0.399	0.469	0.485	0.488	0.512	0.531
534	1.075	-0.017	0.369	0.398	0.467	0.483	0.487	0.511	0.529
536	1.065	-0.016	0.365	0.394	0.464	0.479	0.483	0.506	0.524
538	1.057	-0.017	0.363	0.391	0.461	0.476	0.48	0.503	0.522
540	1.054	-0.018	0.365	0.392	0.461	0.476	0.48	0.503	0.522
542	1.055	-0.019	0.367	0.395	0.461	0.476	0.482	0.504	0.523
544	1.036	-0.017	0.355	0.384	0.452	0.468	0.472	0.496	0.514
546	1.029	-0.017	0.353	0.381	0.451	0.466	0.47	0.493	0.511
548	1.029	-0.016	0.353	0.382	0.45	0.466	0.47	0.491	0.51
550	1.023	-0.015	0.351	0.378	0.447	0.462	0.466	0.489	0.507
552	1.023	-0.017	0.352	0.38	0.447	0.462	0.467	0.489	0.509
554	1.023	-0.018	0.353	0.379	0.446	0.462	0.466	0.489	0.507
556	1.016	-0.017	0.35	0.378	0.444	0.459	0.464	0.487	0.505
558	1.016	-0.018	0.349	0.378	0.443	0.458	0.464	0.486	0.504

560	1.014	-0.018	0.349	0.376	0.444	0.459	0.462	0.485	0.504
562	1.011	-0.019	0.348	0.376	0.442	0.456	0.461	0.483	0.503
564	1.007	-0.019	0.347	0.375	0.441	0.455	0.461	0.481	0.502
566	1.009	-0.02	0.347	0.375	0.44	0.456	0.461	0.482	0.502
568	1.003	-0.019	0.344	0.372	0.439	0.454	0.458	0.479	0.499
570	1	-0.018	0.342	0.371	0.436	0.451	0.456	0.477	0.497
572	1	-0.019	0.342	0.37	0.436	0.452	0.457	0.477	0.497
574	0.997	-0.018	0.34	0.369	0.435	0.45	0.455	0.476	0.496
576	0.991	-0.017	0.338	0.366	0.433	0.447	0.452	0.472	0.493
578	0.985	-0.016	0.336	0.363	0.431	0.445	0.449	0.471	0.491
580	0.98	-0.017	0.334	0.362	0.429	0.443	0.447	0.469	0.489
582	0.978	-0.017	0.334	0.362	0.428	0.443	0.447	0.469	0.488
584	0.98	-0.017	0.334	0.364	0.428	0.444	0.449	0.47	0.489
586	0.98	-0.016	0.335	0.364	0.426	0.443	0.448	0.469	0.488
588	0.981	-0.017	0.335	0.362	0.428	0.442	0.447	0.469	0.489
590	0.978	-0.017	0.335	0.363	0.428	0.442	0.447	0.469	0.489
592	0.973	-0.016	0.333	0.361	0.425	0.441	0.445	0.467	0.487
594	0.972	-0.017	0.332	0.36	0.425	0.44	0.445	0.466	0.486
596	0.973	-0.018	0.333	0.36	0.425	0.44	0.445	0.467	0.486
598	0.97	-0.017	0.332	0.36	0.424	0.44	0.444	0.464	0.485
600	0.962	-0.016	0.327	0.356	0.422	0.436	0.441	0.461	0.481
602	0.966	-0.018	0.328	0.358	0.42	0.436	0.441	0.462	0.482
604	0.97	-0.019	0.332	0.36	0.423	0.438	0.444	0.465	0.485
606	0.964	-0.018	0.33	0.359	0.421	0.436	0.443	0.463	0.483
608	0.958	-0.017	0.326	0.354	0.418	0.434	0.439	0.459	0.48
610	0.956	-0.018	0.326	0.355	0.418	0.434	0.438	0.459	0.479
612	0.955	-0.017	0.324	0.355	0.418	0.432	0.437	0.458	0.479
614	0.948	-0.017	0.321	0.352	0.415	0.43	0.435	0.455	0.477
616	0.948	-0.018	0.323	0.352	0.415	0.43	0.435	0.455	0.476
618	0.952	-0.018	0.324	0.354	0.416	0.43	0.436	0.456	0.478
620	0.956	-0.018	0.325	0.354	0.415	0.431	0.437	0.457	0.479
622	0.952	-0.019	0.325	0.354	0.414	0.43	0.435	0.456	0.476
624	0.951	-0.019	0.324	0.353	0.415	0.43	0.435	0.455	0.477
626	0.952	-0.019	0.325	0.354	0.415	0.431	0.435	0.455	0.478
628	0.948	-0.019	0.324	0.353	0.414	0.429	0.433	0.455	0.476

630	0.944	-0.019	0.321	0.35	0.411	0.427	0.43	0.453	0.473
632	0.937	-0.019	0.32	0.348	0.409	0.425	0.429	0.45	0.471
634	0.938	-0.02	0.32	0.348	0.41	0.424	0.429	0.45	0.47
636	0.936	-0.019	0.318	0.347	0.408	0.422	0.427	0.447	0.469
638	0.929	-0.018	0.315	0.344	0.406	0.421	0.425	0.445	0.468
640	0.929	-0.018	0.314	0.343	0.405	0.419	0.424	0.442	0.466
642	0.926	-0.018	0.313	0.343	0.403	0.418	0.422	0.44	0.464
644	0.923	-0.017	0.311	0.341	0.401	0.417	0.422	0.441	0.463
646	0.923	-0.017	0.31	0.34	0.401	0.416	0.42	0.441	0.463
648	0.92	-0.016	0.31	0.339	0.401	0.415	0.42	0.441	0.461
650	0.916	-0.016	0.31	0.34	0.399	0.414	0.419	0.439	0.461

Table 5: Absorbance spectroscopy data of Plasma, ethambutol and Plasma with ethambutol at different concentrations ranging from 30 µg/ml-1 µg/ml by increments of 5 µg/ml

Wavelength [nm]	**Plasma**	**ETH**	**ETH 1 µg/ml**	**ETH 5 µg/ml**	**ETH 10 µg/ml**	**ETH 15 µg/ml**	**ETH 20 µg/ml**	**ETH 25µg/ml**	**ETH 30 µg/ml**
220	-1.043	-1.555	-0.449	-0.948	-0.226	-0.258	-0.817	0.647	-0.788
222	-0.119	-1.072	-0.049	-0.208	0.856	-0.704	-0.583	-0.197	0.856
224	-0.573	-1.361	-1.188	-1.178	-0.88	-1.712	-1.452	-1.515	-1.394
226	0.323	0.323	-0.222	-0.667	-0.346	-0.613	0.02	-0.132	-1.003
228	0.237	-0.992	-0.551	-0.926	-0.174	-0.13	-0.531	-0.136	-0.397
230	0.134	0.032	0.002	0.134	0.134	-0.269	0.134	-0.164	0.134
232	0.032	-0.061	0.206	-0.285	0.226	-0.065	0.113	-0.632	0.226
234	-0.538	-0.114	0	-0.441	0	0	-0.301	-0.175	0
236	0.064	0.064	0.064	-0.027	0.064	0.064	-0.634	0.026	-0.142
238	0.354	0.354	0.354	0.354	0.354	0.354	0.031	-0.219	0.354
240	0.355	-0.275	0.394	-0.012	0.061	0.041	-0.126	0.078	0.517
242	0.025	0.025	0.025	0.025	0.025	0.025	0.025	0.025	0.025
244	0	-0.208	0	-0.164	0	-0.377	0	0	0
246	0	0	0	0	0	0	0	0	0
248	0	0	0	0	0	0	-0.024	0	0
250	0	-0.059	0	0	0	0	0	0	-0.363
252	0.215	0.016	0.019	0.317	0.176	-0.108	0.425	-0.188	0.04

254	0.043	-0.463	-0.006	0.043	0.043	-0.078	0.043	0.043	0.043
256	0	-0.456	0	0	-0.147	0	0	0	0
258	0	0	0	0	0	0	0	-0.156	0
260	0	0	0	0	0	0	0	-0.401	0
262	0.135	-0.07	0.135	-0.477	0.135	-0.116	-0.051	0.135	-0.135
264	0	0	0	-0.037	0	0	0	0	0
266	0	0	0	-0.386	-0.025	0	-0.147	-0.188	0
268	0	-0.002	-0.297	0	0	-0.028	-0.112	-0.017	0
270	0	0	0	0	0	0	0	0	0
272	0	0	0	0	0	0	0	0	0
274	0.153	-0.318	0.153	-0.22	0.153	0.153	-0.114	0.153	0.077
276	-0.113	0	0	-0.213	0	0	-0.138	0	0
278	-0.482	-0.462	0.024	0.024	0.024	0.024	-0.443	-0.103	0.024
280	0.248	-0.277	0.248	0.248	0.176	0.167	-0.366	0.248	0.248
282	0.871	-0.276	0.568	0.283	0.576	0.282	0.711	0.871	0.871
284	1.34	-0.021	1.34	1.34	1.34	0.854	1.34	1.34	1.34
286	1.809	0.099	1.809	1.809	1.809	1.809	1.809	1.809	1.809
288	1.652	0.102	1.936	1.66	1.93	1.912	1.947	2.147	1.83
290	2.364	0.097	1.902	1.913	1.862	1.898	2.364	1.836	1.802
292	2.481	0.093	2.481	2.3	2.41	2.47	2.169	2.275	2.481
294	2.611	0.091	2.611	2.611	2.611	2.611	2.611	2.611	2.611
296	2.791	0.095	2.791	2.791	2.791	2.791	2.791	2.791	2.791
298	2.938	0.093	2.938	2.938	2.938	2.534	2.938	2.761	2.938
300	2.879	0.092	2.465	2.53	2.993	2.895	2.819	2.666	2.624
302	2.708	0.09	2.454	2.775	2.871	2.556	2.466	2.402	2.726
304	2.73	0.086	2.648	2.212	3.142	2.342	2.565	2.351	2.447
306	2.541	0.086	2.065	2.027	2.339	2.221	2.123	2.32	2.551
308	2.784	0.086	1.639	1.873	1.967	1.839	2.017	2.028	2.21
310	3.215	0.084	1.46	1.614	1.746	1.734	1.836	1.859	2.06
312	2.88	0.083	1.262	1.43	1.493	1.558	1.629	1.618	1.81
314	2.999	0.082	1.126	1.295	1.349	1.464	1.529	1.49	1.636
316	2.548	0.084	1.026	1.206	1.227	1.337	1.397	1.362	1.572
318	2.144	0.082	0.96	1.169	1.192	1.269	1.318	1.299	1.513
320	2.166	0.081	0.915	1.094	1.14	1.215	1.274	1.265	1.445
322	2.599	0.081	0.885	1.061	1.11	1.203	1.252	1.223	1.395

324	2.505	0.082	0.846	1.04	1.067	1.136	1.2	1.212	1.353
326	2.156	0.079	0.829	1.008	1.024	1.094	1.156	1.162	1.325
328	2.175	0.077	0.824	1.001	1.043	1.099	1.164	1.175	1.328
330	2.251	0.08	0.798	0.964	1.013	1.076	1.128	1.156	1.292
332	2.029	0.082	0.784	0.945	0.991	1.052	1.106	1.122	1.257
334	2.011	0.079	0.769	0.949	0.979	1.026	1.09	1.102	1.216
336	1.964	0.078	0.759	0.931	0.98	1.012	1.077	1.107	1.235
338	2.014	0.076	0.739	0.92	0.969	1.018	1.067	1.1	1.222
340	2.165	0.076	0.73	0.911	0.971	0.994	1.051	1.081	1.195
342	2.365	0.076	0.719	0.894	0.934	0.988	1.05	1.067	1.218
344	2.048	0.074	0.692	0.878	0.915	0.972	1.047	1.049	1.176
346	2.044	0.075	0.689	0.879	0.911	0.969	1.028	1.032	1.176
348	2.08	0.076	0.688	0.871	0.897	0.963	1.025	1.024	1.177
350	2.424	0.077	0.691	0.855	0.897	0.948	1.005	1.042	1.152
352	2.089	0.075	0.664	0.835	0.877	0.926	0.96	0.988	1.134
354	2.079	0.076	0.663	0.824	0.871	0.914	0.971	0.993	1.132
356	2.054	0.073	0.653	0.823	0.866	0.916	0.968	0.996	1.136
358	2.034	0.073	0.639	0.817	0.851	0.913	0.965	0.996	1.119
360	1.96	0.071	0.627	0.798	0.845	0.89	0.94	0.976	1.103
362	2.223	0.073	0.624	0.8	0.836	0.895	0.954	0.982	1.105
364	1.961	0.072	0.609	0.787	0.822	0.877	0.929	0.969	1.085
366	1.925	0.071	0.595	0.771	0.808	0.867	0.921	0.951	1.064
368	1.835	0.071	0.591	0.767	0.803	0.85	0.902	0.942	1.059
370	1.809	0.067	0.59	0.752	0.795	0.86	0.893	0.923	1.042
372	1.896	0.068	0.589	0.751	0.798	0.857	0.9	0.938	1.048
374	1.804	0.066	0.58	0.746	0.785	0.849	0.893	0.93	1.044
376	1.824	0.068	0.579	0.749	0.792	0.852	0.893	0.922	1.044
378	1.874	0.068	0.575	0.746	0.792	0.843	0.893	0.911	1.04
380	1.778	0.068	0.569	0.734	0.772	0.818	0.877	0.908	1.02
382	1.841	0.065	0.566	0.734	0.771	0.82	0.888	0.908	1.03
384	1.795	0.065	0.569	0.731	0.77	0.827	0.885	0.91	1.028
386	1.733	0.065	0.565	0.724	0.768	0.821	0.879	0.901	1.02
388	1.778	0.063	0.566	0.734	0.76	0.818	0.879	0.914	1.018
390	1.791	0.062	0.561	0.726	0.761	0.82	0.877	0.908	1.018
392	1.771	0.062	0.564	0.726	0.763	0.823	0.881	0.904	1.018

394	1.766	0.061	0.563	0.725	0.754	0.811	0.872	0.895	1.015
396	1.73	0.06	0.558	0.721	0.751	0.808	0.869	0.892	1.011
398	1.739	0.061	0.562	0.725	0.755	0.816	0.872	0.9	1.014
400	1.781	0.061	0.565	0.726	0.758	0.814	0.87	0.9	1.016
402	1.798	0.059	0.568	0.733	0.764	0.816	0.88	0.91	1.025
404	1.742	0.059	0.573	0.735	0.768	0.822	0.882	0.911	1.021
406	1.745	0.059	0.575	0.738	0.768	0.826	0.883	0.913	1.018
408	1.761	0.058	0.577	0.74	0.769	0.823	0.879	0.91	1.016
410	1.767	0.057	0.576	0.745	0.771	0.825	0.884	0.917	1.016
412	1.781	0.057	0.578	0.744	0.77	0.83	0.881	0.915	1.019
414	1.779	0.055	0.58	0.744	0.769	0.832	0.884	0.915	1.014
416	1.819	0.054	0.582	0.75	0.772	0.835	0.887	0.919	1.02
418	1.851	0.054	0.582	0.751	0.778	0.837	0.888	0.923	1.016
420	1.803	0.052	0.584	0.75	0.778	0.839	0.884	0.921	1.008
422	1.801	0.051	0.582	0.749	0.779	0.838	0.881	0.924	1.007
424	1.816	0.051	0.579	0.749	0.774	0.835	0.876	0.924	1.002
426	1.811	0.052	0.58	0.748	0.773	0.833	0.873	0.92	0.994
428	1.792	0.051	0.579	0.741	0.767	0.829	0.867	0.913	0.986
430	1.788	0.05	0.581	0.744	0.768	0.831	0.866	0.916	0.986
432	1.791	0.05	0.583	0.748	0.771	0.834	0.866	0.922	0.991
434	1.803	0.049	0.583	0.748	0.774	0.835	0.868	0.922	0.986
436	1.808	0.049	0.583	0.747	0.774	0.832	0.869	0.919	0.98
438	1.805	0.048	0.583	0.747	0.772	0.832	0.864	0.919	0.975
440	1.829	0.048	0.585	0.749	0.774	0.833	0.864	0.922	0.977
442	1.774	0.047	0.584	0.747	0.772	0.834	0.859	0.919	0.971
444	1.793	0.047	0.584	0.745	0.77	0.83	0.858	0.916	0.97
446	1.805	0.046	0.585	0.746	0.773	0.833	0.861	0.921	0.973
448	1.816	0.046	0.586	0.751	0.775	0.835	0.86	0.923	0.974
450	1.793	0.045	0.585	0.748	0.774	0.832	0.857	0.922	0.969
452	1.8	0.045	0.588	0.751	0.777	0.834	0.859	0.921	0.97
454	1.822	0.045	0.591	0.753	0.778	0.839	0.86	0.922	0.971
456	1.825	0.044	0.594	0.756	0.78	0.838	0.862	0.927	0.97
458	1.84	0.042	0.596	0.76	0.782	0.84	0.865	0.934	0.973
460	1.833	0.041	0.596	0.762	0.787	0.843	0.869	0.934	0.977
462	1.811	0.042	0.59	0.753	0.778	0.837	0.861	0.923	0.965

464	1.79	0.042	0.585	0.748	0.772	0.832	0.851	0.917	0.959
466	1.788	0.04	0.583	0.745	0.769	0.829	0.848	0.918	0.957
468	1.789	0.04	0.58	0.743	0.767	0.826	0.845	0.915	0.953
470	1.77	0.039	0.573	0.736	0.759	0.815	0.835	0.906	0.942
472	1.76	0.038	0.568	0.731	0.755	0.81	0.83	0.903	0.937
474	1.764	0.038	0.565	0.728	0.753	0.807	0.827	0.9	0.933
476	1.754	0.037	0.561	0.723	0.747	0.805	0.823	0.895	0.925
478	1.766	0.036	0.558	0.719	0.744	0.804	0.821	0.891	0.924
480	1.764	0.035	0.555	0.718	0.742	0.799	0.817	0.889	0.923
482	1.742	0.034	0.553	0.716	0.74	0.798	0.813	0.889	0.919
484	1.738	0.033	0.55	0.715	0.742	0.798	0.815	0.891	0.918
486	1.711	0.037	0.538	0.697	0.721	0.779	0.796	0.873	0.898
488	1.685	0.035	0.528	0.687	0.708	0.769	0.783	0.86	0.884
490	1.656	0.036	0.518	0.675	0.698	0.758	0.771	0.849	0.869
492	1.649	0.034	0.511	0.671	0.692	0.751	0.765	0.844	0.865
494	1.605	0.036	0.497	0.653	0.673	0.733	0.746	0.826	0.844
496	1.587	0.035	0.485	0.642	0.662	0.719	0.735	0.816	0.833
498	1.583	0.034	0.478	0.634	0.658	0.714	0.728	0.812	0.825
500	1.547	0.034	0.466	0.619	0.644	0.701	0.714	0.797	0.814
502	1.527	0.033	0.453	0.608	0.632	0.688	0.703	0.785	0.8
504	1.501	0.033	0.444	0.599	0.622	0.678	0.691	0.776	0.792
506	1.49	0.032	0.434	0.587	0.613	0.67	0.68	0.769	0.784
508	1.464	0.031	0.425	0.578	0.603	0.659	0.671	0.759	0.773
510	1.445	0.031	0.416	0.571	0.595	0.65	0.665	0.751	0.765
512	1.435	0.03	0.41	0.56	0.588	0.643	0.656	0.743	0.755
514	1.416	0.03	0.4	0.554	0.578	0.633	0.646	0.735	0.747
516	1.409	0.029	0.393	0.547	0.571	0.626	0.64	0.729	0.74
518	1.398	0.028	0.389	0.543	0.569	0.622	0.637	0.726	0.736
520	1.384	0.028	0.382	0.534	0.561	0.614	0.628	0.717	0.728
522	1.362	0.028	0.376	0.526	0.551	0.606	0.619	0.709	0.717
524	1.359	0.026	0.372	0.523	0.549	0.605	0.617	0.708	0.715
526	1.354	0.025	0.369	0.522	0.548	0.601	0.614	0.705	0.716
528	1.352	0.024	0.366	0.52	0.546	0.6	0.613	0.704	0.711
530	1.325	0.026	0.358	0.509	0.536	0.59	0.603	0.693	0.699
532	1.299	0.027	0.349	0.499	0.524	0.578	0.589	0.681	0.685

534	1.289	0.026	0.346	0.497	0.522	0.575	0.586	0.678	0.683
536	1.285	0.026	0.342	0.492	0.518	0.57	0.581	0.675	0.677
538	1.276	0.025	0.34	0.489	0.515	0.567	0.578	0.672	0.673
540	1.27	0.024	0.338	0.488	0.515	0.567	0.578	0.671	0.673
542	1.279	0.023	0.338	0.489	0.516	0.568	0.58	0.674	0.676
544	1.257	0.025	0.331	0.479	0.504	0.557	0.568	0.662	0.664
546	1.247	0.024	0.328	0.476	0.501	0.553	0.564	0.658	0.659
548	1.25	0.025	0.327	0.476	0.5	0.554	0.565	0.658	0.66
550	1.243	0.025	0.326	0.472	0.497	0.551	0.561	0.656	0.655
552	1.243	0.023	0.325	0.473	0.498	0.551	0.561	0.658	0.656
554	1.24	0.023	0.325	0.472	0.499	0.55	0.56	0.657	0.655
556	1.237	0.023	0.324	0.47	0.496	0.547	0.558	0.653	0.652
558	1.237	0.022	0.323	0.469	0.494	0.547	0.557	0.653	0.65
560	1.231	0.021	0.322	0.467	0.493	0.546	0.556	0.654	0.65
562	1.227	0.021	0.321	0.467	0.492	0.545	0.554	0.652	0.648
564	1.229	0.02	0.32	0.465	0.491	0.544	0.552	0.651	0.645
566	1.232	0.019	0.319	0.466	0.492	0.546	0.552	0.652	0.645
568	1.221	0.02	0.317	0.463	0.489	0.542	0.548	0.647	0.641
570	1.216	0.02	0.315	0.461	0.486	0.54	0.547	0.645	0.637
572	1.216	0.019	0.315	0.461	0.486	0.54	0.546	0.646	0.638
574	1.211	0.019	0.314	0.461	0.485	0.538	0.544	0.643	0.634
576	1.202	0.019	0.312	0.458	0.482	0.535	0.541	0.64	0.631
578	1.204	0.02	0.311	0.456	0.48	0.533	0.538	0.636	0.627
580	1.194	0.02	0.309	0.454	0.478	0.529	0.535	0.635	0.624
582	1.193	0.019	0.309	0.454	0.477	0.531	0.535	0.636	0.626
584	1.203	0.019	0.31	0.454	0.477	0.533	0.536	0.638	0.627
586	1.201	0.019	0.309	0.454	0.476	0.53	0.535	0.638	0.626
588	1.195	0.019	0.309	0.453	0.477	0.53	0.535	0.637	0.625
590	1.191	0.019	0.309	0.453	0.476	0.529	0.534	0.636	0.624
592	1.194	0.019	0.307	0.451	0.475	0.528	0.533	0.634	0.622
594	1.194	0.018	0.306	0.45	0.475	0.526	0.531	0.635	0.622
596	1.192	0.017	0.306	0.45	0.476	0.527	0.531	0.634	0.622
598	1.194	0.018	0.305	0.449	0.474	0.526	0.53	0.633	0.62
600	1.186	0.018	0.303	0.446	0.47	0.523	0.526	0.63	0.614
602	1.183	0.017	0.304	0.446	0.472	0.522	0.525	0.63	0.615

604	1.189	0.016	0.304	0.449	0.474	0.525	0.528	0.633	0.618
606	1.185	0.016	0.303	0.448	0.473	0.523	0.527	0.631	0.616
608	1.177	0.017	0.302	0.445	0.468	0.521	0.523	0.627	0.612
610	1.173	0.015	0.3	0.444	0.469	0.521	0.522	0.626	0.611
612	1.175	0.016	0.3	0.444	0.468	0.519	0.521	0.625	0.608
614	1.17	0.016	0.298	0.44	0.464	0.516	0.517	0.623	0.605
616	1.168	0.015	0.298	0.44	0.465	0.517	0.518	0.624	0.606
618	1.173	0.015	0.298	0.441	0.466	0.518	0.519	0.625	0.607
620	1.178	0.015	0.299	0.441	0.467	0.519	0.519	0.626	0.608
622	1.171	0.014	0.298	0.441	0.466	0.517	0.518	0.625	0.606
624	1.169	0.013	0.297	0.441	0.466	0.517	0.518	0.625	0.605
626	1.17	0.012	0.297	0.441	0.466	0.517	0.518	0.627	0.604
628	1.167	0.012	0.297	0.44	0.464	0.515	0.517	0.624	0.603
630	1.161	0.013	0.295	0.437	0.462	0.513	0.514	0.619	0.599
632	1.16	0.013	0.294	0.436	0.462	0.512	0.512	0.619	0.597
634	1.162	0.012	0.293	0.436	0.46	0.511	0.511	0.62	0.598
636	1.155	0.012	0.292	0.433	0.458	0.509	0.509	0.616	0.594
638	1.147	0.013	0.291	0.431	0.455	0.507	0.507	0.615	0.59
640	1.143	0.013	0.29	0.431	0.454	0.504	0.505	0.612	0.588
642	1.138	0.012	0.288	0.43	0.453	0.503	0.502	0.612	0.585
644	1.143	0.013	0.288	0.428	0.451	0.502	0.499	0.61	0.586
646	1.142	0.013	0.286	0.427	0.45	0.501	0.499	0.609	0.584
648	1.134	0.013	0.285	0.426	0.449	0.501	0.498	0.608	0.583
650	1.135	0.013	0.285	0.426	0.448	0.502	0.498	0.608	0.583

Table 6: Absorbance spectroscopy data of Plasma, Rif-4 and Plasma with Rif-4 at different concentrations ranging from 30 µg/ml-1 µg/ml by increments of 5 µg/ml.

Wavelength [nm]	**Plasma**	**R-4**	**R-(4) 1 µg/ml**	**R-(4) 5 µg/ml**	**R-(4) 10 µg/ml**	**R-(4) 15 µg/ml**	**R-(4) 20 µg/ml**	**R-(4) 25 µg/ml**	**R-(4) 30 µg/ml**
220	-0.399	-0.554	-0.59	-0.622	-0.904	-1.166	0.647	-0.87	0.647
222	0.856	-0.781	0.018	0.856	-0.373	-0.511	-0.375	-0.601	0.856
224	0.114	-0.797	-	0.114	0.114	0.114	-0.716	-1.489	-0.789

			1.107						
226	-0.849	-0.706	-0.569	-1.079	0.323	-0.689	-0.244	-1.093	0.323
228	0.237	-0.407	-0.857	-0.513	0.204	-0.089	-0.024	-0.111	0.237
230	0.134	0.134	-0.443	-0.412	0.134	0.134	0.134	0.134	-0.263
232	0.226	0.226	-0.043	-0.208	0.226	0.226	0.226	0.226	-0.059
234	-0.056	0	0	0	0	0	0	0	0
236	0.064	-0.319	0.064	-0.497	0.064	0.064	0.064	0.051	-0.444
238	0.354	0.313	0.142	-0.201	0.354	0.354	0.354	0.17	0.354
240	-0.069	-0.277	0.517	-0.257	0.07	0.118	0.038	0.229	0.517
242	0.025	0.025	0.025	0.025	0.025	0.025	0.025	0.025	0.025
244	0	0	-0.341	-0.363	0	0	0	0	0
246	0	-0.017	0	0	0	0	0	-0.083	0
248	0	0	0	0	0	-0.022	0	0	0
250	0	0	0	0	0	-0.396	0	0	-0.057
252	0.149	0.335	-0.215	-0.087	0.296	0.153	-0.065	-0.189	-0.072
254	-0.057	0.043	-0.105	-0.031	0.043	0.043	0.043	-0.014	-0.041
256	0	0	0	-0.186	0	0	0	-0.098	-0.235
258	-0.067	0	0	0	0	0	0	-0.155	0
260	0	0	0	0	0	0	0	0	0
262	0.135	0.123	0.135	0.135	0.135	0.135	0.135	-0.005	-0.08
264	0	0	0	0	0	0	0	0	0
266	0	-0.066	0	0	0	-0.144	0	0	0
268	-0.006	0	-0.168	-0.267	0	0	0	0	-0.021
270	0	0	0	0	0	0	0	0	0
272	0	-0.076	0	0	0	0	0	0	0
274	0.153	0.153	0.153	0.072	0.142	0.153	0.153	-0.004	0.153
276	0	0	0	0	0	0	0	0	0
278	0.024	-0.516	0.024	-0.071	0.024	0.024	0.024	0.024	0.024

280	0.248	0.248	0.248	0.01	0.221	0.248	0.248	0.248	0.248
282	0.664	0.871	0.179	0.457	0.851	0.677	0.648	0.733	0.598
284	1.34	1.24	1.34	1.34	1.34	1.34	1.34	1.34	1.34
286	1.809	1.809	1.809	1.809	1.809	1.809	1.809	1.809	1.809
288	2.147	1.367	2.042	2.147	2.063	1.757	1.943	2.147	1.818
290	2.113	1.284	1.973	2.258	1.982	2.364	1.653	2.106	2.288
292	2.481	1.166	2.101	2.481	2.481	2.364	2.15	2.095	2.481
294	2.611	1.013	2.611	2.611	2.611	2.611	2.611	2.611	2.611
296	2.791	0.869	2.791	2.791	2.791	2.791	2.791	2.791	2.791
298	2.763	0.784	2.938	2.889	2.938	2.938	2.938	2.938	2.938
300	2.185	0.717	2.426	2.537	2.593	2.784	2.944	2.614	2.868
302	2.461	0.674	2.276	2.562	2.483	2.36	2.248	2.404	2.455
304	2.758	0.645	2.575	2.05	2.871	2.655	2.583	2.796	3.109
306	2.969	0.622	1.922	1.922	2.471	2.58	2.816	2.311	2.863
308	2.496	0.598	1.533	1.619	1.935	2.103	2.345	2.052	2.417
310	2.631	0.59	1.337	1.369	1.72	2.087	2.064	1.928	2.31
312	2.651	0.575	1.161	1.187	1.532	1.807	1.769	1.788	1.923
314	2.09	0.565	1.032	1.045	1.402	1.735	1.605	1.718	1.688
316	1.988	0.564	0.939	0.951	1.278	1.629	1.485	1.575	1.669
318	1.983	0.561	0.858	0.884	1.184	1.51	1.419	1.489	1.575
320	1.903	0.557	0.812	0.824	1.139	1.388	1.334	1.39	1.448
322	1.908	0.559	0.777	0.784	1.097	1.376	1.304	1.336	1.37
324	1.743	0.553	0.738	0.75	1.027	1.27	1.253	1.289	1.378
326	1.715	0.545	0.711	0.724	0.989	1.247	1.206	1.263	1.352
328	1.656	0.547	0.696	0.713	0.972	1.236	1.19	1.243	1.325
330	1.594	0.55	0.679	0.687	0.948	1.212	1.13	1.202	1.276
332	1.631	0.545	0.67	0.675	0.921	1.175	1.132	1.168	1.235
334	1.63	0.54	0.649	0.652	0.902	1.149	1.096	1.129	1.182
336	1.568	0.531	0.623	0.643	0.889	1.146	1.097	1.123	1.188
338	1.558	0.516	0.618	0.629	0.866	1.116	1.094	1.127	1.201
340	1.573	0.505	0.602	0.62	0.85	1.084	1.06	1.1	1.149
342	1.548	0.48	0.585	0.606	0.831	1.07	1.057	1.084	1.125
344	1.462	0.438	0.581	0.593	0.804	1.069	1.024	1.06	1.12
346	1.507	0.405	0.564	0.58	0.79	1.05	1.021	1.06	1.099
348	1.525	0.37	0.547	0.566	0.77	1.029	0.993	1.047	1.077

350	1.564	0.342	0.537	0.559	0.761	1.016	0.975	1.024	1.081
352	1.42	0.299	0.527	0.538	0.717	0.957	0.936	0.987	1.036
354	1.451	0.261	0.514	0.526	0.706	0.962	0.934	0.985	1.01
356	1.417	0.232	0.496	0.515	0.694	0.932	0.899	0.965	1.001
358	1.415	0.209	0.485	0.514	0.675	0.908	0.896	0.94	0.977
360	1.389	0.185	0.473	0.498	0.648	0.877	0.869	0.917	0.947
362	1.448	0.169	0.467	0.491	0.637	0.872	0.868	0.912	0.936
364	1.395	0.153	0.456	0.48	0.619	0.85	0.848	0.887	0.923
366	1.346	0.136	0.444	0.472	0.604	0.818	0.828	0.875	0.9
368	1.328	0.122	0.441	0.462	0.595	0.81	0.814	0.864	0.885
370	1.31	0.11	0.433	0.457	0.585	0.793	0.802	0.852	0.864
372	1.323	0.103	0.43	0.451	0.574	0.79	0.802	0.844	0.873
374	1.329	0.093	0.428	0.45	0.566	0.781	0.794	0.837	0.858
376	1.318	0.087	0.422	0.444	0.559	0.776	0.792	0.829	0.851
378	1.311	0.08	0.414	0.438	0.555	0.762	0.78	0.816	0.845
380	1.287	0.075	0.411	0.432	0.542	0.745	0.764	0.814	0.829
382	1.296	0.071	0.408	0.434	0.541	0.747	0.763	0.814	0.826
384	1.3	0.066	0.41	0.43	0.54	0.746	0.764	0.803	0.82
386	1.283	0.062	0.406	0.426	0.533	0.739	0.754	0.796	0.807
388	1.292	0.06	0.406	0.426	0.532	0.735	0.754	0.802	0.809
390	1.289	0.056	0.406	0.426	0.529	0.735	0.75	0.794	0.809
392	1.283	0.055	0.405	0.427	0.53	0.732	0.747	0.789	0.806
394	1.265	0.056	0.403	0.426	0.527	0.727	0.741	0.788	0.8
396	1.259	0.056	0.403	0.426	0.525	0.718	0.741	0.783	0.796
398	1.277	0.055	0.407	0.429	0.526	0.722	0.746	0.788	0.802
400	1.269	0.057	0.409	0.433	0.533	0.725	0.744	0.792	0.8
402	1.293	0.057	0.413	0.437	0.535	0.729	0.748	0.794	0.807
404	1.287	0.059	0.416	0.442	0.537	0.731	0.757	0.802	0.812
406	1.281	0.062	0.42	0.445	0.538	0.732	0.757	0.798	0.813
408	1.281	0.065	0.423	0.449	0.54	0.734	0.757	0.799	0.81
410	1.295	0.068	0.425	0.452	0.545	0.738	0.76	0.805	0.817
412	1.302	0.073	0.427	0.452	0.546	0.741	0.763	0.81	0.817
414	1.316	0.077	0.426	0.454	0.548	0.742	0.764	0.809	0.82
416	1.319	0.081	0.43	0.456	0.551	0.75	0.771	0.812	0.828
418	1.325	0.086	0.431	0.458	0.555	0.75	0.772	0.818	0.832

420	1.329	0.091	0.431	0.458	0.557	0.752	0.771	0.817	0.834
422	1.33	0.097	0.433	0.458	0.558	0.753	0.776	0.819	0.835
424	1.324	0.104	0.433	0.46	0.558	0.755	0.776	0.82	0.835
426	1.322	0.111	0.434	0.461	0.561	0.757	0.777	0.819	0.834
428	1.314	0.119	0.435	0.462	0.563	0.752	0.776	0.814	0.833
430	1.316	0.124	0.437	0.462	0.567	0.756	0.779	0.82	0.838
432	1.325	0.133	0.44	0.467	0.571	0.763	0.782	0.826	0.842
434	1.333	0.139	0.44	0.469	0.573	0.766	0.784	0.83	0.848
436	1.328	0.148	0.442	0.47	0.574	0.768	0.787	0.828	0.847
438	1.33	0.156	0.442	0.471	0.575	0.768	0.79	0.83	0.85
440	1.328	0.163	0.445	0.472	0.579	0.773	0.793	0.835	0.855
442	1.326	0.171	0.446	0.471	0.582	0.776	0.791	0.835	0.853
444	1.328	0.18	0.447	0.472	0.584	0.777	0.793	0.833	0.853
446	1.331	0.187	0.449	0.476	0.589	0.782	0.796	0.839	0.861
448	1.337	0.197	0.452	0.479	0.595	0.786	0.803	0.84	0.863
450	1.329	0.204	0.454	0.48	0.596	0.788	0.802	0.841	0.863
452	1.338	0.211	0.457	0.484	0.601	0.793	0.806	0.847	0.868
454	1.341	0.219	0.458	0.487	0.604	0.798	0.811	0.85	0.876
456	1.353	0.224	0.461	0.489	0.609	0.8	0.815	0.851	0.878
458	1.354	0.228	0.464	0.491	0.613	0.809	0.82	0.856	0.885
460	1.363	0.232	0.465	0.491	0.616	0.815	0.823	0.863	0.89
462	1.345	0.238	0.461	0.488	0.612	0.809	0.818	0.855	0.882
464	1.326	0.241	0.458	0.483	0.608	0.804	0.814	0.851	0.876
466	1.33	0.243	0.455	0.481	0.609	0.803	0.813	0.848	0.879
468	1.329	0.246	0.452	0.477	0.606	0.803	0.811	0.847	0.877
470	1.314	0.249	0.446	0.471	0.601	0.795	0.805	0.842	0.869
472	1.297	0.249	0.441	0.466	0.597	0.792	0.801	0.835	0.867
474	1.295	0.25	0.438	0.461	0.596	0.792	0.799	0.832	0.864
476	1.282	0.249	0.433	0.457	0.591	0.788	0.796	0.827	0.859
478	1.282	0.248	0.431	0.454	0.589	0.786	0.793	0.824	0.861
480	1.28	0.247	0.428	0.451	0.585	0.784	0.791	0.822	0.859
482	1.277	0.242	0.424	0.447	0.583	0.783	0.788	0.822	0.854
484	1.275	0.237	0.421	0.443	0.581	0.784	0.787	0.82	0.856
486	1.244	0.236	0.412	0.434	0.568	0.763	0.771	0.801	0.836
488	1.218	0.229	0.402	0.423	0.558	0.751	0.758	0.79	0.823

490	1.195	0.224	0.391	0.414	0.547	0.739	0.747	0.778	0.811
492	1.187	0.215	0.383	0.403	0.539	0.732	0.739	0.771	0.804
494	1.15	0.21	0.372	0.391	0.523	0.711	0.723	0.752	0.783
496	1.131	0.2	0.361	0.38	0.512	0.699	0.712	0.74	0.772
498	1.12	0.19	0.35	0.367	0.503	0.692	0.704	0.733	0.766
500	1.092	0.18	0.339	0.354	0.489	0.676	0.689	0.715	0.749
502	1.068	0.168	0.325	0.34	0.474	0.663	0.674	0.701	0.734
504	1.049	0.157	0.314	0.329	0.463	0.651	0.664	0.69	0.723
506	1.03	0.147	0.305	0.318	0.451	0.637	0.653	0.677	0.712
508	1.012	0.137	0.296	0.308	0.44	0.625	0.641	0.667	0.699
510	0.999	0.127	0.287	0.298	0.429	0.616	0.631	0.656	0.689
512	0.981	0.116	0.278	0.29	0.419	0.604	0.621	0.647	0.678
514	0.965	0.105	0.27	0.281	0.408	0.592	0.611	0.635	0.666
516	0.953	0.096	0.264	0.274	0.399	0.582	0.602	0.628	0.659
518	0.946	0.086	0.258	0.269	0.393	0.576	0.596	0.622	0.653
520	0.929	0.079	0.252	0.262	0.384	0.565	0.587	0.61	0.641
522	0.914	0.072	0.247	0.256	0.376	0.554	0.576	0.602	0.629
524	0.91	0.062	0.241	0.25	0.369	0.548	0.571	0.598	0.624
526	0.907	0.053	0.236	0.245	0.363	0.544	0.567	0.594	0.621
528	0.901	0.047	0.231	0.24	0.356	0.539	0.563	0.588	0.616
530	0.879	0.044	0.225	0.233	0.347	0.525	0.551	0.575	0.601
532	0.858	0.04	0.219	0.226	0.337	0.51	0.538	0.561	0.587
534	0.85	0.033	0.213	0.22	0.331	0.505	0.532	0.557	0.582
536	0.841	0.03	0.209	0.215	0.326	0.498	0.526	0.551	0.575
538	0.835	0.025	0.206	0.211	0.321	0.492	0.521	0.546	0.57
540	0.834	0.02	0.202	0.209	0.318	0.49	0.519	0.545	0.569
542	0.835	0.016	0.2	0.207	0.316	0.491	0.519	0.544	0.569
544	0.816	0.016	0.196	0.202	0.307	0.478	0.508	0.532	0.555
546	0.807	0.013	0.193	0.199	0.304	0.473	0.504	0.528	0.55
548	0.806	0.011	0.191	0.197	0.302	0.471	0.502	0.527	0.549
550	0.8	0.009	0.19	0.196	0.299	0.467	0.498	0.523	0.545
552	0.802	0.006	0.189	0.194	0.298	0.467	0.499	0.523	0.545
554	0.801	0.004	0.188	0.193	0.297	0.467	0.499	0.522	0.544
556	0.798	0.002	0.186	0.192	0.295	0.463	0.494	0.519	0.541
558	0.796	0.0008	0.186	0.191	0.293	0.46	0.493	0.517	0.539

560	0.793	-7E-04	0.185	0.19	0.292	0.461	0.493	0.517	0.539
562	0.791	-0.002	0.184	0.188	0.291	0.458	0.49	0.514	0.537
564	0.788	-0.004	0.183	0.187	0.29	0.456	0.488	0.513	0.535
566	0.789	-0.005	0.182	0.187	0.289	0.457	0.489	0.512	0.535
568	0.783	-0.005	0.181	0.186	0.287	0.453	0.486	0.509	0.531
570	0.779	-0.005	0.179	0.185	0.285	0.45	0.483	0.507	0.529
572	0.779	-0.007	0.18	0.184	0.285	0.45	0.481	0.507	0.529
574	0.777	-0.007	0.179	0.183	0.284	0.448	0.481	0.505	0.527
576	0.772	-0.007	0.178	0.183	0.282	0.445	0.479	0.502	0.522
578	0.766	-0.006	0.178	0.182	0.28	0.442	0.475	0.498	0.52
580	0.763	-0.007	0.176	0.181	0.279	0.439	0.473	0.496	0.517
582	0.762	-0.008	0.176	0.18	0.278	0.44	0.472	0.496	0.517
584	0.761	-0.009	0.175	0.18	0.278	0.439	0.473	0.495	0.518
586	0.762	-0.008	0.175	0.178	0.278	0.44	0.473	0.495	0.517
588	0.762	-0.009	0.173	0.178	0.276	0.44	0.472	0.494	0.516
590	0.763	-0.009	0.173	0.178	0.275	0.439	0.471	0.494	0.516
592	0.76	-0.009	0.173	0.177	0.275	0.437	0.47	0.493	0.515
594	0.758	-0.01	0.172	0.177	0.274	0.436	0.468	0.492	0.514
596	0.76	-0.011	0.172	0.176	0.274	0.436	0.469	0.491	0.514
598	0.756	-0.01	0.171	0.176	0.274	0.434	0.468	0.489	0.513
600	0.747	-0.01	0.171	0.175	0.272	0.431	0.463	0.487	0.508
602	0.749	-0.011	0.17	0.174	0.271	0.432	0.464	0.487	0.509
604	0.754	-0.012	0.17	0.174	0.271	0.435	0.465	0.489	0.512
606	0.751	-0.012	0.169	0.173	0.27	0.432	0.466	0.486	0.51
608	0.745	-0.011	0.167	0.172	0.267	0.429	0.461	0.483	0.504
610	0.743	-0.013	0.167	0.171	0.267	0.429	0.46	0.482	0.505
612	0.741	-0.012	0.167	0.172	0.266	0.427	0.459	0.481	0.503
614	0.737	-0.012	0.166	0.17	0.265	0.423	0.457	0.477	0.501
616	0.738	-0.013	0.166	0.17	0.265	0.424	0.456	0.478	0.501
618	0.741	-0.014	0.165	0.17	0.265	0.426	0.457	0.479	0.501
620	0.74	-0.014	0.164	0.169	0.265	0.426	0.458	0.479	0.503
622	0.74	-0.015	0.163	0.168	0.264	0.425	0.456	0.477	0.502
624	0.738	-0.015	0.163	0.168	0.263	0.425	0.456	0.477	0.501
626	0.738	-0.015	0.163	0.167	0.263	0.425	0.456	0.478	0.502
628	0.735	-0.015	0.162	0.166	0.262	0.423	0.454	0.475	0.5

630	0.731	-0.015	0.161	0.165	0.26	0.42	0.451	0.474	0.497
632	0.729	-0.015	0.16	0.164	0.258	0.417	0.451	0.47	0.495
634	0.727	-0.016	0.159	0.164	0.258	0.417	0.449	0.47	0.494
636	0.724	-0.016	0.159	0.162	0.257	0.416	0.447	0.467	0.492
638	0.722	-0.015	0.158	0.161	0.256	0.414	0.445	0.464	0.49
640	0.717	-0.015	0.157	0.161	0.254	0.412	0.444	0.463	0.487
642	0.716	-0.015	0.156	0.16	0.254	0.411	0.442	0.462	0.486
644	0.713	-0.014	0.156	0.16	0.253	0.409	0.441	0.461	0.484
646	0.711	-0.015	0.156	0.16	0.253	0.409	0.44	0.46	0.483
648	0.709	-0.014	0.155	0.158	0.251	0.406	0.438	0.457	0.483
650	0.709	-0.014	0.154	0.158	0.251	0.406	0.439	0.457	0.482

Addendum D: Ethics approval letter

UNIVERSITEIT·STELLENBOSCH·UNIVERSITY
jou kennisvennoot · your knowledge partner

Ethics Letter

13-Apr-2017
Vallie, Sarfaraaz S

Ethics Reference #: X17/04/005
Clinical Trial Reference #:
Title: Method development and optimization for Rifampicin, Isoniazide and Esomeprazole in plasma using HPLC and LCMS analytical and Validation techniques

Dear Mr Sarfaraaz Vallie

We acknowledge receipt of your application for your research project to be exempted from ethics review.

The Health Research Ethics Committee has assessed your application and considers this research proposal to meet the requirements for ethics exemption.

This letter confirms that this research is now registered and you can proceed with study related activities.

Where to submit any documentation
Kindly submit **ONE HARD COPY** to Elvira Rohland, RDSD, Room 5007, Teaching Building, and **ONE ELECTRONIC COPY** to ethics@sun.ac.za

Please remember to use your **protocol number (X17/04/005)** on any documents or correspondence with the HREC concerning your research protocol.

Federal Wide Assurance Number: 00001372
Institutional Review Board (IRB) Number: IRB0005240 for HREC1
Institutional Review Board (IRB) Number: IRB0005239 for HREC2

The Health Research Ethics Committee complies with the SA National Health Act No.61 2003 as it pertains to health research and the United States Code of Federal Regulations Title 45 Part 46. This committee abides by the ethical norms and principles for research, established by the Declaration of Helsinki, the South African Good Clinical Pracices Guidelines as well as the Guidelines for Ethical Research: Principles Structures and Processes 2004 (Department of Health).

Sincerely,
Francis Masiye
REC Coordinator
Health Research Ethics Committee 2